SYNTHESIS OF FUNCTIONAL POLYLACTIDES FOR BIOMEDICAL AND PHARMACEUTICAL APPLICATIONS

A Dissertation
Presented to
The Academic Faculty

by

Pranav Pratap Kalelkar

In Partial Fulfillment
of the Requirements for the Degree
Doctor of Philosophy in the
School of Chemistry and Biochemistry/College of Sciences

Georgia Institute of Technology
May 2018

SYNTHESIS OF FUNCTIONAL POLYLACTIDES FOR BIOMEDICAL AND PHARMACEUTICAL APPLICATIONS

Approved by:

Dr. David M. Collard, Advisor
School of Chemistry and Biochemistry
Georgia Institute of Technology

Dr. Will Gutekunst
School of Chemistry and Biochemistry
Georgia Institute of Technology

Dr. Stefan France
School of Chemistry and Biochemistry
Georgia Institute of Technology

Dr. Adegboyega K. Oyelere
School of Chemistry and Biochemistry
Georgia Institute of Technology

Dr. Andrés J. García
Woodruff School of Mechanical Engineering
Georgia Institute of Technology

Date Approved: January 11, 2018

[To my family, the four pillars of support of my life]

ACKNOWLEDGEMENTS

First, I would like to thank Dr. Collard for his guidance, support and constant encouragement. Thank you for being patient with me when I was new to research during my beginning years, for giving me the freedom to come up with new ideas, and most importantly- for teaching me how to tell a story. It was a privilege to work under your guidance and you really did justice to the word “advisor”.

Second, I would like to thank my thesis committee for their guidance, support and time. In particular, I would like to thank Dr. Andrés Garcia for allowing me to use his laboratory facilities as well as for providing me with his guidance. I would also like to thank Dr. M. G. Finn for his inputs and for providing me with the opportunity to collaborate with his research group.

Third, I would like to thank Dr. Rachit Agarwal, a former postdoc from Dr. Garcia’s research group for teaching me biological assays and Zhishuai Geng, a PhD Candidate from Dr. M. G. Finn’s group for carrying out the antimicrobial assays and XPS characterization. In addition to their help with these experiments, I really appreciate the scientific discussions we had which were not necessarily restricted to the projects that we were working on.

Fourth, I would like to thank my colleagues from Collard Research Group. Guillermo Alas for helping me with my research during the early stages. Bronson and Chinmay for being great friends and for always being their when I needed to discuss science. Thank you, Elizabeth, Jessie and Ashley for your support and for maintaining a cheerful and positive atmosphere in the lab.

Fifth, I would like to thank all my friends in the US and in India for their support and friendship.

And finally, I would like to thank my mom, Mrs. Rajashri Kalelkar, my dad, Mr. Pratap Kalelkar, and my two sisters, Mrs. Rasika Samant and Dr. Rachana Kalelkar for their unconditional support. They celebrated even the smallest of my achievements, which gave me the courage and motivation to pursue greater things in life. Special mention to Rachana for her unwavering support throughout my PhD journey and her spot-on advice. Seriously, it wouldn't have been possible without you guys.

TABLE OF CONTENTS

LIST OF TABLES

LIST OF FIGURES

LIST OF SYMBOLS AND ABBREVIATIONS

ATRP	atom-transfer radical polymerization
BPO	benzoyl peroxide
Bpy	2,2'-bipyridine
CMC	critical micellar concentration
dd	doublet of doublet
DIPEA	*N*,*N*-diisopropylethyl amine
DCM	dichloromethane
DCC	*N, N'*-dicyclohexylcarbodiimide
DCU	dicyclohexylurea
DLS	dynamic light scattering
DSC	differential scanning calorimetry
FDA	Food and Drug Administration
FT-IR	fourier-transform infrared spectroscopy
GPC	gel permeation chromatography
HOBt	1-hydroxybenzotriazole
HRMS	high resolution mass spectrometry
IR	infrared
J	coupling constant
m	multiplet
M_w	weight-average molecular weight
M_n	number-average molecular weight
MA	methyl acrylate
MMA	methyl methacrylate

MIC_{90}	lowest concentration of the antibiotic at which 90 % of the isolates were inhibited
M.P.	melting point
MS	mass spectrometry
NBS	*N*-bromosuccinimide
NMR	nuclear magnetic resonance spectroscopy
OEGMA	oligoethylene glycol methacrylate
ppm	parts per million
PDI	polydispersity index
PEG	polyethylene glycol
PG	polyglycolide
PL	polylactide
QAMA	quaternary ammonium methacrylate
RGD	arginine-glycine-aspartic acid
ROP	ring-opening polymerization
s	singlet
SI- ATRP	surface initiated atom-transfer radical polymerization
t	triplet
TFA	trifluoroacetic acid
THF	tetrahydrofuran
TLC	thin layer chromatography
UV-vis	ultraviolet-visible
ZMA	zwitterion methacrylate
Δ	heat or reflux
ΔH_c	enthalpy of crystallization during cooling

ΔH_{cc}	enthalpy of cold crystallization during heating
ΔH_{m}	enthalpy of melting
ΔT_{c}	crystallization temperature
ΔT_{cc}	temperature of cold crystallization during heating
ΔT_{m}	melting temperature
δ	chemical shift

SUMMARY

Poly(lactide) (PL) is an aliphatic, biodegradable polyester that is approved by the FDA for use in contact with humans. These characteristics make PL an attractive material for use in biomedical devices and medical implants. However, the lack of functional groups appended along the backbone limits its applications. Incorporation of functional groups would allow for the conjugation of drugs or biomolecules that would further enhance the utility of the polymer for biomedical and pharmaceutical applications.

To improve the properties of PL, analogs bearing alkyl, carboxyl, hydroxyl and amino side chains have been synthesized, Figure 1. Further modification of carboxyl, hydroxyl and amino substituted analogs with biomolecules is possible by coupling using active ester chemistry. However, the synthesis of polyesters and the conjugation of biomolecules remain as significant challenges.

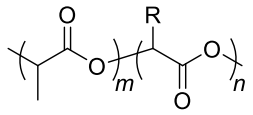

R
alkyl
alkenyl
alkynyl
$(CH_2)_xS(CH_2)_2O(CH_2)_2N_3$
$(CH_2)_xCOOH$
$(CH_2)_xOH$
$(CH_2)_xNH_2$
$L[O(CH_2)_2]_yOMe$

Figure 1. Examples of functional polylactides. L: linker group.

To overcome this limitation, I have synthesized five new functional copolylactides, Figure 2. This required multi-step monomer synthesis, ring-opening copolymerization, and post-polymerization modifications. A bromine-substituted analog of PL was prepared by direct bromination of PL in solution and at the surface of thin films of PL.

These PL analogs allow for the coupling of molecules under mild conditions. The coupling of thiols to ene-PL and the addition of thiol-PL to electron deficient alkenes sets a precedence for the potential bioconjugation of both nucleophilic and electrophilic biomolecules. The azide-substituted analog undergoes [3+2] cycloaddition "click" chemistry with a variety of alkynes. Addition of quaternary ammonium-substituted alkynes onto azido-PL imparts antimicrobial activity that could improve the utility of PL as a packaging material.

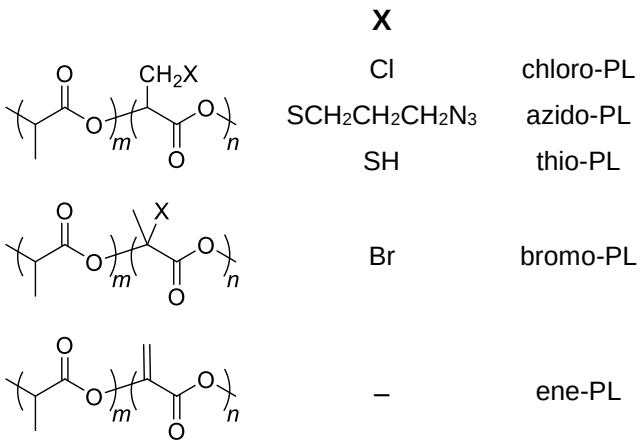

Figure 2. Examples of new functional polylactides described in this thesis.

The use of bromo-PL as a macroinitiator for the atom-transfer radical polymerization (ATRP) of oligo(ethylene glycol) methacrylate results in the formation of an amphiphilic brush copolymer that self assembles into nanoparticles that might have potential for drug delivery. Finally, surface brominated PL objects undergo surface-initiated atom-transfer radical polymerization (SI ATRP) that allow the grafting of hydrophilic and antimicrobial polymethacrylate brushes on the surface. Thus, the biodegradable nature of PL, combined with a variety of reactive functional group that are amenable to facile modification, provides researchers with access to materials with a wide array of potential application.

CHAPTER 1

Recent advances in functional copolymers of polylactides for biomedical applications

1.1. INTRODUCTION

1.1.1. Background

The availability of petroleum based thermoplastics such as polyethylene (PE), polypropylene (PP) and polyethylene terephthalate (PET) has supported technological innovation for the last century. These materials are ubiquitous in modern life in areas as diverse as consumer packaging, electronic devices and transportation. However, the dependence on non-renewable resources and their resistance to degradation places a severe burden on the environment. To address these concerns, significant investment has been made to develop new plastics that can be obtained from biorenewable resources and which are biodegradable.[1]

1.1.2. Properties

Thermoplastic poly(α-hydroxy acid)s (PHAs) such as polylactide (PL), polyglycolide (PG), and their copolymers (e.g., PLGA), have gained attention because of their biocompatible and biodegradable nature.[2,3,4] The polyester backbone of PHAs allows for hydrolytic degradation that produces the constituent α-hydroxy acid (lactic acid or glycolic acid, respectively) which are further broken down to release CO_2 and H_2O following the Krebs's cycle. The low toxicity and the innocuous nature of the degradation products has resulted in the use of PL and its copolymers in a number of biomedical devices and pharmaceutical formulations that have been approved by the Food and Drug Administration (FDA) for use in contact with humans. These include, bone

fixation devices (Bioscrew®, Phusiline® and Sysorb®), prosthetic reinforcements (Vicryl®, Galactin910®) and drug delivery matrices (Decapeptyl®, Enantone®, Sandostatine®, Zoladex®).[5]

In addition to being biocompatible and biodegradable, PL also displays good mechanical and optical properties. In a comparison study, PL displayed tensile modulus and flexural modulus higher than polystyrene (PS), poly(ε-croplactone) PCL and Low density polyethylene (LDPE), and barrier properties to CO_2 and H_2O that are comparable to poly(ethylene terephthalate) (PET), Table 1.1.[1] However, the brittle nature, low thermal degradation temperature of PL, relatively high cost of production and lack of reactive functional groups are some of the shortcomings associated with PL.

Table 1.1. Comparison of typical biodegradable polymer properties with LDPE, PS and PET (recreated from Jamshidian et al.)[1]

	T_g (°C)	T_m (°C)	Tensile strength (MPa)	Tensile modulus (MPa)	Elongation break (%)
PLA	40-70	130-180	48-53	3500	30-240
LDPE	-100	98-115	8-20	300-500	100-1000
PCL	-60	59-64	4-28	390-470	700-1000
Starch	-	110-115	35-80	600-850	580-820
PS	70 -115	100	34-50	2300-3300	1.2-2.5
PET	73-80	245-265	48-72	200-4100	30-300

1.1.3. Preparation

Common methods to prepare PL are shown in Figure 1.1. The first of these, dating back to 1914, consists of polycondensation of lactic acid.[6] The equilibrium nature of the esterification and the need for the constant removal of the condensate (H_2O) from the polymerization to achieve high conversion places a high energy requirement on this process. Moreover, since condensation polymerization follows a step-growth mechanism, the PL obtained from this route usually has a low molecular weight (a few tens of thousands of kDa) with a broad distribution of chain lengths.

Recent advances in the design of catalysts and optimization of the polymerization process has resulted in molecular weights as high as 600 kDa, albeit with a high polydispersity.[7]

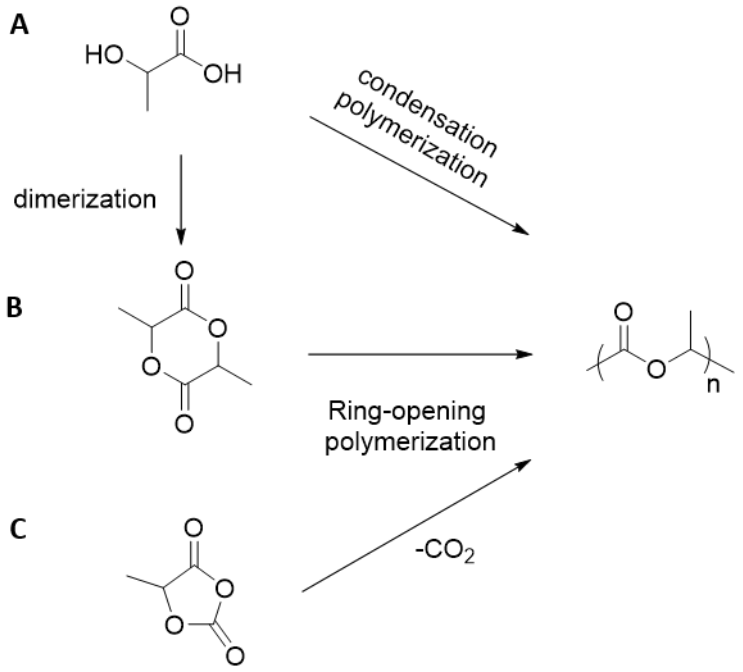

Figure 1.1. Synthesis of PLA. A, condensation polymerization of lactic acid; B, ring-opening polymerization of the cyclic dimer lactide; and C, ring-opening polymerization of lactic acid O-carboxy anhydride

A second route to synthesize PL entails ring-opening polymerization (ROP) of lactide, Figure 1.1B.[8] The processes is often initiated by addition of an alcohol, or it may be initiated by adventitious water (moisture) present in the reaction mixture. The cyclic diester undergoes polymerization following a chain-growth mechanism, resulting in the formation of relatively high molecular weight polymers with a narrow molecular weight distribution. ROP of lactide has been the subject of extensive studies that has resulted in the development of various catalysts to provide control over the molecular weight, PDI and stereochemistry of PL.[9,10,11,12,13] The industrial production of PL is typically carried out using ROP of lactide in the melt with tin(II) octoate as a catalyst. ROP of lactic acid O-carboxy anhydride (lacOCA) using tertiary amines or metal oxides as initiators is third strategy to synthesize PL, Figure 1.1C.[14] The higher ring strain associated with

lacOCA, as well as the release of CO_2 during polymerization serves, as driving forces for the polymerization of lacOCAs at a lower temperature than is typically used for the polymerization of lactic acid or the cyclic lactide.[15]

1.1.4. Chemically modified PLs

With the potential for the utilization of PL in biomedical applications, there is a growing interest in the development of analogs that are substituted with reactive functional groups. The reactive chain ends of PL have been extensively utilized to prepare diblock and triblock copolymers, as discussed elsewhere.[16,17,18] The presence of additional functional groups along the backbone of the polymer would facilitate, for example, the immobilization of biomolecules and the preparation of new branched block copolymers. Examples of copolylactides bearing reactive functional groups include examples with carboxyl,[19,20,21,22,23,24] hydroxyl[25,26,27,28,29] and amino side chains[30,31] Table 1.2. These functional repeat units have been used both to modulate the thermomechanical properties of the copolymers and to graft various units to the polymer backbone.

Although these functional analogs provide a cornucopia of potential opportunities to expand the utility of PL in biomedical applications by way of bioconjugation, the post-polymerization modification of many of these analogs is challenging because of the susceptibility of the polyester backbone to nucleophilic cleavage and the need for use of coupling agents (e.g., for activated ester-promoted esterification or amidation). Given this, there is value to the preparation of functionalized PL derivatives which may be modified using conditions under which the polyester backbone is stable. Thus, this review focuses on recent advances which include the synthesis of PL bearing alkyne and azido-substituted side chains that allow for post-polymerization

bioconjugation via Huisgen azide-alkyne cycloaddition “click” chemistry; direct functionalization of the PL backbone; and surface modification of PL.

Table 1.2. Functional co-polylactides

Poly(3-functionalized lactide(X'=CH_3)/glycolide(X'=H)-co-lactide)s

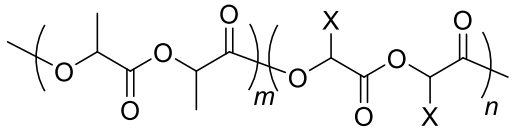

			reference
X/X'=	$(CH_2)_pOH$		
	$(CH_2)_pCOOH$		
	$CH_2OCCH_2CH_2COOH$		
	$(CH_2)_pNH_2$		
	$CH_2CH=CH_2$		
	$CH_2C\equiv CH$	poly**1**	32
	$CH_2O(CH_2)C\equiv CH$	poly**2**	33
X =	$CH_2C\equiv CH$; X' = H	poly**3**	34
X =	$CH_2C\equiv CH$; X' = CH_3	poly**4**	35
X =	$CH_2CH_2N_3$; X' = H	poly**5**	36
X =	$CH_2S(CH_2)_2(OCH_2CH_2)_2N_3$; X' = CH_3	poly**6**	37,38
X/X'=	$CH_2S(CH_2)_3N_3$	**azido-PL**	this thesis
	CH_2SH	**thiol-PL**	this thesis
	CH_2Cl	**Cl-PL**	this thesis

Poly(2-functionalized lactic acid-co-lactic acid)s

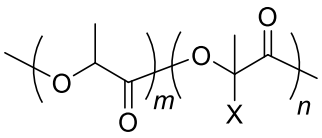

X = Br	**Br-PL**	this thesis
poly(methyl acrylate)	**PL-g-PMA**	
poly(methyl methacrylate)	**PL-g-PMMA**	
poly((oligo(ethylene glycol) methacrylate)	**PL-g-POEGMA**	

Poly(lactide-co-methylene glycolide)

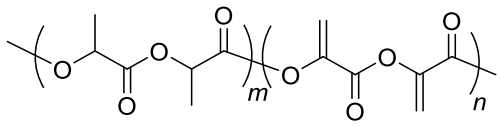

ene-PL	this thesis

1.2. POLYMER CHEMISTRY

1.2.1. Functional PL synthesized by esterification of functional lactic acid followed by ROP of the functional lactide with L-lactide

1.2.1.1. "Clickable" PL analogs

With the resurgence of copper-catalyzed azide-alkyne "click" chemistry, a variety of polymers bearing azido or alkynyl side chains have been synthesized.[39,40] These functional handles can be used to couple a variety of molecules so as to modify the properties of the polymer. This approach has gained particular attention as a method to conjugate biological molecules to polymers and as a method to prepare block copolymers.[41] The advantage of azide-alkyne click chemistry is that it affords almost quantitative addition without the formation of side products in most cases. The reaction is also tolerant of numerous other functional group.[39,40,42]

A variety of new copolymers of PL bearing azide or alkyne functional groups have been synthesized by condensation polymerization of new substituted lactic acids, ROP of new functional lactides, and by post-polymerization modification of functional polylactides. An alkyne-substituted copolylactide (poly**1**, Table 1.2) was first prepared by Baker et al. in 2008 by the ring opening copolymerization of propargyl glycolide **1** (Figure 1.2A) with L-lactide.[32] Propargyl glycolide **1** was synthesized by the acid-catalyzed esterification of 2-hydroxy-4-pentynoic acid, which was, in turn, synthesized by a Reformatsky reaction between propargyl bromide and ethyl glyoxylate followed by hydrolysis of the ester, Figure 1.3A. Baker demonstrated optimization of the azide-alkyne [3+2] cycloaddition with a variety of azides, Figure 1.4. Recently, Baker et al. also reported the synthesis of a new copolymer of PL bearing propargyloxymethyl side chains poly**2**, that was prepared by the copolymerization of substituted lactide **2** (Figure 1.2A) with L-lactide.[33] The multi-step synthesis of 2-hydroxyl-3-propargyloxypropanoic acid (Figure

1.3B) which is the precursor to the alkyne-lactide **2**, has the advantage of being high yielding (>85 %) with the intermediate at each step requiring minimal purification. Click chemistry of both of these copolymer (poly**1** and poly**2**) with PEGylated azide yields materials that display reversible thermoresponsive properties.

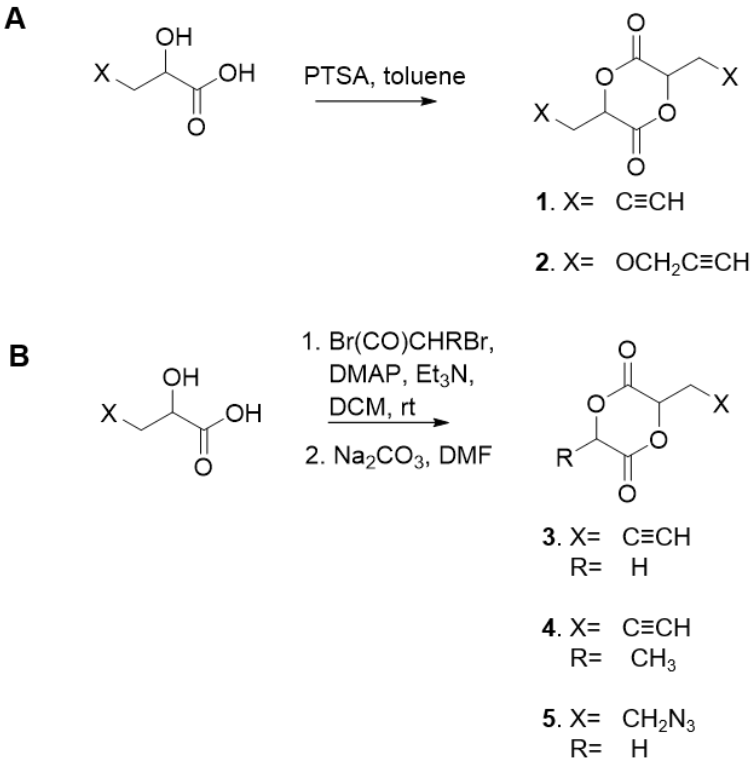

Figure 1.2. Synthesis of substituted lactides. A, cyclodimerization of modified lactic acid to afford symmetrically substituted lactides; B, treatment of modified lactic or glycolic acid with bromoacetyl bromide (R = H) or 2-bromopropionyl bromide (R = CH_3) followed by base-promoted cyclization to afford unsymmetrically substituted cyclic dimer.

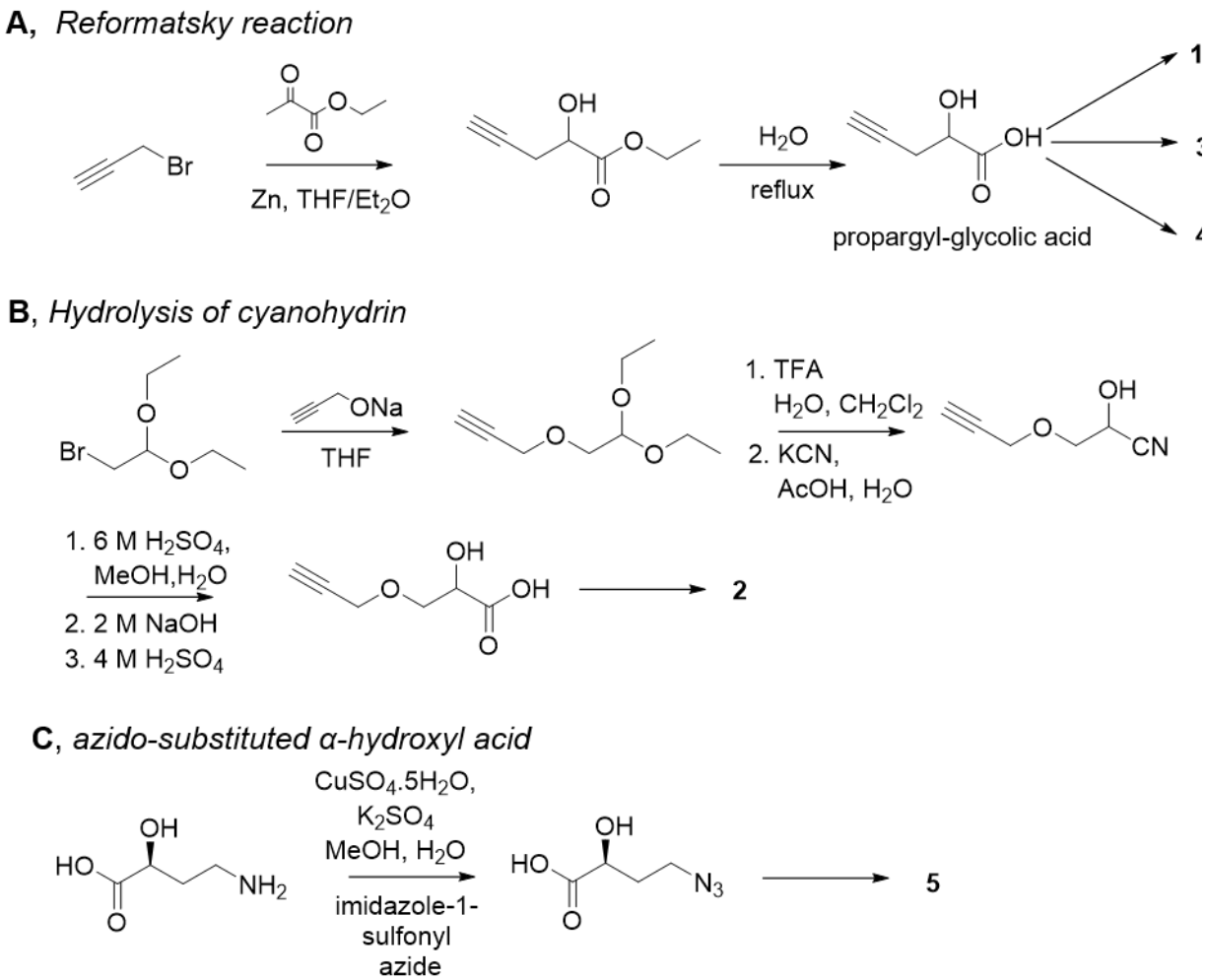

Figure 1.3. Synthesis of substituted lactic acids. A, 2-hydroxy-4-pentynoic acid; B, 2-hydroxy-3-propargyloxypropanoic acid; C, 4-azido-2-hydroxybutanoic acid.

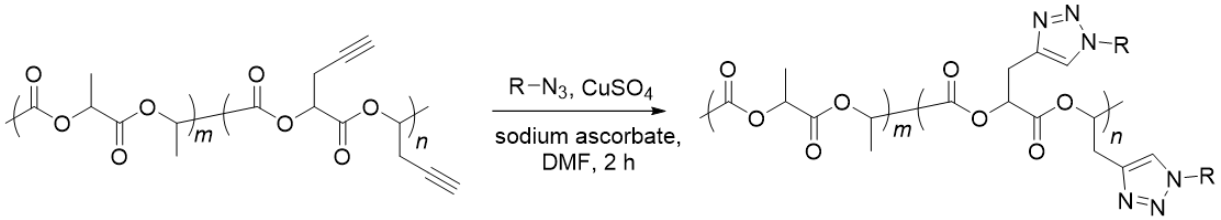

Figure 1.4. Copper-catalyzed [3+2] alkyne-azide- cycloaddition "click" chemistry of an alkyne-substituted PL analog.

Copolymers of monosubstituted propargyl glycolide **3** and monosubstitued propargyl lactide **4** (Figure 1.2B) were also prepared using ROP.[35,34] The asymmetric substitution of these analogs, along with the absence of methyl group in the asymmetric polyglycolide, poly**3**, alters the rate of degradation of these copolymers, which opens new avenues for the application of these functional copolymers. The functional monomers **3** and **4** were synthesized by esterification of 2-hydroxy-4-pentynoic acid with bromoacetyl bromide or 2-bromopropionoyl bromide, respectively, followed by based-promoted ring closure, Figure 1.2B.

Compared to the synthesis of alkyne-substituted copolylactides, synthesis of azido-substituted copolylactides appears to be more challenging. The incorporation of an azide by nucleophilic substitution of a halide with azide anion is hindered by the labile nature of the ester linkages in both the cyclic lactide and PL. Pugh et al. reported the synthesis of an azido-substituted poly(lactic acid-co-glycolic acid) (azido-PLGA) by the displacement of the bromide from the bromo-substituted-glycolide repeat units in a PLGA copolymer (Br-PLGA) with sodium azide, Figure 1.5.[43]

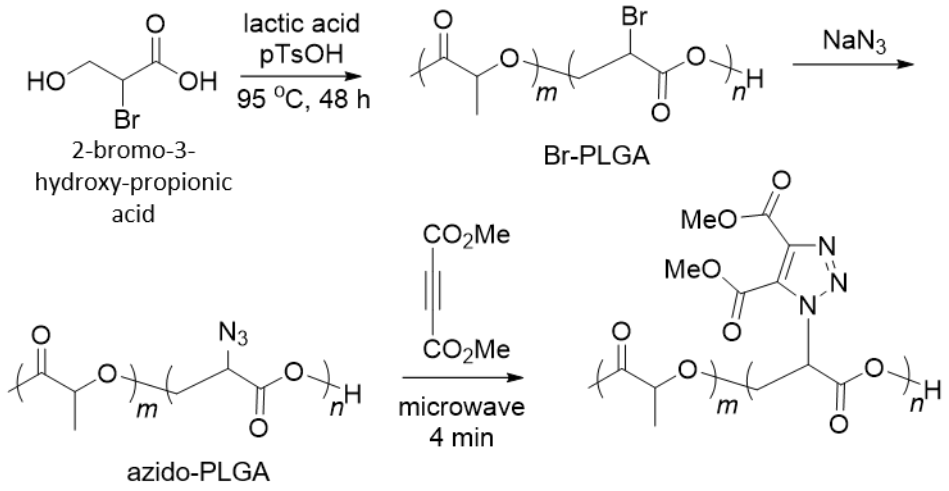

Figure 1.5. Condensation copolymerization of 2-bromoglycolic acid with lactic acid, nucleophilic displacement of bromine with azide, and azide-alkyne click chemistry.

In this case, the brominated copolymer of PL was synthesized by condensation copolymerization of 2-bromo-3-hydroxypropionic acid with lactic acid or glycolic acid. The challenges of direct substitutions with an azide nucleophile post-polymerization are evident, with their attempts yielding non-quantitative substitution of the secondary alkyl bromide substituents. The substitution reaction proceeded with concomitant cleavage of the polyester backbone with a 22% decrease in the molecular weight of the copolymer upon reaction with sodium azide. Moreover, the azido-substituted copolymer underwent degradation when exposed to conditions that are required to carry out copper-catalyzed click chemistry in the presence of basic ligands such as *N*,*N*,*N*′,*N*″,*N*″-pentamethyldiethylenetriamine (PMEDTA). Click chemistry was achieved only with an activated alkyne such as dimethyl acetylenedicarboxylate that do not require the use of basic ligands under microwave-assisted conditions. Our own attempts to achieve substitution of a bromine-substituted copolymer of PL (Br-PL), which contains a tertiary alkyl bromide, with sodium azide were also unsuccessful and resulted in the cleavage of the polyester backbone (see chapter 5). These results clearly demonstrate the challenges associated with the post-polymerization substitution of functional copolymers of PL, especially when the substituent is attached close to the polyester backbone.

In 2013, Weck reported the synthesis of an azide-substituted PL analog poly**6**, Table 1.2. This copolymer was synthesized by copolymerization of L-lactide and azide-substituted lactide,**6** (Figure 1.6) that is connected to the lactide unit via a diethyleneglycol linker.[37,38] The substituted lactide was synthesized by the radical-catalyzed addition of a thiol bearing a terminal azide to allylic lactide **7**, Figure 1.6. Allylic lactide **7** was synthesized following procedure reported by Hennik et al.[44]

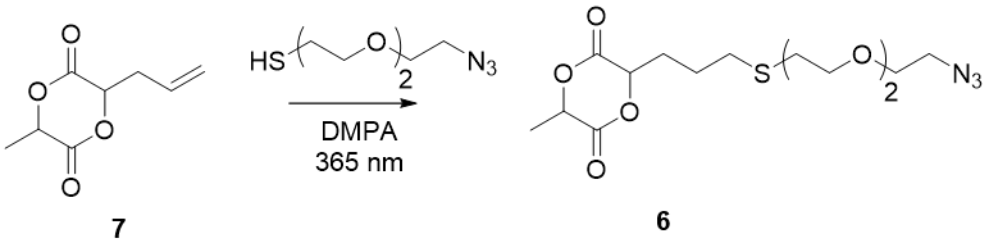

Figure 1.6. Synthesis of azido-substituted lactide by thiol-ene addition to allyl-lactide.

Since complete removal of the copper catalyst used in the azide-alkyne cycloaddition reaction is cumbersome, Weck explored the Staudinger ligation by the treatment of the copolymer with a variety of triarylphosphine-containing molecules including a Gly-Arg-Gly-Asp-Ser substituted phosphine, Figure 1.7. This chemistry, which does not require the use of copper, expands the utility of PL copolymers bearing an azide functional group for applications in which even trace amounts of copper is detrimental.

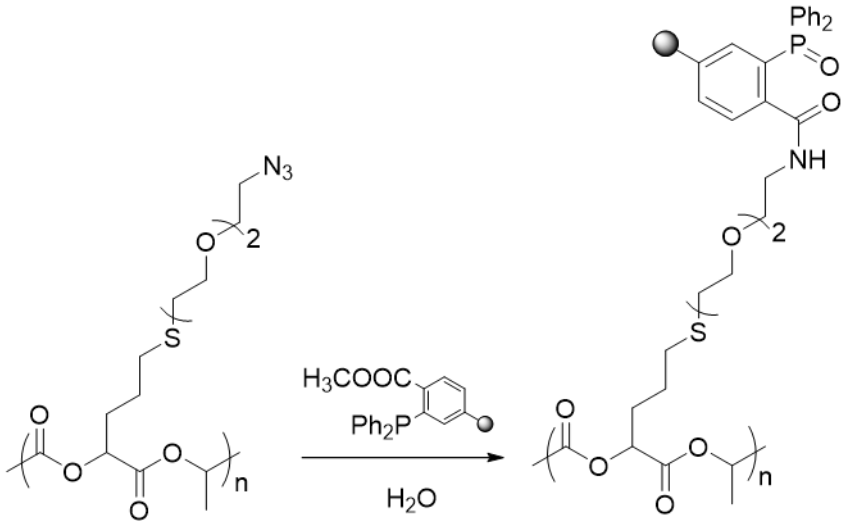

Figure 1.7. Staudinger ligation: addition of Phosphine−GRGDS to an azide-substituted PL.

In 2017, Almutairi reported azido-substituted glycolide **5** (Figure 1.2B and Figure 1.3C) that can be synthesized in just two steps from a commercially available starting materials.[36] The first step involves the conversion of 4-amino-2-hydroxybutanoic acid to the azido-substituted α-hydroxy analog, Figure 1.3C. Treatment of the hydroxyl acid with bromoacetyl bromide followed

by ring closure in the presence of a base affords the azido-glycolide **5**, Figure 1.2B. ROP of substituted glycolide affords azido-PG. This work successfully demonstrates the stability of azide functional group to withstand the conditions necessary to carry out ROP, the lack of need for a linker chain longer than an ethylene bridge connecting the azide to lactide, and avoids post-polymerization reaction to install the azido group. Using copper-free azide-alkyne cycloaddition of strained alkyne bearing folate on the azido-PG nanoparticles Almutairi displayed improved biological interaction of the nanoparticles with a potential application for targeted drug delivery.

1.2.2. Functional PL synthesized by direct modification of L-lactide followed by copolymerization

1.2.2.1. Bromo-lactide

Direct modification of the cyclic lactide dimer without concomitant ring-opening is challenging. Scheibelhoffer et al. demonstrated the synthesis of a bromo-substituted lactide **8** (Figure 1.8) by treatment of L-lactide with *N*-bromosuccinimide (NBS) and benzoylperoxide (BPO). Dubois at al. used this bromolactide as an initiator to carry out atom-transfer radical polymerization (ATRP) of methyl methacrylate to afford lactide-terminated PMMA macromer **12**, Figure 1.8.[45] Their work demonstrates the mild nature of ATRP, which proceeds without ring-opening of lactide. Copolymerization of the lactide-terminated PMMA macromer **12** with L-lactide in the presence of an *N*-heterocyclic carbene, 1,3-dimesitylimidazol-2-ylidene, which act as a transesterification agent, affords a macrocyclic polyester poly**12** with a narrow PDI, that adopts jellyfish macromolecular assembly, Figure 1.8.

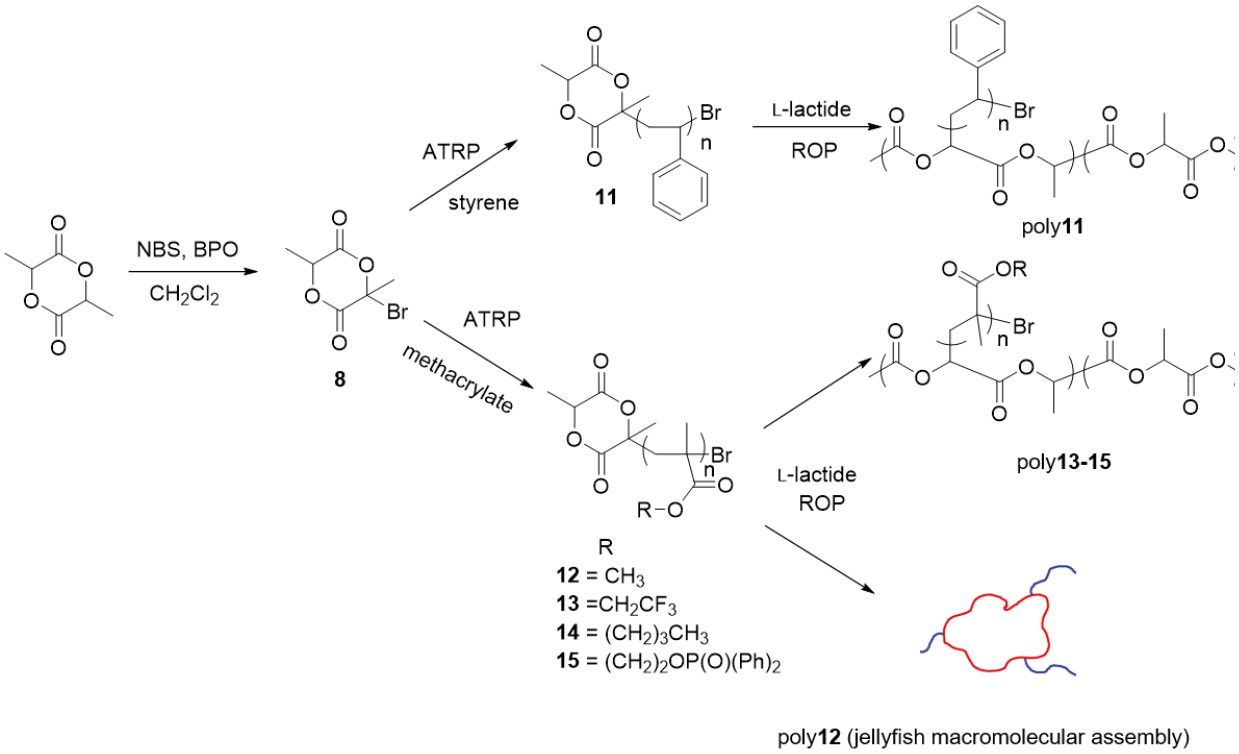

Figure 1.8. Radical-catalyzed bromination of lactide, atom-transfer radical polymerization (ATRP) using bromolactide as an initiator, and ring-opening copolymerization of lactide macromer with L-lactide.

Bromolactide **8** has also been used as an initiator to carry out ATRP of styrene, 1-butyl methacrylate, trifluoroethyl methacrylate, and diphenyl(methacryloyloxyethyl)phosphinate using CuBr-PMDETA as catalyst system, Figure 1.8.[46,47,48,49] ROP of the resulting lactide-terminated macroinitiator (**11**, **13-15**, Figure 1.8) with L-lactide in presence of tin(II) octoate as a catalyst and benzyl alcohol as an initiator affords graft copolymers consisting of a PL backbone bearing polymeric side chains. In a series of patents, the copolymer (poly**15**) bearing poly(diphenyl(methacryloyloxyethyl)phosphinate) is claimed to impart flame retardancy to PL, the copolymer (poly**14**) with poly(1-butyl methacrylate) side chains is claimed to toughen PL, and poly(trifluoroethyl methacrylate) copolymer (poly**13**) is claimed to lower the moisture vapor transmission rate of PL.

1.2.2.2. Methylene lactide

Bromolactide **8** undergoes dehydrobromination to afford methylene lactide **9**, Figure 1.9, which has been subjected to free radical polymerization by initiation with AIBN to afford poly(methylene lactide), Figure 1.9.[50] The dipolar interactions between the neighboring lactide units confers different reactivity to the two esters of a lactide and renders these esters highly active. Recently, the Ritter group demonstrated the capacity of methylene lactide to undergo reversible addition-fragmentation chain transfer (RAFT) polymerization which provides for a greater level of control over polydispersity.[51] While neither methylene lactide **9** nor poly(methylene lactide) have been copolymerized with L-lactide, they provide potential opportunities in the design of new materials along with inspiration for some of our recent work on related structures (Chapter 2).

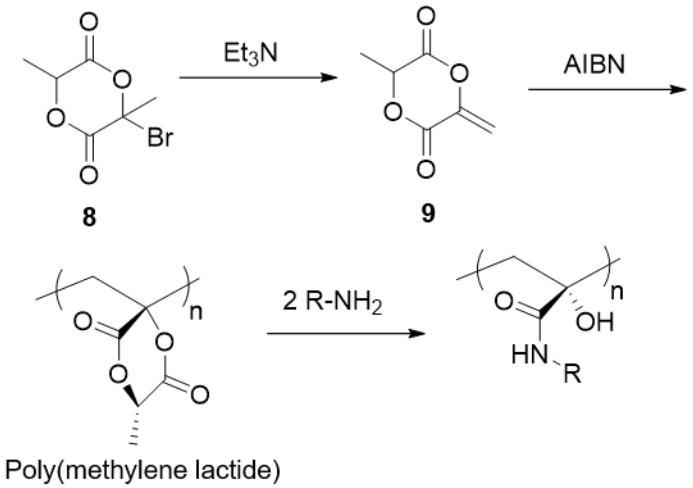

Figure 1.9. Dehydrobromination of bromo-lactide, free radical polymerization and aminolysis.

1.2.2.3. Norbornene-lactide

The captodative alkene of methylene lactide undergoes Diels-Alder reaction with cyclopentadiene to afford a lactide with a spiro-fused norbornene ring **10**, as demonstrated by Hillmyer et al.[52] Figure 1.10A. ROP of norbornene-substituted lactide affords a PL analog, poly**10** Figure 1.10A, that has a glass transition temperature (T_g) of 113 °C, which is the highest reported

T_g for a modified PL bearing non-polymeric side chains. The increase in the T_g is a result of the rigidity induced in the polyester backbone on account of the presence of the norbornene ring. Ring-opening metathesis polymerization (ROMP) of lactide-fused norbornene **10** with 1,5-cyclooctadiene affords a lactide-substituted polyoctadiene **16**, Figure 1.10. ROP of **16** with L-lactide affords a PL-polyoctadiene graft copolymer poly**16**, Figure 1.10. The polymers (poly**10** and poly**16**) display improved physical properties compared to PL and serve as a compatibilizer for a blend of PL and polybutadiene.

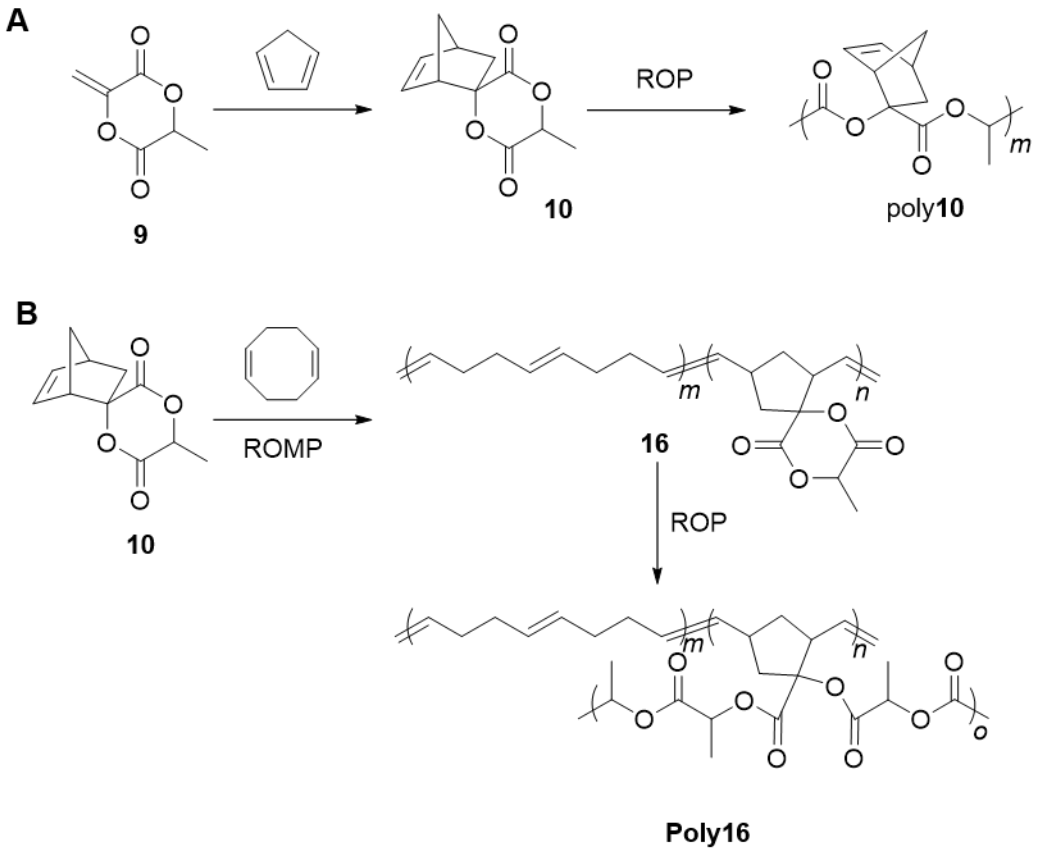

Figure 1.10. A, Diels-Alder reaction of enne-PL and ring-opening polymerization; B, ring-opening metathesis copolymerization of **10** and 1,4-cyclooctadiene followed by ring-opening copolymerization with lactide.

1.2.3. Direct modification of PL

Some of the challenges associated with the preparation of functional PL outlined above include the need for multi-step syntheses and purification of the functional comonomers, or analogs in which the lactide is substituted with a precursor to the desired functional group, along with the requirement to perform post-polymerization modifications to install the functional group (often by deprotection of the precursor). These severely limit the potential for commercialization of these materials. However, the lack of modifiable functional groups, along with the susceptibility of PL backbone toward hydrolysis, pose significant challenges to performing direct chemical modification of PL.

One approach to directly modify the polyester backbone proceeds by deprotonation of the methine of PL by treatment with lithium diisopropylamide (LDA) followed by reaction with an electrophile, Figure 1.11.[5] Coudane demonstrated the tritiation of PL using this approach, along with modification of PL with napthoyl chloride, to afford poly**17** and poly**18** respectively, Figure 1.11. While these approaches led to substitution of just 0.25 % of the repeat units, the authors also noted extensive cleavage of the polyester backbone.

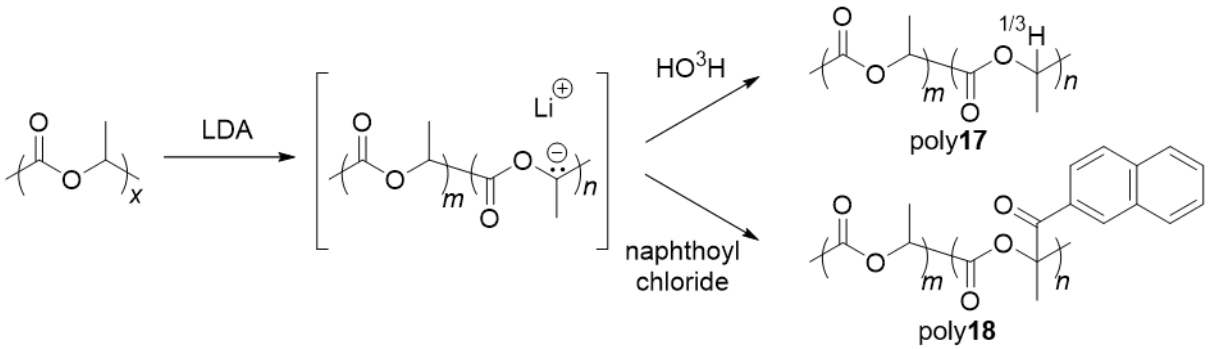

Figure 1.11. Base-promoted modification of PL backbone.

PL also undergoes free radical grafting upon reactive extrusion with maleic anhydride and glycidyl methacrylate to afford graft copolymers.[53] These have been prepared to improve the

compatibilization of PL/starch blends.[54,55] However, this method is generally conducted to incorporate only low grafting densities. Chain scission and cross-linking of the intermediate macroradicals present additional challenges to the general applicability of approach.

1.2.4 Modification of a PL surface

The ability to conjugate biomolecules to the surface of a medical device to impart resistance to biofouling, or to elicit specific biological responses, offers tremendous potential benefits. The selective modification of the surface of a fabricated device, without altering the bulk material that provides the structural integrity, would provide new opportunities to tailor interactions with the host. Functionalization of the surface of PL has been achieved by the treatment of polymeric objects with the reagents in solution and by UV and photo-initiated grafting of polymers.

Intentional mild hydrolysis of the PL surface provides hydroxyl and carboxylic acid end groups that can be subjected to coupling reactions.[56] Alternatively, aminolysis with 1,6-hexanediamine provides amines on the surface. For example, Yang carried out aminolysis of a PL film using 1,6-hexanediamine and treated the resulting film with bromoisobutyryl bromide to provide an immobilized initiator for ATRP on the surface, Figure 1.12.[57] ATRP of sodium methacrylate (MAAS) provided an acid-decorated polymer brush to which various biomolecules may be coupled. For example, immobilization of gelatin using this approach provides films with improved cell adhesion. Copper-White carried out coupling of chitosan to carboxylic acid and amine-decorated surfaces of PLGA films,[56] and Bertóti reported PEGylation of PLGA surfaces by the treatment of the aminolysed surfaces with a PEG bearing a succinimide active ester at the terminus.[58] They demonstrated that the PEG-substituted surfaces are significantly more hydrophilic than PLGA and that the modified films display a lower propensity to adsorb proteins.

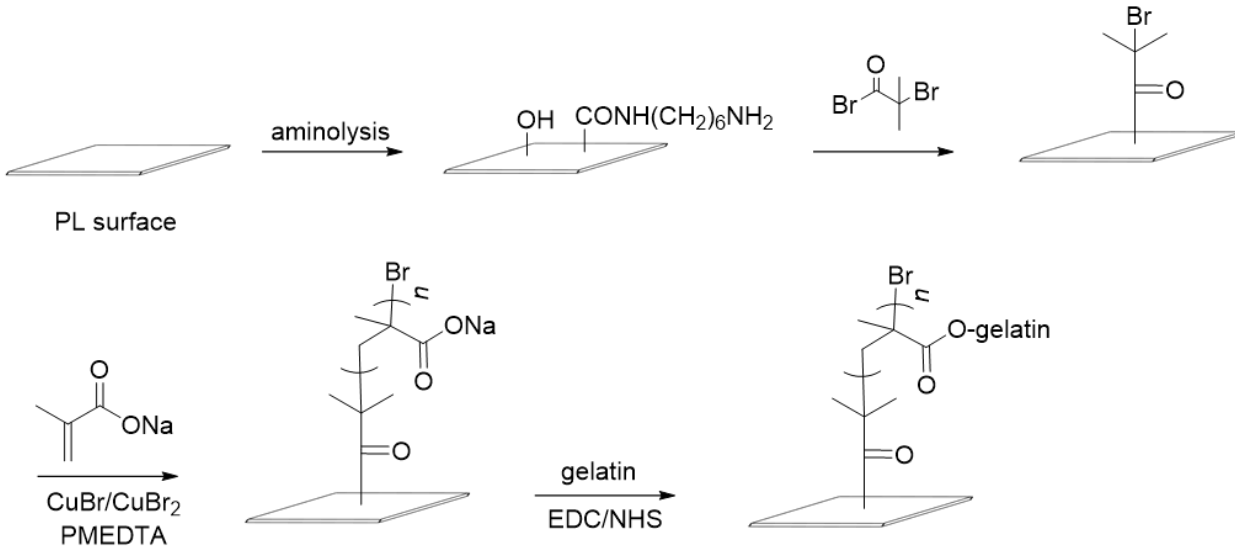

Figure 1.12. Surface modification of PL. Aminolysis, immobilization of surface initiator, atom-transfer radical polymerization of sodium methacrylate and coupling of gelatin.

Photo-induced grafting polymerization provides a relatively non-destructive route for the modification of PL surfaces. The process involves generation of a macroradical by the abstraction of the hydrogen atom from the methine of PL at the surface in the presence of a photoinitiator. The macroradical initiates polymerization of a vinyl monomer, Figure 1.13. For example, Albertsson demonstrates grafting of poly(acrylic acid)) on the surface of PL films by photoinitiation in presence of benzoquinone, Figure 1.13A.[59] The acid provides electrophilic sites that allow the coupling of nucleophilic species. In a similar fashion, Gaona-Lozano et al. carried out photoinitiated grafting of *N*-vinylpyrrolidone (NVP) on PL films, Figure 1.13B.[60] Upon complexation of polyvinylpyrrolidone with iodine the surface is rendered antimicrobial. Photoinitiated grafting has also been employed to achieve covalent grafting of polymers from the surface of PL particles. Albertson demonstrates grafting of poly(acrylamide), poly(acrylic acid) and poly(maleic anhydride) on PL particles.[61] The particles retained their spherical shape after grafting, which demonstrates the non-destructive nature of photinitiated grafting process. Grafting of polymers on PL particles improved the surface hydrophilicity of PL and provided reactive

functional groups to carry out further modification. This study provides a precedence for future modification of PL particles to improve its utility as a drug delivery vehicle.

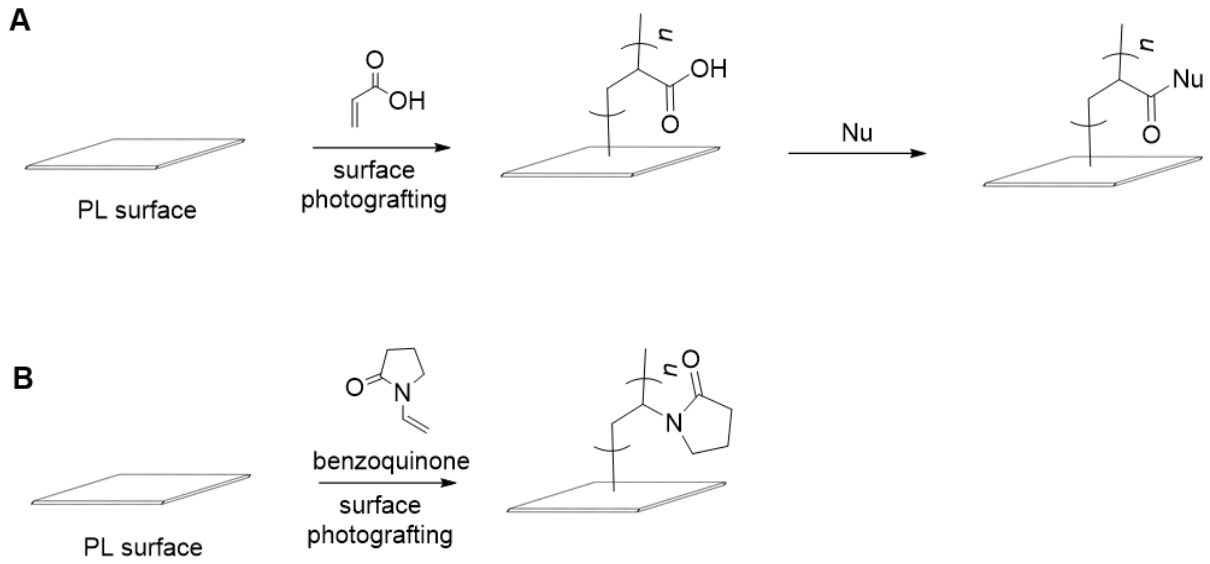

Figure 1.13. Non-destructive photoinitiated modification of PL. A, photoinitiated grafting of acrylic acid followed by coupling; B, photoinitiated grafting of *N*-vinylpyrolidone.

Coudane et al extended their work on the treatment of PL with LDA in solution to propargylate the surface of PL, Figure 1.14. By carrying out the procedure at -50 to -30 °C for a short time, they demonstrated incorporation of alkyne functionality without polyester cleavage.[62,63,64] Such an alkyne-substituted PL object could be used to carry out azide-alkyne click chemistry or photochemical thiol-yne click chemistry to couple a variety of molecules to the surface. Grafting a quaternary ammonium methacrylate polymer (M_n = 6.5 kg/mol) bearing a terminal azide to the alkyne substituted PL object rendered the object antimicrobial.

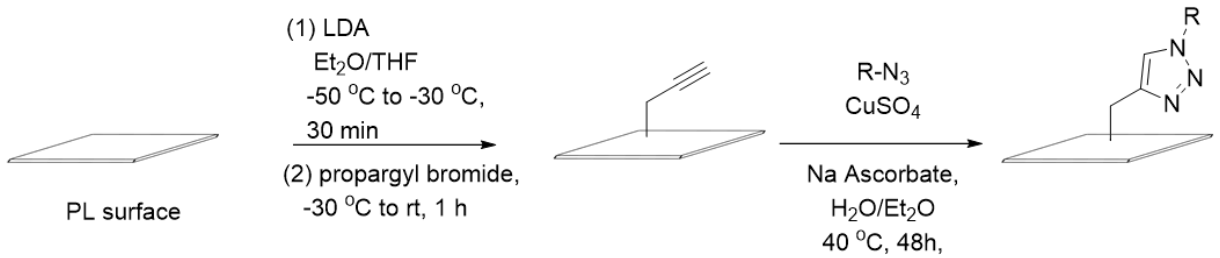

Figure 1.14. Chemical modification of PL surface. Base mediated propargylation of PL followed by alkyne-azide click chemistry.

1.3. SCOPE OF THIS THESIS

Although a variety of functional copolymers of PL have been synthesized, there is a significant level of interest in (1) the design new analogs of PL that can be used in bioconjugation, especially using of click chemistries such as thiol-ene, 1,4-conjugate additions and cycloaddition reactions, (2) the development of additional routes to azido-substituted PL copolymers, and (3) the potential to perform direct functionalization of PL, both in solution and at surfaces. In this thesis, I describe the synthesis of five different copolymers of PL bearing reactive functional groups. I demonstrate the utility of these materials to manipulate cell adhesion and render PL antimicrobial, and to design drug delivery vehicles.

In Chapter 2, I describe the synthesis of an α,β-unsaturated ester analog of PL (ene-PL) by dehydrochlorination of chloro-PL (Table 1.2) and explore its capacity to undergo addition reactions with a variety of thiols, Figure 1.15. The demonstration of coupling of thiols on ene-PL serves as a proof-of-concept for the bioconjugation of a variety of cysteine containing peptides on ene-PL.

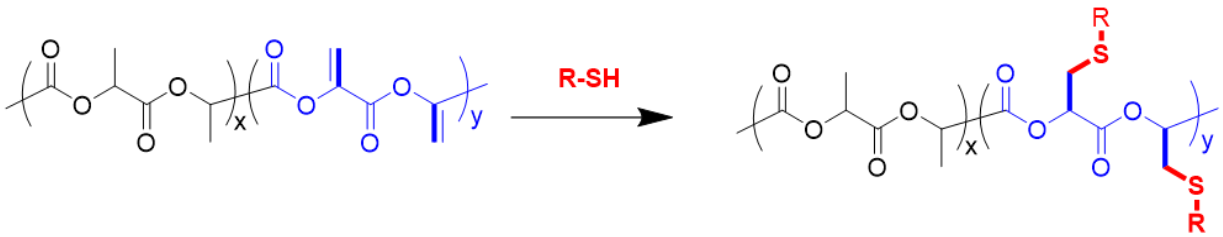

Figure 1.15. Thiol addition to α,β-unsaturated ester analog of PL, Chapter 2.

In Chapter 3, I describe the synthesis of a thiol-substituted copolymer of PL and explore its reactivity towards electron deficient alkenes, Figure 1.16. The thiol polymer is prepared by debenzylation of a 4-methoxybenzylthio-substituted PL which in turn may be prepared either from ene-PL or by ring opening copolymerization of a new substituted lactide with L-lactide. Between

ene-PL (chapter 2) and thiol-PL (chapter 3), I present two copolymers of PL that have the ability to quantitatively couple a variety of nucleophiles and electrophiles, respectively.

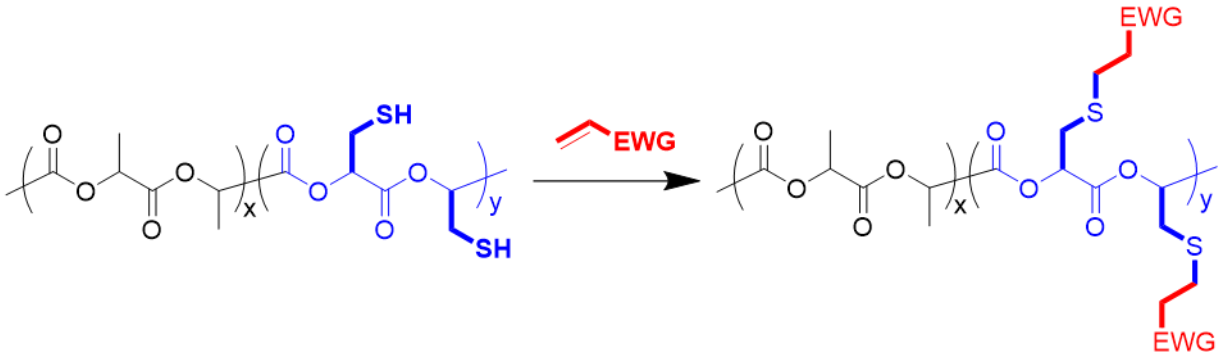

Figure 1.16. Addition of thiol-substituted PL to electron-deficient alkenes, Chapter 3.

In Chapter 4, I describe the synthesis of an azido-substituted copolymer of PL by the addition of 3-azido-1-propanethiol to ene-PL and demonstrate its ability to undergo azide-alkyne click chemistry, Figure 1.17. Using this strategy, I designed a new antimicrobial PL by coupling a quaternary ammonium-substituted alkyne. The alkyne coupled PL adduct displays antimicrobial activity against gram negative bacteria both in solution and as a film.

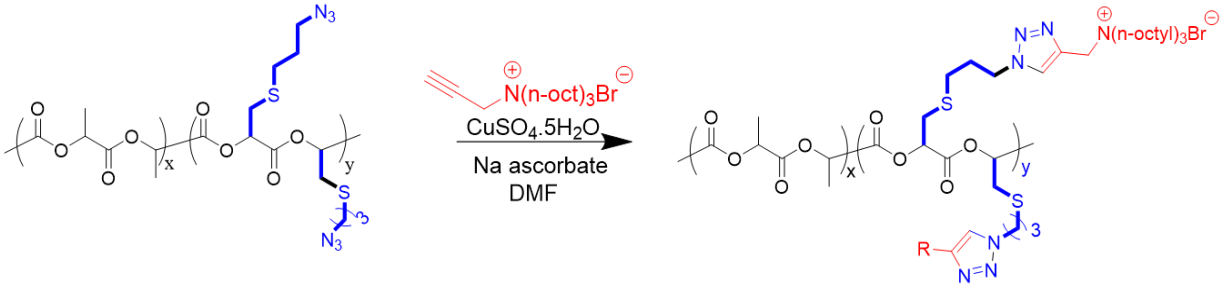

Figure 1.17. Azide-alkyne click chemistry of a new azido-substituted PL to afford antimicrobial plastic, Chapter 4.

In Chapter 5, I demonstrate a route to carry out radical bromination of PL in solution by reaction with NBS and BPO. The brominated PL analog (Br-PL) serves as a multisite macroinitiator to carry out atom-transfer radical polymerization (ATRP), Figure 1.18. I formulate

nanoparticles from the graft copolymer of PL and poly(ethylene glycol) methacrylate and study its capacity to encapsulate and release a variety of dye molecules.

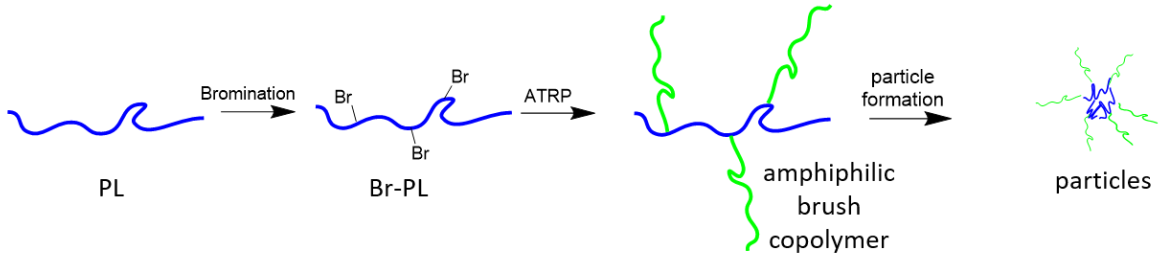

Figure 1.18. Radical bromination of PL, atom-transfer radical polymerization, and particle formation, Chapter 5.

Finally, in Chapter 6, I describe the bromination of the surfaces of thin films of PL followed by surface-initiated ATRP of a quaternary ammonium methacrylate and a zwitterion methacrylate to grow polymeric brushes, Figure 1.19. The growth of these brushes renders the surfaces antibacterial and bacterial resistant.

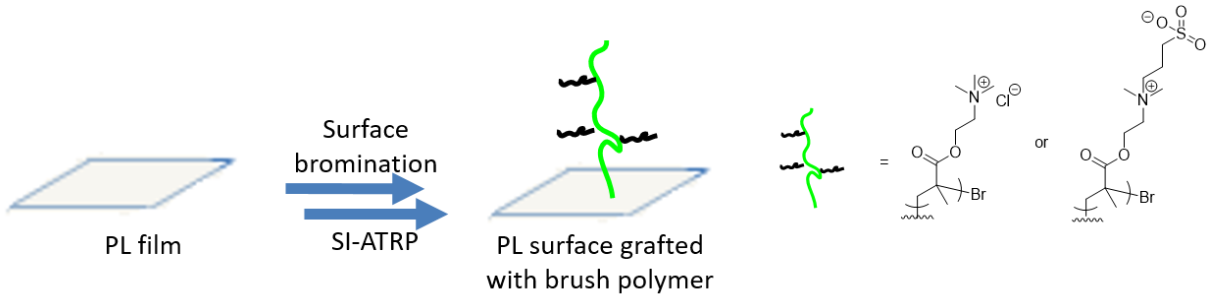

Figure 1.19. Surface bromination and SI-ATRP to provide antimicrobial films, Chapter 6.

1.4. REFERENCES

1. Jamshidian, M.; Tehrany, E. A.; Imran, M.; Jacquot, M.; Desobry, S., Poly-Lactic Acid: Production, Applications, Nanocomposites, and Release Studies. *Comprehensive Reviews in Food Science and Food Safety* **2010,** *9* (5), 552-571.
2. Lasprilla, A. J. R.; Martinez, G. A. R.; Lunelli, B. H.; Jardini, A. L.; Filho, R. M., Poly-lactic acid synthesis for application in biomedical devices — A review. *Biotechnol. Adv.* **2012,** *30* (1), 321-328.
3. Jiao, Y.-H.; Li, Y.; Wang, S.; Zhang, K.; Jia, Y.-G.; Fu, Y., Layer-by-Layer Assembly of Poly(lactic acid) Nanoparticles: A Facile Way to Fabricate Films for Model Drug Delivery. *Langmuir* **2010,** *26* (11), 8270-8273.
4. Ren, K.; Zhang, M.; He, J.; Wu, Y.; Ni, P., Preparation of Polymeric Prodrug Paclitaxel-Poly(lactic acid)-b-Polyisobutylene and Its Application in Coatings of a Drug Eluting Stent. *ACS Appl. Mater. Interfaces* **2015,** *7* (21), 11263-71.
5. Ponsart, S.; Coudane, J.; Morgat, J. L.; Vert, M., Synthesis of 3H and fluorescence-labelled poly (DL-Lactic acid). *J. Labelled Compd. Radiopharm.* **2001,** *44* (10), 677-687.
6. Tsuji, H., Poly(l-Lactide). In *Encyclopedia of Polymeric Nanomaterials*, Kobayashi, S.; Müllen, K., Eds. Springer Berlin Heidelberg: Berlin, Heidelberg, 2014; pp 1-12.
7. Moon, S.-I.; Taniguchi, I.; Miyamoto, M.; Kimura, Y.; Lee, C.-W., Synthesis and Properties of High-Molecular-Weight Poly(L-Lactic Acid) by Melt/Solid Polycondensation under Different Reaction Conditions. *High Perform. Polym.* **2001,** *13* (2), S189-S196.
8. Dechy-Cabaret, O.; Martin-Vaca, B.; Bourissou, D., Controlled Ring-Opening Polymerization of Lactide and Glycolide. *Chem. Rev.* **2004,** *104* (12), 6147-6176.
9. Feng, Q.; Zhong, Y.; Xie, L.; Tong, R., Recent Advances in Ring-Opening Polymerization of O-Carboxyanhydrides. *Synlett* **2017,** *28* (15), 1857-1866.
10. Csihony, S.; Culkin, D. A.; Sentman, A. C.; Dove, A. P.; Waymouth, R. M.; Hedrick, J. L., Single-Component Catalyst/Initiators for the Organocatalytic Ring-Opening Polymerization of Lactide. *J. Am. Chem. Soc.* **2005,** *127* (25), 9079-9084.
11. Kamber, N. E.; Jeong, W.; Waymouth, R. M.; Pratt, R. C.; Lohmeijer, B. G. G.; Hedrick, J. L., Organocatalytic Ring-Opening Polymerization. *Chem. Rev.* **2007,** *107* (12), 5813-5840.
12. Coady, D. J.; Fukushima, K.; Horn, H. W.; Rice, J. E.; Hedrick, J. L., Catalytic insights into acid/base conjugates: highly selective bifunctional catalysts for the ring-opening polymerization of lactide. *Chem. Commun.* **2011,** *47* (11), 3105-3107.
13. Kiesewetter, M. K.; Shin, E. J.; Hedrick, J. L.; Waymouth, R. M., Organocatalysis: Opportunities and Challenges for Polymer Synthesis. *Macromolecules* **2010,** *43* (5), 2093-2107.
14. Zhuang, X.-l.; Yu, H.-y.; Tang, Z.-h.; Oyaizu, K.; Nishide, H.; Chen, X.-s., Polymerization of lactic O-carboxylic anhydride using organometallic catalysts. *Chin. J. Polym. Sci.* **2011,** *29* (2), 197-202.

15. Thillaye du Boullay, O.; Marchal, E.; Martin-Vaca, B.; Cossío, F. P.; Bourissou, D., An Activated Equivalent of Lactide toward Organocatalytic Ring-Opening Polymerization. *J. Am. Chem. Soc.* **2006,** *128* (51), 16442-16443.

16. Saffer, E. M.; Tew, G. N.; Bhatia, S. R., Poly(lactic acid)-poly(ethylene oxide) block copolymers: new directions in self-assembly and biomedical applications. *Curr. Med. Chem.* **2011,** *18* (36), 5676-86.

17. Xiao, R. Z.; Zeng, Z. W.; Zhou, G. L.; Wang, J. J.; Li, F. Z.; Wang, A. M., Recent advances in PEG–PLA block copolymer nanoparticles. *International Journal of Nanomedicine* **2010,** *5*, 1057-1065.

18. Aluthge, D. C.; Xu, C.; Othman, N.; Noroozi, N.; Hatzikiriakos, S. G.; Mehrkhodavandi, P., PLA–PHB–PLA Triblock Copolymers: Synthesis by Sequential Addition and Investigation of Mechanical and Rheological Properties. *Macromolecules* **2013,** *46* (10), 3965-3974.

19. Kimura, Y.; Shirotani, K.; Yamane, H.; Kitao, T., Ring-opening polymerization of 3(S)-[(benzyloxycarbonyl)methyl]-1,4-dioxane-2,5-dione: a new route to a poly(.alpha.-hydroxy acid) with pendant carboxyl groups. *Macromolecules* **1988,** *21* (11), 3338-3340.

20. du Boullay, O. T.; Saffon, N.; Diehl, J.-P.; Martin-Vaca, B.; Bourissou, D., Organo-Catalyzed Ring Opening Polymerization of a 1,4-Dioxane-2,5-dione Deriving from Glutamic Acid. *Biomacromolecules* **2010,** *11* (8), 1921-1929.

21. Ouchi, T.; Fujino, A., Synthesis of poly(α-malic acid) and its hydrolysis behavior in vitro. *Die Makromolekulare Chemie* **1989,** *190* (7), 1523-1530.

22. Pounder, R. J.; Dove, A. P., Synthesis and Organocatalytic Ring-Opening Polymerization of Cyclic Esters Derived from l-Malic Acid. *Biomacromolecules* **2010,** *11* (8), 1930-1939.

23. Pounder, R. J.; Fox, D. J.; Barker, I. A.; Bennison, M. J.; Dove, A. P., Ring-opening polymerization of an O-carboxyanhydride monomer derived from l-malic acid. *Polym. Chem.* **2011,** *2* (10), 2204-2212.

24. Kolitz, M.; Cohen-Arazi, N.; Hagag, I.; Katzhendler, J.; Domb, A. J., Biodegradable Polyesters Derived from Amino Acids. *Macromolecules* **2009,** *42* (13), 4520-4530.

25. Samadi, N.; van Nostrum, C. F.; Vermonden, T.; Amidi, M.; Hennink, W. E., Mechanistic Studies on the Degradation and Protein Release Characteristics of Poly(lactic-co-glycolic-co-hydroxymethylglycolic acid) Nanospheres. *Biomacromolecules* **2013,** *14* (4), 1044-1053.

26. Leemhuis, M.; van Nostrum, C. F.; Kruijtzer, J. A. W.; Zhong, Z. Y.; ten Breteler, M. R.; Dijkstra, P. J.; Feijen, J.; Hennink, W. E., Functionalized Poly(α-hydroxy acid)s via Ring-Opening Polymerization: Toward Hydrophilic Polyesters with Pendant Hydroxyl Groups. *Macromolecules* **2006,** *39* (10), 3500-3508.

27. Stayshich, R. M.; Weiss, R. M.; Li, J.; Meyer, T. Y., Periodic Incorporation of Pendant Hydroxyl Groups in Repeating Sequence PLGA Copolymers. *Macromol. Rapid Commun.* **2011,** *32* (2), 220-225.

28. Saulnier, B.; Ponsart, S.; Coudane, J.; Garreau, H.; Vert, M., Lactic acid-based functionalized polymers via copolymerization and chemical modification. *Macromol. Biosci.* **2004,** *4* (3), 232-7.

29. Noga, D. E.; Petrie, T. A.; Kumar, A.; Weck, M.; García, A. J.; Collard, D. M., Synthesis and Modification of Functional Poly(lactide) Copolymers: Toward Biofunctional Materials. *Biomacromolecules* **2008,** *9* (7), 2056-2062.

30. Gerhardt, W. W.; Noga, D. E.; Hardcastle, K. I.; García, A. J.; Collard, D. M.; Weck, M., Functional Lactide Monomers: Methodology and Polymerization. *Biomacromolecules* **2006,** *7* (6), 1735-1742.

31. Lim, Y.-b.; Kim, C.-h.; Kim, K.; Kim, S. W.; Park, J.-s., Development of a Safe Gene Delivery System Using Biodegradable Polymer, Poly[α-(4-aminobutyl)-l-glycolic acid]. *J. Am. Chem. Soc.* **2000,** *122* (27), 6524-6525.

32. Jiang, X.; Vogel, E. B.; Smith, M. R.; Baker, G. L., "Clickable" Polyglycolides: Tunable Synthons for Thermoresponsive, Degradable Polymers. *Macromolecules* **2008,** *41* (6), 1937-1944.

33. Zhang, Q.; Ren, H.; Baker, G. L., Synthesis and click chemistry of a new class of biodegradable polylactide towards tunable thermo-responsive biomaterials. *Polym. Chem.* **2015,** *6* (8), 1275-1285.

34. Coumes, F.; Darcos, V.; Domurado, D.; Li, S.; Coudane, J., Synthesis and ring-opening polymerisation of a new alkyne-functionalised glycolide towards biocompatible amphiphilic graft copolymers. *Polym. Chem.* **2013,** *4* (13), 3705-3713.

35. Yu, Y.; Zou, J.; Yu, L.; Ji, W.; Li, Y.; Law, W.-C.; Cheng, C., Functional Polylactide-g-Paclitaxel–Poly(ethylene glycol) by Azide–Alkyne Click Chemistry. *Macromolecules* **2011,** *44* (12), 4793-4800.

36. Olejniczak, J.; Collet, G.; Nguyen Huu, V. A.; Chan, M.; Lee, S.; Almutairi, A., Biorthogonal click chemistry on poly(lactic-co-glycolic acid)-polymeric particles. *Biomaterials Science* **2017,** *5* (2), 211-215.

37. Borchmann, D. E.; ten Brummelhuis, N.; Weck, M., GRGDS-Functionalized Poly(lactide)-graft-poly(ethylene glycol) Copolymers: Combining Thiol–Ene Chemistry with Staudinger Ligation. *Macromolecules* **2013,** *46* (11), 4426-4431.

38. Borchmann, D. E.; Tarallo, R.; Avendano, S.; Falanga, A.; Carberry, T. P.; Galdiero, S.; Weck, M., Membranotropic Peptide-Functionalized Poly(lactide)-graft-poly(ethylene glycol) Brush Copolymers for Intracellular Delivery. *Macromolecules* **2015,** *48* (4), 942-949.

39. Meldal, M.; Tornøe, C. W., Cu-Catalyzed Azide−Alkyne Cycloaddition. *Chem. Rev.* **2008,** *108* (8), 2952-3015.

40. Kolb, H. C.; Finn, M. G.; Sharpless, K. B., Click Chemistry: Diverse Chemical Function from a Few Good Reactions. *Angew. Chem. Int. Ed. Engl.* **2001,** *40* (11), 2004-2021.

41. Binder, W. H.; Sachsenhofer, R., 'Click' Chemistry in Polymer and Material Science: An Update. *Macromol. Rapid Commun.* **2008,** *29* (12-13), 952-981.

42. Nwe, K.; Brechbiel, M. W., Growing Applications of "Click Chemistry" for Bioconjugation in Contemporary Biomedical Research. *Cancer Biother. Radiopharm.* **2009,** *24* (3), 289-302.

43. Wright, C.; Banerjee, A.; Yan, X.; Storms-Miller, W. K.; Pugh, C., Synthesis of Functionalized Poly(lactic acid) Using 2-Bromo-3-hydroxypropionic Acid. *Macromolecules* **2016,** *49* (6), 2028-2038.

44. Leemhuis, M.; Akeroyd, N.; Kruijtzer, J. A. W.; van Nostrum, C. F.; Hennink, W. E., Synthesis and characterization of allyl functionalized poly(α-hydroxy)acids and their further dihydroxylation and epoxidation. *Eur. Polym. J.* **2008,** *44* (2), 308-317.

45. Coulembier, O.; Moins, S.; De Winter, J.; Gerbaux, P.; Leclère, P.; Lazzaroni, R.; Dubois, P., From Jellyfish Macromolecular Architectures to Nanodoughnut Self-Assembly. *Macromolecules* **2010,** *43* (1), 575-579.

46. Boday, D. J.; Mauldin, T. C., Polylactic acid (PLA) with low moisture vapor transmission rates by grafting through of hydrophobic polymers directly to PLA backbone. US9725548B2, 2017.

47. Boday, D. J.; Mauldin, T. C., Toughened polylactic acid (PLA) by grafting through of impact-modifying polymers directly to PLA backbone. US9193818B1, 2015.

48. Boday, D. J.; Mauldin, T. C., Versatile, facile and scalable route to polylactic acid-backbone graft and bottlebrush copolymers. US9228050B2, 2016.

49. Boday, D. J.; Mauldin, T. C., Flame-retardant polylactic acid (PLA) by grafting through of phosphorus-containing polymers directly to PLA backbone. US9187597 B1, 2015.

50. Britner, J.; Ritter, H., Methylenelactide: vinyl polymerization and spatial reactivity effects. *Beilstein J. Org. Chem.* **2016,** *12*, 2378-2389.

51. Britner, J.; Ritter, H., Self-Activation of Poly(methylenelactide) through Neighboring-Group Effects: A Sophisticated Type of Reactive Polymer. *Macromolecules* **2015,** *48* (11), 3516-3522.

52. Jing, F.; Hillmyer, M. A., A Bifunctional Monomer Derived from Lactide for Toughening Polylactide. *J. Am. Chem. Soc.* **2008,** *130* (42), 13826-13827.

53. Carlson, D.; Nie, L.; Narayan, R.; Dubois, P., Maleation of polylactide (PLA) by reactive extrusion. *J. Appl. Polym. Sci.* **1999,** *72* (4), 477-485.

54. Plackett, D., Maleated Polylactide as an Interfacial Compatibilizer in Biocomposites. *J. Polym. Environ.* **2004,** *12* (3), 131-138.

55. Zhang, J.-F.; Sun, X., Mechanical Properties of Poly(lactic acid)/Starch Composites Compatibilized by Maleic Anhydride. *Biomacromolecules* **2004,** *5* (4), 1446-1451.

56. Croll, T. I.; O'Connor, A. J.; Stevens, G. W.; Cooper-White, J. J., Controllable Surface Modification of Poly(lactic-co-glycolic acid) (PLGA) by Hydrolysis or Aminolysis I: Physical, Chemical, and Theoretical Aspects. *Biomacromolecules* **2004,** *5* (2), 463-473.

57. Xu, F. J.; Yang, X. C.; Li, C. Y.; Yang, W. T., Functionalized Polylactide Film Surfaces via Surface-Initiated ATRP. *Macromolecules* **2011,** *44* (7), 2371-2377.

58. Kiss, É.; Kutnyánszky, E.; Bertóti, I., Modification of Poly(lactic/glycolic acid) Surface by Chemical Attachment of Poly(ethylene glycol). *Langmuir* **2010,** *26* (3), 1440-1444.

59. Guo, B.; Finne-Wistrand, A.; Albertsson, A.-C., Electroactive Hydrophilic Polylactide Surface by Covalent Modification with Tetraaniline. *Macromolecules* **2012,** *45* (2), 652-659.

60. Gutierrez-Villarreal, M. H.; Ulloa-Hinojosa, M. G.; Gaona-Lozano, J. G., Surface functionalization of poly(lactic acid) film by UV-photografting of N-vinylpyrrolidone. *J. Appl. Polym. Sci.* **2008,** *110* (1), 163-169.

61. Nugroho, R. W. N.; Odelius, K.; Höglund, A.; Albertsson, A.-C., Nondestructive Covalent "Grafting-from" of Poly(lactide) Particles of Different Geometries. *ACS applied materials & interfaces* **2012,** *4* (6), 2978-2984.

62. El Habnouni, S.; Darcos, V.; Garric, X.; Lavigne, J.-P.; Nottelet, B.; Coudane, J., Mild Methodology for the Versatile Chemical Modification of Polylactide Surfaces: Original Combination of Anionic and Click Chemistry for Biomedical Applications. *Adv. Funct. Mater.* **2011,** *21* (17), 3321-3330.

63. El Habnouni, S.; Lavigne, J.-P.; Darcos, V.; Porsio, B.; Garric, X.; Coudane, J.; Nottelet, B., Toward potent antibiofilm degradable medical devices: A generic method for the antibacterial surface modification of polylactide. *Acta Biomater.* **2013,** *9* (8), 7709-7718.

64. Sardo, C.; Nottelet, B.; Triolo, D.; Giammona, G.; Garric, X.; Lavigne, J.-P.; Cavallaro, G.; Coudane, J., When Functionalization of PLA Surfaces Meets Thiol–Yne Photochemistry: Case Study with Antibacterial Polyaspartamide Derivatives. *Biomacromolecules* **2014,** *15* (11), 4351-4362.

CHAPTER 2

Synthesis of an alkene-containing copolylactide and its facile modification by the addition of thiols[*]

2.1. INTRODUCTION

With the continued interest to design new copolymers of PL bearing reactive functional groups, herein I report the preparation of a new PLA copolymer that contains unsaturated ester linkages (ene-PL) by dehydrochlorination of a chloro-substituted PLA copolymer. The addition of thiols to the electrophilic α,β-unsaturated ester groups to the copolymer is demonstrated in solution by a nucleophilic conjugate addition under mildly basic conditions, and by a radical catalyzed process in the presence of AIBN. The addition of thiols to alkenes is an efficient approach for bioconjugation of peptides,[1,2] proteins,[3,4] and nucleic acids[5] to synthetic polymers. We have also explored the potential to use this approach to modify the surface of films of the functional copolymer.

[*] The work presented here is published in Macromolecules. Kalelkar et al. *Macromolecules*, **2016**, *49*, 2609-2617.The monomer synthesis was initially explored by Guillermo Alas, a PhD. Candidate in Dr. Collard's research Group. First few polymerization attempts were carried out in conjunction with Guillermo Alas.

2.2. RESULTS AND DISCUSSION

2.2.1. Monomer synthesis.

The synthesis of the cyclic monomer 3,6-bis(chloromethyl)-1,4-dioxane-2,5-dione, (chlorolactide monomer, Figure 2.1) begins with the selective oxidation of the primary alcohol of 3-chloropropane-1,2-diol by treatment with nitric acid to produce 3-chlorolactic acid. Once the reaction mixture is heated to 80 °C an exothermic oxidation reaction takes place with the release of a dense red-brown gas. Over-oxidation of 3-chlorolactic acid to oxalic acid was observed when the reaction was allowed to continue for a prolonged time or until complete cessation of gas formation. Higher yields of 3-chlorolactic acid were obtained by cooling and quenching the reaction by the addition of water once the evolution of gas had substantially subsided.

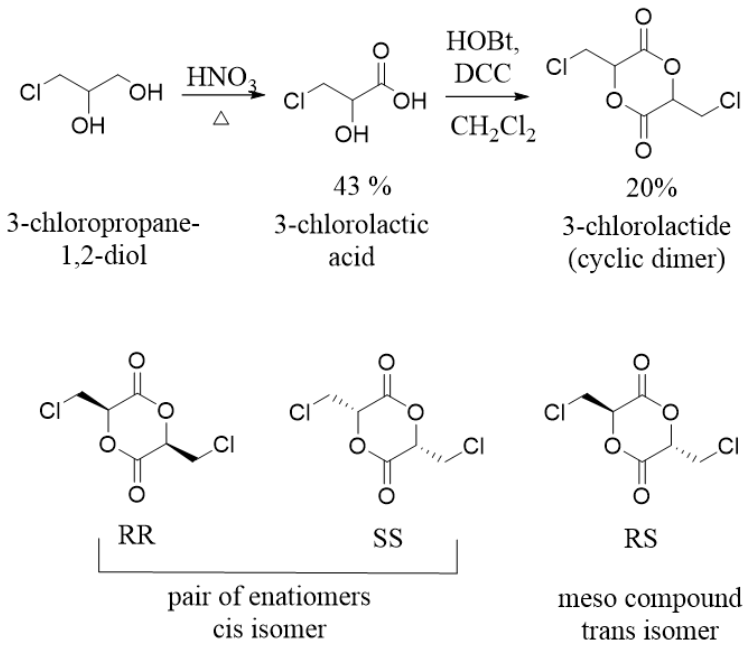

Figure 2.1. Monomer synthesis and stereochemistry of the chlorine-substituted lactide monomer.

Modified lactides have previously been synthesized by a number of different methods: Reacting substituted lactic acids with bromopropionyl chloride followed by ring closure, esterification by treatment with *p*-toluenesulfonic acid, partial esterification to afford linear oligomeric esters followed by thermal cracking and distillation,[6] and by the use of activated esters.[7] We chose to synthesize the cyclic lactide monomer by the treatment of 3-chlorolactic acid with HOBt and DCC in CH_2Cl_2 at room temperature, Figure 2.1. This approach addresses some of the challenges associated with the previous methods as it avoids the need for high temperature or harsh reaction conditions in the synthesis of this new functional lactide and affords a monomer with two functional unit per mole of the monomer. While the substrate was completely consumed within 4 h, the separation of the cyclic monomer from excess reagents (HOBt and DCC) and byproducts (DCU and linear chain oligomers) presented a significant challenge. Attempts to isolate the monomer using column chromatography resulted in ring opening. Nevertheless, we were successful in isolating the cyclic monomer from the reaction mixture by performing two filtrations to remove precipitated DCC and DCU, and passing a CH_2Cl_2 solution through a short plug of silica to remove HOBt and the linear oligomers.

Since the 3-chlorolactic acid is a racemic mixture, the esterification reaction leads to the formation of three stereoisomers of the lactide; the cis compound (a racemic mixture of the *R,R* and *S,S* enantiomers) and the trans isomer (the meso compound), Figure 2.1. The ^{1}H NMR spectrum of the material isolated directly from the reaction mixture indicated to the presence of both the cis and the trans isomers, Figure 2.2 A. The methine hydrogen of one of the isomers appears as a doublet of doublets (δ = 5.51 ppm, with coupling constants of 3 Hz and 2.7 Hz) by virtue of being adjacent to the two diastereotopic hydrogen atoms of the exocyclic methylene

group. Another doublet of doublets (δ = 5.23 ppm) with coupling constants 6 Hz and 3.9 Hz corresponds to the other isomer, Figure 2.2A.

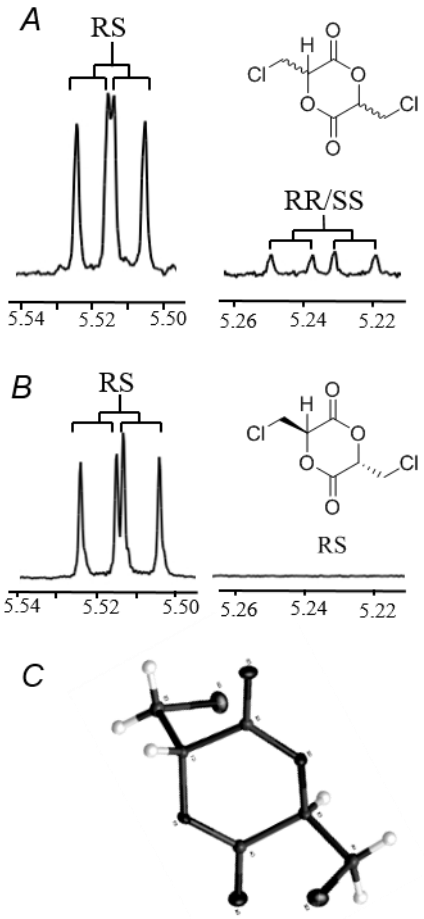

Figure 2.2. 3-Chlorolactide monomer structure: A, ^{1}H NMR spectrum of the mixture showing the presence of both the cis and trans isomers obtained from the esterification reaction. B, ^{1}H NMR spectrum of the separated meso stereoisomer. C, X-ray crystal structure of meso (trans) isomer.

Recrystallization of the mixture of stereoisomers from CH_2Cl_2 afforded colorless crystals of the stereoisomer for which the methine proton appears further downfield in the ^1H NMR spectrum, Figure 2.2B. Single crystal X-ray diffraction was performed to unequivocally define the stereochemistry of the recrystallized monomer, which proved to be the trans (i.e., meso) isomer, which adopts a pseudo diequatorial conformation, Figure 2.2C. Purification of the cis isomer proved to be challenging and was not pursued extensively.

2.2.2. Copolymerization

The recrystallized meso chlorolactide cyclic monomer was copolymerized with L-lactide in a molar ratio of 5:95, Figure 2.3. The ring-opening copolymerization was carried out in the absence of solvent at 135 ºC using stannous octoate as a catalyst. No external initiator was added to the reaction since the minute impurities present in the monomer such as lactic acid and residual water can initiate the copolymerization.[8] During the reaction, the mixture of the two monomers melted at approximately 95 ºC, which allowed for a uniform mixing with the catalyst even in the absence of solvent. The reaction flask was maintained at 135 ºC for 16 h, during which the mixture solidified. After cooling, the copolymer was dissolved in CH_2Cl_2 and purified by precipitation upon addition to MeOH. Attempts to carry out the stannous octoate-promoted copolymerization in toluene resulted in low molecular weight copolymers.

The ^1H NMR spectrum of the precipitated copolymer shows the presence of a quartet (δ5.15 ppm, signal *p*) and a doublet (δ1.57 ppm, signal *q*) for the methine and the methyl hydrogens, respectively, of the lactide component of the copolymer, Figure 2.4A. Broad multiplets appear at

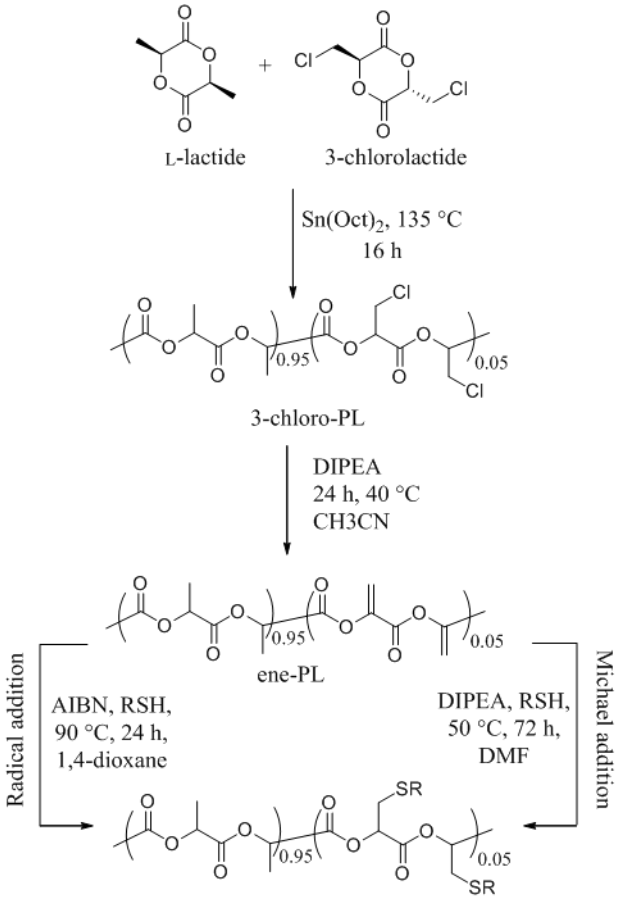

Figure 2.3. Copolymerization and post-polymerization addition of thiols.

δ5.4-5.6 ppm and δ3.8-4.1 ppm for the methine and the methylene hydrogens, respectively, of the chlorolactide unit of the copolymer, Figure 2.4A. Comparison of the integrals of the signals for the lactide unit and the chlorolactide unit of the copolymer confirms that the chloro-substituted unit constitutes 5% of the copolymer, in agreement with ratio of monomers used.

The appearance of a small peak in the base of the signal for the methine hydrogen of the lactide component (signal *p*, Figure 2.4A) can be attributed to the methine hydrogen of the lactide units that are adjacent to a chlorolactide unit. This shifts the signal slightly downfield from that of a regular lactide unit that is flanked by two lactide units. A small quartet at δ 4.35 ppm (signal x) and a singlet δ 3.74 ppm (signal *y*) can be assigned to the methine hydrogen at the hydroxyl

terminus and methyl hydrogen at the methoxy ester terminus of the copolymer respectively, Figure 2.4A. Comparison of the integrals of these signals to that of signal *p* (for the methine of lactide units within the chain of the polymer) suggests a number average molecular weight (M_n) of ~15 kDa. GPC analysis confirmed this molecular weight, Table 2.1.

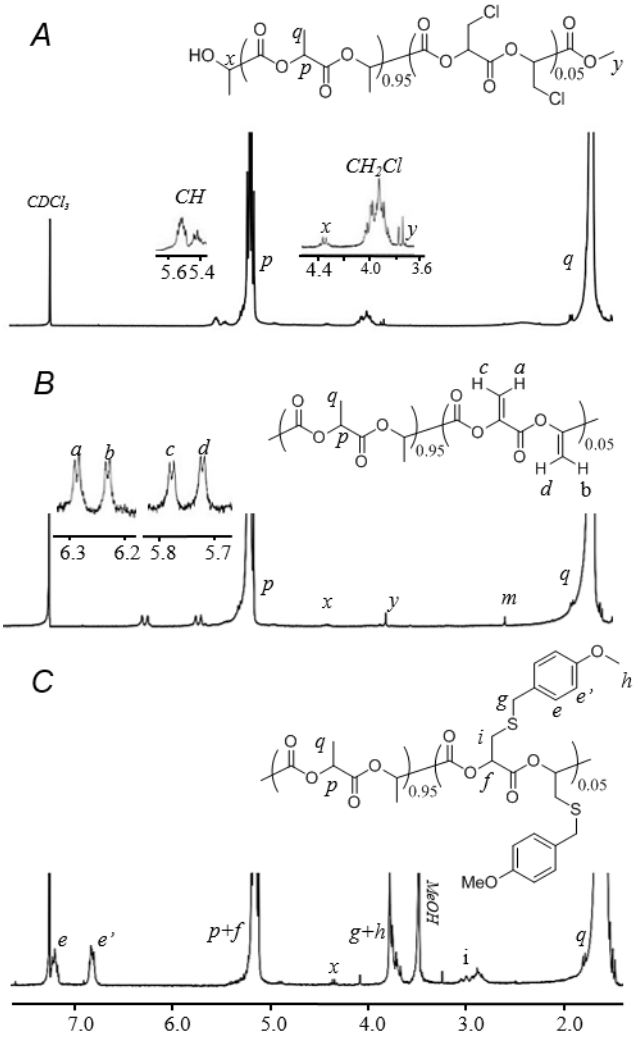

Figure 2.4.[1]H NMR spectra (300 MHz, $CDCl_3$) of copolymers: A, 3-chloro-PL; B, ene-PL; C, MBT-PL.

Table 2.1. DSC[a], NMR[b] and GPC[c] characterization.

	T_g[a] °C	T_c[a] on heating °C	T_m[a] °C	T_c[a] on cooling °C	ΔH_{melt}[a] J/g	ΔH_{cryst}[a] J/g on heating	ΔH_{cryst}[a] J/g on cooling	M_n (NMR)[b]	M_n (GPC)[c]	PDI (GPC)[c]
chloro-PL	30	96	133	-	11.63	19.9	-	15.7	15.3	1.81
ene-PL	32	95	138	-	19.8	16.7	-	15.1	14.1	1.52
MBT-PL[d]	40	81	156	85	39.9	14.2	16.2	15.6	16.6	1.58
LPLA	60-65	121 -	173-178 amorphous	-	42.4 -	41 -	- -	- -	- -	- -
DLPLA[f]	50-55									

[a]10 °C/min, 3 cycles, -20 °C to 250 °C. [b]From ^{1}H NMR chain end analysis. [c]Polystyrene standards; THF eluent. [d]Obtained by nucleophilic base catalyzed addition mechanism. [f]Poly(DL-lactide [Ref[9]].

Attempts to synthesize a 20 percent by mole of chloro-PL resulted in lower monomer conversions. However, these conditions yielded a 20% copolymer which matched with the monomer feed ratio. The ^{1}H NMR spectrum of the 20 % copolymer showed an increase in the size of the peak at the base of the quartet (base of signal *p*, Figure 2.5) as compared to the corresponding peak in the 5% copolymer (base of signal *p*, Figure 2.4A). Since this peak at the base of the quartet is associated with the methine hydrogen of the lactide component of the copolymer adjacent to a chlorolactide unit, the increase in its size was expected with the increase in the percentage of the comonomer from 5 % to 20 %.

The increase in the percentage of chlorolactide unit of the copolymer also resulted in the appearance of a quartet at 4.7 ppm (signal *z*, Figure 2.5). This quartet can be assigned to the methine hydrogen of the chlorolactide component of the copolymer at the hydroxyl terminus. The relative size of this quartet compared to the quartet associated with the methine hydrogen of the lactide component of the copolymer at the hydroxyl terminus (signal *x*, Figure 2.5) shows that the

molecules of the copolymer bearing chlorolactide unit at the hydroxyl terminus are three time that of those bearing lactide units. Comparison of the integration of both of these signals together with that of the backbone methine hydrogen (signal *p*) showed that the increase in the molar ratio of the

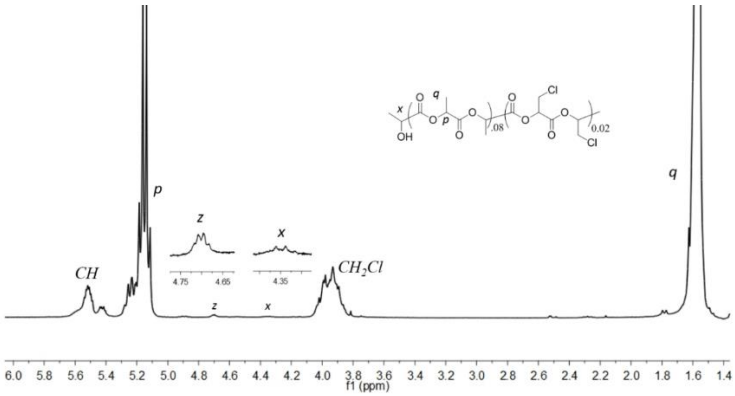

Figure 2.5.[1]H NMR spectrum (300 MHz, $CDCl_3$) of 20 % chloro-PL. Signal labelled z is associated with the methine hydrogen of the chlorolactide unit at the hydroxyl terminus of the copolymer.

functional comonomer to 20 % did not drastically affect the molecular weight (M_n) of chloro-PL, which turned out to be ~10 kDa.

2.2.3. Post-polymerization dehydrochlorination

The chloro-substituted repeat units of the copolymer undergo dehydrochlorination upon treatment of the copolymer with *N*,*N*-diisopropyl-*N*-ethylamine (Hunig's base) in acetonitrile, Figure 2.3. The copolymer was precipitated by addition of the reaction mixture in MeOH and isolated by filtration. The extent of the reaction was characterized using ^{1}H NMR spectroscopy, Figure 2.4B. The appearance of a series of four doublets in the alkene region of the ^{1}H NMR spectrum (signals a, b, c, d) along with the disappearance of the peaks of the methylene hydrogens and methine hydrogen of the chloromethyl pendant group, suggest that the elimination reaction proceeds quantitatively to give the alkene-containing copolymer ene-PL. The relative size of the quartet at δ4.35 ppm (signal x), that is associated with the methine hydrogen of the hydroxyl terminus, remains unchanged. Thus, the dehydrochlorination reaction under these basic conditions

proceeds without rupture of the polyester backbone. This is confirmed by the molecular weight of ene-PL determined by GPC, Table 2.1.

The appearance of four doublets in the vinylic region of the ^{1}H NMR spectrum of ene-PL results from the nonequivalent chemical environments of the four vinylic hydrogen atoms of the alkene-containing diads. This indicates the creation of diads in the polymer that are derived from the two separate lactide comonomers, and the absence of other transesterification reactions that would scramble the individual repeat units. A relatively large difference in the chemical shift of these hydrogen atoms can be ascribed to the presence of different substituents on the 1,1-disubstituted double bond whereby one hydrogen atom on each double bond is cis to a carbonyl carbon of an ester functional group (which results in a relatively large downfield shift), while the other is cis to the oxygen atom of an ester. Thus, hydrogen atoms a and b appear further downfield than the hydrogen atoms c and d, Figure 2.4B. Further inequivalency of the four vinylic protons of the ene-diad results from the effect of resonance of the unsaturated esters, Figure 2.6. The carbon-carbon double bonds of the two α,β unsaturated ester groups affect both the electron withdrawing ability of the carbonyl bonds and the electron donating ability of the oxy substituents of each ester. Thus, the α,β unsaturated oxy substituent is a weaker electron donor to the attached carbonyl than the corresponding saturated alkoxy substituent, Figure 2.6. This renders the β-carbon of the α,β unsaturated ester labeled β_1 more electron-deficient than the one labeled β_2, Figure 2.6.

This would suggest that the signals for hydrogen atoms a and c should appear further downfield than the atoms b and d respectively, Figure 2.4B. A COSY experiment shows that the hydrogen atoms labeled a and c couple to one another other, suggesting that they are on the same β-carbon atom, and that the hydrogen atoms labeled b and d couple with one another, thereby confirming the peak assignments (Appendix A, Figure A-2).

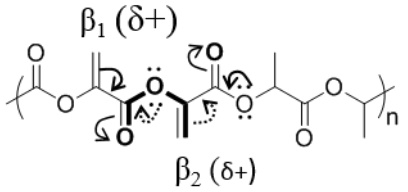

Figure 2.6. Electron density of the two β carbons of ene-PL diad. Bold bond highlights the vinyl ester. Bold arrows show stronger electron donating ability.

Alkene-containing units at the hydroxyl terminus of the copolymer chain tautomerize into the keto form. This is corroborated by the fact that prolonged exposure of the ene-PL copolymer to basic conditions (10 equivalents of Et_3N, 48 h) leads to an increase in the relative size of a singlet at δ 2.5 ppm in the ^1H NMR spectrum, (peak labelled m in Figure 2.4B). This singlet arises from the methyl group of the keto tautomer; peaks corresponding to the enol tautomer are absent. Along with the increase in the size of this singlet, a new set of peaks appears in the alkene region of the ^1H NMR spectrum (a', b', c', d') that can be assigned to the vinylic protons at the carboxylic methyl ester chain end of ene-PL, Figure 2.7B. These chain ends are generated by nucleophilic acyl transfer of the unsaturated ester containing diad of the copolymer with Et_3N and methanolysis upon precipitation of the copolymer in MeOH, Figure 2.7A. These basic conditions lead to extensive cleavage of the unsaturated ester of the copolymer over the saturated ester. Control over the rate of degradation of poly(lactic acids) (PLA) has been studied extensively in the field of biomaterial fabrication and drug delivery.[10] The presence of α,β unsaturated linkages might provide a new approach to tune the rate of hydrolytic degradation.

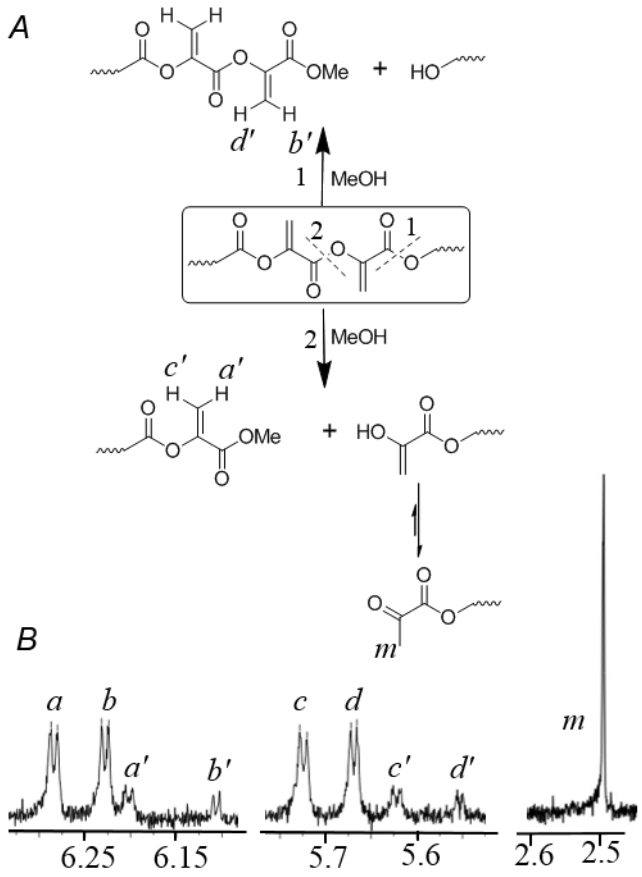

Figure 2.7. A, Methanolysis of ene-PL under basic conditions. Cleavage of the alkyl ester (pathway1) and the vinyl ester (pathway 2) produce end group that give signals *b'*, *d'* and *a'*, *c'*, *m* respectively; B, ^{1}H NMR of ene-PL in $CDCl_3$.

2.2.4. Thermal analysis

Thermogravimetric analysis (TGA) was performed to determine the degradation temperatures of the copolymers. The copolymers are stable up to approximately 300 °C and degraded rapidly above 350 °C. Differential Scanning Calorimetry (DSC) was performed to determine the T_g, T_m and T_c, ΔH_{melt}, and $\Delta H_{crystal}$ of the copolymers, Table 2.1. Consistent data were obtained for the second and the third cycle of all the copolymers.

The second thermal cycle of 3-choro-PL indicated that after undergoing a glass transition (T_g = 30 °C) the copolymer cold crystallizes (T_c = 96 °C). This is followed by melting at 133 °C.

Supercooling on freezing of the copolymer resulted in the formation of predominantly amorphous material. This amorphous copolymer cold crystallized upon subsequent heating. The enthalpy of fusion (ΔH_{melt}) absorbed upon melting was approximately equal to the heat of crystallization ($\Delta H_{crystal}$) released during a single thermal cycle. Similar to chloro-PL, ene-PL copolymer underwent cold crystallization (T_c = 95 °C) upon heating above the glass transition phase (T_g = 32 °C) and the semi-crystalline copolymer melted upon further heating, (T_m = 138 °C). The similarity in the 2nd and the 3rd thermogram of ene-PL suggest that no crosslinking took place between the alkene units of ene-PL. To corroborate this finding, ene-PL was heated to 170 °C and characterized using ^{1}H NMR spectroscopy. The dissolution of ene-PL in $CDCl_3$, as well as the presence of alkene units in the NMR spectrum confirms the thermal stability of the copolymer. The thermogram of MBT-PL showed the features of glass transition phase (T_g = 40°C), crystallization phase (T_c = 81°C) and melting phase (T_m =156 °C), Table 2.1. However, in contrast to chloro-PL and ene-PL, the bulky sidechains of the copolymer allow for the copolymer to solidify into a semi-crystalline state upon cooling. The lowering in the glass transition temperature (T_g) of the copolymers compared to regular PLA is as expected and might be ascribed to the presence of flexible side chains that act as plasticizers.

2.2.5. Radical thiol-ene reaction

The ene-PL copolymer was treated with (4-methoxyphenyl)methanethiol in the presence of AIBN as a radical initiator to explore the addition of thiols to the unsaturated ester repeat units. Use of one equivalent of the thiol relative to the amount of unsaturated ester in the ene-PL copolymer led to complete disappearance of the vinylic hydrogen peaks (a, b, c, d, Figure 2.4B) in the ^{1}H NMR spectrum in 24 hrs. However, the integration of the peaks in the ^{1}H NMR spectrum

for the 4-methoxyphenyl unit of the copolymer, compared to the signal for the polymeric backbone, indicated that only 23% of the thiol had undergone addition to the alkene, Table 2.2. This could be a result of a competing radical catalyzed cross-linking of the alkene containing diads of ene-PL. This was corroborated by the decrease in the solubility of the thiol-added copolymer as compared to that of the starting copolymer (ene-PL), which precluded GPC characterization.

Table 2.2. Radical-catalyzed thiol-ene addition of 4-methoxybenzylthiol to ene-PL.[a]

Ratio of C=C in ene-PL to thiol	% consumption of C=C in ene-PL	% thiol addition
1:1	100%	23%
1:10	100%	40%
1:25	76%	56%

[a] AIBN, 1,4-dioxane, 90°C, 24 h.

Changing the temperature or time of the reaction did not lead to an increase in the amount of thiol addition. However, the quantity of thiol played an important role: Use of 10 equivalents of thiol resulted in addition to 40% of the alkene units, Table 2.2. This behavior is similar to that observed by Dove et al. for the radical addition of thiols to allyl-functional poly(carbonate)s, and rises from an increased statistical chance of thiol addition over crosslinking. However, with a larger excess of thiol (25 equivalents) the addition reaction was still incomplete. This incomplete addition of thiol, even when it is present in a large stoichiometric excess, may be ascribed to the reaction of thiol radicals to form disulfide, rather than addition to ene-PL.

2.2.6. Nucleophilic conjugate addition of thiol to ene-PL

The treatment of ene-PL with thiols in the presence of base was explored as a method to add thiols to the copolymer via a nucleophilic conjugate addition reaction. Reaction parameters such as the duration of the reaction, amount of base and temperature were optimized by carrying

out the reaction in $CDCl_3$ and monitoring the rate of disappearance of the vinylic peaks in the ^1H NMR spectrum. The four doublets associated with the vinylic hydrogens of the unsaturated diad of ene-PL (a, b, c, d), Figure 2.4B) were diminished at different rates during the reaction. The pair of doublets labeled a and c disappeared at a faster rate than signals b and d. This observation is in agreement with the expected electron density of the carbon atoms labeled β_1 and β_2 and is consistent with the chemical shifts of the vinylic hydrogen atoms (Figure 2.6). The addition of thiol is faster at the more electron deficient β_1 carbon of the alkene diad of ene-PL, which is relatively more deshielded than the β_2 carbon of the diad.

Using optimized conditions, near quantitative addition was achieved with a variety of thiols: aromatic (thiophenol), benzylic ((4-methoxyphenyl)methanethiol) and aliphatic (octanethiol). These additions took place without a decrease in the molecular weight of the copolymer, as confirmed by the relative size of the peaks associated with the chain-end hydrogen of the copolymer in the ^1H NMR spectroscopy, Figure 2.4C, Table 2.3. GPC characterization of the copolymers was consistent with the lack of chain session under these conditions (Table 2.1). The addition of cysteine onto the polymer was performed to explore the potential to conjugate thiol-containing biomolecules. While treatment of ene-PL with cysteine under optimized reaction conditions resulted in addition across the double bond, this procedure resulted in a concomitant eight-fold increase in the size of the peaks in the ^1H NMR spectrum that are associated with the lactide unit at the hydroxyl end of the copolymer, Table 3. This corresponds to a decrease in the molecular weight of the copolymer which might result from the nucleophilic attack of the α-amino group of cysteine on the ester linkages in the polymeric backbone. To prevent this side reaction, we treated ene-PL with *N*-acetyl cysteine. This reaction proceeded smoothly with quantitative addition of the thiol to the alkene without a decrease in the molecular weight, Table 3.

Table 2.3. Nucleophilic base-catalyzed conjugate addition of thiols to ene-PL.[a]

Thiol	% thiol addition	M_n of product / kD [b]
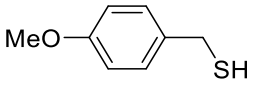	100	16.6
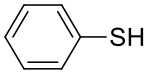	97.2	15.9
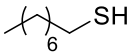	98	16.1
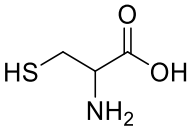	100	5.3
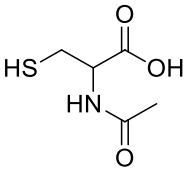	100	15.8

[a] DIPEA, TCEP-HCl, DMF, 50 °C, 3 d. [b] Estimated by ^{1}H NMR chain end analysis.

2.2.7. Exploration of surface chemistry

The ability to modify the surface properties of a polymer by immobilization of peptides to render it more compatible with biological environments has tremendous potential value in the development of biomedical devices.[11] To explore the modification of ene-PL we treated films of ene-PL copolymer with a thiol-containing fluorescent dye, SAMSA fluorescein, under conditions which result in the nucleophilic conjugate addition.

SAMSA fluorescein contains a thioacetate group which is subjected to deacylation to afford a free thiol group. It has been extensively used to demonstrate the conjugation of thiols to biomaterials by monitoring fluorescence.[12,13]

Films of ene-PL were prepared by drop-casting a solution of the polymer in CH_2Cl_2 followed by slow evaporation of the solvent at room temperature. Drop-casting of polymer from other solvents ($CHCl_3$, EtOAc, acetone resulted in poor quality of films. Films were immersed in an aqueous solution of deprotected SAMSA fluorescein for 5 h. They were then subjected to rigorous aqueous washes to remove any physisorbed dye. The slides were dried under Ar and imaged using fluorescence microscopy, Figure 2.8.

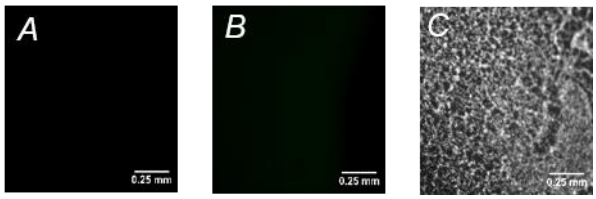

Figure 2.8. Fluorescence from polymer films after treatment with SAMSA fluorescein dye: A, PLA film + deprotected dye; B, ene-PL film + protected dye; C, ene-PL film + deprotected dye; bar, 250 μm.

Along with the combination of ene-PL and deprotected SAMSA fluorescein, two control experiments were imaged: (i) Films of regular poly(lactic acid) (PLA) that had been treated with deprotected SAMSA fluorescein, and (ii) films of ene-PL that had been treated with acyl-protected SAMSA fluorescein (i.e., with no free thiol group). The intensity of fluorescent emission from the deprotected SAMSA-treated ene-PL films, along with the absence of emission from the control films, suggests that the retention of the dye occurred due to covalent attachment by addition of thiol to the functional copolymer. Consistent results obtained over six replicates of sample films

treated under these conditions and reproducible results obtained across different batches demonstrates the ability of the ene-PL surface to undergo conjugate addition of thiols.

2.3. EXPERIMENTAL SECTION

2.3.1. Materials and methods.

Reagents were obtained from the following sources and were used without further purification: 3-Chloropropane-1,2-diol and (4-methoxyphenyl)methanethiol (Alfa Aesar); 1-octanethiol, L-cysteine, thiophenol, *N*,*N*-diisopropylethylamine (DIPEA), azobisisobutyronitrile (AIBN), anhydrous DMF and anhydrous acetonitrile (Sigma-Aldrich); hydroxybenzotriazole (HOBt) and *N*,*N'*-dicyclohexylcarbodiimide (DCC) (AAPPTec Corporation); tris(2-carboxyethyl)phosphine (TCEP-HCl) and 5-((2-(and-3)-S-(acetylmercaptosuccinoylamino) fluorescein (SAMSA fluorescein) (Thermo Fisher Scientific Life Technologies). All other solvents were purchased from VWR. Commercial L-lactide (Alfa Aesar) was recrystallized twice from EtOAc. Flash chromatography silica gel was obtained from Dynamic Adsorbents, Inc.)

NMR spectra were recorded using a Varian Mercury spectrometer (^{1}H NMR, 300 MHz; ^{13}C, 75 MHz) and a Bruker Avance IIIHD 500 (COSY, 500 MHz). IR spectra were recorded using a Bruker ALPHA FT-IR spectrometer. Mass spectrometry analysis was performed using a Quattro LC spectrometer. Fluorescence microscopy was performed using a Nikon Eclipse E400 upright fluorescent microscope. Differential Scanning Calorimetry (DSC) (3 cycles, -20 °C to 250 °C, at 10° C/min), and Thermogravimetric Analysis (TGA) (10 °C/min) were recorded using Q200 Differential scanning calorimeter, and a Pyris 1 Thermogravimetric Analyzer, respectively. Gel permeation chromatography was performed on a Shimadzu gel permeation chromatography setup using THF as an eluent; chromatographs were calibrated against polystyrene standards.

2.3.2. Synthesis

2.3.2.1. 3-Chloro-2-hydroxypropanoic acid (3-chlorolactic acid).

43 %

3-chloropropane-1,2-diol — 3-chlorolactic acid

The title compound was prepared according to the method described by Hope et al.[14] 3-Chloropropane-1,2-diol (100 g, 904 mmol) was stirred in a beaker that was immersed in an ice bath in a well-vented hood. Concentrated nitric acid (308 mL) was added over a period of 30 min. Following the addition, the beaker was removed from the ice bath and the temperature was raised gradually to 80 °C at which point an exothermic reaction began with the rapid evolution of a dense brown gas. Heating was stopped when the evolution of gas began to subside (approximately 15 to 25 minutes) The reaction flask was allowed to cool to room temperature, water (200 mL) was added, followed by the slow addition of $NaHCO_3$ (66 g, 0.78 mol). The resulting mixture was filtered, and the filtrate was extracted with Et_2O (8 × 50 mL). The combined organic extracts were dried over $MgSO_4$, and the solvent was removed under reduced pressure. The residue was recrystallized twice from a minimum amount of $CHCl_3$/THF (10:1 v/v) to afford 3-chlorolactic acid as a colorless crystalline solid (47.3 g, 42%); mp: 77–79 °C (lit: 78–80 °C). ^{1}H NMR (300 MHz, $CDCl_3$): δ 4.61 (t, *J* = 3.3 Hz, 1H, C2-CH), 3.94 (dd, *J* = 11.7 Hz, 3.9 Hz, 1H, diastereotopic C3-CH_2), 3.83 (dd, *J* = 11.7 Hz, 3.3 Hz, 1H, diastereotopic C3-CH_2).

2.3.2.2. Meso-3,6-bis(chloromethyl)-1,4-dioxane-2,5-dione (chlorolactide monomer).

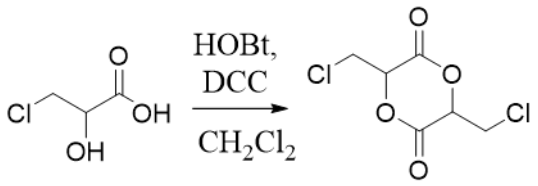

43 %
3-chlorolactic acid

20%
3-chlorolactide (cyclic dimer)

3-Chloro-2-hydroxypropanoic acid (10 g, 80 mmol) was added to solution of HOBt (15.6 g, 100 mmol) and DCC (21.1 g, 100 mmol) in CH_2Cl_2 (700 mL) under N_2 and the mixture was stirred at room temperature for 6 h. The reaction mixture was filtered twice, and the solvent was removed under reduced pressure. The residue was dissolved in CH_2Cl_2, the solution was passed through a short silica plug, and the solvent was removed. The latter process was repeated to afford a crude mixture of the cis (R,R and S,S isomers) and trans (meso) cyclic lactide (2.80 g, 33%) The mixture was recrystallized from a small volume of CH_2Cl_2 to obtain *meso*-3,6-bis(chloromethyl)-1,4-dioxane-2,5-dione as a colorless crystalline solid (1.79 g, 21%); mp: 125-127 °C. ^{1}H NMR (300 MHz, $CDCl_3$): δ 5.51 (dd, *J* = 3 Hz and 2.7 Hz, 1H, CH), 4.18 (dd, *J* = 12.3 Hz and 2.7 Hz, 1H, diastereotopic CH_2Cl), 3.99 (dd, *J* = 12.3 Hz and 3Hz, 1H, diastereotopic CH_2Cl). ^{13}C NMR (75 MHz, $CDCl_3$): δ 76.13 (CH–O), 44.78 (CH_2Cl), 161.49 (C=O). MS (ESI) *m*/*z* (relative intensity): 228.8 ($[M + OH]^-$, 100 %), 230.8 ($[(M + 2) + OH]^-$, 65%), 232.7 ($[(M + 4) + OH]^-$, 10 %); HRMS (EI) calculated for $C_6H_6O_4Cl_2$: 211.9643, observed: 211.9644, Δ = 0.5 ppm. IR: 3000-2840 (w, C–H, str.), 1740 (s, C=O, str.), 1250 (s, C–O str.), 690 (s, C–Cl str.) cm^{-1}.

2.3.2.3. Poly(lactide-co-chlorolactide) (chloro-PL).

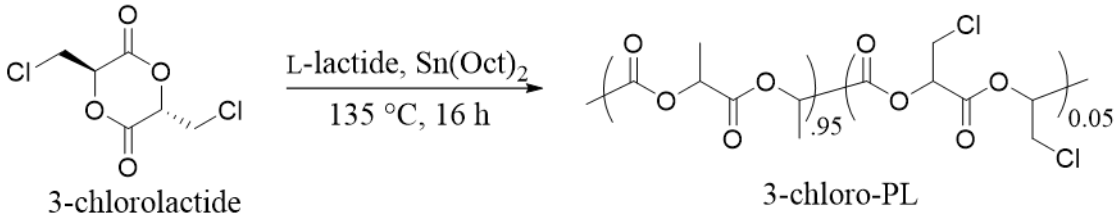

3-chlorolactide 3-chloro-PL

A mixture of chlorolactide monomer (30 mg, 0.14 mmol) and L-lactide (273 mg, 1.91 mmol) was placed in a round-bottomed flask. The flask was purged with Ar, and a solution of tin(II) octoate in benzene (40 µL of a 0.8 M stock solution, 32 µmol) was added. The mixture was kept under vacuum for 24 h and the flask was back-filled with Ar. The flask was then heated to 135 °C for 16 h. The resulting solid was dissolved in CH_2Cl_2 (2 mL) and the solution was added slowly to room temperature MeOH (100 mL) with stirring. The precipitated solid was removed by filtration and dried to afford the 95:5 copolymer as a colorless solid (281.7 mg, 93 %). ^{1}H NMR (300 MHz, $CDCl_3$): δ 5.4-5.6 (m, 1H, chlorolactide unit), 5.15 (q, *J* = 6 Hz, 19H) 3.8-4.1 (m, 2H, chlorolactide), 1.57 (d, *J* = 6 Hz, 57H).

2.3.2.4. Poly(lactide-co-methylene glycolide) (ene-PL).

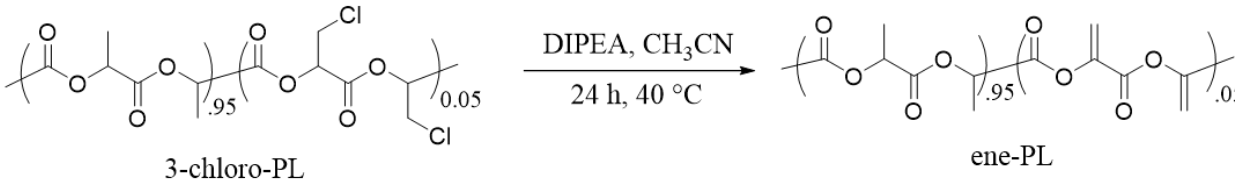

3-chloro-PL ene-PL

A solution of chloro-PL (100 mg) and DIPEA (11.2 µL, 67.8 µmol) in anhydrous acetonitrile was stirred at 40 °C under Ar for 24 h. The solvent was removed under reduced pressure, and the resulting solid residue was dissolved in a minimum amount of CH_2Cl_2. This solution was added slowly to room temperature MeOH (50 mL) with stirring. The precipitated solid was filtered and dried to afford the 95:5 ene-PL copolymer as a colorless solid (79.1 mg, 81 %). ^{1}H NMR (300 MHz, $CDCl_3$): δ 6.28 (d, *J* = 2.1 Hz, 1H), 6.23 (d, *J* = 2.4 Hz, 1H), 5.72 (d, *J* = 2.4 Hz, 1H), 5.67 (d, *J* = 1.8 Hz, 1H) – see Results and Discussion section for assignments, 5.15 (q, *J* = 6 Hz, 19H, lactide CH), 1.57 (d, *J* = 6 Hz, 57H, lactide CH_3).

2.3.2.5. General procedure for conjugate addition of thiol to ene-PL

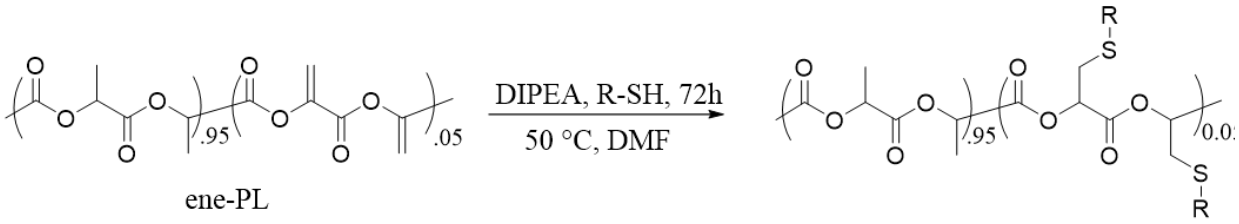

ene-PL

A solution of thiol (678 µmol, 10 equivalents relative to the amount of unsaturated ester in the copolymer), DIPEA (118 µL, 678 µmol) and TCEP-HCl (194 mg, 678 µmol) in DMF (2 mL) was stirred for 2h. ene-PL (100 mg) was added, and the reaction mixture was stirred at 50 °C for 72 h. DI H_2O (10 mL) was added, and the mixture was extracted with dichloromethane (1 × 5 mL). The organic extract was dried over $MgSO_4$ and added slowly to room temperature MeOH (50 mL) with stirring. The precipitated solid was collected by filtration and dried to afford the addition product as a colorless solid.

95:5 % Poly(lactide-co-(4-methoxyphenyl)methanethiolactide) (MBT-PL): Prepared by addition of 4-methoxyphenylmethanethiol to ene-PL: 88.5 mg, 80% isolated yield; quantitative addition reaction. ^{1}H NMR (300 MHz, $CDCl_3$): δ 7.15-7.23 (m, 2H, Ar-2,6 CH), 6.75-6.9 (m, 2H, Ar-3,5 CH), 5.15 (q, *J* = 6 Hz, 20H, lactide CH), 3.50-3.81 (m, 5H, OCH_3 and $ArCH_2S$), 2.7-3.1 (m, 2H, SCH_2), 1.57 (d, *J* = 6 Hz, 60H, lactide CH_3).

2.3.2.6. Radical catalyzed addition of thiol to ene-PL

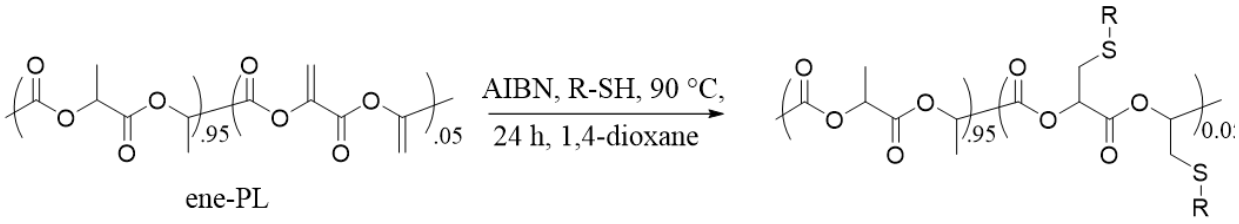

ene-PL

A solution of ene-PL (100 mg), (4-methoxyphenyl)methanethiol (678 µmol, 10 eq relative to the alkene) and AIBN (135.6 µmol) in 1,4-dioxane was stirred at 90 °C under Ar for 24 h. The solvent was removed under reduced pressure, and the solid residue was dissolved in minimum amount of CH_2Cl_2. The solution was added slowly to stirred MeOH (50 mL) at room temperature. The precipitated copolymer was collected by filtration and dried to afford the addition product as a colorless solid (71.9 mg, 64%).

Poly(lactide-co-(4-methoxyphenyl)methanethiolactide): Prepared by addition of 4-methoxyphenylmethanethiol to ene-PL: 71.9 mg, 64% isolated yield; 40% addition reaction. ^{1}H NMR (300 MHz, $CDCl_3$): δ 7.15-7.23 (m, 0.7H, Ar-2,6 CH), 6.75-6.9 (m, 0.7H, Ar-3,5 CH), 5.15 (q, J = 6Hz, 19H, lactide CH), 3.50-3.81 (m, 1.7H, OCH_3 and $ArCH_2S$), 2.7-3.1 (m, 0.7H, SCH_2), 1.57 (d, J = 6 Hz, 57H, lactide CH_3).

2.3.2.7. Surface Modification

Glass slides (12 mm micro cover glass slides, VWR) were washed with concentrated HNO_3, water, and acetone, and then dried under a stream of Ar. Films were formed by drop-casting 200 µL of a 50 mg/mL solution of the 95:5 ene-PL copolymer in CH_2Cl_2 on to the glass slides. The slides were kept covered overnight in a glass vial to allow the solvent to evaporate slowly. A stock solution of SAMSA fluorescein was deprotected and diluted to a final concentration of 50 µL/mL. DIPEA (20 µL, 114 µmol) and TCEP-HCL (10 mg, 39 µmol) were added to the stock solution of the dye. Slides were immersed in the dye solution (1mL) under Ar, and the solution was placed on a single tier VWR rocking platform for 5 h. The slides were removed from the solution, washed three times by immersion into water, and dried under a stream of Ar. Slides were imaged using an upright fluorescence microscope (10X, emission λ = 520 nm, shutter speed 653 ms, gain = 16).

2.4. CONCLUSION

We have demonstrated the synthesis and characterization of a novel PLA copolymer that contains electrophilic α,β-unsaturated esters. The successful post-polymerization addition of a variety of thiols by the radical thiol-ene pathway and by nucleophilic conjugated addition reactions demonstrates the potential utility of these materials for bioconjugation. Under optimized conditions, these addition reactions take place without a decrease in the molecular weight of the polymer. The treatment of thin films of ene-PL with a thiol-containing fluorescent dye demonstrated the potential for conjugation of thiol-containing biomolecules to the surface of the copolymer. Successful addition of the thiol containing fluorescent dye onto films of ene-PL provides a promising precedence for the application of the copolymer as a biomaterial.

2.5. REFERENCES

1. Singha, N. K.; Gibson, M. I.; Koiry, B. P.; Danial, M.; Klok, H.-A., Side-Chain Peptide-Synthetic Polymer Conjugates via Tandem "Ester-Amide/Thiol–Ene" Post-Polymerization Modification of Poly(pentafluorophenyl methacrylate) Obtained Using ATRP. *Biomacromolecules* **2011,** *12* (8), 2908-2913.
2. Obermeier, B.; Frey, H., Poly(ethylene glycol-co-allyl glycidyl ether)s: A PEG-Based Modular Synthetic Platform for Multiple Bioconjugation. *Bioconjugate Chem.* **2011,** *22* (3), 436-444.
3. Slavin, S.; Khoshdel, E.; Haddleton, D. M., Biological surface modification by 'thiol-ene' addition of polymers synthesised by catalytic chain transfer polymerisation (CCTP). *Polym. Chem.* **2012,** *3* (6), 1461-1466.
4. Jones, M. W.; Mantovani, G.; Ryan, S. M.; Wang, X.; Brayden, D. J.; Haddleton, D. M., Phosphine-mediated one-pot thiol-ene "click" approach to polymer-protein conjugates. *Chem. Commun.* **2009,** (35), 5272-5274.
5. Kow, S. C.; McCarroll, J.; Valade, D.; Boyer, C.; Dwarte, T.; Davis, T. P.; Kavallaris, M.; Bulmus, V., Dicer-Labile PEG Conjugates for siRNA Delivery. *Biomacromolecules* **2011,** *12* (12), 4301-4310.
6. Noda, M.; Okuyama, H., Thermal Catalytic Depolymerization of Poly(L-Lactic Acid) Oligomer into LL-Lactide : Effects of Al, Ti, Zn and Zr Compounds as Catalysts. *Chem. Pharm. Bull. (Tokyo)* **1999,** *47* (4), 467-471.
7. Hayashi, Y.; Kinoshita, Y.; Hidaka, K.; Kiso, A.; Uchibori, H.; Kimura, T.; Kiso, Y., Analysis of Amide Bond Formation with an α-Hydroxy-β-amino Acid Derivative, 3-Amino-2-hydroxy-4-phenylbutanoic Acid, as an Acyl Component: Byproduction of Homobislactone. *The Journal of Organic Chemistry* **2001,** *66* (16), 5537-5544.
8. Dijkstra, P. J.; Du, H.; Feijen, J., Single site catalysts for stereoselective ring-opening polymerization of lactides. *Polym. Chem.* **2011,** *2* (3), 520-527.
9. Middleton, J. C.; Tipton, A. J., Synthetic biodegradable polymers as orthopedic devices. *Biomaterials* **2000,** *21* (23), 2335-2346.
10. Shasteen, C.; Choy, Y. B., Controlling degradation rate of poly(lactic acid) for its biomedical applications. *Biomedical Engineering Letters* **2011,** *1* (3), 163.
11. Ikada, Y., Surface modification of polymers for medical applications. *Biomaterials* **1994,** *15* (10), 725-36.
12. Gillitzer, E.; Willits, D.; Young, M.; Douglas, T., Chemical modification of a viral cage for multivalent presentation. *Chem. Commun.* **2002,** (20), 2390-2391.
13. Kipper, M. J.; Kleinman, H. K.; Wang, F. W., Covalent surface chemistry gradients for presenting bioactive peptides. *Anal. Biochem.* **2007,** *363* (2), 175-184.
14. Hope, D. B.; Walti, M., Synthesis of the α-hydroxy-analogues of S-benzylcysteine and cysteine. *Journal of the Chemical Society C: Organic* **1970,** *0* (18), 2475-2478.

CHAPTER 3

Thiol-substituted copolylactide: Synthesis, characterization and post-polymerization modification using thiol-ene chemistry[†]

3.1. INTRODUCTION

In Chapter 2, I have described an electrophilic PL analog in which nucleophiles add to α,β-unsaturated ester units that are present in the polyester backbone.[1] To extend the potential utility of PHAs we set out to develop a route to thiol-substituted PL copolymers. Such thiol-substituted PL copolymers would provide a soft nucleophile that undergoes irreversible addition to electron-deficient alkenes via thiol-ene click chemistry.[2] Thiol-ene addition has been extensively used as a tool to modify polymers, both in solution as well as on surfaces. For example, thiol groups generated from the thiocarbonylthio endgroups of polymers prepared by reversible addition-fragmentation chain-transfer (RAFT) polymerization undergo addition to electron-deficient alkenes,[3,4,5] and a thiol-substituted polymethacrylate undergoes coupling with maleimides via thiol-ene addition.[6]

The nucleophilicity and oxidative instability of thiols might be expected to interfere with the ring-opening polymerization of a thiol-bearing lactide and the polycondensation of a thiol-substituted lactic acid. Accordingly, we chose to synthesize a new lactide monomer that bears a 4-methoxybenzylthio substituent. Ring opening copolymerization of 4-methoxybenzylthio-substituted lactide with L-lactide followed by subsequent debenzylation affords a thiol-substituted polylactide, thiol-PL. The 4-methoxybenzyl group has been extensively used as a protecting group

[†] The work presented here is accepted in the journal *Polymer Chemistry*. Kalelkar et. al *Polymer Chemistry* **2018**, *9*, 1022–1031.

for thiols in the multistep synthesis of small molecules.[7] Moreover, it withstands the conditions required for the ring-opening polymerization of lactides.[8,9,10] We explore the addition of thiol-PL to a variety of electron-deficient alkenes to demonstrate its potential utility to expand the scope of functional group chemistries that maybe used to modify PHAs.

3.2. RESULTS AND DISCUSSION

3.2.1. Monomer synthesis

The synthesis of 4-methoxybenzylthio-substituted lactide monomer commences with the synthesis of 3-chlorolactic acid, which was prepared by oxidation of 3-chloro-1,2-propanediol as previously described.[1,11,] Treatment of 3-chlorolactic acid with 4-methoxybenzylthiol under basic conditions affords 4-methoxybenzyl-protected 3-mercaptolactic acid, as shown in Figure 3.1. The ^{1}H NMR spectrum of the 4-methoxybenzylthio-substituted acid consists of a one-hydrogen doublet of doublets for the hydrogen atom of the methine (Figure 3.2A, signal *a*) and a pair of doublet of doublets for the diastereotopic pair of hydrogen atoms of the methylene group (signal *b*), along with the expected peaks for the 4-methoxybenzyl group.

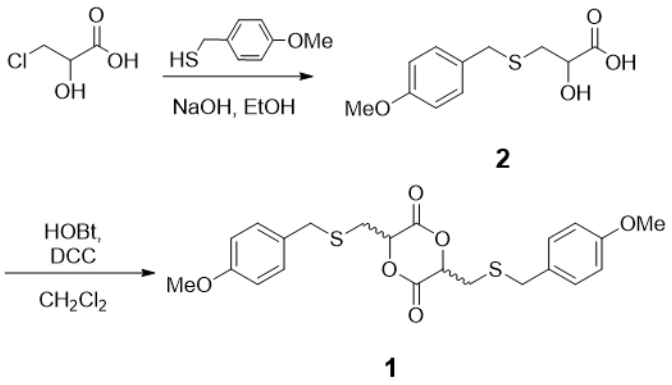

Figure 3.1. Synthesis of 4-methoxybenzylthio-substituted lactide monomer.

α-Hydroxy acid was subjected to esterification by treatment with *N*-hydroxybenztriazole (HOBt) and *N*,*N*'-dicyclohexylcarboximide (DCC) to afford the cyclic monomer 3,6-bis(4-methoxybenzylthiomethyl)-1,4-dioxane-2,5-dione. The conditions used for the esterification reaction (room temperature, CH_2Cl_2, 4 h) results in complete consumption of the α-hydroxy acid. We have previously demonstrated that this is a robust method for the synthesis of lactides that bear

other functional groups, albeit that excess reagents (HOBt, DCC), the formation of side products (linear chain oligomers, dicyclohexylurea (DCU)), and the sensitivity of the functional cyclic monomer to prolonged exposure to silica, necessitate an elaborate purification process.[1,12]

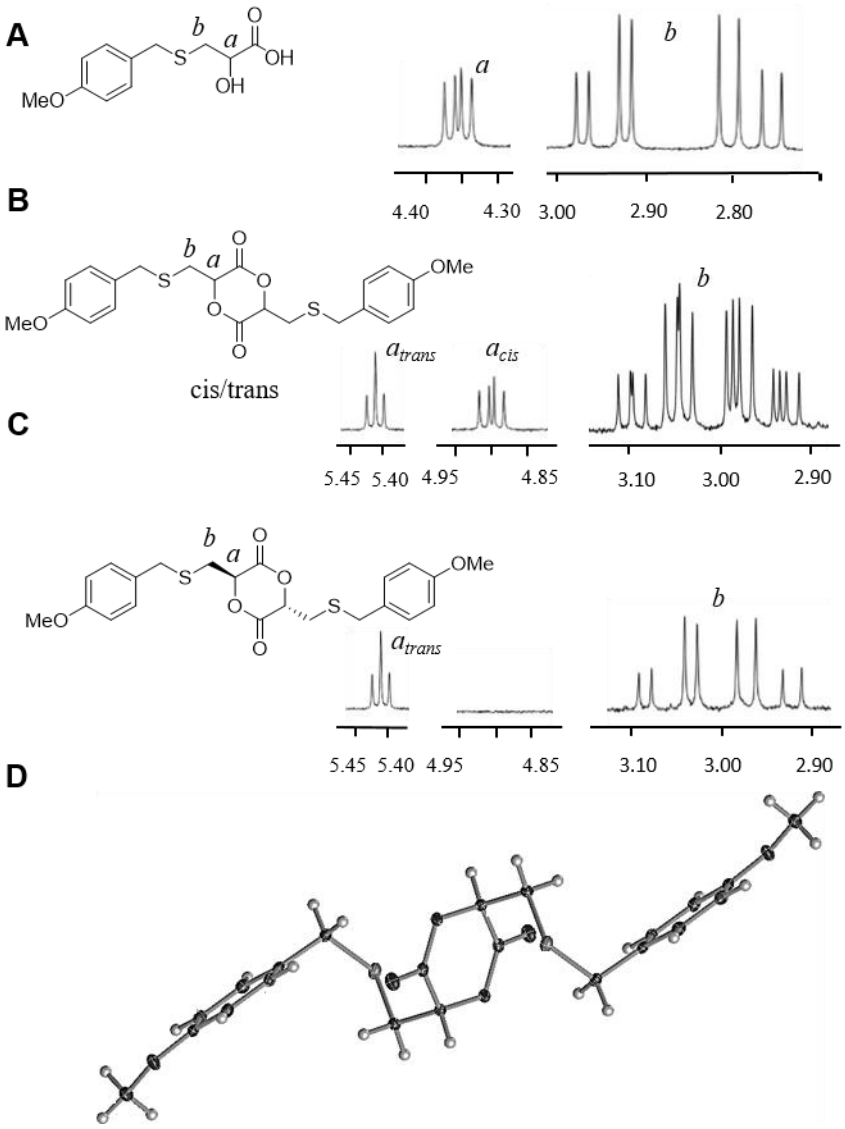

Figure 3.2. A-C, ^{1}H NMR spectra (300 MHz, $CDCl_3$): A, 3-(4-Methoxybenzylthio)lactic acid; B, 4-methoxybenzylthio-substituted lactide (mixture of diastereomers); C, trans 4-methoxybenzylthio-substituted lactide obtained by recrystallization; and D, crystal structure of trans 4-methoxybenzylthio-substituted lactide monomer.

The purification of monomer required two triturations of the crude product with CH_2Cl_2 to remove unreacted DCC and byproduct (DCU), followed by treatment with saturated aqueous $NaHCO_3$ to remove HOBt. Finally, the solution obtained from this treatment was passed through a short silica plug to remove linear chain oligomers.

The ^{1}H NMR spectrum of the product obtained from this procedure exhibits a doublet of doublets at δ 4.9 (J = 6.3 Hz, 4.2 Hz) and a triplet (δ 5.41 ppm J = 3.9 Hz) for the stereogenic methine hydrogen of the cis and the trans isomer of the substituted lactide (signals a_{cis} and $a_{trans,}$ respectively). The diastereotopic methylene hydrogens of the two diastereomers gives rise to two pairs of doublet of doublets between δ 2.9 and 3.1 ppm, Figure 3.2B. The relative chemical shift of the methine signals of the cis and trans substituted lactides depends on the type of substituents on the ring. However, the assignment of the two signals to a specific diastereomer (i.e., cis or trans) is not possible based solely on the chemical shift of these signals. For example, in the case of the chloro-substituted lactide the methine hydrogen of the trans stereoisomer appears downfield relative to the cis form,[1] whereas for the benzyloxy-substituted lactide it is the opposite.[12] However, in both of these prior cases the coupling constants of signal for the methine hydrogen of the trans diastereomer are smaller than those of the cis stereoisoform.[1, 12] These three-bond coupling constants (^3J) depend on the dihedral angles between the methine and the pair of diastereotopic methylene hydrogen atoms. Thus, based on coupling constants we tentatively assigned the triplet at 5.41 ppm to the methine of the trans diastereomer of the new benzylthio-substituted lactide.

The mixture of cis and trans isomers was recrystallized from chloroform. The ^{1}H NMR spectrum of the recrystallized material exhibited only one triplet for the methine hydrogen (signal a_{trans} at 5.4 ppm, 3.9 Hz) and two doublet of doublets at δ 3.08 (J = 15.3 Hz and 3.9 Hz) and δ 2.96

(J = 15.3 Hz and 3.9 Hz), Figure 3.2C. Single crystal X-ray diffraction was used to unequivocally assign the stereochemistry of the recrystallized diastereomer. The crystal structure indicates that the recrystallized product is the trans diastereomer, which adopts a diequatorial conformation in the crystalline state, Figure 3.2D. Thus, this confirms our earlier assignment of the stereochemistry of the structure based on the analysis of coupling constants in the AX_2 spin systems in the ^{1}H NMR spectrum.

The cis stereoisomer was purified by removing the solvent from the mother liquor obtained from the recrystallization followed by recrystallization of the residue from CH_2Cl_2. The ^{1}H NMR spectrum of the crystalline material obtained from this process showed a signal for methine hydrogen of the cis diastereomer at δ 4.9 ppm (signal a_{cis}), and the absence of the corresponding peak for the trans compound. The methylene hydrogens appear as a pair of doublet of doublets at 3.06 ppm (J =15.3 Hz and 4.2 Hz) and 2.95 ppm (J = 15.3 Hz and 6.3 Hz).

3.2.2. Copolymerization of protected thiol-substituted comonomer

The bulk copolymerization of L-lactide and *trans* 4-methoxybenzylthio-substituted lactide was carried out using tin(II) octanoate as a catalyst (1 mole %), Figure 3.3. In the absence of any added initiator, adventitious water or a trace of uncyclized α-hydroxy acid acts as an initiator.[13] A 95:5 mixture of the two comonomers was heated in the presence of catalyst in a closed flask. The mixture of comonomers melted at approximately 95 °C, which allowed for uniform mixing. The temperature was then raised to 140 °C and heating was continued for 16 h. The reaction mixture became viscous and eventually solidified (typically after ~7 h). Since the melting point of the copolymer is higher than that of the comonomers, solidification of the reaction mixture is an indication of the formation of a relatively high molecular weight copolymer. Heating was

continued after the mixture had solidified to achieve higher conversion of monomer and to increase the molecular weight.

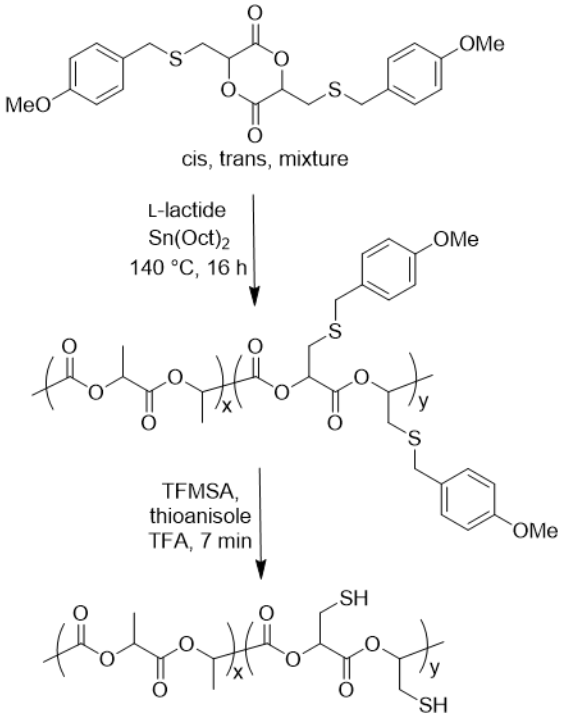

Figure 3.3 Copolymerization of MBT-substituted monomer with L-lactide, and debenzylation of MBT-PL.

During the entire heating process, care was taken to maintain a uniform temperature throughout the reaction flask to prevent the loss of lactide monomer from the reaction mixture by vaporization, condensation and crystallization at a cold spot in the closed system. An analysis of the crude reaction mixture using ^{1}H NMR spectroscopy demonstrated that greater than 95% the comonomers had been consumed. The reaction mixture was dissolved in minimum amount of CH_2Cl_2 (approximately 5 mL/g) and the solution was added to MeOH to precipitate the copolymer as a colorless, fibrous solid that was isolated by filtration.

The ^{1}H NMR spectrum of the precipitated copolymer shows the presence of a quartet at δ 5.15 ppm (Figure 3.4A, signal *p*) and a doublet at 1.57 ppm (signal *q*) that can be assigned to the

methine and the methyl hydrogens of the lactide component of the copolymer, respectively. The signals associated with the methoxy group (signal *e*, 3H) and the benzylic hydrogen atoms (signal *c*, 2H) of the 4-methoxybenzylthio-substituted repeat units give rise to a multiplet at δ 3.5-3.8 (5H). The diastereotopic hydrogen atoms of the methylene unit of the functional repeat unit that is directly attached to the polyester backbone appear as a broad multiplet at δ 2.7-3.1 (signal *b*).

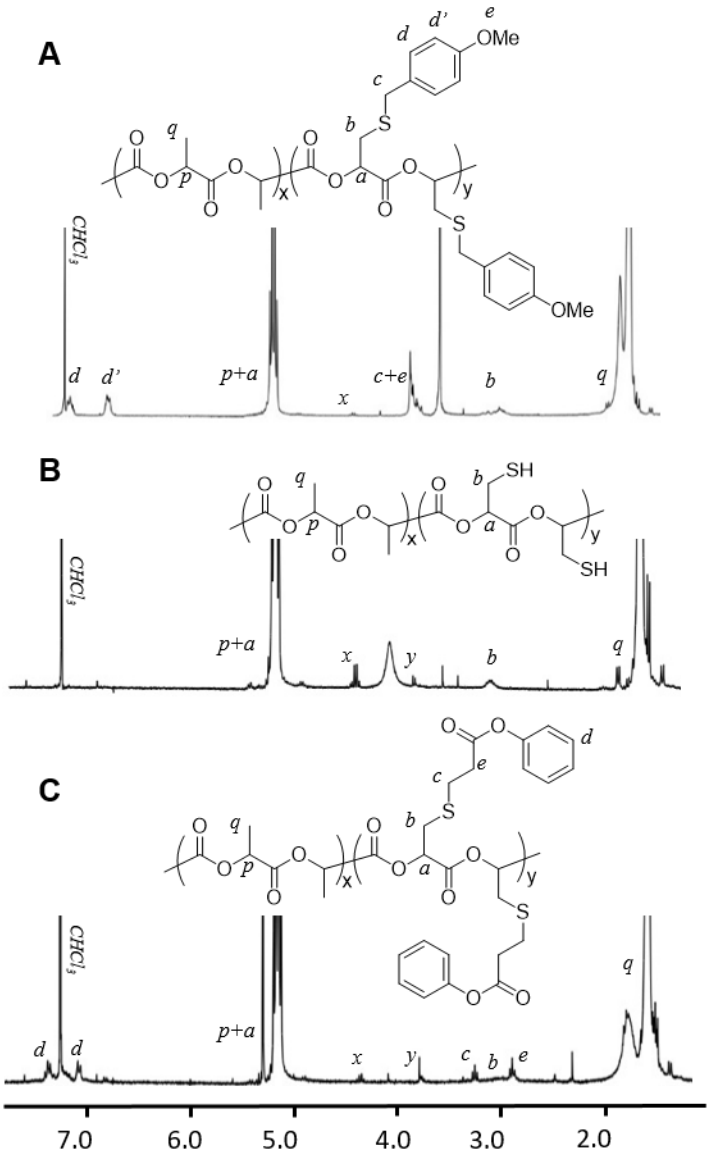

Figure 3.4. ^{1}H NMR spectra (300 MHz, $CDCl_3$). A, MBT-PL; B, thiol-PL; and C, thiol-PL adduct with phenyl acrylate.

Comparison of the integrations of the signals associated with the aromatic, methoxy, benzylic and methylthio hydrogen atoms of the thio-substituted repeat unit with that of methine hydrogen atoms of the copolymer (hydrogen atoms *a* and *p* in Figure 3.4A) confirms that the copolymer contains 5% of the functional monomer, which matches the monomer feed ratio in the polymerization reaction. A small quartet at 4.35 ppm (signal *x*) can be assigned to the methine hydrogen at the hydroxyl chain end of the copolymer. A comparison of the integral of this signal with that of the signal at δ 5.15 (signals *p* and *a*) indicates a number-average molecular weight (M_n) of 15 kDa. GPC studies are consistent with this polymer chain end analysis by ^{1}H NMR spectroscopy, Table 3.1.

Table 3.1. Structural and thermal characterization.

	DSC[a]							Molecular weight		PDI
	T_g (°C)	T_{cc}[b] (°C)	T_m (°C)	T_c[c] (°C)	ΔH_{melt} (J/g)	ΔH_{cc}[b] (J/g)	ΔH_c[c] (J/g)	NMR (kDa)[d] M_n	GPC (kDa)[e] M_n	(GPC)
5% MBT-PL (trans)	30	78	149	78	30.3	15.3	11.7	15.7	15.3	1.81
5% MBT-PL (cis)	45	105	144	42	28.2	24.5	0.23	12.1	11.4	1.47
4% Thiol-PL	20	-	-	-	-	-	-	9.2	7.7	1.3
4% Acrylate-PL	30	81	142	83	22.1	10.4	10.9	11	10.8	1.42

[a]Second of three cycles, −20 °C to 200 °C at 5 °C/min. [b]Cold crystallization during heating. [c]Crystallization during cooling. [d]From ^{1}H NMR chain end analysis. [e]Polystyrene standards; THF eluent.

To determine if the stereochemistry of the 4-methyoxybenzylthio-substituted lactide monomer has any effect on the polymerization process, we went on to separately copolymerize the cis stereoisomer of the monomer with L-lactide, and also a mixture of stereoisomers (containing a

1:1 mole ratio of the cis and trans diastereomers) with L-lactide. In both cases, the mixture of comonomers melted at approximately 95 °C. In the case of the cis stereoisomer, the polymerization mixture solidified within 4 h, compared to ~7 h for the mixture of diastereomers. In both cases the copolymer obtained showed the same features in the ^{1}H NMR spectrum as those of the copolymer obtained from the trans stereoisomer. Moreover, the molecular weight, monomer conversion and the ratio of repeat units in the copolymer were all similar (11-15 kDa; >95% conversion; 5:95 copolymer composition, matching the monomer feed ratio).

Attempts to synthesize copolymers that contain higher amounts of 4-methyoxybenzylthio-substituted repeat units (i.e., 10-20 mole %) were also successful. However, increasing the proportion of the substituted lactide monomer resulted in lower conversion of the monomer and lower molecular weight copolymers. The copolymerization was attempted at a lower concentration of tin(II) octoate (0.1 mol %) at 135 °C to improve the monomer conversion and obtain higher molecular weight copolymer. However, during this polymerization, the mixture did not solidify even after heating for 2 days; it only solidified after addition of more tin(II) octoate and further heating. On extended heating the reaction mixture turned dark brown. In the case of the polymerizations with a higher percentage of functional lactide monomer, the ratio of repeat units in these polymers was consistently lower than expected, as determined by ^{1}H NMR spectroscopy. For example, a 1:9 monomer feed ratio of thio-substituted lactide to L-lactide resulted in a 7% functional copolymer, while a 1:4 monomer feed ratio resulted in only 13% incorporation of the functional repeat unit. The need for a higher concentration of tin(II) octoate to obtain high molecular weight materials and better monomer conversion in this particular case might arise because of complexation or side reactions between the tin catalyst and the sulfur atoms of the monomer, thereby reducing the amount of the catalyst that is available to promote the

polymerization or by lowering its reactivity. Over the past few years a lot of development has taken place on different types of organocatalysts to carry out ROP of L-lactide. Though not explored in this work, in the future, different catalyst systems could be investigated to synthesize high molecular weight MBT-PL with higher amounts of 4-methyoxybenzylthio-substituted repeat units (i.e., 10-20 mole %).

3.2.3. Debenzylation

MBT-PL can be debenzyated to afford thiol-PL upon treatment with thioanisole under acidic conditions. While exposure of PL to acidic conditions can lead to cleavage of the polyester backbone,[14] successful removal of the 4-methoxybenzyl group from a thio-substituted ester-amide copolymer[15-16] provided a promising precedence for the use of strong acids such as trifluoromethanesulfonoic acid (TFMSA) and trifluoroacetic acid (TFA) for the deprotection of MBT-PL. Under optimized conditions, brief exposure of MBT-PL to a mixture of TFMSA and thioanisole (2:1:1 mole ratio of TFMSA, thioanisole, and MBT units in the copolymer) followed by precipitation in MeOH results in successful debenzylation of MBT-PL to afford thiol-PL, as shown in Figure 3.3. The ^{1}H NMR spectrum of the precipitated copolymer showed the absence of signals corresponding to the 4-methoxybenzyl group, Figure 3.4B. The signal for the thiol-substituted methylene hydrogens appears as a multiplet at δ 3.0–3.1 ppm (Figure 3.4B, signal *b*) while the signal for the methine hydrogen β to the thiol coincides with that of the methine hydrogen of the lactide repeat unit of the copolymer at 5.15 ppm. In some batches of thiol-PL obtained using these optimized conditions the methylene hydrogens (signal *b*) appeared as a broader multiplet (δ 2.8-3.5 ppm), which we ascribe to the formation of inter or intramolecular disulfide bonds. Integration of the signals corresponding to the methine and the methyl hydrogens of the lactide

and thiol-lactide units indicate that the copolymer contains ~4% of the thiol-substituted unit. The copolymer was also characterized using IR spectroscopy and the spectrum was compared to that of MBT-PL. The IR spectrum of MBT-PL shows the presence of a signal at 1506 cm^{-1} corresponding to the carbon-carbon stretch of the aromatic rings, Figure 3.5. Absence of this signal in the IR spectrum of thiol-PL further corroborates the success of the debenzylation reaction, Figure 3.5.

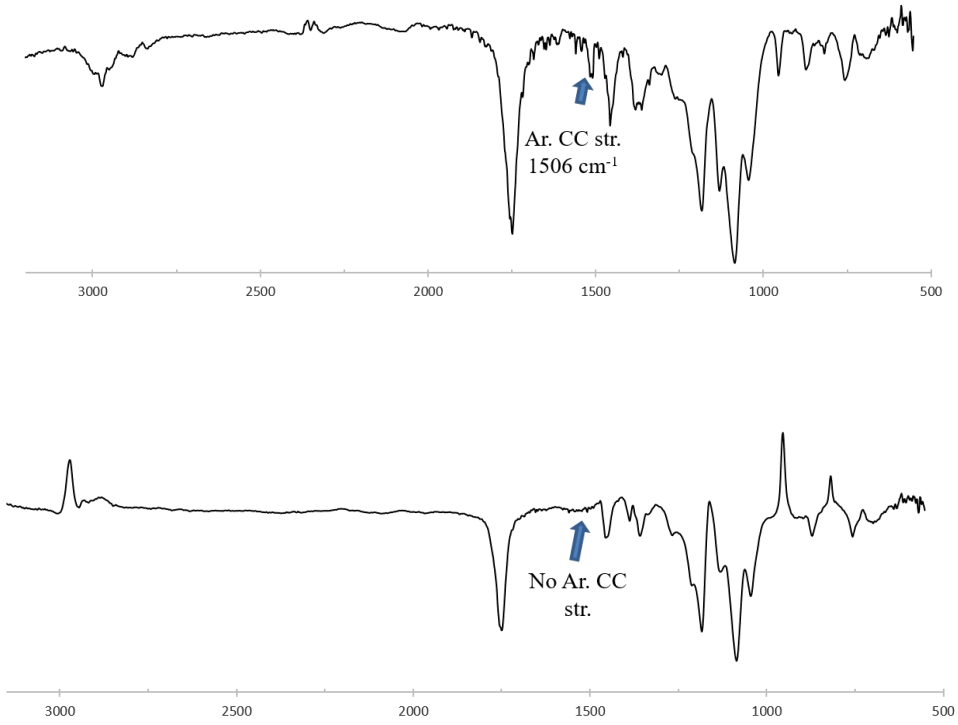

Figure 3.5. Top, IR spectrum of 5 % MBT-PL. Bottom IR spectrum of 4 % thiol-PL.

The molecular weight of the precipitated copolymer, as determined by ^{1}H NMR end group analysis and by GPC indicated a decrease in the number-average molecular weight to ~9 kDa, Table 3.2. The decrease in the molecular weight of the copolymer, as well as in the decrease in the amount of functional comonomer in the debenzylated material suggests that the use of acidic conditions resulted in some cleavage of the polyester even under these optimized conditions. However, decreasing the reaction time to under 7 min or lowering the concentration of reagents

resulted in incomplete debenzylation. Increasing the reaction time, or exposure of MBT-PL to higher concentrations of the reagents, resulted in more cleavage of the polyester backbone, as shown in Table 3.2.

Table 3.2. Reaction conditions for debenzylation of MBT-PL[a]

Reaction conditions		Starting material	Deprotected copolymer			
TFMSA/ Thioanisole	Time (min)	% MBT in copolymer	% thiol-lactide in copolymer	M_n post ppt (kD)	% mass recovered	% deprotection
10:6	10	5	1.2	5.2	17	100
4:2	7	5	2.0	7.1	42	100
2:1	7	5	4.0	9.2	57	100
2:1	7	10	6.0	10.8	60	97
1:0.5	7	5	5.0	10.9	72	80

[a] TFMSA-thioanisole in TFA.

3.3.4. Thermal Analysis

The thermal properties of the copolymers were characterized using differential scanning calorimetry (DSC) to evaluate the glass transition temperature (T_g), cold crystallization (T_{cc}), melting point (T_m), enthalpy of melting (ΔH_m) and enthalpy of crystallization (ΔH_c). The 5% copolymer of MBT-PL obtained from copolymerization of cis stereoisoform of the monomer with L-lactide undergoes a glass transition at 45 °C. Upon further heating the copolymer cold crystallizes at 105 °C, releasing an enthalpy of 24.5 J/g. The crystallized copolymer melts at 144 °C, absorbing an enthalpy of 28.2 J/g. Upon cooling, the copolymer undergoes crystallization at 42 °C. MBT-PL obtained by copolymerization of trans stereoisomer of the monomer demonstrates similar thermal phase behavior, while the one obtained from the copolymerization of diastereotopic mixture results in the formation of an amorphous copolymer that undergoes a glass transition at 30 °C and does not crystalize upon subsequent thermal cycling.

Thiol-PL obtained by debenzylation of MBT-PL undergoes a glass transition at ~20 °C, Table 3.1. However, upon further heating the copolymer does not display melting or crystallization transitions. The lowering of the T_g and T_m of MBT-PL and thiol-PL compared to that of PL homopolymer is consistent with other PL copolymers in which irregularly spaced side chains disrupt crystalline packing to provide amorphous materials.

3.3.5. Conjugate addition of thiol-PL to electron deficient alkenes

Thiol-PL was treated with a variety of electron-deficient alkenes (phenyl acrylate, acrylonitrile, *N*-phenylmaleimide) under basic conditions to explore the utility of the copolymer to prepare adducts via conjugate addition of the thiol group. Since free thiols have a propensity to form disulfide bonds under oxidizing conditions, thiol-PL was treated with tris(2-carboxyethyl)phosphine hydrochloride (TCEP-HCl), a reducing agent, prior to treatment with the alkene. Successful addition of thiol-PL to phenyl acrylate was achieved under optimized conditions (1:3:10 mole ratio of thiol units in PL, Hunig's base, and electrophile), Figure 3.6.

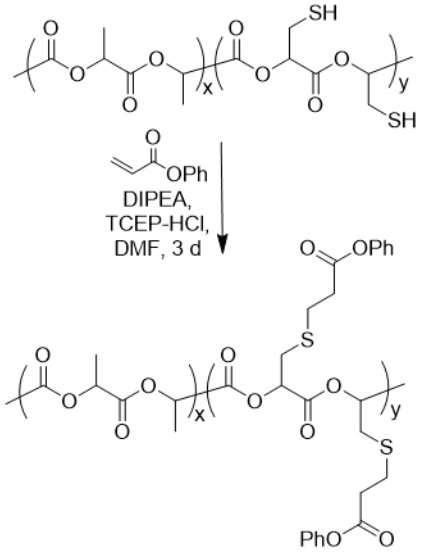

Figure 3.6. Conjugate addition of thiol-PL to phenyl acrylate.

The ^{1}H NMR spectrum of the precipitated copolymer adduct, Figure 3.4C, shows the presence of two triplets at 3.2 ppm and 2.9 ppm, corresponding to the methylene groups of the 2-(phenoxycarbonyl)ethylthio side chain, along with the signals corresponding to the phenyl group, Figure 3.4C. Comparison of the integration of these signals to that of the backbone methine hydrogen indicates that these conditions result in the quantitative addition of the polymer-appended thiols to the acrylate. These reaction conditions did not lead to the cleavage of the polymeric backbone, as is evident from the size of the signal in the ^{1}H NMR spectrum that is associated with the methine hydrogen for the repeat unit at the hydroxyl terminal of the copolymer, Figure 3.4C. GPC characterization shows that the copolymer has a M_n of 11 kDa and a polydispersity index (PDI) of 1.4, Table 3.1.

The thermal properties of the copolymer-acrylate adduct, as characterized by DSC, shows that it undergoes thermal phase transitions that are similar to those of MBT-PL, Table 3.1. Upon heating, the semicrystalline copolymer undergoes a glass transition at 30 °C, followed by cold crystallization at 81 °C releasing an enthalpy of 10.4 J/g. Upon further heating, the crystalline portion of the copolymer melts at a temperature of 142 °C (ΔH_m = 22.1 J/g). Upon cooling, the melted copolymer crystallizes at 83 °C releasing an enthalpy of 10.9 J/g. A similar thermogram is obtained for the subsequent cycles.

Treatment of thiol-PL with other electron-deficient alkenes (*N*-phenylmaleimide and acrylonitrile) under the same optimized conditions resulted in quantitative addition of thiol without concomitant polyester cleavage. The presence of a base is critical to carrying out the addition reaction. No addition occurred in 3 days in the absence of base. The identity of the base is also critical to the success of the reaction because of the lability of the polyester backbone in the

presence of nucleophiles. For example, use of Et_3N in place of Hunig's base resulted in cleavage of the polyester backbone, as demonstrated by NMR spectroscopy and GPC.

3.3. EXPERIMENTAL SECTION

3.3.1. Materials and Methods

Reagents were purchased from the following sources: 4-Methoxybenzylthiol (99%) and trifluoromethanesulfonic acid (TFMSA, 98+%) (Alfa Aesar); *N*,*N*-diisopropylethylamine (DIPEA), anhydrous DMF and anhydrous acetonitrile (Sigma-Aldrich); *N*-hydroxybenzotriazole (HOBt) and *N*,*N'*-dicyclohexylcarbodiimide (DCC) (AAPPTec Corporation); $MgSO_4$ (VWR); tris(2-carboxyethyl)phosphine hydrochloride (TCEP-HCl) (Pierce); trifluoroacetic acid (HPLC grade) and NaOH (EMD). Flash silica gel was obtained from Dynamic Adsorbents, Inc. L-lactide (Alfa Aesar) was recrystallized twice from EtOAc and dried under vacuum prior to copolymerization. All other solvents were purchased from VWR and were used without further purification. All reactions were carried out under Ar (Nexair). 3-Chlorolactic acid was synthesized as previously reported.[11]

NMR spectral analysis was performed using a Varian Mercury spectrometer (^{1}H NMR, 300 MHz; ^{13}C, 75 MHz). IR spectra were recorded using a Shimadzu IR Affinity-1 spectrometer. Mass spectrometry analysis was performed using a Quattro LC spectrometer. Differential scanning calorimetry (DSC) (3 cycles, -20° C to 200° C, at 5° C/min) was performed using a TA Q200 instrument under N_2. Gel permeation chromatograms were recorded on a Shimadzu gel permeation chromatograph using THF as the eluent; chromatographs were calibrated against polystyrene standards. Melting points were recorded using a Mel-Temp II.

3.3.2. Synthesis

3.3.2.1. 2-Hydroxy-3-(4-methoxybenzylthio)propanoic acid

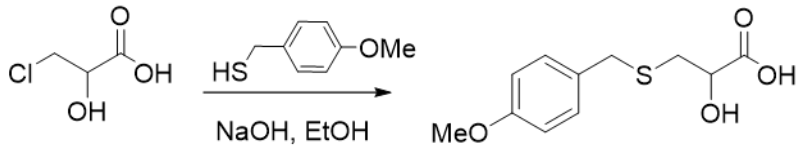

A solution of 3-chlorolactic acid (5.0 g, 40 mmol) and NaOH (1.6 g, 40 mmol) in EtOH (23 mL) was added to a solution of 4-methoxybenzyl thiol (5.6 mL, 40 mmol) and NaOH (1.6 g, 40 mmol) in ethanol (23 mL). The volume was made up to 200 mL with EtOH and the mixture was heated at reflux for 12 h. The mixture was allowed to cool to room temperature and the solvent was removed under reduced pressure to afford a pale yellow solid. The residue was suspended in water and the aqueous suspension was acidified with 1 N sulfuric acid. The mixture was extracted with Et_2O (4 × 50 mL). The organic extracts were dried over $MgSO_4$ and the solvent was removed under reduced pressure to give a yellow solid. The solid was dissolved in CH_2Cl_2 (5 mL) and the solution was passed through a short silica plug which was then flushed with additional CH_2Cl_2. The solvent was removed under reduced pressure and the residue was dried under vacuum to afford the product as a colorless solid (8.1 g, 84%). ^{1}H NMR (300 MHz, $CDCl_3$): δ 7.25 (d, *J* = 8.7 Hz, 2H, $Ar_{2,6}$), 6.85 (d, *J* = 8.7 Hz, 2H, $Ar_{3,5}$), 4.36 (dd, *J* = 6.3 Hz, 4.2 Hz, 1H, CH), 3.8 (s, 3H, OCH_3), 3.75 (s, 2H, SCH_2), 2.95 (dd, *J* = 14.4 Hz, 4.2 Hz, 1H, diasterotopic CH_2), 2.79 (dd, *J* = 14.4 Hz, 6.3 Hz, 1H, diasterotopic CH_2). ^{13}C NMR (75 MHz, $CDCl_3$): δ 158.9, 130.1, 129.4, 114.1 (Ar), 69.5 (OCH_3), 55.3 (SCH_2), 36.1, 34.9. MS (ESI): *m*/*z* (relative intensity) 240.9 ($[M - H]^-$, 100 %), 241.9 ([M] 12.1 %), 242.9 ([M+2], 7.1 %). IR (neat) 3400-2400 (w, O–H str.), 1750 (s, C=O str.), 1250 (s, C–O str.), 1100 (s, C–OH str.), 1500 (s, C=C str.), 820 (s, para opp. bend) cm^{-1}.

3.3.2.2. 3,6-bis(4-Methoxybenzylthiomethyl)-1,4-dioxane-2,5-dione, (MBT-lactide)

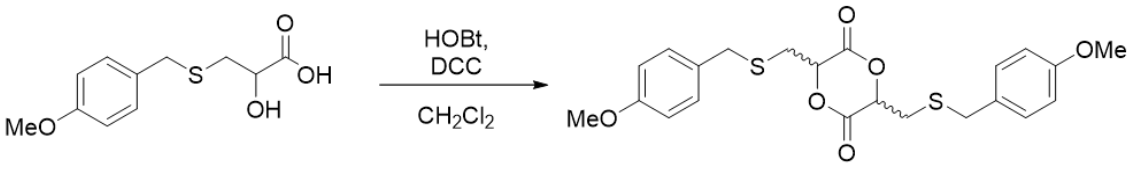

2-Hydroxy-3-(4-methoxybenzylthio)propanoic acid (5.0 g, 21 mmol) was added to a solution of HOBt (4.1 g, 27 mmol) and DCC (5.5 g, 27 mmol) in CH_2Cl_2 (300 mL) under Ar. The solution was stirred for 4 h at room temperature. The mixture was filtered and the solvent was removed under reduced pressure to afford a yellow solid. The solid was redissolved in CH_2Cl_2 (100 mL), the solution was filtered, and the solvent was removed under reduced pressure. The residue was washed with saturated aqueous $NaHCO_3$ and the product was extracted using Et_2O (6 × 50 mL). The organic extract was dried over $MgSO_4$, filtered, and the solvent was removed under reduced pressure. The residue was dissolved in CH_2Cl_2 and the solution was passed through a short silica plug that was then flushed with CH_2Cl_2. The solvent was removed under reduced pressure to afford a mixture of cis (RR/SS) and trans (RS) diastereomers as a yellow solid. (1.9 g, 42% yield). The solid was recrystallized from $CHCl_3$ to afford trans 3,6-bis(4-methoxybenzylthiomethyl)-1,4-dioxane-2,5-dione (0.81 g, 17 % yield of the single stereoisomer) as a colorless crystalline solid. mp 99-100 °C. ^{1}H NMR (300 MHz, $CDCl_3$): δ 7.26 (d, *J* = 9 Hz, 2H, $Ar_{2,6}$), 6.85 (d, *J* = 9 Hz, 2H, $Ar_{3,5}$), 5.41 (t, *J* = 3.9 Hz, 1H, stereogenic CH), 3.80 (s, 3H, OCH_3), 3.76 (s, 2H, SCH_2), 3.08 (dd, *J* = 15.3 Hz, 3.9 Hz, 1H, diastereotopic CH_2), 2.96 (dd, *J* = 15.3 Hz, 3.9 Hz, 1H, diastereotopic CH_2). ^{13}C NMR (75 MHz, $CDCl_3$), δ 164 (C=O), 159, 130, 128, 114 (Ar), 55, 37 (C-S), 33. IR 3080-3000 (w, sp^2 C−H str.), 3000-2810 (w, sp^3 C−H str.), 1743 (s, C=O str.), 1510 (s, C=C str.), 1240 (s, C−O str.), 1170 (s, Ar−O str.), 1074 (s, O−CH_3

str.), 1040 (s, C−O, str.), 839 cm^{-1} (s, para opp. bending). HRMS (ESI) calculated for $C_{22}H_{24}O_6S_2$ + Na + MeOH: m/z = 503.1174, observed: 503.1154.

The mother liquor from the recrystallization was removed under reduced pressure and the residue was recrystallized from CH_2Cl_2 to afford cis 3,6-bis(4-methoxybenzylthiomethyl)-1,4-dioxane-2,5-dione (0.52 g, 11 % of the single stereoisomer) as a colorless crystalline solid. ^1H NMR (300 MHz, $CDCl_3$): δ 7.26 (d, *J* = 9 Hz, 2H, $Ar_{2,6}$), 6.85 (d, *J* = 9 Hz, 2H, $Ar_{3,5}$), 4.89 (dd, *J* = 6.3 Hz, 4.2 Hz, 1H, stereogenic CH), 3.81 (s, 2H, SCH_2), 3.79 (s, 3H, OCH_3), 3.06 (dd, *J* = 15.3 Hz, 4.2 Hz, 1H, diastereotopic CH_2), 2.95 (dd, *J* = 14.4 Hz, 6.3 Hz, 1H, diastereotopic CH_2).

3.3.2.3. Poly(lactide-co-(4-methoxybenzylthio)methylglycolide) (MBT-PL)

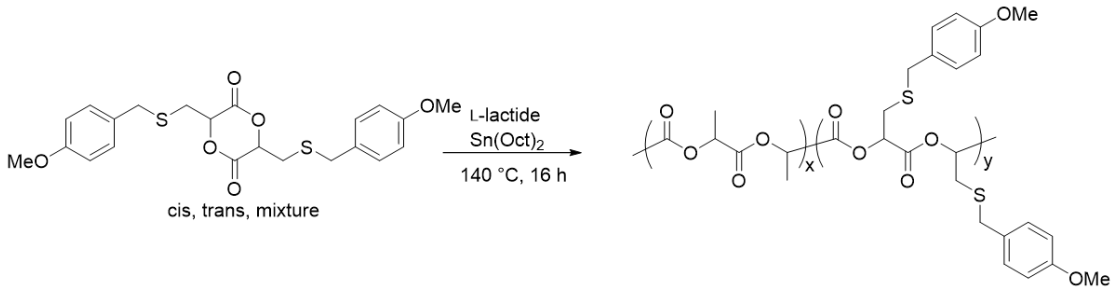

L-lactide (250.4 mg, 1.738 mmol) and MBT-lactide (41 mg, 91 µmol; i.e., a 95:5 ratio of comonomers) were mixed in a mortar and pestle and placed in a pear-shaped flask under Ar. A solution of tin(II) octoate (29 µL of a 0.8 M stock solution in dry benzene, 23.2 µmol) was added to the flask. The reaction vessel was kept under vacuum for 24 h and then backfilled with Ar. The temperature was raised to 140 °C over ca. 2 h, and heating was continued for an additional 14 h. The flask was allowed to cool to room temperature and the reaction mixture was dissolved in CH_2Cl_2 (ca. 1 mL). The solution was added dropwise to MeOH (50 mL) with stirring and the precipitated yellow solid was collected by filtration, (209 mg, 71% yield).

5% MBT containing copolymer, MBT-PL. ^{1}H NMR (300 MHz, $CDCl_3$): δ 7.15-7.23 (m, 2H, $Ar_{2,6}$), 6.75-6.90 (m, 2H, $Ar_{3,5}$), 5.15 (q, J = 6Hz, 20H, CH of lactide and substituted lactide repeat unit), 3.5-3.8 (m, 5H, OCH_3 and benzylic hydrogens of substituted lactide), 2.7-3.1 (m, 2H, CH_2 of substituted lactide), 1.57 (d, J = 6 Hz, 57H, CH_3 of lactide repeat unit). IR 3040-3000 (w, sp^2 C−H str.), 3000-2800 (w, sp^3 C−H str.), 1749 (s, C=O str.), 1506 (w, C=C str.), 1180 (s, C−O str.), 1040 (s, C−O, str.) cm.$^{-1}$ This ^{1}H NMR data is consistent with that described previously.[1]

3.3.2.4. Poly(lactide-co-mercaptomethylglycolide) (thiol-PL)

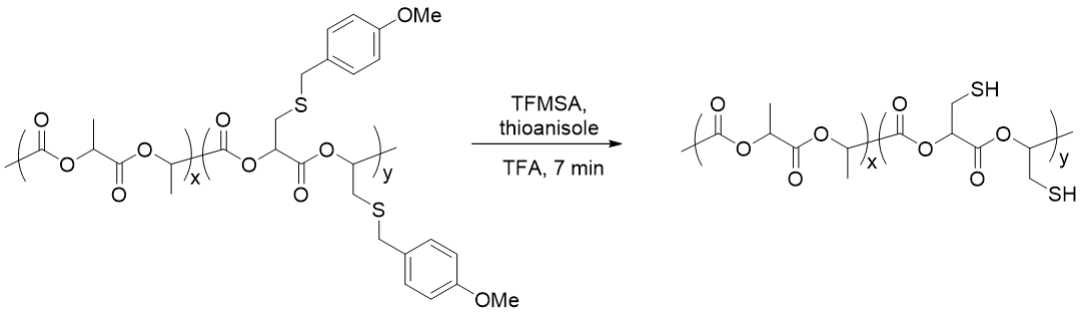

MBT-PL (100 mg, 62.8 µmol) was dissolved in trifluoroacetic acid (1 mL) under Ar. Thioanisole (7 µL, 62.8 µmol, 1 equivalents relative to the amount of thiobenzyl-substituted lactide units in the copolymer) and trifluoromethane sulfonic acid (18.5 µL, 125.6 µmol, 2 eq) was added. The mixture was stirred for 7 min and then added to MeOH (20 mL) with stirring. The precipitated solid was filtered and dried to afford the thiol-substituted copolylactide as an off-white solid, (56 mg, 61%).

4 % thiol-substituted copolymer, thiol-PL. ^{1}H NMR (300 MHz, $CDCl_3$), δ 5.15 (q, *J* = 6 Hz, 25H, CH of lactide and substituted lactide unit), 3.0-3.1 (m, 2H, CH_2SH), 1.57 (d, *J* = 6 Hz, 72H, CH_3 of lactide unit). IR 2950-2820 (w, sp^3 C−H str.), 1749 (s, C=O str.), 1180 (s, C−O str.), 1080 (s, C−O, str.) $cm.^{-1}$

3.3.2.5. General procedure for 1,4-conjugate addition to thiol-substituted copolylactide

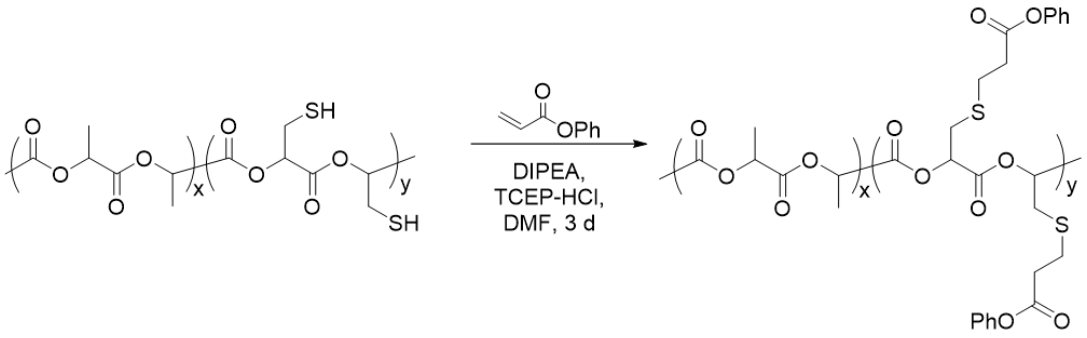

A solution of thiol-PL and TCEP HCl (1 equivalent relative to the amount of thiol-substituted lactide units) in anhydrous DMF was stirred at room temperature for 24 h. The α,β-unsaturated substrate (10 equivalents relative to the amount of thiol in the copolymer) was added. A (50 µL/mL) solution of DIPEA (3 equivalents) in DMF was slowly added to the mixture, which was stirred at room temperature for 3 d. The reaction mixture was poured into water (10 mL) and the precipitated solid was collected by filtration. The solid was dissolved in minimum amount of CH_2Cl_2 and the solution was added dropwise to MeOH (50 mL) with stirring. The precipitated solid was filtered and dried under vacuum.

Reaction with phenyl acrylate. Thiol-PL (100 mg, 67.9 µmol of thiol group) was treated with phenyl acrylate (80 µL, 679 µmol, 10 equivalents) according to the general procedure described above to afford the addition product as a colorless solid (74 mg, 67 %).

4% poly(lactide-co-2-(phenoxycarbonyl)ethylthiomethylglycolide). From treatment of thiol-PL with phenyl acrylate. ^{1}H NMR (300 MHz, $CDCl_3$): δ 7.40-7.05 (m, 5H ,Ar), 5.15 (q, *J* = 6Hz, 25H, CH of lactide and substituted lactide units), 3.24 (t, *J* = 6.9 Hz, 2H, SCH_2CH_2COOPh), 3.0-3.1 (m, 2H, $\underline{CH_2}SCH_2CH_2COOPh$), 2.88 (t, *J* = 6.9 Hz, 2H, SCH_2CH_2COOPh), 1.57 (d, *J* = 6 Hz, 72H, CH_3 of lactide unit).

4% poly(lactide-co-2-cyanoethylthiomethylglycolide). From treatment of thiol-PL with acrylonitrile. ^{1}H NMR (300 MHz, $CDCl_3$): δ 5.15 (q, *J* = 6Hz, 25H, CH of lactide and substituted lactide units), 2.8-2.2 (m, 6H, $CH_2SCH_2CH_2CN$), 1.57 (d, *J* = 6 Hz, 72H, CH_3 of lactide unit).

4% poly(lactide co-1-phenylpyrrolidine-3-thiomethylglycolide). From treatment of thiol-PL with N-phenyl maleimide. ^{1}H NMR (300 MHz, $CDCl_3$), δ 7.55-7.22 (m, 5H, Ar), 5.15 (q, *J* = 6Hz, 25H, CH of lactide and substituted lactide units), 3.00-3.42 (m, 3H, CH_2SCH), 2.40-2.60 (m, 2H, CH_2-CO-N(CO)-Ph), 1.57 (d, *J* = 6 Hz, 72H, CH_3 of lactide unit).

3.4. CONCLUSION

In this work we have described the synthesis of a new protected thio-substituted lactide monomer followed by its copolymerization with L-lactide. Debenzylation of MBT-PL under acidic conditions affords thiol-PL. Quantitative addition of thiol-PL to electron-deficient alkenes demonstrates the ability of the copolymer to undergo thiol-ene addition reactions. Demonstration of the quantitative addition of thiol-PL to electron deficient alkenes establishes a good precedence for its potential application to bioconjugate chemistry with, for example, maleimide-substituted biomolecules. This capability, coupled with the biocompatible and biodegradable nature of the copolymer, suggests opportunities to expand the utility of PL in biomedical applications.

3.5. REFERENCES

1. Kalelkar, P. P.; Alas, G. R.; Collard, D. M., Synthesis of an Alkene-Containing Copolylactide and Its Facile Modification by the Addition of Thiols. *Macromolecules* **2016,** *49* (7), 2609-2617.
2. Hoyle, C. E.; Bowman, C. N., Thiol–Ene Click Chemistry. *Angew. Chem. Int. Ed.* **2010,** *49* (9), 1540-1573.
3. Li, M.; De, P.; Gondi, S. R.; Sumerlin, B. S., End group transformations of RAFT-generated polymers with bismaleimides: Functional telechelics and modular block copolymers. *J. Polym. Sci., Part A: Polym. Chem.* **2008,** *46* (15), 5093-5100.
4. Yu, B.; Chan, J. W.; Hoyle, C. E.; Lowe, A. B., Sequential thiol-ene/thiol-ene and thiol-ene/thiol-yne reactions as a route to well-defined mono and bis end-functionalized poly(N-isopropylacrylamide). *J. Polym. Sci., Part A: Polym. Chem.* **2009,** *47* (14), 3544-3557.
5. Nair, D. P.; Podgórski, M.; Chatani, S.; Gong, T.; Xi, W.; Fenoli, C. R.; Bowman, C. N., The Thiol-Michael Addition Click Reaction: A Powerful and Widely Used Tool in Materials Chemistry. *Chem. Mater.* **2014,** *26* (1), 724-744.
6. Pauloehrl, T.; Delaittre, G.; Bastmeyer, M.; Barner-Kowollik, C., Ambient temperature polymer modification by in situ phototriggered deprotection and thiol-ene chemistry. *Polym. Chem.* **2012,** *3* (7), 1740-1749.
7. Harris, K. M.; Flemer, S., Jr.; Hondal, R. J., Studies on deprotection of cysteine and selenocysteine side-chain protecting groups. *J. Pept. Sci.* **2007,** *13* (2), 81-93.
8. Ouchi, T.; Nozaki, T.; Ishikawa, A.; Fujimoto, I.; Ohya, Y., Synthesis and enzymatic hydrolysis of lactic acid–depsipeptide copolymers with functionalized pendant groups. *J. Polym. Sci., Part A: Polym. Chem.* **1997,** *35* (2), 377-383.
9. Ouchi, T.; Shiratani, M.; Jinno, M.; Hirao, M.; Ohya, Y., Synthesis of poly[(glycolic acid)-alt-(L-aspartic acid)] and its biodegradation behavior in vitro. *Die Makromolekulare Chemie, Rapid Communications* **1993,** *14* (12), 825-831.
10. Ouchi, T.; Ohya, Y., Design of lactide copolymers as biomaterials. *J. Polym. Sci., Part A: Polym. Chem.* **2004,** *42* (3), 453-462.
11. Hope, D. B.; Walti, M., Synthesis of the [small alpha]-hydroxy-analogues of S-benzylcysteine and cysteine. *Journal of the Chemical Society C: Organic* **1970,** *0* (18), 2475-2478.
12. Noga, D. E.; Petrie, T. A.; Kumar, A.; Weck, M.; García, A. J.; Collard, D. M., Synthesis and Modification of Functional Poly(lactide) Copolymers: Toward Biofunctional Materials. *Biomacromolecules* **2008,** *9* (7), 2056-2062.
13. Dijkstra, P. J.; Du, H.; Feijen, J., Single site catalysts for stereoselective ring-opening polymerization of lactides. *Polym. Chem.* **2011,** *2* (3), 520-527.
14. Jung, J. H.; Ree, M.; Kim, H., Acid- and base-catalyzed hydrolyses of aliphatic polycarbonates and polyesters. *Catal. Today* **2006,** *115* (1), 283-287.

15. Ouchi, T.; Seike, H.; Nozaki, T.; Ohya, Y., Synthesis and characteristics of polydepsipeptide with pendant thiol groups. *J. Polym. Sci., Part A: Polym. Chem.* **1998,** *36* (8), 1283-1290.

16. Ouchi, T.; Seike, H.; Miyazaki, H.; Tasaka, F.; Ohya, Y., Synthesis of a block copolymer of L-lactide and depsipeptide with pendant thiol groups. *Designed Monomers and Polymers* **2000,** *3* (3), 279-287.

CHAPTER 4

Antimicrobial copolylactide polymers via "click" chemistry attachment of simple quaternary amines‡

4.1. INTRODUCTION

Polylactide (PL) is an aliphatic polyester that is obtained from bio-renewable monomers by either ring-opening polymerization (ROP) of cyclic lactide, or by polycondensation of lactic acid.[1,2] PL is an attractive candidate as an alternative to petroleum-based plastics for packaging and coating applications,[3] in the design of biomedical devices,[4,5,6,7,8] and as a drug delivery vehicle.[9,10,11] These potential applications are a consequence of the biorenewable nature of the monomers, together with the biocompatibility, biodegradability and high tensile strength of PL.

An important attribute of a coating material that is to be used in a sterile environment is the ability to resist bacterial growth.[12] Coudane[15,16,17]and Gaona-Lozano[18] have independently demonstrated that the surface of PL can be rendered antimicrobial by the attachment of an antimicrobial agent. However, the biodegradable nature of the PL backbone[19,20] provides a mechanism for the loss of bactericide from the surface due to erosion.

The covalent conjugation of bactericidal agents requires access to PL analogs that bear pendent functional groups. A number of copolylactides have been prepared that have functional side chains,[21,22] including analogs with unsaturated groups (alkenes[23,24,25,26] and alkynes[27,28,29,30,31]), as well as hydroxyl,[32,33,34,35,36,37] amino,[38,39] carboxylic acid,[40,41,42,43,44,45,46] thiol[47] and azido group.[48,49] Copolymers of PL that are substituted with azide or alkyne groups are

‡ The work presented in this chapter is carried in collaboration with Zhishuai Geng, a PhD candidate in Dr. M. G. Finn's research group. Antimicrobial assays were performed by Zhishuai.

valuable additions to this list of functional analogs by virtue of their ability to undergo facile coupling by azide-alkyne [3+2] cycloaddition "click" chemistry. Azide-substituted copolylactides however, have received less attention than alkyne-substituted analogs. Weck prepared an azide-substituted PL via ROP of an azido-substituted lactide at elevated temperature (above 100 °C).[48] Pugh reported the preparation of an azido-substituted poly(lactic acid-*co*-glycolic acid) by post-polymerization substitution of a bromo-substituted copolymer of poly(lactic acid-*co*-glycolic acid) with sodium azide.[49] However, this route resulted in inefficient substitution of the bromide and concomitant cleavage of the polyester backbone.

Here we describe a mild alternate route for the synthesis of an azide-substituted copolylactide (azido-PL, Figure 4.1.) by post-polymerization modification of a chlorine substituted PL with an azido-substituted alkanethiol. This pathway allows for the quantitative substitution of the chloro substituents without cleavage of the polyester backbone. This route avoids the need to handle azide salts or organic azides at high temperatures. We demonstrate the ability of azido-PL to undergo copper-catalyzed [3+2] cycloaddition reactions with alkynes and use this approach to couple a variety of quaternary ammonium salts to the polymer backbone. Many quaternary ammonium compounds (QACs) are antimicrobial by virtue of the combination of a cationic charge that interacts with the negatively charged lipophilic bacterial wall and the lipophilic alkyl chains which penetrate the lipid bilayer, thereby resulting in cell lysis.[50,51,52,53] The advantage of cationic compounds over other antimicrobial agents is their non-specific mode of action which makes it difficult for microbes to develop resistance towards them.[50, 54, 55] We report an exploration of the antimicrobial potency of the quaternary ammonium coupled PL.

4.2. RESULTS AND DISCUSSION

4.2.1. Azido-PL

Our exploration of the synthesis of azido-PL began with the addition of 3-azido-1-propanethiol to a copolymer of PL containing 5% α,β-unsaturated ester units (ene-PL) under basic conditions, Figure 4.1. We have previously described the synthesis of ene-PL by the base-promoted dehydrochlorination of chloro-PL.[26] Chloro-PL in turn was synthesized by the ring-opening copolymerization of L-lactide with chloromethylglycolide.

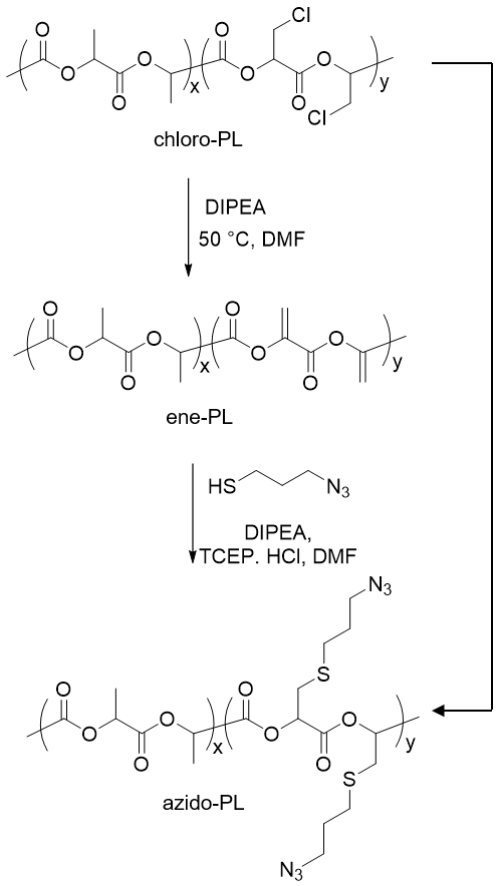

Figure 4.1. Synthesis of azido-PL. Dehydrochlorination and 1-4-conjugate addition of 3-azido-1-propanethiol to afford azido-PL.

Azido-PL was isolated by pouring the reaction mixture into MeOH and filtration to recover the precipitated material. The ^{1}H NMR spectrum of the precipitated copolymer shows the presence of a quartet at 5.15 ppm (signal *p*, Figure 4.2B) and a doublet at 1.57 ppm (signal *q*) which correspond to the methine and the methyl groups, respectively, of the lactide units of the copolymer. Four multiplets between 2.0 and 3.5 ppm (signals *b*, *c* and *d*, and *e* Figure 4.2B) can be assigned to the hydrogen atoms of the methylene units in the azidopropylthiomethyl side chain on the substituted-lactide units of the copolymer.

Comparison of the integrals of these signals with those of the methine quartet (signals *p* and *a*) shows that the product contained 5% of the functional comonomer, which is similar to the composition of the starting ene-PL. Complete disappearance of the signals corresponding to the alkene units of ene-PL (Figure 4.2A) confirmed the quantitative addition of the thiol under these conditions. The spectrum of azido-PL also shows the presence of a quartet at 4.3 ppm (signal *x*, Figure 4.2B) that can be assigned to the methine hydrogen atom at the hydroxyl end of the copolymer. Integration of this signal with respect to the quartet at 5.15 ppm for the methine hydrogen atoms of the polymer backbone suggests a number-average molecular weight (M_n) of 8 kDa (average degree of polymerization 110) which is comparable to that of the starting ene-PL, thereby demonstrating that the reaction conditions did not lead to cleavage of the polyester backbone. The presence of a signal at 2100 cm^{-1} in the IR spectrum of azido-PL, corresponding to the stretching vibrational frequency of azide functional group, further corroborated the success of the synthesis of azido-PL, Figure 4.3A.

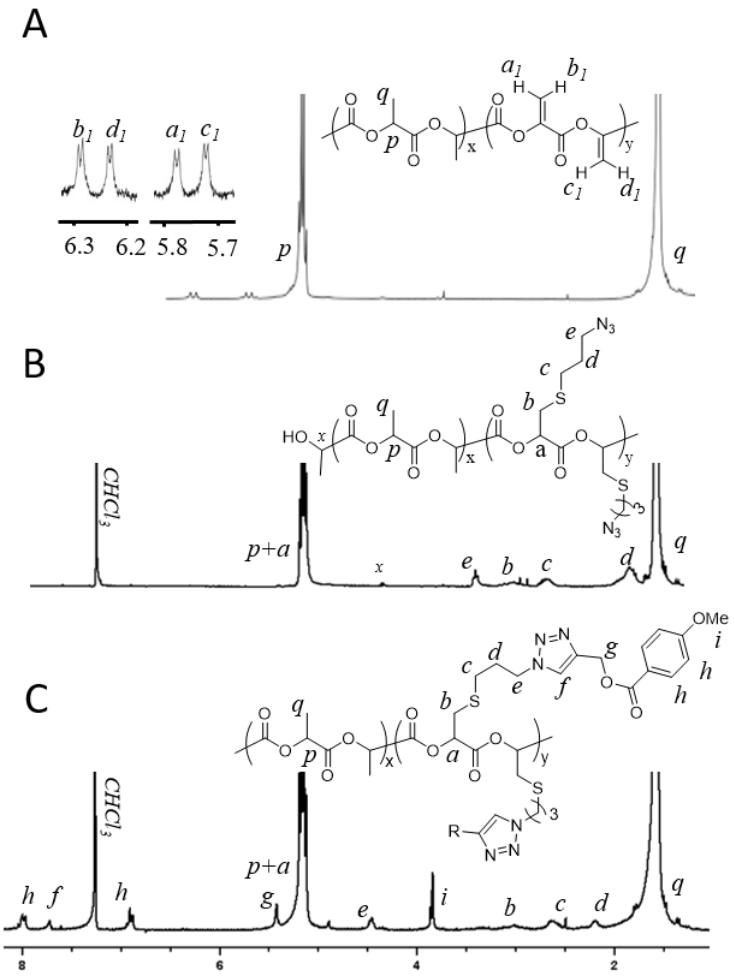

Figure 4.2. ^{1}H NMR spectra (300 MHz, $CDCl_3$). A, 5% ene-PL; B, 5% azido-PL; C, 5% adduct of azido-PL with propargyl-4-methoxybenzoate.

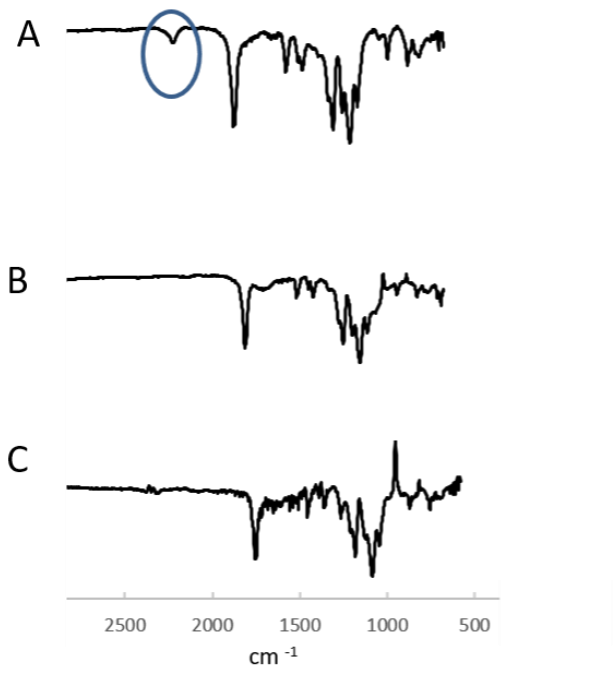

Figure 4.3. IR spectra A, 5% azido-PL; B, 5% dimethyloctylammonium-substituted PL; C, 5% trioctylammonium-substitutedPL.

Since both the synthesis of ene-PL by dehydrochlorination of chloro-PL and the addition of 3-azido-1-propanethiol to ene-PL were carried out in the presence of *N*,*N*-diisopropylethylamine (DIPEA), we explored a one-pot process to avoid the need to isolate ene-PL, Figure 4.1. Treatment of chloro-PL with DIPEA in DMF for 24 h followed by the addition of a 1:1 (mol/mol) mixture of 3-azido-1-propanethiol and DIPEA resulted in complete replacement of chlorine substituents to afford azido-PL. Some batches of chloro-PL underwent incomplete dehydrochlorination in 24 h in the presence of DIPEA but still resulted in a 5% azido-substituted copolymer after treatment with 3-azido-1-propanethiol. This could be because the conditions used for the second part of the procedure support both dehydrochlorination of any remaining chloro-PL along with the addition of thiol to the *in situ*-generated ene-PL or because of direct substitution of chloro-PL by the thiol. The ^{1}H NMR spectrum of the copolymer obtained by this one-pot reaction

showed the same signals as that of azido-PL obtained by addition of 3-azido-1-propanethiol to isolated ene-PL. Moreover, the molecular weight of the copolymer calculated by ^{1}H NMR chain end analysis matched that of azido-PL obtained by sequential dehydrochlorination and thiol addition. GPC analysis confirmed that the copolymer had an average number molecular weight (M_n) of around 7 kDa with a PDI of 1.4, Figure S-2.

Irrespective of the route used to synthesize azido-PL, the choice of amine base was critical to the success of the reaction because of the susceptibility of the polyester backbone to aminolysis. For example, use of Et_3N resulted in cleavage of the polyester backbone, as evident by the observation of an increase in the size of signal *x* in ^{1}H NMR spectrum of the copolymer, corresponding to an increase in the number of chain ends. However, use of Hunig's base under anhydrous conditions promoted both dehydrochlorination and thiol addition without any concomitant cleavage of the polyester chain. Since thiols have a propensity to oxidize in the presence of oxygen to form disulfides, the reaction was carried out under an inert atmosphere. As an additional precaution, tris(2-carboxyethyl)phosphine hydrochloride (TCEP-HCl), a reducing agent, was added to the reaction mixture to convert any oxidized disulfide back to its nucleophilic thiol form. Though TCEP HCl has a propensity to react with azides to form phosphazene which can undergo hydrolysis to afford an amine, quantitative formation of azido-PL as well as a lack of reduction in the molecular weight of the copolymer which could result due to the nucleophilicity of an amine suggests minimal formation of the amine side product, presumably because of the mild reaction conditions.

The thermal properties of azido-PL were characterized by differential scanning calorimetry (DSC). On heating, the semicrystalline copolymer underwent a glass transition at 37 °C, Figure 4.4. On further heating the copolymer cold crystallized at 82 °C and eventually melted at 153 °C.

Cooling of the copolymer resulted in its crystallization at 85 °C. Similar thermal transitions were obtained for subsequent cycles. The lowering of T_g and T_m compared to those of PL homopolymer (60-65 °C and 173-178 °C, respectively)[6] is consistent with the thermal transitions of other copolylactides that are substituted with side chains which act as a plasticizer and disrupt the packing of the polymer chains.

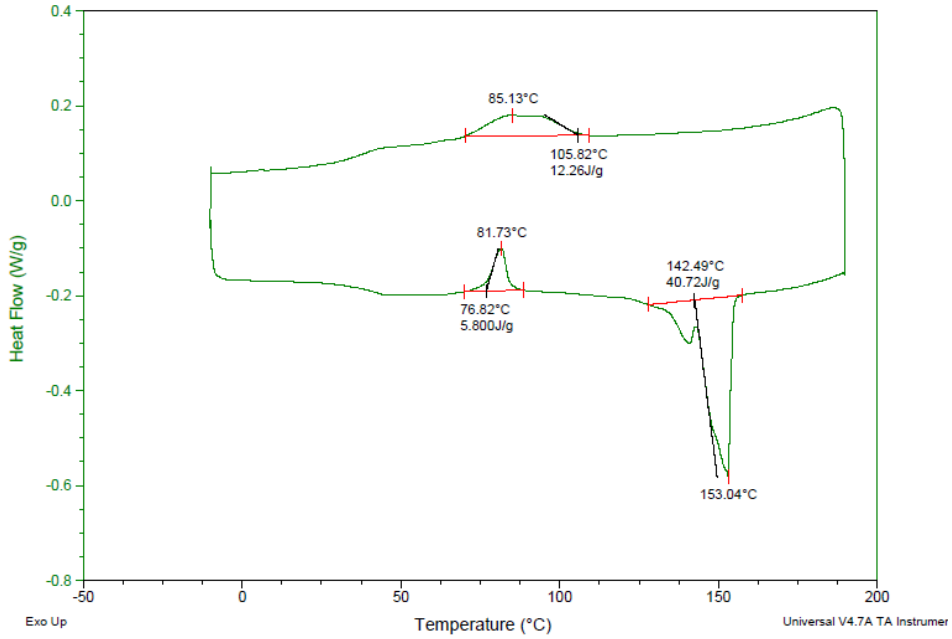

Figure 4.4. Differential Scanning Calorimetry (DSC) (5 °C/min, from -10 °C to 180 °C**)**. N_3-PL.

4.2.2. Azide-alkyne click chemistry

Azido-PL was treated with propargyl 4-methoxybenzoate in the presence of sodium ascorbate and a catalytic amount of $CuSO_4$ in DMF to explore its ability to undergo azide-alkyne click chemistry, Figure 4.5. The ^{1}H NMR spectrum of the copolymer shows a quartet and a doublet at 5.15 and 1.57 ppm, respectively, corresponding to the AX_3 spin system of the lactide unit of the copolymer, Figure 4.2C. Along with these peaks, the spectrum shows signals corresponding to the 4-methoxybenzoate group (2H doublets at 8.0 and 6.9 ppm, and a 3H singlet at 3.8 ppm). These peaks, in addition to the appearance of a singlet at 7.7 ppm corresponding to the triazole hydrogen,

indicated the success of the cycloaddition reaction. Integration of these peaks suggested the quantitative addition of alkyne to the pendent azide group under these reaction conditions.

The azide-alkyne cycloaddtion reaction performed under these conditions did not result in any cleavage of the polyester backbone. The molecular weight of the copolymer, as determined by both chain-end analysis using ^{1}H NMR spectroscopy and by GPC indicated a number-average molecular weight (M_n) of ~7 kDa, which was similar to that of the precursor azido-PL.

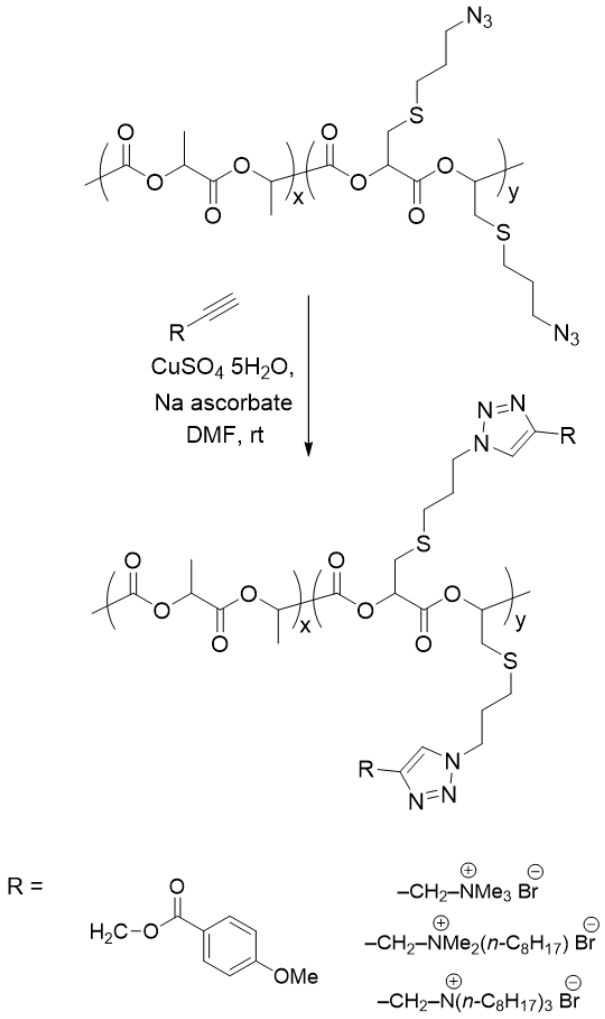

Figure 4.5. Azide-alkyne click chemistry. Conditions: $CuSO_4 \cdot 5H_2O$ (5 mol%), sodium ascorbate (10 mol%) and alkyne (10 eq relative to the moles of azide in azido-PL)

The thermal transitions of the copolymer as characterized by DSC suggest that the precipitated copolymer was highly crystalline, Figure 4.6. Upon heating, the copolymer underwent cold crystallization at 57 °C, with a release of an enthalpy of 7.6 J/g. Further heating resulted in the melting of the copolymer at 113 °C, with an absorption of 14.5 J/g. Upon cooling, the copolymer underwent crystallization at 70 °C with a release of 7.6 J/g. Similar thermal transitions were obtained for subsequent cycles, in which there is a good agreement between the sum of the enthalpies of crystallization and cold crystallization with the enthalpy for melting of the copolymer.

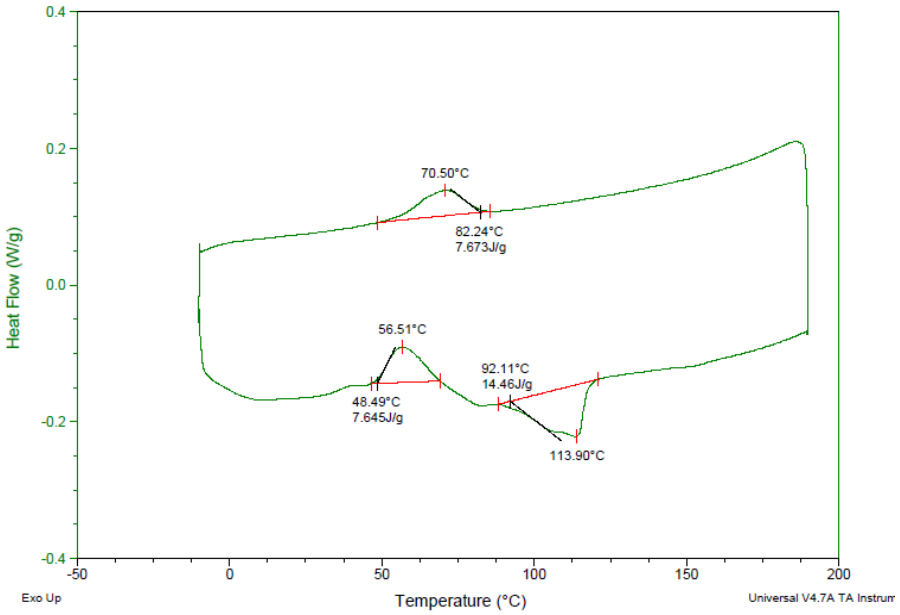

Figure 4.6. Differential Scanning Calorimetry (DSC) (5 °C/min, from -10 °C to 200 °C. 4-methoxybenzoate-substituted PL

Having successfully demonstrated the addition of propargyl 4-methoxybenzoate to the pendent functional groups of azido-PL, we explored the addition of quaternary ammonium-substituted alkynes, Figure 4. The reactions of the functional copolymer with *N*,*N*,*N*-trimethyl-*N*-propargylammonium bromide and *N*-octyl-*N*,*N*,-dimethyl-*N*-propargylammonium bromide were performed in DMF. The reaction with *N*,*N*,*N*-trioctyl-*N*-propargylammonium bromide was

performed in DMSO, which is a better solvent for the more hydrophobic trioctyl analogue. At the end of each reaction, the copolymers were precipitated by addition of the reaction mixture to MeOH. The solubility of the three cation-substituted copolymers was drastically different from that of azido-PL. The copolymers were insoluble in water, barely soluble in the solvents in which PL is highly soluble (e.g., CH_2Cl_2, and $CHCl_3$); and had low solubility in DMF and DMSO (solubility <5 mg/mL). We ascribe the change in the solubility of the copolymers to the charged nature of the PL chain bearing multiple ammonium-substituted side chains.

The presence of the signals in the ^{1}H NMR spectrum (Figure A-23 Appendix A) that correspond to the tetraalkyl ammonium-substituted unit of the copolymer, and the integration of these signals with respect to the hydrogen atom of the methine unit of the PL backbone, suggests quantitative addition of the alkyne and the formation of a polylactide in which 5% of the repeat units are substituted with the quaternary ammonium salt. The absence of the peaks for the propargyl ammonium bromide indicates that the precipitation of the copolymer in MeOH affords complete separation of the copolymer from any unreacted ammonium salt. The precipitated copolymers were also characterized using IR spectroscopy. The absence of a peak at 2100 cm^{-1} in the spectrum of the precipitated copolymer obtained after treatment with propargyl ammonium salts confirms that the reaction conditions result in complete consumption of azido groups, Figure 4.3B and 4.3C. Lack of a peak at ~2100 cm^{-1} for a carbon-carbon triple bond stretching vibration indicates the complete removal of unreacted ammonium salt. This result, together with the NMR, indicate the successful addition of the quaternary ammonium alkyne to azide-PL.

4.2.3. Antimicrobial assay: Polymer suspension

The antimicrobial efficacy of the cationic copolymers was evaluated by the following procedure. A suspension of copolymer in DMSO was treated with CupriSorb for 24 h to remove any residual copper from the cycloaddition reaction. The suspension was serially diluted with PBS buffer to provide various concentrations of polymer, the resulting suspensions containing no more than 2% DMSO. Well-dispersed suspensions of cationic copolymer were added to suspensions of *E. coli* and incubated for 4 h. The suspension was then loaded onto an agar plate and incubated for 24 h. A suspension of azido-PL and a solution of the alkyne in the same medium were used as controls, along with a 2 % DMSO solution in buffer.

N,*N*,*N*-Trimethylammonium-substituted PL and *N*,*N*-dimethyl-*N*-octylammonium-substituted PL did not display significant antimicrobial activity, while the *N*,*N*,*N*-trioctylammonium-substituted PL displayed potent activity. Enhanced activity of relatively hydrophobic quaternary ammonium compounds is a common observation, usually attributed to the ability of such molecules to better penetrate the bacterial membrane and facilitate cell lysis.[56] The *N*,*N*,*N*-trioctylammonium-substituted PL inhibited *E. coli* growth completely down to a polymer concentration of 31 μg/mL, Figure 4.7. The components (precursor azido-PL and *N*,*N*,*N*-trioctyl-*N*-propargyl alkyne) each exhibited no antimicrobial activity at the highest concentrations tested (1 mg/mL polymer and 80 μg/mL alkyne, Figure 4.7). Arraying the ammonium species on the polymer support can present high local concentrations of positive charge and allow the hydrophobic polymer to reinforce the ability of the alkylammonium chains to disrupt the lipid bilayer of the microbe.

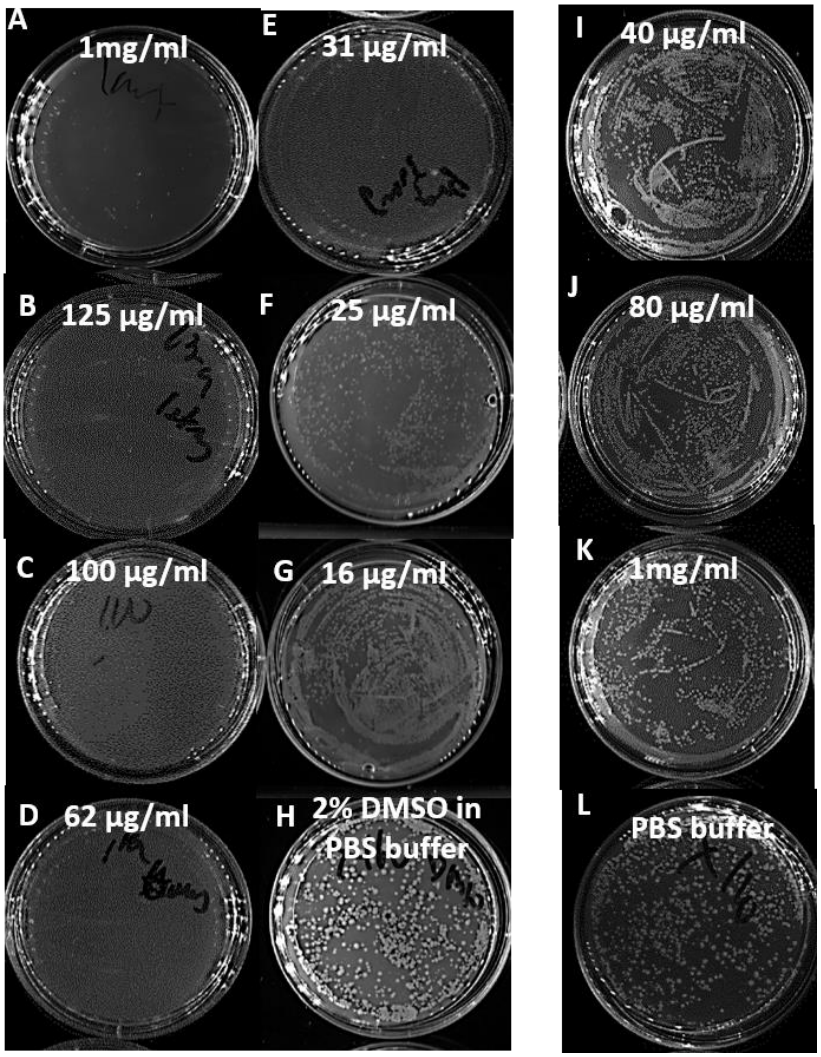

Figure 4.7. Agar plate obtained post treatment of *E. coli* with-A to G, increasing concentration of trioctylammonium-substituted PLA; H, 2% DMSO solution, I-J trioctylpropargyl ammonium bromide; K, azido-PL; L, PBS buffer.

4.2.4. Antimicrobial efficacy: Polymer surfaces

Since our overall goal was to develop antimicrobial PL materials for packaging and coating applications, we evaluated the antimicrobial efficacy of films of copolymers with a variety of bacterial strains. Films of *N,N,N*-trioctylammonium-substituted PL were prepared by drop casting a DMSO solution of the polymer onto glass substrates. The efficacy of the films was tested against two Gram-negative bacteria (*E. coli*, *P. aeruginosa*), as these are generally regarded as

being harder to kill with cationic materials. Control experiments were performed with unfunctionalized PL that had been treated with the alkyne, $CuSO_4$ and sodium ascorbate. The cationic copolymeric films displayed antimicrobial efficacy against both bacterial strains, Figure 4.8. The absence of bactericidal activity of the control material showed that covalent attachment of the ammonium salt to the copolymer is required for bactericidal behavior.

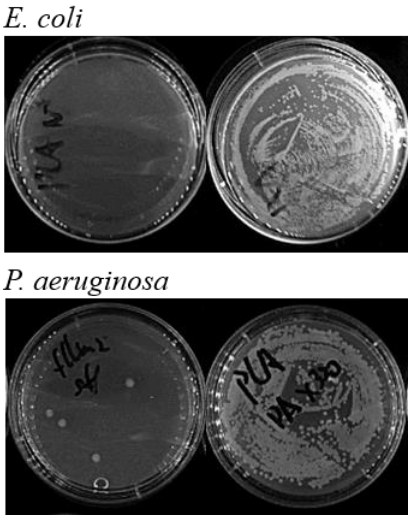

Figure 4.8. Agar plate loaded with solutions obtained from antimicrobial assay. (Films). trioctylammonium-substituted films (left); control films of unfunctionalized PLA treated with alkyne, $CuSO_4$, and sodium ascorbate, followed by the standard isolation and washing procedure (right).

The cationic films were challenged with increasing concentrations of *E. coli* cells, Figure 4.9. The films displayed antimicrobial activity against a bacterial concentration as high as 5×10^8 cfu/mL, with a killing efficiency of 2.5×10^8 cfu/cm^2. This is higher than the potency of an antimicrobial glass surface bearing quaternized poly(2-(*N*,*N*-dimethylamino)ethyl methacrylate) polymer brushes, which displayed incomplete inhibition of bacterial growth when challenged with $<10^8$ cfu/cm^2 *E. coli*.[57-58] To test the minimum exposure time required for the films to kill bacteria, the films were immersed in a bacterial suspension and assayed at different time points. The films

were able to kill all the cultured bacteria within 1 h, but not within 30 min, Figure 4.10. This was also observed at a lower initial bacterial concentration (6.4 x 10^6 cfu/mL).

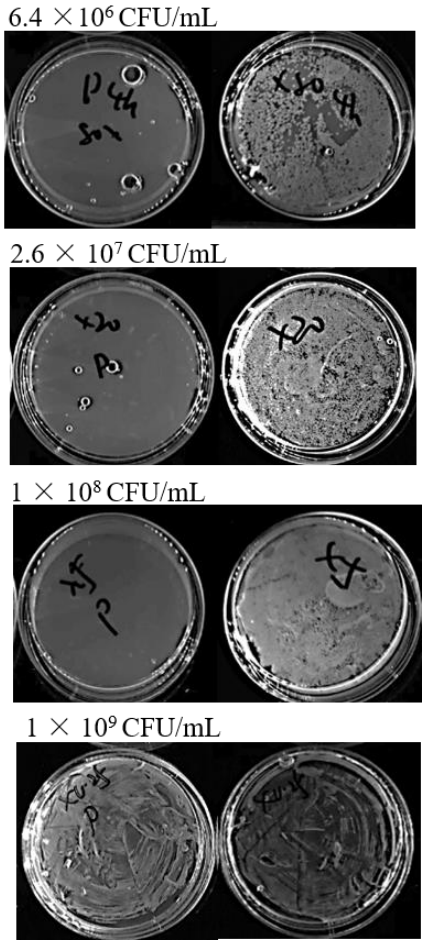

Figure 4.9. Agar plate post treatment of increasing concentration of *E. coli* with the films for 4h. trioctylammonium-substituted films (left); and control PLA films (right).

The films were found to retain their antimicrobial activity in a second cycle of exposure. Thus, after eradication of a sample of *E. coli* as above, the films were extensively rinsed with PBS buffer and sonicated in buffer for a few minutes to remove any adhered bacteria. Upon immersion to another suspension of *E. coli*, the resulting films retained their full antimicrobial efficacy (complete eradication within one hour, data not shown).

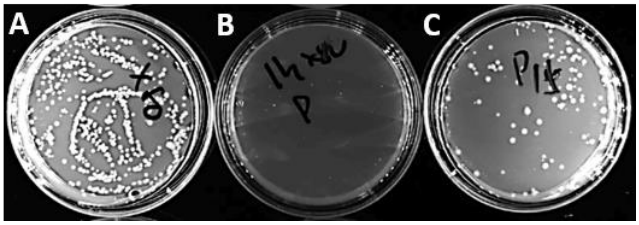

Figure 4.10. Agar plate post treatment of films with 6.4 ×10^6 CFU/ml *E. coli* A, Control PLA film treated for 1 h; B, Trioctylammonium-substituted PL film treated for 1h; C, Trioctylammonium-substituted PL film treated for 30 min.

4.2.5. Toxicity to mammalian cells

Hela cells were treated with different concentrations of the well-dispersed copolymeric suspensions to determine the toxicity of the insoluble copolymer against mammalian cells, Figure 4.11. A 125 µg/mL suspension of copolymer resulted in killing approximately 90% of the mammalian cell population (MIC_{90}). This is approximately five times higher than the MIC_{90} towards bacteria cells. With other conditions the same, considering that the initial seeding concentration of the bacteria was three orders of magnitude higher than that of the mammalian cells, and the bacterial cells have a propensity to grow at a significantly faster rate, this assay provides a preliminary demonstration of the selectivity of the polymer towards bacteria.

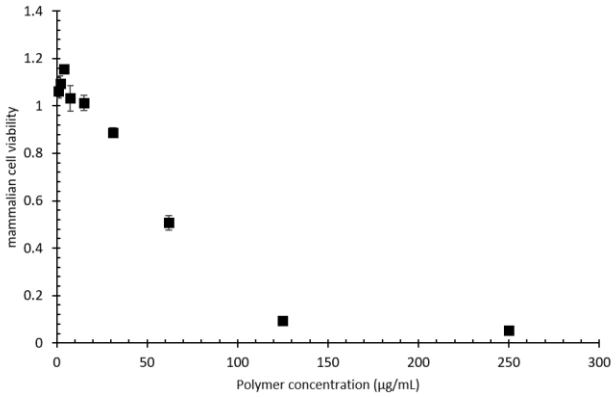

Figure 4.11. Mammalian cell viability. Hela cells treated with increasing concentration of cationic PL suspension.

4.3. EXPERIMENTAL SECTION

4.3.1. Materials and methods

The following reagents were obtained from Sigma Aldrich and were used without further purification: propargyl alcohol, 4-methoxybenzoyl chloride, *N*,*N*-diisopropylethylamine (DIPEA) and anhydrous DMF. Copper(II) sulfate was obtained from Fisher Scientific company, sodium ascorbate from Alfa Aesar and tris(2-carboxyethyl)phosphine hydrochloride (TCEP-HCl) from Pierce. All other solvents were purchased from VWR. Flash chromatography silica gel was obtained from Dynamic Adsorbents, Inc. Poly(lactide-*co*-methylene glycolide) (ene-PL) and poly(lactide-*co*-chlorolactide) (chloro-PL) were prepared following procedures described elsewhere. *N*,*N*,*N*-trimethyl-*N*-propargylammonium bromide[59] and *N*,*N*-dimethyl-*N*-octyl-*N*-propargylammonium bromide[60] were prepared following procedures described elsewhere. 3-Azido-1-propanethiol was synthesized by deacetylation of 3-azidopropylthioacetate that was obtained from Sigma Aldrich.

NMR spectra were recorded using a Varian Mercury spectrometer (^{1}H NMR, 300 MHz; ^{13}C, 75 MHz). IR spectra were recorded using a Shimadzu IRAffinity-1 spectrometer. Differential scanning calorimetry (DSC) (3 cycles, -10° C to 200° C, at 5° C/min) was performed using a Q200 Differential Scanning Calorimeter. Gel permeation chromatography was performed on a Shimadzu chromatograph setup using THF as an eluent; chromatographs were calibrated against polystyrene standards. UV-vis spectra were recorded using a Varioskan Flash plate reader (Thermo Fisher, Waltham, MA).

4.3.2. Synthesis

4.3.2.1. Progargyl 4-methoxybenzoate

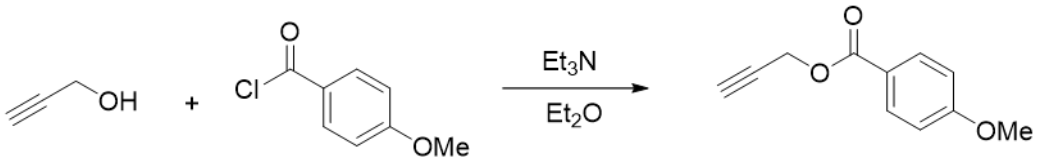

The target compound was synthesized as described elsewhere.[61,62] A solution of 4-methoxybenzoyl chloride (5.60 mL, 41.4 mmol) in Et_2O was added dropwise over a period of 30 min to a solution of propargyl alcohol (2.00 g, 35.6 mmol) and Et_3N (6.30 mL, 45.3 mmol) in Et_2O immersed in a salt-ice bath. The solution was stirred for 1 h at -20 °C and at room temperature for 15 h. The mixture was filtered and the filtrate was washed with 6% aqueous Na_2CO_3 solution. The organic extract was separated, dried over $MgSO_4$, filtered and the solvent was removed under reduced pressure. The residue was dissolved in EtOAc and the solution was passed through a silica plug with (1:5 EtOAc/hexane) as eluent. The eluent was collected and the solvent was removed under reduced pressure to afford the product as a colorless solid. ^{1}H NMR (300 MHz, $CDCl_3$): δ 8.01 (d, *J* = 8.9 Hz, 2 H, $Ar_{2,6}$), 6.92 (d, *J* = 8.9 Hz, 2 H, $Ar_{3,5}$), 4.89 (d, *J* = 2.5 Hz, 2 H, O-CH_2), 3.86 (s, 3 H, OCH_3), 2.50 (t, *J* = 2.5 Hz, 1 H, C≡CH).

4.3.2.2. 95:5 Poly(lactide-co-(3-azido-1-propyl)thiolactide) (azido-PL) from ene-PL

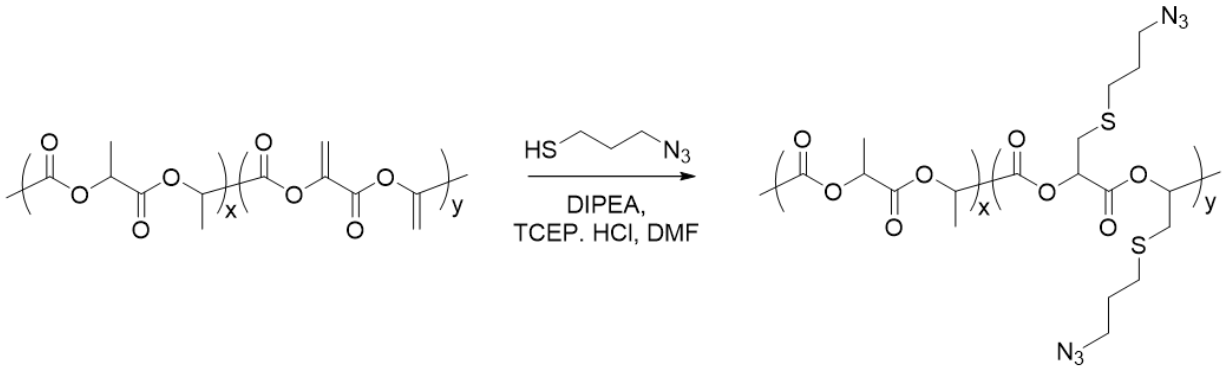

A solution of 3-azido-1-propanethiol (80 mg, 0.67 mmol, 10 equivalents per unsaturated ester in ene-PL), TCEP-HCl (97 mg, 0.34 mmol) and DIPEA (118 µL, 0.670 mmol) in DMF (2 mL) was stirred at room temperature for 2 h. A solution of ene-PL (100 mg) in DMF (2 mL) was added. The mixture was stirred at room temperature under Ar for 3 d. The solvent was removed under reduced pressure to yield a yellow residue. The residue was dissolved in minimum amount of CH_2Cl_2 (approx. 1 mL) and this solution was added to MeOH (20 mL) with stirring. The precipitated solid was collected by filtration and dried under reduced pressure to yield azido-PL as a colorless solid. ^{1}H NMR (300 MHz, $CDCl_3$): δ 5.15 (q, J = 6 Hz, 20 H, lactide and substituted lactide CH), 3.41 (m, 2 H, CH_2N_3), 2.8-3.2 (m, 2 H, CH_2 of substituted lactide), 2.6-2.8 (m, 2 H, SCH_2), 1.86-2.1 (m, 2 H, β-CH_2), 1.57 (d, J = 6 Hz, 57 H, lactide CH_3). IR: 3000-2840 (w, C–H, str.), 2100 (m, N_3 str.), 1740 (s, C=O, str.), 1190 (s, C–O str.) cm^{-1}.

4.3.2.3. 95:5 Poly(lactide-co-(3-azido-1-propyl)thiolactide) (azido-PL) in one-pot synthesis from chloro-PL

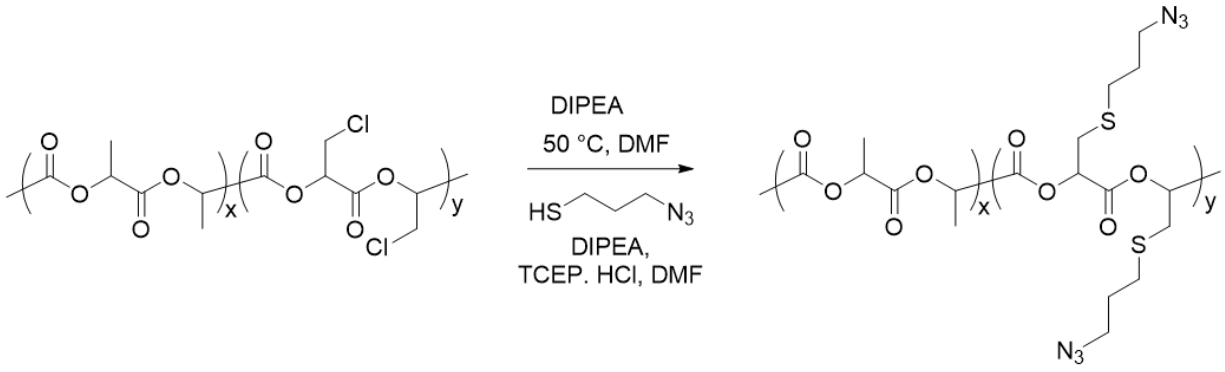

A solution of 3-azido-1-propanethiol (80 µL, 0.67 mmol, 10 equivalents relative to chloride in chloro-PL), TCEP-HCl (97 mg, 0.34 mmol) and DIPEA (118 µL, 0.670 mmol), in DMF (2 mL) was stirred for 4 h at room temperature. In a separate flask, a solution of 5% chloro-PL (100 mg) and DIPEA (12µL, 68 µmol) in DMF (2 mL) was stirred at 50 °C for 24 h. The solutions were combined and the mixture was stirred for 3 d. The solvent was removed under reduced pressure, and the solid residue was dissolved in minimum amount of CH_2Cl_2. The solution was added slowly to MeOH (15 mL) and the precipitated colorless solid was filtered and dried under vacuum. The collected material had the same spectral characteristics as that prepared by addition to ene-PL.

4.3.2.4. Azide-alkyne cycloaddition: General procedure

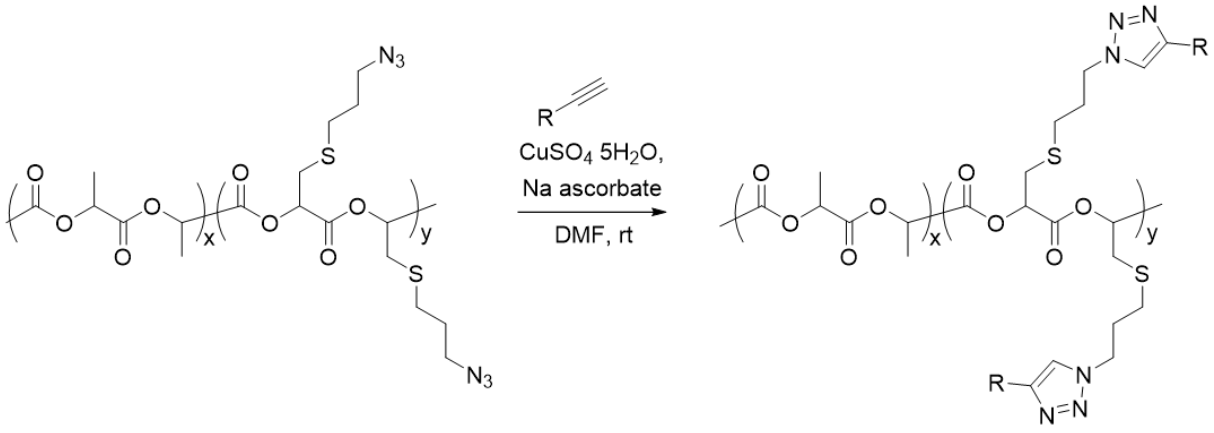

A solution of azido-PL (100 mg), $CuSO_4.\ 5H_2O$ (5 mol%), sodium ascorbate (10 mol%) and alkyne (10 eq relative to the moles of azide in azido-PL) in DMF (2 mL) was degassed by three freeze-pump-thaw cycles. The flask was backfilled with Ar and the mixture was stirred at room temperature for 12 hours. The mixture was poured into MeOH (20 mL) under stirring and the precipitated solid was isolated by filtration and dried overnight to yield quaternary ammonium-substituted PL as a colorless solid.

Propargyl-4-methoxybenzoate adduct. ^{1}H NMR (300 MHz, $CDCl_3$): δ 8.0 (d, *J* = 8.9 Hz, 2 H, $Ar_{2,6}$ CH), 7.7 (s, 1 H, triazole CH) 6.95 (d, *J* = 8.9, 2 H, $Ar_{3,5}$ CH), 5.4 (s, 2 H, $COOCH_2$), 5.15 (q, *J* = 7 Hz, 20H, lactide and substituted-lactide CH), 4.41 (m, 2 H, CH_2 adjacent to the triazole ring), 3.81 (s, 3 H, OMe), 2.8-3.2 (m, 2 H, CH_2 of substituted lactide), 2.5-2.7 (m, 2 H, SCH_2), 2.1-2.2 (m, 2 H, SCH_2CH_2), 1.57 (d, *J* = 7 Hz, 60 H, lactide CH_3).

N,N,N-Trimethyl-N-propargylammonium bromide adduct. IR 2950-2820 (w, sp^3 C−H str.), 1755 (s, C=O str.), 1452 (w, sp^3 C−H, bend), 1355 (w, sp^3 C−H, bend), 1180 (s, C−O str.), 1080 (s, C−O, str.) $cm.^{-1}$

N,N-Dimethyl-N-octyl-N-propargylammonium bromide adduct. IR 2940-2840 (w, sp^3 C−H str.), 1755 (s, C=O str.), 1457 (w, sp^3 C−H, bend), 1357 (w, sp^3 C−H, bend), 1186 (s, C−O str.), 1080 (s, C−O, str.) $cm.^{-1}$

N,N,N-Trioctyl-N-propargylammonium bromide adduct. IR 2950-2820 (w, sp^3 C−H str.), 1749 (s, C=O str.), 1456 (w, sp^3 C−H, bend), 1357 (w, sp^3 C−H, bend), 1180 (s, C−O str.), 1085 (s, C−O, str.) $cm.^{-1}$

4.3.2.5. Antimicrobial assay

Assays were performed by Zhishuai Geng, a PhD. Candidate in M. G. Finn's research group. Bacteria suspensions (*E. coli*) were grown in Mueller-Hinton Broth (MHB) overnight at 37 °C. The resulting culture was used to inoculate a second culture in 2 mL of MHB medium until an optical density of 0.8 was reached at 600 nm was obtained. The bacteria were collected by centrifugation at 4,000 x g for 3 min at 4 °C, washed with sterile PBS (pH 7.4) and suspended in PBS to get a specific final concentration. Polymer films (0.01-0.04 cm^2) were prepared by drop-casting a 1 mg/mL solution of the copolymer in DMSO on a glass cover slip. Polymer suspension were prepared by serial dilution of the copolymer suspension in DMSO with PBS buffer. The films or a suspension of the copolymer was added to the suspension of bacteria and the vial was shaken for 0.5 to 4 h on a rocker. A 25 µL aliquot of the suspension was spread onto a layer of LB medium containing 0.8% agar (previously autoclaved and cooled to 37 °C) in a sterile Petri dish. Bacterial colonies were counted after incubation overnight at 37 °C. The MIC_{90} was defined as the minimum concentration of the polymer suspension at which the colony forming unit (CFU) number on the agar plate reached no more than 10 % of the control plate.

4.3.2.6. Toxicity of materials made from copolymer towards mammalian cells

Assay was performed by Zhishuai Geng, a PhD. Candidate in M. G. Finn's research group. Approximately 1×10^4 Hela cells/well in 100 μL of complete growth media were plated in the wells of a 96-well plate and allowed to adhere overnight at 37 °C. After 24 hours, media in each well was replenished with polymer suspension at specific concentration in media. Control wells were only treated with equal volume of PBS buffer. The cells were incubated for 4 h. Cells were then assayed for viability by using a standard MTT assay. MTT (3-(4,5-dimethylthiazol-2-yl)-2,5-diphenyltetrazolium bromide, 5 mg/mL, 25 μL per well) was added, and the solutions were incubated at 37 °C for approximately 1 h (the assay was stopped when accumulated purple formazan crystals were visible in the control wells). The medium was carefully aspirated with multi-channel pipettes, and DMSO was added (200 μL per well) to dissolve the purple MTT–formazan crystals. The absorbance of the dissolved formazan was quantified at 570 nm by using a UV-Vis plate reader, and cell viability was determined as a fraction of absorbance relative to control wells.

4.4. CONCLUSIONS

We have described a convenient synthesis of an azido-substituted PL by the reaction of 3-azido-1-propanethiol with an α,β-unsaturated PL (ene-PL) or chloro-substituted PL (Cl-PL), respectively. We have demonstrated the addition of quaternary ammonium-substituted alkynes onto azido-PL and evaluated the antimicrobial efficacy of the resulting ammonium-substituted PL analogs against two gram-negative bacterial strains. The copolymer displayed potent antimicrobial efficacy with substitution of just 5% of the repeat units of PL with trioctylammonium bromide. This provides promise for the development of PL as a coating or packaging material to maintain a sterile environment and for imparting antimicrobial activity to PL-containing biomedical devices.

4.5. REFERENCES

1. Lasprilla, A. J. R.; Martinez, G. A. R.; Lunelli, B. H.; Jardini, A. L.; Filho, R. M., Poly-lactic acid synthesis for application in biomedical devices — A review. *Biotechnology Advances* **2012,** *30* (1), 321-328.
2. Inkinen, S.; Hakkarainen, M.; Albertsson, A.-C.; Södergård, A., From Lactic Acid to Poly(lactic acid) (PLA): Characterization and Analysis of PLA and Its Precursors. *Biomacromolecules* **2011,** *12* (3), 523-532.
3. Busolo, M. A.; Fernandez, P.; Ocio, M. J.; Lagaron, J. M., Novel silver-based nanoclay as an antimicrobial in polylactic acid food packaging coatings. *Food Additives & Contaminants: Part A* **2010,** *27* (11), 1617-1626.
4. Hu, W.; Huang, Z.-M., Biocompatibility of braided poly(L-lactic acid) nanofiber wires applied as tissue sutures. *Polymer International* **2010,** *59* (1), 92-99.
5. Huh, B. K.; Kim, B. H.; Kim, S.-N.; Park, C. G.; Lee, S. H.; Kim, K. R.; Heo, C. Y.; Choy, Y. B., Surgical suture braided with a diclofenac-loaded strand of poly(lactic-co-glycolic acid) for local, sustained pain mitigation. *Materials Science and Engineering: C* **2017,** *79*, 209-215.
6. Middleton, J. C.; Tipton, A. J., Synthetic biodegradable polymers as orthopedic devices. *Biomaterials* **2000,** *21* (23), 2335-2346.
7. Eppley, B. L.; Morales, L.; Wood, R.; Pensler, J.; Goldstein, J.; Havlik, R. J.; Habal, M.; Losken, A.; Williams, J. K.; Burstein, F.; Rozzelle, A. A.; Sadove, A. M., Resorbable PLLA-PGA plate and screw fixation in pediatric craniofacial surgery: clinical experience in 1883 patients. *Plastic and Reconstructive Surgery* **2004,** *114* (4), 850-6; 857.
8. Gupta, B.; Revagade, N.; Hilborn, J., Poly(lactic acid) fiber: An overview. *Progress in Polymer Science* **2007,** *32* (4), 455-482.
9. Conti, B.; Pavanetto, F.; Genta, I., Use of polylactic acid for the preparation of microparticulate drug delivery systems. *Journal of microencapsulation* **1992,** *9* (2), 153-66.
10. Hyon, S. H., Biodegradable poly (lactic acid) microspheres for drug delivery systems. *Yonsei Medical Journal* **2000,** *41* (6), 720-734.
11. Rancan, F.; Papakostas, D.; Hadam, S.; Hackbarth, S.; Delair, T.; Primard, C.; Verrier, B.; Sterry, W.; Blume-Peytavi, U.; Vogt, A., Investigation of Polylactic Acid (PLA) Nanoparticles as Drug Delivery Systems for Local Dermatotherapy. *Pharmaceutical Research* **2009,** *26* (8), 2027-2036.
12. Su, L.; Yu, Y.; Zhao, Y.; Liang, F.; Zhang, X., Strong Antibacterial Polydopamine Coatings Prepared by a Shaking-assisted Method. *Scientific Reports* **2016,** *6*, 24420.
13. Wu, Y.; Qin, Y.; Yuan, M.; Li, L.; Chen, H.; Cao, J.; Yang, J., Characterization of an antimicrobial poly(lactic acid) film prepared with poly(ε-caprolactone) and thymol for active packaging. *Polymers for Advanced Technologies* **2014,** *25* (9), 948-954.

14. Tawakkal, I. S. M. A.; Cran, M. J.; Miltz, J.; Bigger, S. W., A Review of Poly(Lactic Acid)-Based Materials for Antimicrobial Packaging. *Journal of Food Science* **2014,** *79* (8), R1477-R1490.

15. El Habnouni, S.; Darcos, V.; Garric, X.; Lavigne, J.-P.; Nottelet, B.; Coudane, J., Mild Methodology for the Versatile Chemical Modification of Polylactide Surfaces: Original Combination of Anionic and Click Chemistry for Biomedical Applications. *Advanced Functional Materials* **2011,** *21* (17), 3321-3330.

16. Sardo, C.; Nottelet, B.; Triolo, D.; Giammona, G.; Garric, X.; Lavigne, J.-P.; Cavallaro, G.; Coudane, J., When Functionalization of PLA Surfaces Meets Thiol–Yne Photochemistry: Case Study with Antibacterial Polyaspartamide Derivatives. *Biomacromolecules* **2014,** *15* (11), 4351-4362.

17. El Habnouni, S.; Lavigne, J.-P.; Darcos, V.; Porsio, B.; Garric, X.; Coudane, J.; Nottelet, B., Toward potent antibiofilm degradable medical devices: A generic method for the antibacterial surface modification of polylactide. *Acta Biomaterialia* **2013,** *9* (8), 7709-7718.

18. Gutierrez-Villarreal, M. H.; Ulloa-Hinojosa, M. G.; Gaona-Lozano, J. G., Surface functionalization of poly(lactic acid) film by UV-photografting of N-vinylpyrrolidone. *Journal of Applied Polymer Science* **2008,** *110* (1), 163-169.

19. Lunt, J., Large-scale production, properties and commercial applications of polylactic acid polymers. *Polymer Degradation and Stability* **1998,** *59* (1), 145-152.

20. Farah, S.; Anderson, D. G.; Langer, R., Physical and mechanical properties of PLA, and their functions in widespread applications — A comprehensive review. *Advanced Drug Delivery Reviews* **2016,** *107*, 367-392.

21. Pounder, R. J.; Dove, A. P., Towards poly(ester) nanoparticles: recent advances in the synthesis of functional poly(ester)s by ring-opening polymerization. *Polymer Chemistry* **2010,** *1* (3), 260-271.

22. Yu, Y.; Zou, J.; Cheng, C., Synthesis and biomedical applications of functional poly([small alpha]-hydroxyl acid)s. *Polymer Chemistry* **2014,** *5* (20), 5854-5872.

23. Leemhuis, M.; Akeroyd, N.; Kruijtzer, J. A. W.; van Nostrum, C. F.; Hennink, W. E., Synthesis and characterization of allyl functionalized poly(α-hydroxy)acids and their further dihydroxylation and epoxidation. *European Polymer Journal* **2008,** *44* (2), 308-317.

24. Jing, F.; Hillmyer, M. A., A Bifunctional Monomer Derived from Lactide for Toughening Polylactide. *Journal of the American Chemical Society* **2008,** *130* (42), 13826-13827.

25. Fiore, G. L.; Jing, F.; Young, J. V. G.; Cramer, C. J.; Hillmyer, M. A., High Tg aliphatic polyesters by the polymerization of spirolactide derivatives. *Polymer Chemistry* **2010,** *1* (6), 870-877.

26. Kalelkar, P. P.; Alas, G. R.; Collard, D. M., Synthesis of an Alkene-Containing Copolylactide and Its Facile Modification by the Addition of Thiols. *Macromolecules* **2016,** *49* (7), 2609-2617.

27. Zhang, Z.; Yin, L.; Xu, Y.; Tong, R.; Lu, Y.; Ren, J.; Cheng, J., Facile Functionalization of Polyesters through Thiol-yne Chemistry for the Design of Degradable, Cell-Penetrating and Gene Delivery Dual-Functional Agents. *Biomacromolecules* **2012,** *13* (11), 3456-3462.

28. Jiang, X.; Vogel, E. B.; Smith, M. R.; Baker, G. L., "Clickable" Polyglycolides: Tunable Synthons for Thermoresponsive, Degradable Polymers. *Macromolecules* **2008,** *41* (6), 1937-1944.

29. Yu, Y.; Zou, J.; Yu, L.; Ji, W.; Li, Y.; Law, W.-C.; Cheng, C., Functional Polylactide-g-Paclitaxel–Poly(ethylene glycol) by Azide–Alkyne Click Chemistry. *Macromolecules* **2011,** *44* (12), 4793-4800.

30. Yu, Y.; Chen, C.-K.; Law, W.-C.; Mok, J.; Zou, J.; Prasad, P. N.; Cheng, C., Well-Defined Degradable Brush Polymer–Drug Conjugates for Sustained Delivery of Paclitaxel. *Molecular Pharmaceutics* **2013,** *10* (3), 867-874.

31. Zhang, Q.; Ren, H.; Baker, G. L., Synthesis and click chemistry of a new class of biodegradable polylactide towards tunable thermo-responsive biomaterials. *Polymer Chemistry* **2015,** *6* (8), 1275-1285.

32. Kolitz, M.; Cohen-Arazi, N.; Hagag, I.; Katzhendler, J.; Domb, A. J., Biodegradable Polyesters Derived from Amino Acids. *Macromolecules* **2009,** *42* (13), 4520-4530.

33. Samadi, N.; van Nostrum, C. F.; Vermonden, T.; Amidi, M.; Hennink, W. E., Mechanistic Studies on the Degradation and Protein Release Characteristics of Poly(lactic-co-glycolic-co-hydroxymethylglycolic acid) Nanospheres. *Biomacromolecules* **2013,** *14* (4), 1044-1053.

34. Leemhuis, M.; van Nostrum, C. F.; Kruijtzer, J. A. W.; Zhong, Z. Y.; ten Breteler, M. R.; Dijkstra, P. J.; Feijen, J.; Hennink, W. E., Functionalized Poly(α-hydroxy acid)s via Ring-Opening Polymerization: Toward Hydrophilic Polyesters with Pendant Hydroxyl Groups. *Macromolecules* **2006,** *39* (10), 3500-3508.

35. Stayshich, R. M.; Weiss, R. M.; Li, J.; Meyer, T. Y., Periodic Incorporation of Pendant Hydroxyl Groups in Repeating Sequence PLGA Copolymers. *Macromolecular Rapid Communications* **2011,** *32* (2), 220-225.

36. Saulnier, B.; Ponsart, S.; Coudane, J.; Garreau, H.; Vert, M., Lactic acid-based functionalized polymers via copolymerization and chemical modification. *Macromolecular bioscience* **2004,** *4* (3), 232-7.

37. Noga, D. E.; Petrie, T. A.; Kumar, A.; Weck, M.; García, A. J.; Collard, D. M., Synthesis and Modification of Functional Poly(lactide) Copolymers: Toward Biofunctional Materials. *Biomacromolecules* **2008,** *9* (7), 2056-2062.

38. Gerhardt, W. W.; Noga, D. E.; Hardcastle, K. I.; García, A. J.; Collard, D. M.; Weck, M., Functional Lactide Monomers: Methodology and Polymerization. *Biomacromolecules* **2006,** *7* (6), 1735-1742.

39. Lim, Y.-b.; Kim, C.-h.; Kim, K.; Kim, S. W.; Park, J.-s., Development of a Safe Gene Delivery System Using Biodegradable Polymer, Poly[α-(4-aminobutyl)-l-glycolic acid]. *Journal of the American Chemical Society* **2000,** *122* (27), 6524-6525.

40. Nottelet, B.; Di Tommaso, C.; Mondon, K.; Gurny, R.; Möller, M., Fully biodegradable polymeric micelles based on hydrophobic- and hydrophilic-functionalized poly(lactide) block copolymers. *Journal of Polymer Science Part A: Polymer Chemistry* **2010,** *48* (15), 3244-3254.

41. Kimura, Y.; Shirotani, K.; Yamane, H.; Kitao, T., Ring-opening polymerization of 3(S)-[(benzyloxycarbonyl)methyl]-1,4-dioxane-2,5-dione: a new route to a poly(.alpha.-hydroxy acid) with pendant carboxyl groups. *Macromolecules* **1988,** *21* (11), 3338-3340.

42. Thillaye du Boullay, O.; Bonduelle, C.; Martin-Vaca, B.; Bourissou, D., Functionalized polyesters from organocatalyzed ROP of gluOCA, the O-carboxyanhydride derived from glutamic acid. *Chemical Communications* **2008,** (15), 1786-1788.

43. Ouchi, T.; Fujino, A., Synthesis of poly(α-malic acid) and its hydrolysis behavior in vitro. *Die Makromolekulare Chemie* **1989,** *190* (7), 1523-1530.

44. Pounder, R. J.; Dove, A. P., Synthesis and Organocatalytic Ring-Opening Polymerization of Cyclic Esters Derived from l-Malic Acid. *Biomacromolecules* **2010,** *11* (8), 1930-1939.

45. Pounder, R. J.; Fox, D. J.; Barker, I. A.; Bennison, M. J.; Dove, A. P., Ring-opening polymerization of an O-carboxyanhydride monomer derived from l-malic acid. *Polymer Chemistry* **2011,** *2* (10), 2204-2212.

46. du Boullay, O. T.; Saffon, N.; Diehl, J.-P.; Martin-Vaca, B.; Bourissou, D., Organo-Catalyzed Ring Opening Polymerization of a 1,4-Dioxane-2,5-dione Deriving from Glutamic Acid. *Biomacromolecules* **2010,** *11* (8), 1921-1929.

47. Kalelkar, P. P.; Collard, D. M., Thiol-substituted copolylactide: synthesis, characterization and post-polymerization modification using thiol-ene chemistry. *Polym. Chem.* **2018,** *9* (8), 1022-1031.

48. Borchmann, D. E.; ten Brummelhuis, N.; Weck, M., GRGDS-Functionalized Poly(lactide)-graft-poly(ethylene glycol) Copolymers: Combining Thiol–Ene Chemistry with Staudinger Ligation. *Macromolecules* **2013,** *46* (11), 4426-4431.

49. Wright, C.; Banerjee, A.; Yan, X.; Storms-Miller, W. K.; Pugh, C., Synthesis of Functionalized Poly(lactic acid) Using 2-Bromo-3-hydroxypropionic Acid. *Macromolecules* **2016,** *49* (6), 2028-2038.

50. Jennings, M. C.; Minbiole, K. P. C.; Wuest, W. M., Quaternary Ammonium Compounds: An Antimicrobial Mainstay and Platform for Innovation to Address Bacterial Resistance. *ACS Infectious Diseases* **2015,** *1* (7), 288-303.

51. Chakraborty, S.; Liu, R.; Hayouka, Z.; Chen, X.; Ehrhardt, J.; Lu, Q.; Burke, E.; Yang, Y.; Weisblum, B.; Wong, G. C. L.; Masters, K. S.; Gellman, S. H., Ternary Nylon-3 Copolymers as Host-Defense Peptide Mimics: Beyond Hydrophobic and Cationic Subunits. *Journal of the American Chemical Society* **2014,** *136* (41), 14530-14535.

52. Kuroda, K.; DeGrado, W. F., Amphiphilic polymethacrylate derivatives as antimicrobial agents. *J Am Chem Soc* **2005,** *127* (12), 4128-9.

53. Lienkamp, K.; Madkour, A. E.; Musante, A.; Nelson, C. F.; Nusslein, K.; Tew, G. N., Antimicrobial polymers prepared by ROMP with unprecedented selectivity: a molecular construction kit approach. *J Am Chem Soc* **2008,** *130* (30), 9836-43.

54. Liu, S.; Ono, R. J.; Wu, H.; Teo, J. Y.; Liang, Z. C.; Xu, K.; Zhang, M.; Zhong, G.; Tan, J. P. K.; Ng, M.; Yang, C.; Chan, J.; Ji, Z.; Bao, C.; Kumar, K.; Gao, S.; Lee, A.; Fevre, M.; Dong, H.; Ying, J. Y.; Li, L.; Fan, W.; Hedrick, J. L.; Yang, Y. Y., Highly potent antimicrobial polyionenes with rapid killing kinetics, skin biocompatibility and in vivo bactericidal activity. *Biomaterials* **2017,** *127*, 36-48.

55. Geng, Z.; Finn, M. G., Thiabicyclononane-Based Antimicrobial Polycations. *Journal of the American Chemical Society* **2017,** *139* (43), 15401-15406.

56. Ilker, M. F.; Nusslein, K.; Tew, G. N.; Coughlin, E. B., Tuning the hemolytic and antibacterial activities of amphiphilic polynorbornene derivatives. *J Am Chem Soc* **2004,** *126* (48), 15870-5.

57. Murata, H.; Koepsel, R. R.; Matyjaszewski, K.; Russell, A. J., Permanent, non-leaching antibacterial surface--2: how high density cationic surfaces kill bacterial cells. *Biomaterials* **2007,** *28* (32), 4870-9.

58. Lee, S. B.; Koepsel, R. R.; Morley, S. W.; Matyjaszewski, K.; Sun, Y.; Russell, A. J., Permanent, Nonleaching Antibacterial Surfaces. 1. Synthesis by Atom Transfer Radical Polymerization. *Biomacromolecules* **2004,** *5* (3), 877-882.

59. Späth, A.; König, B., Ditopic crown ether–guanidinium ion receptors for the molecular recognition of amino acids and small peptides. *Tetrahedron* **2010,** *66* (10), 1859-1873.

60. Chen, Y.; Wang, F.; Yun, D.; Guo, Y.; Ye, Y.; Wang, Y.; Tan, H., Preparation of a C6 quaternary ammonium chitosan derivative through a chitosan schiff base with click chemistry. *Journal of Applied Polymer Science* **2013,** *129* (6), 3185-3191.

61. Wilkins, L. C.; Lawson, J. R.; Wieneke, P.; Rominger, F.; Hashmi, A. S. K.; Hansmann, M. M.; Melen, R. L., The Propargyl Rearrangement to Functionalised Allyl-Boron and Borocation Compounds. *Chemistry – A European Journal* **2016,** *22* (41), 14618-14624.

62. Quémener, D.; Hellaye, M. L.; Bissett, C.; Davis, T. P.; Barner-Kowollik, C.; Stenzel, M. H., Graft block copolymers of propargyl methacrylate and vinyl acetate via a combination of RAFT/MADIX and click chemistry: Reaction analysis. *Journal of Polymer Science Part A: Polymer Chemistry* **2008,** *46* (1), 155-173.

63. Luo, J.; Oliver, A. G.; Scott McIndoe, J., A detailed kinetic analysis of rhodium-catalyzed alkyne hydrogenation. *Dalton Transactions* **2013,** *42* (31), 11312-11318.

CHAPTER 5

Atom-transfer radical polymerization of oligo(ethylene glycol) methacrylate (OEGMA) on polylactide bearing bromide side chains to afford amphiphilic brush copolymer

5.1. INTRODUCTION

Polylactide (PL), a renewable thermoplastic polyester, has gained attention for various biomedical and pharmaceutical applications as a result of its biocompatible and biodegradable nature. However, its hydrophobicity, lack of reactive functional side chains, and low glass transition temperature (T_g) limit its applications. To overcome these shortcomings, a variety of copolymers of PL have been synthesized with functional comonomers including substituted lactones and lactides.[1-6,7,8,9] The functional groups on the comonomer units have been used to improve the T_g, impart hydrophilicity, and install ligands to enhance the potential for the use of PL in biomedical applications.[10,11] Drawbacks associated with these approaches include the need for multi-step syntheses of the comonomers and the use of excess reagents in the post-polymerization modification step. These severely limit the potential for commercialization of these materials. Thus, the direct modification of PL to impart new functionality might prove to be advantageous.

One approach to the direct modification of PL proceeds by treatment with LDA to deprotonate the methine, followed by reaction of the polymeric carbanion with an electrophile. This process allowed for acylation and tritiation of 0.25% of the PL repeat units.[12] However, the use of a strong base resulted in extensive cleavage of the polyester backbone. This process was recently optimized to allow for modification of the surface of PL.[13,14,15] Another approach to chemically modify PL involves free radical grafting polymerizations via a reactive extrusion process. Graft copolymers of PL bearing maleic anhydride side chains have been prepared to

improve the compatibilization of PL/starch blends.[16,17,18] However, low grafting densities, as well as side reactions such as chain scission and cross-linking of the intermediate macroradicals present some challenges.

Herein we describe direct functionalization of PL by bromination under radical conditions to achieve up to 10% bromine substitution along the polymeric backbone. The presence of a tertiary bromine substituent along the polymer backbone provides opportunities to perform nucleophilic displacement reactions, dehydrobromination and atom-transfer radical polymerization (ATRP) to prepare brush copolymers. We demonstrate the ability of the brominated polymer (Br-PL) to undergo ATRP with acrylate and methacrylate monomers, including oligo(ethylene glycol) methacrylate (OEGMA), to afford amphiphilic brush copolymers.

Amphiphilic brush copolymers have attracted considerable attention in the field of drug delivery due to their ability to self-assemble into polymeric particles in aqueous solution. These assemblies provide a hydrophobic reservoir into which pharmaceuticals that are sparingly soluble in water may be sequestered. In addition, the hydrophilic exterior of the nanoparticles prevent biofouling and provide the potential to attach ligands to so as to direct delivery to specific sites.[19] Previously, diblock,[20,21] and triblock[22] copolymers consisting of PLA with poly(ethylene glycol) (PEG) or poly(olegoethylene glycol methacrylate) (POEGMA) blocks have been synthesized by chain end modification of PLA. Graft block copolymers consisting of a PLA main chain with PEG side chains have been synthesized by copolymerization of alkyne-substituted lactide with L-lactide followed by grafting of an azide terminating PEG polymer using azide-alkyne "click" chemistry.[3,23] However, low grafting density as a result of steric crowding between the polymeric chains is a challenge associated with the grafting to approach.[24]

In contrast, a graft from strategy allows for the grafting of long polymeric side chains in high density. Moreover, a brush copolymer bearing branched poly(OEGMA) side chains would provide more stability to nanoparticles compared to a PL copolymer that bears linear PEG side chains.[22] Thus, we set out to carry ATRP of OEGMA using a 5 % Br-PL as a multisite macroinitiator to prepare PL-POEGMA graft copolymer. Self-assembly of this polymer in aqueous results in the formation of nanoparticles. We explore the capacity of PL-POEGMA polymeric nanoparticles to encapsulate and release curcumin, an antioxidant, antiinflammatory and anticancer agent.

5.2. RESULTS AND DISCUSSION

5.2.1. Bromination of PL

Treatment of PL (number-average molecular weight, M_n = 26.7 kDa; polydispersity index, PDI = 2.5) with *N*-bromosuccinimde (NBS), in the presence of benzoyl peroxide (BPO) acting as an initiator, results in bromination of the polymer backbone, Figure 5.1. Addition of BPO after every 24 h over a five-day period results in substitution of ~5% of the repeat units of the polymer. Gel permeation chromatography (GPC) of the resulting brominated polymer shows a number average molecular weight of 22 kDa with a PDI of 2.2. These values are similar to those of the PL used for the reaction, indicating that the reaction conditions do not result in crosslinking of the copolymer or rupture of the polyester backbone.

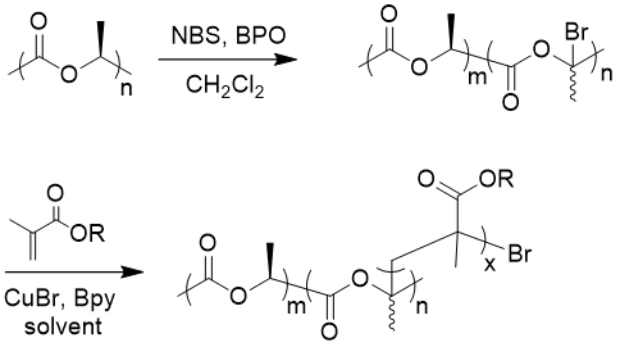

Figure 5.1. Radical bromination of PLA and atom-transfer radical polymerization.

The ^{1}H NMR spectrum of the copolymer (Figure 5.2A) shows the presence a quartet at 5.16 ppm (signal *p*) and a doublet at 1.57 ppm (signal *q*) corresponding to the methine and the methyl hydrogen atoms of the unsubstituted repeat unit of the copolymer respectively, along with singlets at 2.25 ppm and 2.28 ppm (signal *a* and *a'*) corresponding to the methyl group of bromine-substituted repeat units. The comparison of the integral of these two singlets with that of the signals associated with the methyl group of unsubstituted lactide units of the polymer (signal *q*) suggests that 5% of the units are brominated. The appearance of two singlets can be attributed to the tacticity

of the bromine-substituted copolymer. Ring-opening polymerization (ROP) of L-lacitde results in the formation of isotactic PL.[25] The generation of a planar radical intermediate, which can undergo bromination on either face, and the presence of chiral centers on the two neighboring repeat units, results in bromination of the two faces at different rates via diastereomeric transition states. This results in a ~3:1 ratio of diastereomeric brominated triads in the polymer as demonstrated by the difference in the size of the two singlets arising from the bromo-substituted repeat units, Figure 5.3.

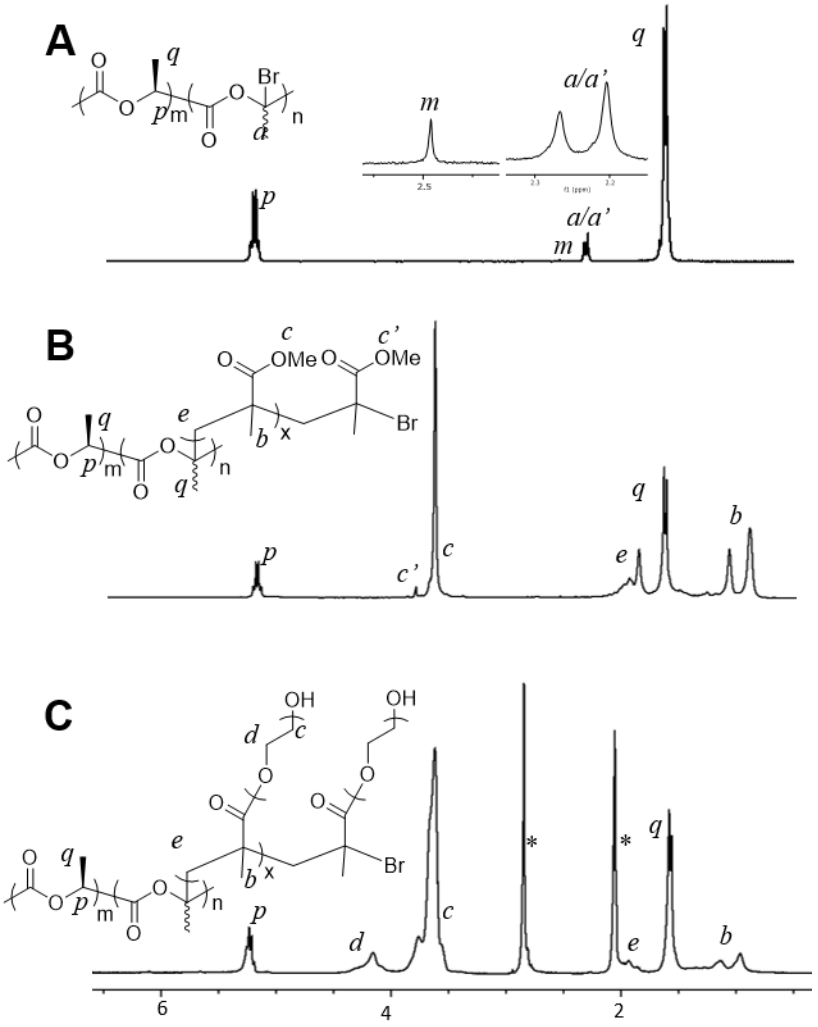

Figure 5.2. ^{1}H NMR spectra (300 MHz, $CDCl_3$). A, Br-PL. B, PL-PMMA. C, ^{1}H NMR spectra (300 MHz, acetone-d_6) PL-POEGMA. * Residual solvents: H_2O, acetone

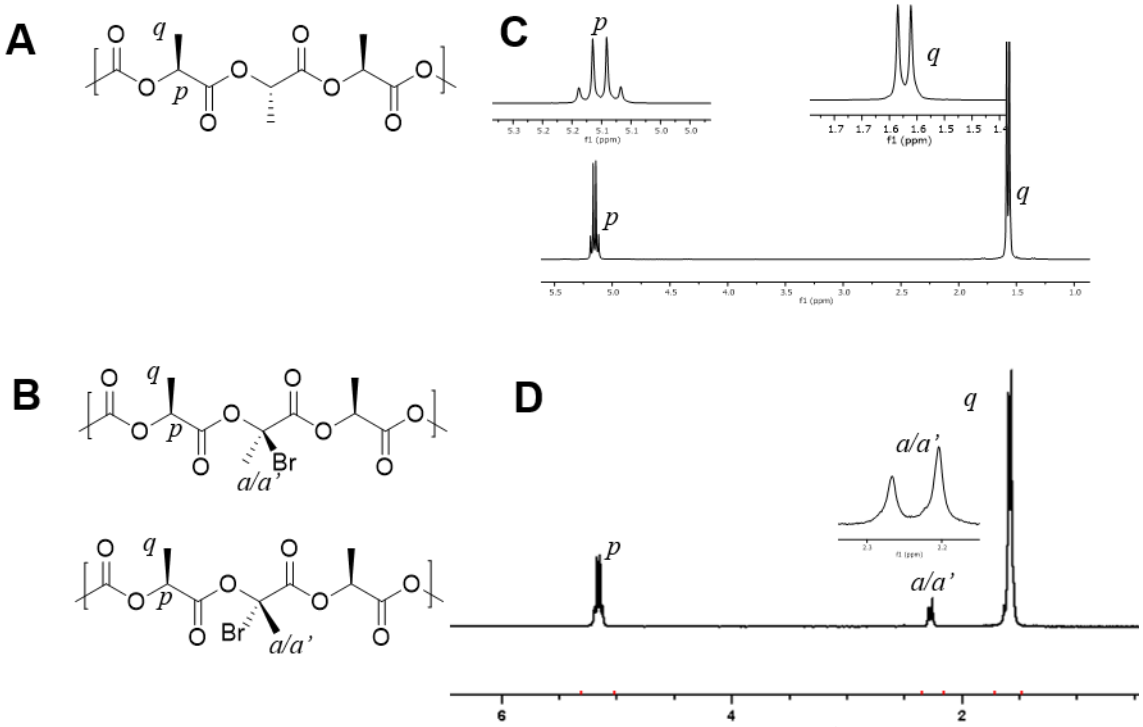

Figure 5.3. A, Isotactic PL triad. B, Diastereomeric Br-PL triad. ^{1}H NMR spectra (300 MHz, $CDCl_3$). C, PL. D, Br-PL.

Prior attempts to brominate PL by Coudane resulted in selective bromination at the hydroxyl chain end.[26] Under the reaction conditions used (NBS, BPO in benzene/anisole/trifluorotoluene for 3-16 h, 80-110 °C) no bromination of the main chain polyester backbone took place. Their attempts to brominate PL with acetylated hydroxyl terminus were also unsuccessful. Their evidence for bromination at the hydroxyl chain end was the appearance of a singlet at 2.45 ppm in the ^{1}H NMR spectrum of the brominated copolymer. An α-hydoxy bromine chain end generated as a result of selective bromination at the hydroxyl end group of PL would be susceptible to dehydrobromination and would result in the generation of a methyl ketone chain end, Figure 5.4. Indeed, MALDI characterization of the chain-end brominated polymer synthesized by Coudane group displayed a significant amount of dehydrobrominated polymer.[26]

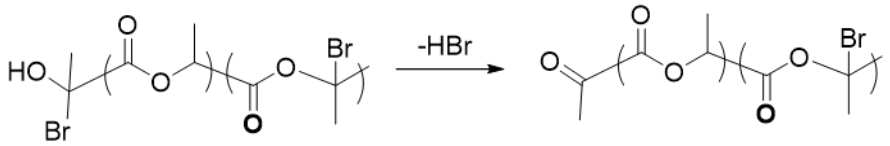

Figure 5.4. dehydrobromination of the brominated hydroxyl chain-end

The ^{1}H NMR spectrum of 5 % Br-PL synthesized under the reaction conditions (NBS, BPO in CH_2Cl_2 for 5 d, 40 °C), shows the presence of a small singlet at 2.49 ppm (Figure 5.2A, signal *m*) which we assign to the methyl ketone end group of the copolymer generated by dehydrobromination of the α-hydoxy bromine chain end of the polymer. This assignment is consistent with methyl ketone chain ends formed by hydrolysis of a copolymer of PL bearing α,β-unsaturated repeat units (ene-PL).[1] The ketone end group is generated on prolonged exposure of ene-PL to basic conditions which results in the rupture of the polyester backbone of the functional units of the copolymer giving rise to an enol chain end that tautomerizes to its thermodynamically favored keto form. Bromination at the hydroxyl chain end of PL would lead to the formation of a labile chain end that can undergo dehydrobromination to generate the same methyl ketone chain end as observed with ene-PL. Absence of any additional signals in the region between 1.8 and 2.5 ppm of the ^{1}H NMR spectrum indicates that the majority of the brominated polymer chain ends undergo dehydrobromination.

Attempts on the generation on copolymer of PL with higher bromine content were successful. Continuation of the reaction over a ten-day period resulted in ~10 % bromination, which was evident from the integration of the signals corresponding to the methyl group of the bromide-substituted unit of the copolymer (signal *a* and *a'*) with those associated with the lactide unit of the copolymer (signal *p*) in the ^{1}H NMR spectrum. Elemental analysis confirmed the molar ratio of bromide units in Br-PL. However, increasing the concentration of the reagents (NBS, BPO), or the duration of the reaction (>10 days) did not afford more than 10 % bromination.

Different brominating agents and initiators were explored in attempts to achieve higher incorporation of bromide within the polyester backbone. Bromination using Br_2 in CH_2Cl_2 in the presence of UV light resulted in the degradation of the polyester backbone as evident by the increase in the size of the signal corresponding to the hydrogen atom of the methine at the hydroxyl terminus in the ^{1}H NMR spectrum. The use of AIBN in place of BPO did not result in more than 10% incorporation of bromide. Reactions attempted with NBS in the absence of BPO, but in the presence of light resulted in bromination at both the methine carbon and the methyl group of PL in a ca 1:1 ratio, Figure 5.5

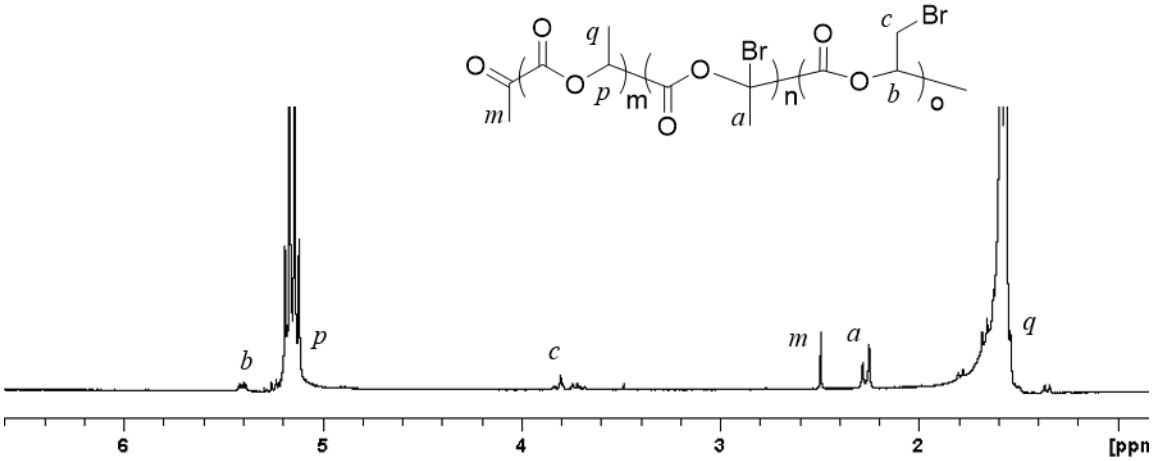

Figure 5.5. ^{1}H NMR spectra (300 MHz, $CDCl_3$). Bromination in the absence of BPO and in the presence of light.

As additional evidence to confirm the success of bromination throughout the polyester backbone of PL using our reaction conditions, bromination was attempted on O-aceytylated-PL. In contrast to Coudane's observation that the acylated PL does not undergo bromination (at the chain ends or along the chain)[26] we determined 2.5% incorporation of bromine in three days, Figure 5.6. This further attest to the ability to directly brominate PL upon heating with NBS in the presence of BPO over an extended period, whereas reaction carried for a shorter duration appears to be restricted to the chain ends.

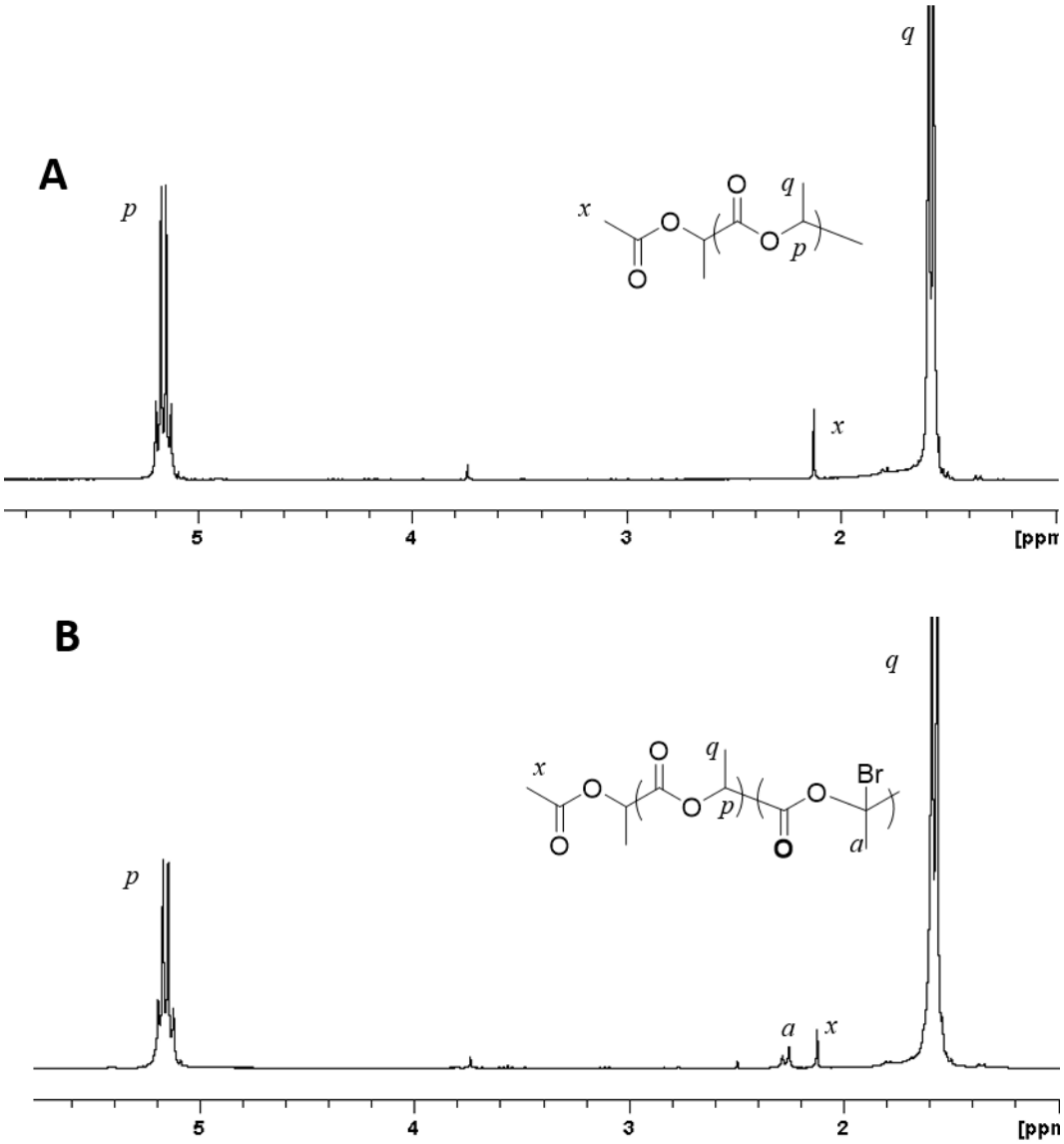

Figure 5.6. ^{1}H NMR spectra (300 MHz, $CDCl_3$). A, O-acetylated-PL. B, O-acetylated-Br-PL.

Differential scanning calorimetry indicates that 5% Br-PL undergoes a glass transition at a 43 °C, Table 5.1. Continued heating results in cold crystallization at 103 °C followed by melting at 137 °C. Upon cooling, the melted polymer crystalizes at 89 °C. Heating of Br-PL beyond 175 °C results in the degradation of the polymer. Heating Br-PL in a melting point capillary results in the evolution of HBr, as detected by the change in the color of a piece of moist pH universal indicator paper kept at the opening of the capillary. Moreover, the ^{1}H NMR spectrum of the

brominated polymer exposed to elevated temperature shows complete loss of signals corresponding to the methyl group of the bromine-substituted repeat units, along with an increase in the size of the signal for the methyl ketone end group. The lowering of the T_g of Br-PL in comparison to PL (T_g = 50-60 °C) is consistent with other examples of copolymers of PL bearing reactive functional groups.

5.2.2. Elimination and nucleophilic displacement of Br-PL

Successful dehydrobromination of a bromo-substituted lactide, (3*R*,6*S*)-3-bromo-3,6-dimethyl-1,4-dioxane-2,5-dione, upon treatment with Et_3N was demonstrated by Hillmyer as a method to prepare (6*S*)-3-methylene-6-methyl-1,4-dioxane-2,5-dione. This provided a strong precedence to attempt dehydrobromination of bromo-PL. However, treatment of Br-PL with Et_3N, and a variety of other non-nucleophilic bases (DIPEA, DBU, NaH) did not afford the α,β-unsaturated analog of PL (ene-PL) as evident by the complete absence of signals in the alkene region of the NMR spectrum corresponding to the hydrogen atoms of α,β unsaturated ester linkage, Figure 5.7B. This is in contrast to our previous demonstration of the dehydrochlorination of 3-chlorolactide repeat units to afford ene-PL.[1] Instead, the basic reaction conditions of the brominated PL resulted in the rupture of the polymeric backbone at the 2-bromo lactide units of the copolymer. The presence of a good leaving group renders the ester susceptible to a nucleophilic attack even by a mild base, resulting in the rupture of the backbone, Figure 5.7A. The ^{1}H NMR spectrum of the polymer obtained post reaction shows complete disappearance of the methyl hydrogens of the bromide-substituted units of the copolymer, along with an equivalent increase in the size of the singlet at δ 2.49 corresponding to the methyl ketone chain end of the copolymer.

The commensurate increase in the size of the singlet at 2.49 ppm with the decrease in the size of signals *a* and *a'* further corroborates our assignment of the singlet to the methyl ketone chain end.

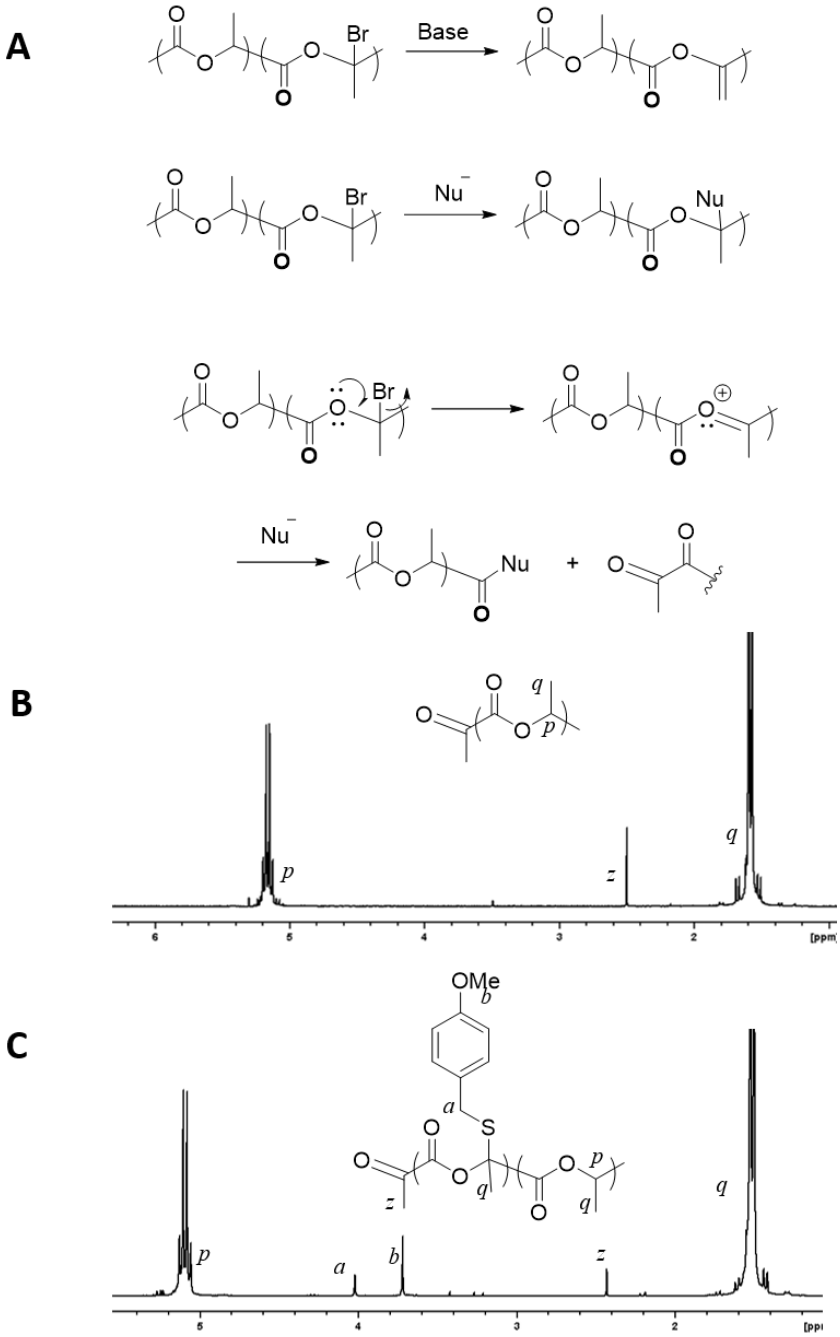

Figure 5.7. A, Synthetic scheme for dehydrobromination and nucleophilic substitution of Br-PL Proposed mechanism of preferential cleavage of the functional polyester. B, ^{1}H NMR spectra (300 MHz, $CDCl_3$). C, Br-PLA treated with NaN_3. D, Br-PLA treated with methoxybenzyl thiol

Treatment of the copolymer with nucleophiles such as NaN_3, 4-methoxybenzylthiol and octanethiol also resulted in the rupture of the polyester backbone due to the attack of the nucleophile at the ester rather than nucleophilic substitution of the bromine, Figure 5.7C. Thus, these attempts to perform nucleophilic substitution and elimination reactions on Br-PL simply demonstrate the labile nature of the polyester backbone.

5.2.3. Atom-transfer radical polymerization

The brominated PL was used as a multisite macroinitiator for the atom-transfer radical polymerization (ATRP) of methyl methacrylate (MMA), methyl acrylate (MA) and oligo(ethylene glycol) methacrylate (OEGMA). The graft polymerization of MMA was carried out with various monomer:initiator molar ratios (M:Br) in THF, using CuBr as the catalyst and 2,2′-bipyridine (bpy) as a complexing agent, to provide a series of PL graft copolymers which have side chains of different lengths, Table 5.1.

Table 5.1. Characterization of 5% PL-PMMA graft copolymers.

	monomer/ initiator, [M]/[I]	Grafted PMMA chain length[a]	M_n[b] kDa	PDI[b]	T_g[c] °C	T_m[c] °C	T_c[c] °C
PL	-	-	26.7	2.5	50-60	173-178	121
5% Br-PL	-	-	21.5	2.2	43	137	103
PL-PMMA	25	14	19.6	2.3	58	-	-
PL-PMMA	50	22	25.6	1.9	65	-	-
PL-PMMA	100	41	28.3	2.5	75	-	-
PL-PMMA	150	53	45.4	3.1	90	-	-
PMMA	-	-	-	-	110	180	-

[a]From ^{1}H NMR chain end analysis. [b]Obtained by GPC; polystyrene standards, THF eluent. [c]DSC (5 °C/min, 3 cycles, -10 °C to 200 °C).

The reaction was terminated after 2 h by exposure of the reaction mixture to air. The solvent was removed under reduced pressure, the residue was dissolved in CH_2Cl_2, and addition of the

solution to MeOH precipitated the graft polymer which could be isolated by filtration. The reaction conditions afford complete consumption of the macroinitiator sites bromo-substituted repeat units. The efficiency of monomer conversion of up to 50% was observed over the duration of the reaction. A linear increase in the number-average molecular weight (M_n) of the copolymer with an increase in the M:Br was observed, Table 5.1.

The ^{1}H NMR spectrum (Figure 5.2B) of the precipitated copolymer obtained by treating Br-PL with MMA (M:Br = 50:1) shows the presence of a quartet at 5.12 ppm and a doublet at 1.5 ppm corresponding to the methine and methyl hydrogens of the PLA main chain (signals *p* and *q* respectively), along with complete absence of the two singlets corresponding to the methyl group of the bromine-substituted repeat units (signal *a* and *a'* in Figure 5.2A), indicating complete consumption of macroinitiator sites. The singlet at 3.54 ppm (signal *c*) can be assigned to the methyl ester groups of the grafted PMMA chains. A small peak at 3.7 ppm (signal *c'*) corresponds to the ester at the terminus of the side chains. The downfield chemical shift of the terminal ester signal is consistent with the effect of an α-bromo substituent on the chemical shift of methyl esters. The integration of the two singlets for the methyl esters (signal *c* and *c'*) suggest that the ATRP grafting process afforded a 22mer of PMMA. The integration of the singlet at 3.7 ppm (signal *c'*) with respect to the quartet at 5.12 ppm (signal *p*) indicates a 5% grafting density of PMMA to Br-PL, which is consistent with the molar composition of 5% Br-PL used for the reaction. Moreover, this indicates that all of the PMMA chains are grafted from the PL backbone and that there are no unbound linear PMMA chains generated by other initiation processes. This conclusion is further corroborated by the appearance of a single peak in the gel permeation chromatogram for the graft copolymer, appendix A, Figure A-25. A broad multiplet at between 1.95 and 1.75 ppm in the ^{1}H NMR spectrum (signal *e*) corresponds to the hydrogen atoms of the methylene units of the graft

PMMA chains. Finally, broad singlets at 0.95 ppm and 0.77 ppm correspond to the methyl groups attached to the PMMA backbone, which is consistent with the expected atacticity of the grafted copolymer chains. Similar features are observed in the NMR spectrum of the copolymers obtained with different M:Br molar ratios. The ^{1}H NMR spectrum of the copolymer of PL grafted with poly(methyl acrylate) side chains displays signals corresponding to the methine and methyl group associated with the PL backbone (signals *p* and *q*, Figure 5.8), along with the expected signals associated with poly(methyl acrylate) side chain.

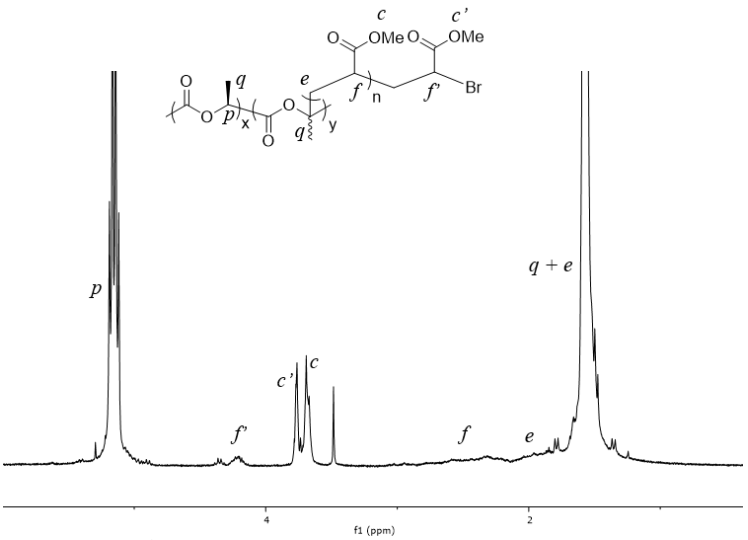

Figure 5.8. ^{1}H NMR spectra (300 MHz, $CDCl_3$). PL-PMA_2

Thermal analysis shows that the PL-*graft*-PMMA copolymers are amorphous. The graft copolymers undergo a single glass transition. The glass transition temperature (T_g) for this set of graft copolymers increases with the degree of polymerization of PMMA over the range of 58 to 90 °C, Table 5.1. The low T_g of PL (50-60 °C) limits its applications. There are a few examples of PL analogs bearing polymeric side chain that have an improved T_g. Here we observe an increase in the T_g of PL to 90 °C with a grafting density of just 5 % of $PMMA_{53}$.

We carried out ATRP of oligo(ethylene glycol) methacrylate (OEGMA) with Br-PL as the macroinitiator under the same reaction conditions as used for the polymerization of MMA and

MA. OEGMA has been extensively used to yield polymers that resist biofouling.[27,28] Graft-polymerization was carried out with $OEGMA_{360}$ macromers at various macromer:initiator (OEGMA:Br) molar ratios. The graft-polymers were purified by precipitation in Et_2O. The ^1H NMR spectrum of the precipitated brush copolymer (OEGMA:Br = 25:1) shows the presence of signals corresponding to the methine and the methyl hydrogens of the PLA units, along with signals that can be assigned to the poly(OEGMA) side chains, Figure 5.2C. The spectrum shows the complete absence of signals corresponding to the vinylic hydrogen atoms of OEGMA, indicating that the purification process was successful in separating the unreacted OEGMA macromer from the grafted copolymer. Integration of the signals corresponding to the PL backbone with those corresponding to the PEG side chains of the grafted poly(OEGMA) shows that the ATRP afforded a 20-mer. Polymerization with $OEGMA_{360}$ with OEGMA:Br ratios of 5:1 or 10:1 afforded brush copolymers that were soluble in acetone, chloroform and THF, whereas while higher OEGMA:Br ratios (20:1, 25:1 and 50:1) afforded graft copolymers that were soluble only in acetone. A liner increase in the degree of polymerization of the poly(OEGMA) side chain was observed with an increase in the OEGMA:Br ratio, Figure 5.9.

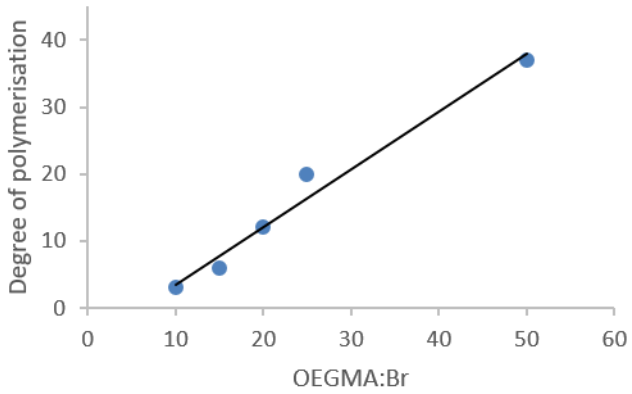

Figure 5.9. Linear dependence of the degree of polymerization of PL-POEGMA on the ratio of macromer to the initiator (OEGMA:Br).

A higher molar ratio of $OEGMA_{360}$ (OEGMA:Br = 100) afforded reaction mixture that gelled during the reaction. The copolymer obtained from the latter reaction was insoluble in CH_2Cl_2, $CHCl_3$, DMF, acetone, MeOH and hexane, even at elevated temperatures.

5.2.4. Particle formation

The amphiphilic nature of the PL-$POEGMA_{37}$ graft block copolymer should allow for its self-assembly into particles in an aqueous environment by aggregation of the PL chains as a hydrophobic core and formation of a hydrophilic poly(OEGMA) shell. The fluorescence of pyrene was recorded as a function of copolymer concentration to determine the critical micelle concentration (CMC), the minimum concentration at which the copolymer self-assembles into particles in an aqueous environment. In the absence of the polymer, pyrene fluoresces in the aqueous solution with a maximum excitation at 334 nm. In the presence of aggregated polymer, partition of pyrene into the less polar phase of the particle results in a shift in the excitation at 337 nm. The CMC of the copolymer, calculated by the intersection of the best fit lines on the plot of the ratio of intensities at these two wavelengths (I_{337}/I_{334}) versus the log of concentration provides a CMC of 2 mg/L, Figure 5.10.

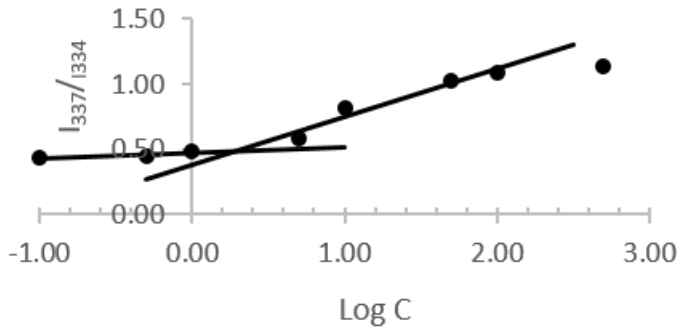

Figure 5.10. Fluorescence studies to determine the CMC of the copolymer. A ratio of intensity of fluorescence excitation of pyrene at I_{337}/I_{334} as a function of log of the concentration of PL-$POEGMA_{37}$.

Dynamic light scattering (DLS) and transmission electron microscopy (TEM) were used to determine the diameter of the particles formed by the brush copolymer. Particles were formed by nanoprecipitation at a concentration above the CMC of the brush copolymer by addition of a solution of the polymer in acetone to H_2O followed by stirring of the aqueous solution for 24 h to allow for the evaporation of acetone. DLS of 5% PL-POEGMA$_{37}$ showed a unimodal distribution of particle diameter over a range of 70-90 nm, Figure 5.11. A change in the solvent used for nanoprecipitation from acetone to chloroform afforded particle of with a similar range of diameter (80-100 nm).

TEM showed that the amphiphilic graft copolymers self-assemble into a spherical particle with a diameter of 90-110 nm, Figure 5.11. To determine the stability of the particles in an aqueous medium, the aqueous suspension was dialyzed against water for 5 days and the particle size was measured every 24 h. No change in the particle size was observed during the first 4 days, with a slight increase in the diameter of the particles on the fifth day indicating the onset of particle aggregation.

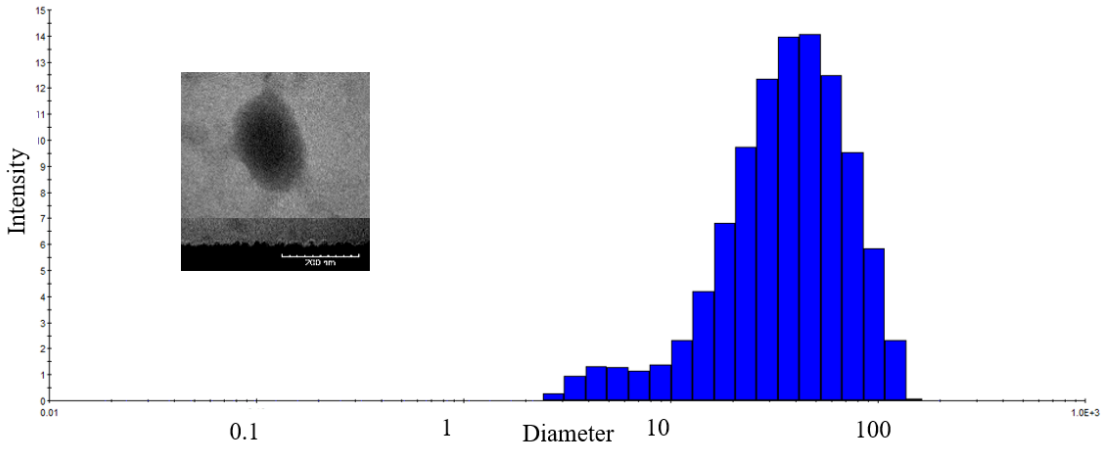

Figure 5.11. Particle size characterization. DLS of aqueous suspension of PL-POEGMA$_{37}$ prepared by nanoprecipitation and filtered through a 4 µ syringe filter. Inset, TEM of PL-POEGMA$_{37}$ prepared by drop casting of the aqueous solution of PL-POEGMA$_{37}$ on the copper grid followed by evaporation of the solvent. scale bar = 200 nm.

A preliminary qualitative assessment of the capacity of these particles to load a fluorescent dye, 1,1′-Dioctadecyl-3,3,3′,3′-tetramethylindocarbocyanine perchlorate (Dil), was performed to evaluate the potential utility of these particles to serve as an agent for *in vivo* delivery of pharmaceuticals or imaging dyes. Dye-loaded nanoparticles were prepared by the addition of an acetone solution containing both Dil and the polymer to water. The aqueous mixture was stirred for 24 h which allowed for the evaporation of acetone. The mixture was filtered to remove any insoluble dye and the filtrate was characterized using fluorescence spectroscopy. The fluorescence intensities of a saturated aqueous solution of the dye and unloaded nanoparticles were recorded as control experiments. Emission of a strong fluorescence from the Dil-loaded particle solution and the absence of fluorescence from the control solutions provided preliminary evidence of the capacity of the particles to load a hydrophobic molecule, Figure 5.12.

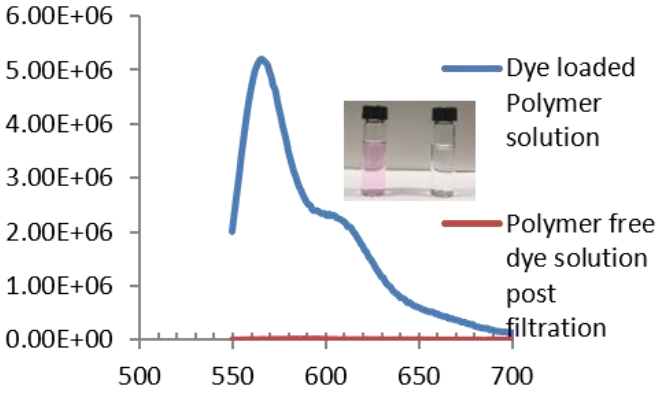

Figure 5.12. Fluorescence emission of aqueous solution of Dil-loaded PL-POEGMA$_{37}$ particles after filtration and fluorescence emission of control solution of Dil in water after filtration. Inset, Picture of the aqueous solution of Dil-loaded PL-POEGMA$_{37}$ particles after filtration (left) and aqueous Dil solution after filtration (right)

After successful loading of the fluorescent dye within the polymeric nanoparticles, we went on to quantify the encapsulation efficiency and release profile of curcumin. Curcumin is a phenolic, hydrophobic molecule with potential therapeutic attributes; it has anti-inflammatory, antioxidant and antitumor activities. Curcumin-loaded particles were prepared following the procedure

explained in the experimental section. Prior to the quantification of the encapsulation efficiency of the nanoparticles, a standard curve was prepared by plotting the UV absorbance of known concentrations of curcumin in 4:1 v/v mixture of H_2O and acetone. The amount of curcumin loaded in the nanoparticle was calculated with reference to the standard curve. An encapsulation efficiency of 61 ±5 % was achieved for a 15:100 ratio of curcumin to the graft copolymer by weight, while 41 ±4 % efficiency was observed for a 5:100 ratio of curcumin to the graft copolymer. Langer group observed a similar trend for poly(lactic-co-glycolic acid) based nanoparticles where the encapsulation efficiency increased with the increase in initial drug input to the weight of the copolymer, with a maximum encapsulation efficiency at 15:100 ratio of the drug to the polymer by weight.[29]

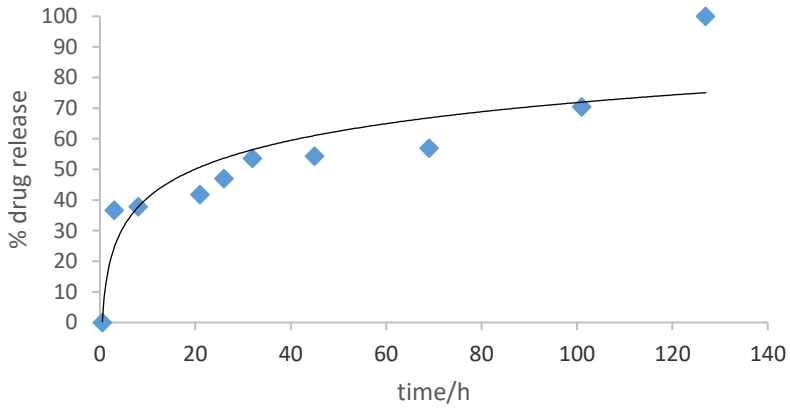

Figure 5.13. Preliminary study of the release profile of curcumin from curcumin-loaded $POEGMA_{37}$ particles loaded at a weight ratio of 15:100 (curcumin: $POEGMA_{37}$).

To study the release profile of curcumin from the nanoparticles, the curcumin-loaded solution was placed in a dialysis bag and the bag was placed in a beaker containing water. The absorbance of the solution in the dialysis bag was measured periodically. The decrease in the absorbance over time was used to calculate the rate of release of curcumin from the nanoparticles. The release profile of curcumin from PL-$POEGMA_{37}$ particles shows a rapid release in the first

30 min, followed by a sustained release of the drug over a period of 130 hours. The initial burst release could be a result of the loss of the drug adsorbed on the outer surface of the particles, Figure 5.13. The sustained release of curcumin for an extended period of time after the initial burst release provides promising preliminary results for the use of these nanoparticles for the delivery of drugs and imaging agents.

5.3. EXPERIMENTAL SECTION

5.3.1. Materials and Methods

The reagents required for the synthesis of the polymers were obtained from the following sources: *N*-bromosuccinimide (NBS), CuBr (Aldrich); anhydrous methylene chloride, methyl methacrylate (MMA), methyl acrylate (MA), oligo(ethylene glycol) methacrylate $(OEGMA)_{360}$, 2,2′-bipyridine (bpy) (Sigma Aldrich); and benzoyl peroxide (BPO) (Alfa Aeser). L-lactide (Alfa Aeser) was recrystallized twice from EtOAc, and copolymerized using tin(II) 2-ethylhexanoate following a procedure described elsewhere.[7] All other solvents were purchased from VWR and were used directly without further purification. All reactions were carried out under Ar (Nexair).

NMR spectral analysis was performed using a Varian Mercury spectrometer (^{1}H NMR, 300 MHz; ^{13}C, 75 MHz). Differential scanning calorimetry (DSC) (3 cycles, -20° C to 200° C, at 5° C/min) were recorded using a Q200 under N_2. Thermogravimetric analysis (TGA) (5° C/min), was recorded on a Pyris 1 thermogravimetric analyzr. Gel permeation chromatograms were recorded on a Tosoh EcoSEC with Wyatt 8-angle MALLS instrument with THF as the eluent; chromatograms were calibrated against polystyrene standards. DLS measurements were taken using a Wyatt DynaPro NanoStar Dynamic Light Scattering Spectrophotometer. Critical micellar concentration (CMC) was determined using Horiba Jobin Yvon Fluorometer using pyrene (Sigma Aldrich) as a fluorescent dye, following the procedure described elsewhere.[30] TEM samples were prepared by adding a solution of the nanoparticle (5 mg/mL) on a TEM copper grid. The solution was allowed to air dry overnight and the samples were imaged using a JEOL 100CX-II TEM. Elemental analysis was provided by Atlantic Microlab Inc. UV Vis and fluorescence spectroscopy were performed using a Cary 5E UV-Vis-NIR Spectrophotometer and Horiba Jobin Yvon Fluorometer respectively.

5.3.2. Synthesis

5.3.2.1. Poly(lactide-co-bromolactide), Br-PL

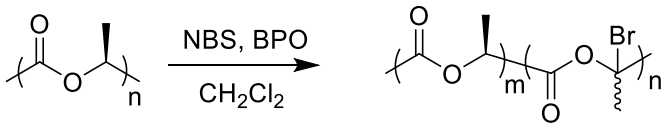

Polylactide (200 mg) and *N*-bromosuccinimide (543 mg) were placed in an Ar-purged, oven-dried round-bottomed flask. Anhydrous CH_2Cl_2 was added to the flask and the mixture was stirred for 2 h at reflux. A solution of benzoyl peroxide (BPO) (20 mg) in CH_2Cl_2 (1 mL) was added drop-wise to the polymer solution and the reaction mixture was stirred at reflux. Additional BPO (20 mg in 1 mL of CH_2Cl_2) was added to the reaction mixture after every 24 h. After 5 days, the reaction mixture was allowed to cool to room temperature and the solvent was removed under reduce pressure to obtain a yellow residue. The solid was dissolved in minimum amount of CH_2Cl_2 (~2 mL) and the solution was added to room-temperature MeOH (50 mL). The resulting solid was collected by filtration and dried under reduce pressure to afford the copolymer as a colorless solid (170 mg). ^{1}H NMR (300 MHz, $CDCl_3$), δ 5.16 (q, *J* = 7.2 Hz, 19 H, CH of lactide unit), δ 2.28 (s, CH_3 of substituted lactide), δ 2.25 (s, CH_3 of substituted lactide), δ 1.57 (d, *J* = 7.2 Hz, 57H, CH_3 of lactide repeat unit).

5.3.2.2. General procedure for ATRP polymerization

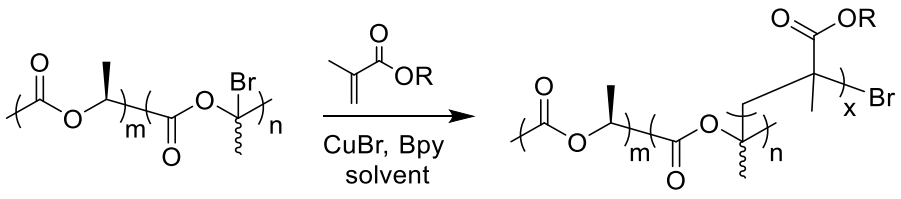

An Ar-purged, oven-dried flask was charged with 5% Br-PL (100 mg), CuBr (29 mg, 3 mol eq of bromine-substituted repeat units in the polymer) and the acrylate monomer. Distilled THF was added and the mixture was degassed using 6-7 freeze-pump-thaw cycles. Bpy (21 mg, 2 mol eq of bromine-substituted units in the polymer) was added, and the reaction mixture was heated to 50 °C with stirring for 2 h. The reaction mixture was cooled to room temperature, and the solvent was removed under reduced pressure. For MA and MMA-grafted materials, the residue was dissolved in minimum amount of CH_2Cl_2 ~(2 mL) and the solution was added to MeOH (50 mL) with stirring. For OEGMA-grafted materials the residue was dissolved in 2 mL of acetone which was then added to stirred Et_2O. The precipitated solid was filtered and dried under reduced pressure to afford the grafted copolymer.

95:5 Poly(lactic acid)-gr-poly(methyl methacrylate). ^{1}H NMR (30 MHz, $CDCl_3$), δ 5.10 (q, *J* = 6.9 Hz, 19 H, CH of lactide unit), δ 3.69 (s, OCH_3 of PMMA chain terminus), δ 3.53 (s, OCH_3 PMMA chain), δ 1.95-1.75 (m, CH_2 of PMMA side chain), δ 1.57 (d, *J* = 7.2 Hz, 57H, CH_3 of lactide repeat unit) δ 0.95, 0.77 (s, CH_3 of PMMA side chain).

95:5 Poly(lactic acid)-gr-poly(methyl acrylate). ^{1}H NMR (300 MHz, $CDCl_3$), δ 5.15 (q, *J* = 6.9 Hz, 19 H, CH of lactide unit), δ 4.2-4.3 (m, CH-Br, PMA chain terminus), δ 3.79 (s, OCH_3 of PMA chain terminus), δ 3.68 (s, OCH_3 PMMA side chain), δ 2.2-2.6 (m, CH-Br, PMA side chain), δ 2.1-1.75 (m, CH_2 of PMA side chain), δ 1.57 (d, *J* = 7.2 Hz, 57H, CH_3 of lactide repeat unit).

95:5 Poly(lactic acid)-gr-poly((oligoethyleneglycol) methacrylate). ^{1}H NMR (300 MHz, acetone d-6), δ 5.21 (q, *J* = 6.9 Hz, 19 H, CH of lactide unit), δ 4.15 (m, $COOCH_2$ of PEG chain), δ 3.6 (m, OCH_2 PEG chain), δ 2.08-1.93 (m, CH_2 of PMMA side chain), δ 1.57 (d, *J* = 6.9 Hz, 57H, CH_3 of lactide repeat unit) δ 1.15-0.72 (m, CH_3 of PMMA side chain).

5.3.2.3. General procedure for preparing nanoparticles of PL-POEGMA

Nanoparticles were prepared by a nanoprecipitation process.[29] Briefly, a 10 mg/mL solution of the polymer in acetone was added drop-wise to stirred deionized H_2O to give a final concentration of 1 mg/mL. The aqueous solution was stirred overnight and left open to allow the acetone to evaporate. The aqueous solution was filtered and characterized using DLS to measure the particle size.

5.3.2.4. Dye/Drug loading and release

A solution of curcumin (100 µL of a 15 mg/mL stock solution in acetone) was added to a solution of polymer (1.0 mL of a 10 mg/mL solution of the polymer in acetone) and the mixture was placed on a laboratory rocker for 2 h. The mixture was added dropwise to 10 mL of stirred deionized H_2O and the vial was kept open to allow acetone to evaporate over 24 h (final concentration of the polymer = 1 mg/mL; final concentration of the curcumin: 0.15 mg/mL). The solution was filtered to remove insoluble curcumin. A 100 µL aliquot of the filtered solution was made up to 2.5 mL by adding a 4:1 mixture of water and acetone and the solution was analyzed using UV-Vis spectroscopy. The concentration of curcumin solubilized by the nanoparticles was determined using a standard curve of known concentrations of curcumin (0.01 mM to 0.1 mM) in H_2O-acetone (4:1).

A control solution of curcumin was prepared by dropwise addition of an acetone solution of curcumin (1 mL of 1.5 mg/mL) to 10 mL of deionized H_2O and the solution was stirred in an open vial to allow acetone to evaporate. After 24 hours, the suspension was filtered and the filtrate was characterized using UV Vis spectroscopy. Curcumin-free nanoparticles were prepared following the general procedure for preparing nanoparticles.

Encapsulation efficiency was calculated using the following formula:

$$\%\ Encapsulation\ efficiency = \frac{Amount\ of\ curcumin\ in\ nanoparticles}{Total\ amount\ of\ curcumin\ originally\ added} \text{X } 100$$

The aqueous solution of curcumin-loaded nanoparticle was added to three different dialysis bags (MW cut off 10k) and each bag was kept in a separate 50 mL beaker containing deionized H_2O. The water in the beakers was replaced with fresh water after every 24 hours. At a certain interval, an aliquot was taken from each of the three dialysis bags, was diluted to make up a volume

of 2.5 mL using 4:1 H_2O-acetone and analyzed using UV Vis spectroscopy. The release profile of curcumin was obtained by plotting percentage release of curcumin against time.

5.4. CONCLUSIONS

A novel synthesis of bromination of PL backbone is described. Brominated PL undergoes atom-transfer radical polymerization with methyacrylate and a variety of methacrylate monomers. ATRP of oligo(ethylene glycol)methacrylate on Br-PL results in the formation of amphiphilic graft copolymer that self-assembles into nanoparticles in aqueous environment. PL-POEGMA form nanoparticles of a diameter of 70-90 nm and are able to sequester hydrophobic dye molecules with an encapsulation efficiency of >60 %. A sustained release profile of curcumin from the nanoparticles displays promising preliminary results for the development of these nanoparticle for drug delivery application.

5.5. REFERENCES

1. Kalelkar, P. P.; Alas, G. R.; Collard, D. M., Synthesis of an Alkene-Containing Copolylactide and Its Facile Modification by the Addition of Thiols. *Macromolecules* **2016,** *49* (7), 2609-2617.
2. Kimura, Y.; Shirotani, K.; Yamane, H.; Kitao, T., Ring-opening polymerization of 3(S)-[(benzyloxycarbonyl)methyl]-1,4-dioxane-2,5-dione: a new route to a poly(.alpha.-hydroxy acid) with pendant carboxyl groups. *Macromolecules* **1988,** *21* (11), 3338-3340.
3. Jiang, X.; Vogel, E. B.; Smith, M. R.; Baker, G. L., "Clickable" Polyglycolides: Tunable Synthons for Thermoresponsive, Degradable Polymers. *Macromolecules* **2008,** *41* (6), 1937-1944.
4. Wright, C.; Banerjee, A.; Yan, X.; Storms-Miller, W. K.; Pugh, C., Synthesis of Functionalized Poly(lactic acid) Using 2-Bromo-3-hydroxypropionic Acid. *Macromolecules* **2016,** *49* (6), 2028-2038.
5. Olejniczak, J.; Collet, G.; Nguyen Huu, V. A.; Chan, M.; Lee, S.; Almutairi, A., Biorthogonal click chemistry on poly(lactic-co-glycolic acid)-polymeric particles. *Biomaterials Science* **2017,** *5* (2), 211-215.
6. Pounder, R. J.; Dove, A. P., Towards poly(ester) nanoparticles: recent advances in the synthesis of functional poly(ester)s by ring-opening polymerization. *Polym. Chem.* **2010,** *1* (3), 260-271.
7. Noga, D. E.; Petrie, T. A.; Kumar, A.; Weck, M.; García, A. J.; Collard, D. M., Synthesis and Modification of Functional Poly(lactide) Copolymers: Toward Biofunctional Materials. *Biomacromolecules* **2008,** *9* (7), 2056-2062.
8. Yu, Y.; Zou, J.; Cheng, C., Synthesis and biomedical applications of functional poly([small alpha]-hydroxyl acid)s. *Polym. Chem.* **2014,** *5* (20), 5854-5872.
9. Pounder, R. J.; Fox, D. J.; Barker, I. A.; Bennison, M. J.; Dove, A. P., Ring-opening polymerization of an O-carboxyanhydride monomer derived from l-malic acid. *Polym. Chem.* **2011,** *2* (10), 2204-2212.
10. Borchmann, D. E.; ten Brummelhuis, N.; Weck, M., GRGDS-Functionalized Poly(lactide)-graft-poly(ethylene glycol) Copolymers: Combining Thiol–Ene Chemistry with Staudinger Ligation. *Macromolecules* **2013,** *46* (11), 4426-4431.
11. Simmons, T. L.; Baker, G. L., Poly(phenyllactide): Synthesis, Characterization, and Hydrolytic Degradation. *Biomacromolecules* **2001,** *2* (3), 658-663.
12. Ponsart, S.; Coudane, J.; Morgat, J. L.; Vert, M., Synthesis of 3H and fluorescence-labelled poly (DL-Lactic acid). *J. Labelled Compd. Radiopharm.* **2001,** *44* (10), 677-687.
13. El Habnouni, S.; Darcos, V.; Garric, X.; Lavigne, J.-P.; Nottelet, B.; Coudane, J., Mild Methodology for the Versatile Chemical Modification of Polylactide Surfaces: Original Combination of Anionic and Click Chemistry for Biomedical Applications. *Adv. Funct. Mater.* **2011,** *21* (17), 3321-3330.

14. El Habnouni, S.; Lavigne, J.-P.; Darcos, V.; Porsio, B.; Garric, X.; Coudane, J.; Nottelet, B., Toward potent antibiofilm degradable medical devices: A generic method for the antibacterial surface modification of polylactide. *Acta Biomater.* **2013,** *9* (8), 7709-7718.

15. Sardo, C.; Nottelet, B.; Triolo, D.; Giammona, G.; Garric, X.; Lavigne, J.-P.; Cavallaro, G.; Coudane, J., When Functionalization of PLA Surfaces Meets Thiol–Yne Photochemistry: Case Study with Antibacterial Polyaspartamide Derivatives. *Biomacromolecules* **2014,** *15* (11), 4351-4362.

16. Carlson, D.; Nie, L.; Narayan, R.; Dubois, P., Maleation of polylactide (PLA) by reactive extrusion. *J. Appl. Polym. Sci.* **1999,** *72* (4), 477-485.

17. Plackett, D., Maleated Polylactide as an Interfacial Compatibilizer in Biocomposites. *J. Polym. Environ.* **2004,** *12* (3), 131-138.

18. Zhang, J.-F.; Sun, X., Mechanical Properties of Poly(lactic acid)/Starch Composites Compatibilized by Maleic Anhydride. *Biomacromolecules* **2004,** *5* (4), 1446-1451.

19. Cao, Z.; Jiang, S., Super-hydrophilic zwitterionic poly(carboxybetaine) and amphiphilic non-ionic poly(ethylene glycol) for stealth nanoparticles. *Nano Today* **2012,** *7* (5), 404-413.

20. Bakkour, Y.; Darcos, V.; Coumes, F.; Li, S.; Coudane, J., Brush-like amphiphilic copolymers based on polylactide and poly(ethylene glycol): Synthesis, self-assembly and evaluation as drug carrier. *Polymer* **2013,** *54* (7), 1746-1754.

21. Qian, W.; Song, X.; Feng, C.; Xu, P.; Jiang, X.; Li, Y.; Huang, X., Construction of PEG-based amphiphilic brush polymers bearing hydrophobic poly(lactic acid) side chains via successive RAFT polymerization and ROP. *Polym. Chem.* **2016,** *7* (19), 3300-3310.

22. Coumes, F.; Beaute, L.; Domurado, D.; Li, S.; Lecommandoux, S.; Coudane, J.; Darcos, V., Self-assembly of well-defined triblock copolymers based on poly(lactic acid) and poly(oligo(ethylene glycol) methyl ether methacrylate) prepared by ATRP. *RSC Advances* **2016,** *6* (58), 53370-53377.

23. Zhang, Q.; Ren, H.; Baker, G. L., Synthesis and click chemistry of a new class of biodegradable polylactide towards tunable thermo-responsive biomaterials. *Polym. Chem.* **2015,** *6* (8), 1275-1285.

24. Falatach, R.; McGlone, C.; Al-Abdul-Wahid, M. S.; Averick, S.; Page, R. C.; Berberich, J. A.; Konkolewicz, D., The best of both worlds: active enzymes by grafting-to followed by grafting-from a protein. *Chem. Commun.* **2015,** *51* (25), 5343-5346.

25. Dechy-Cabaret, O.; Martin-Vaca, B.; Bourissou, D., Controlled Ring-Opening Polymerization of Lactide and Glycolide. *Chem. Rev.* **2004,** *104* (12), 6147-6176.

26. Beuille, E.; Darcos, V.; Coudane, J.; Lacroix-Desmazes, P.; Nottelet, B., Regioselective Halogenation of Poly(lactide) by Free-Radical Process. *Macromolecular Reaction Engineering* **2014,** *8* (2), 141-148.

27. Raynor, J. E.; Petrie, T. A.; García, A. J.; Collard, D. M., Controlling Cell Adhesion to Titanium: Functionalization of Poly[oligo(ethylene glycol)methacrylate] Brushes with Cell-Adhesive Peptides. *Adv. Mater.* **2007,** *19* (13), 1724-1728.

28. Alas, G. R.; Agarwal, R.; Collard, D. M.; García, A. J., Peptide-functionalized poly[oligo(ethylene glycol) methacrylate] brushes on dopamine-coated stainless steel for controlled cell adhesion. *Acta Biomater.* **2017,** *59* (Supplement C), 108-116.

29. Zhang, L.; Chan, J. M.; Gu, F. X.; Rhee, J.-W.; Wang, A. Z.; Radovic-Moreno, A. F.; Alexis, F.; Langer, R.; Farokhzad, O. C., Self-Assembled Lipid−Polymer Hybrid Nanoparticles: A Robust Drug Delivery Platform. *ACS Nano* **2008,** *2* (8), 1696-1702.

30. Nederberg, F.; Zhang, Y.; Tan, J. P. K.; Xu, K.; Wang, H.; Yang, C.; Gao, S.; Guo, X. D.; Fukushima, K.; Li, L.; Hedrick, J. L.; Yang, Y.-Y., Biodegradable nanostructures with selective lysis of microbial membranes. *Nat. Chem.* **2011,** *3*, 409.

CHAPTER 6

Surface bromination followed by atom-transfer radical polymerization on thin films of polylactide to afford bacterial resistant surfaces[§]

6.1. INTRODUCTION

The biocompatible and biodegradable nature of Polylactide (PL), together with the approval of US Food and Drug Administration (FDA) for the use of some of its devices in contact in humans has resulted in the fabrication of PL into a variety of medical devices such as sutures, stents, and scaffolds for bone regeneration.[1,2,3,4] However, the hydrophobicity of PL supports biofouling which results in the potential for the accumulation and growth of bacteria on the device and inception of an infection that leads to medical complications.[5]

The attachment of a cationic or zwitterion polymer by a "grafting to" approach, or growing polymeric chains from a surface-bound initiator by a "grafting from" approach, are two strategies that have been used to covalently modify the surface so as to render the substrates antibacterial.[6-8] For example Wang et al rendered silicon substrate resistant against *S. aureus* and *E. coli* by coupling an antimicrobial polypeptide bearing an azide functional group on the alkynyl group present on the silicone substrate via azide alkyne click chemistry.[9] In contrast, Pranantyo et al carried out ATRP of cationic and zwitterion methacrylates by initiation from brominated tanic acid anchored to a stainless steel surface to improve the antifouling properties of the stainless steel.[10]

Similarly, PL surface has been modified via photo-initiated free radical grafting of a polymer such as *N*-vinylpyrrolidone.[11] Complexation of poly(vinylpyrrolidone) brushes with

[§] The work presented in this chapter is carried in collaboration with Zhishuai Geng, a PhD candidate in Dr. M. G. Finn's research group. The antimicrobial assay and XPS were performed by Zhishuai.

iodine rendered the surface antimicrobial. However, a lack of control of the growth of the graft polymer is a limitation associated with free radical polymerization. Another strategy to modify the surface of PL involved deprotonation of methine of PL by the use of a strong base (e.g. LDA) followed by coupling of the polymeric carbanion to propargyl bromide.[8] A quaternary ammonium methacrylate was grafted to the polymer surface via azide-alkyne click chemistry to render the surface antimicrobial polymer.[12] However, use of a strong base that can potentially lead to degradation of the polymer and low grafting density on the surface associated with the "grafting to" approach due steric crowding leads to inefficient modification of the surface. Herein we demonstrate a two-step modification of the surface of PL to impart bacterial resistance and antimicrobial behavior.

6.2. RESULTS AND DISCUSSION

Bromination of surface of films of PL followed by surface initiated atom-transfer radical polymerization (SI-ATRP) of [2-(methacryloyloxy)ethyl]trimethylammonium chloride, a quaternary ammonium methacrylate (QAMA) imparts bactericidal properties, Figure 6.1.

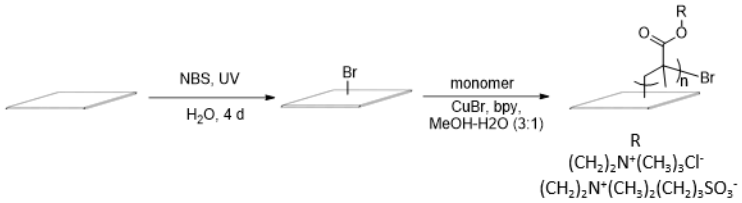

Figure 6.1. Radical bromination of PL film and surface-initiated atom-transfer radical polymerization of methacrylate monomers.

Films were prepared by drop-casting a solution of PL in CH_2Cl_2 onto a glass coverslip followed by evaporation of the solvent. Treatment of PL films with a solution of *N*-bromosuccinimide (NBS) in H_2O (14 mg/mL) and UV irradiation for 4 days followed by rinsing results in the incorporation of up to 3.8 % of bromine on the surface of PL, as characterized by XPS, Figure 6.2B, Table 6.1.

Table 6.1. XPS characterization and water contact angle measurements of the films

Polymer film	XPS (Atomic percentage)						Water contact angle
	C	O	N	Br	Cl	S	
PL[a]	69.0	25.4	–	–	–	–	89±5°
Surface brominated PL	67.9	25.9	–	3.8	–	–	
SI-ATRP with QAMA	67.3	18.1	7.6	0.8	5.0	–	15±5°
SI-ARTP with ZMA	63.0	26.4	5.7	-	-	4.9	

[a]PL film treated with ATRP conditions (QAMA, CuBr, bpy, MeOH/H_2O)

The lack of a signal for nitrogen in the spectrum indicates the absence of physically-adsorb NBS on the surface. A lack of decrease in the mass of the film after bromination suggests that the

reaction conditions does not result in degradation of the polymer. Carrying out the reaction in the absence of UV light, or in the presence of a different initiator such as benzoyl peroxide (BPO) in MeOH resulted in incorporation of only 0.8 % bromine on the film. Attempts on bromination of PL surface with 1 % Br_2 led to the dissolution of the films over the duration of reaction.

Brominated PL surface serves as a macroinitiator to carry out SI-ATRP of quaternary ammonium methacrylate (QAMA) in the presence of CuBr and 2,2'-bipyridyl (bpy) as catalyst. The ratio of CuBr to bpy was kept at 2:1 to reduce the concentration of free bpy at any given time to prevent its nucleophilic attack on the polyester backbone of PL. XPS spectra of the QAMA-treated films show the presence of two new signals corresponding to the binding energy of nitrogen and chlorine, indicating the success of the reaction, Figure 6.2C. The C/O (3.71) and C/N (8.85) ratios of the films are consistent with the composition of poly(QAMA) brushes on the surface. This indicate that the surface of the films predominately consists of the grafted copolymer as a result of which the signals of PL backbone are drastically attenuated, Table 6.1. Moreover, the increase in the ratio of C/Br compared to brominated PL films indicates that the conditions results in the formation of a relatively dense layer of the graft polymer.

Prior attempts by Coudane to attach poly(QAMA) (M_n = 6.5 kg/mol) on PL surfaces by a "grafting to" approach resulted in a surface with a C/N ratio of 72.2.[12] The high C/N ratio indicate low grafting of poly(QAMA) brushes. Thus, surface bromination of PL followed by SI-ATRP provides an opportunity to graft a much denser layer of polymethacrylate on PL surface. Static water contact angle measurements were performed to evaluate the change in the surface properties upon polymerization. The hydrophobic nature of the PL backbone leads to a large water contact angle for PL films before ATRP. A drastic decrease in the water contact angle of the films post

ATRP indicates towards the successful grafting of the hydrophilic polymer on the PL surface Table 6.1.

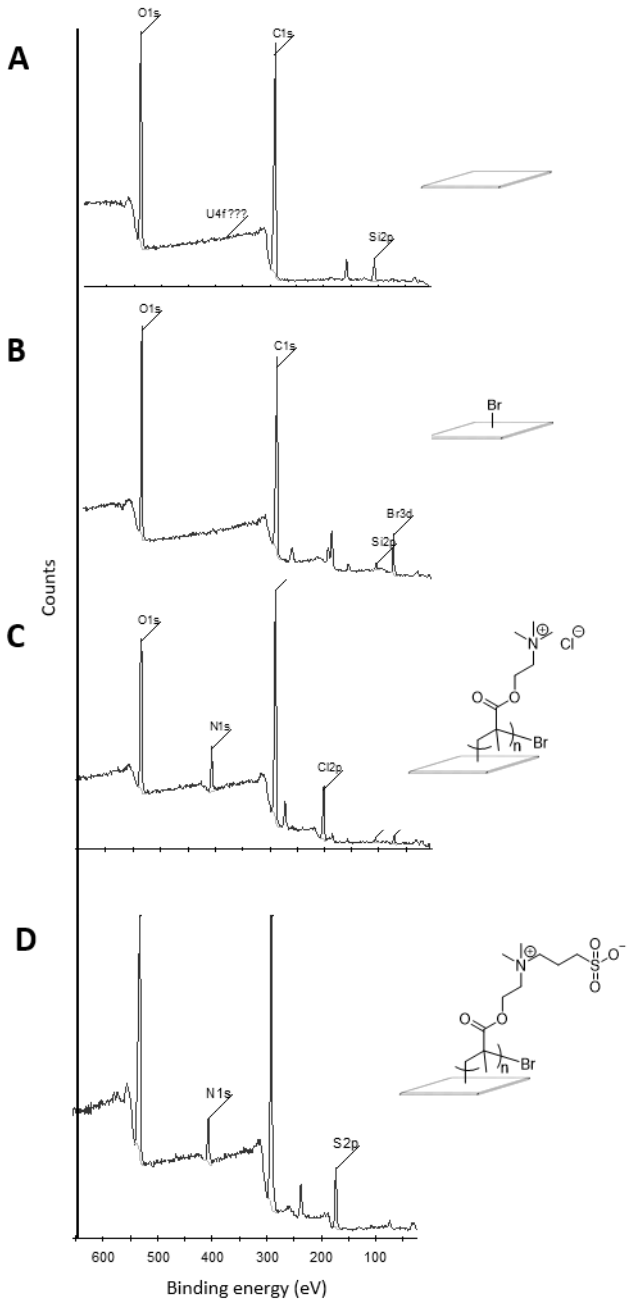

Figure 6.2. XPS survey spectra of polymeric thin films. A, PL film exposed to ATRP conditions (CuBr, bpy, QAMA, MeOH-H_2O); B, Surface brominated PL; C, SI-ATRP QAMA modified PL. D, SI-ATRP with ZMA modified PL.

To further demonstrate the versatility of brominated PL we also performed SI-ATRP of [2-(methacryloyloxy)ethyl]dimethyl-(3-sulfopropyl)ammonium hydroxide, a zwitterion methacrylate (ZMA), under the same reaction conditions. The appearance of new signals with the binding energy of nitrogen and sulfur in the ZMA modified films indicates the success of the reaction, Figure 6.2D. The complete disappearance of the Br signal, along with the agreement of the C/N (11.05) and C/S (12.85) ratio of the films with that of poly(ZMA) (C/N = C/S = 11) suggests that the protocol resulted in grafting a relatively dense layer of poly(ZMA) brush on top of the PL film, Table 6.1.

Though the films were extensively washed post ATRP, to confirm that the signals observed in the XPS were not as a result of physical adsorption of the monomer on the surface, following set of controls were employed: i) non-brominated PL films exposed to ATRP conditions; ii) surface brominated PL films treated with the monomer, CuBr in MeOH/H_2O (no bpy). The absence of signals corresponding to the binding energy of nitrogen and chlorine (or sulfur in case of ZMA) in the XPS for both the set of controls confirm that these condition does not lead to physical adsorption of the monomer on the film.

The antimicrobial efficacy of the graft polymerized surfaces was determined against *E. coli* cells. Treatment of *E. coli* cells with the films bearing the graft poly(QAMA) polymer on the surface (area of the film 0.5 X 0.5 mm) displayed potent antimicrobial potency compared to non-grafted PL films, Figure 6.3. Quantification of the antimicrobial potency was performed by loading serial dilutions of the aliquot of bacterial suspension treated with the films on an agar plate. Poly(QAMA) grafted films displayed a 2.5 order of magnitude increase in the antimicrobial potency as compared to PL film, Figure 3D.

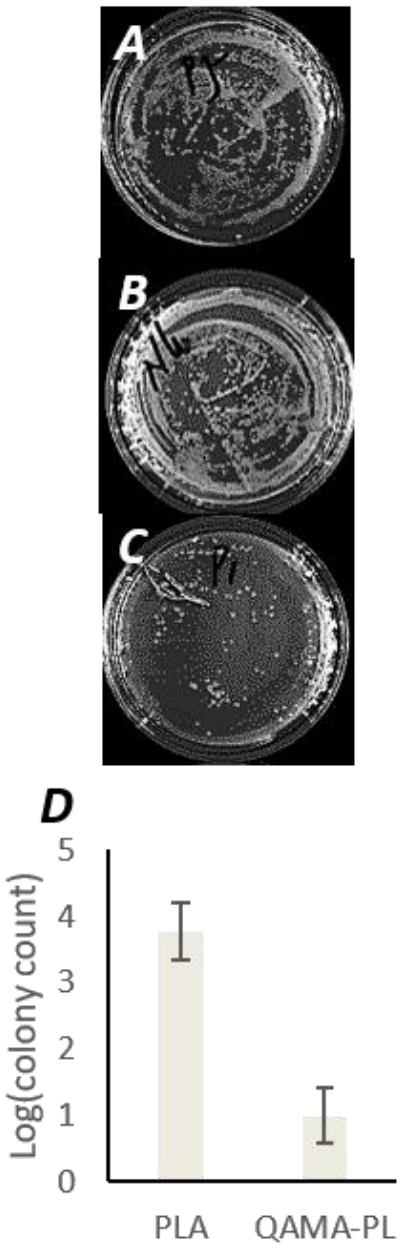

Figure 6.3. Antimicrobial assay: Agar plates obtained after treatment of *E. coli* with A, PL film exposed to ATRP conditions (CuBr, bpy, QAMA, MeOH-H_2O). B, Surface brominated PL. C, SI-ATRP with QAMA. D, Quantification of bacterial colonies

6.3. EXPERIMENTAL SECTION

6.3.1. Materials and methods

All the reagents were obtained from the sources listed below and were used without further purification unless otherwise specified: *N*-bromosuccinimide (NBS), CuBr (Aldrich); [2-(methacryloyloxy)ethyl]trimethylammonium chloride 75 wt % in water (QAMA), 2,2′-bipyridine (bpy), (Sigma Aldrich); [2-(methacryloyloxy)ethyl]dimethyl-(3-sulfopropyl)ammonium hydroxide (ZMA) (Alfa Aeser). All solvents were purchased from VWR and were used directly without further purification. X-ray photoelectron spectroscopy (XPS) characterizations were performed using a Thermo K-Alpha spectrometer with an Al-K_α source. UV-vis spectra were recorded using a Varioskan Flash plate reader (Thermo Fisher, Waltham, MA).

6.3.2. Synthesis

6.3.2.1. Surface bromination of PL

Glass coverslips were washed sequentially with hexane, acetone and H_2O and dried under a stream of Ar. PL films were prepared by drop casting a solution of PL in CH_2Cl_2 (25 mg/mL) onto the coverslips. The edges of the films were taped to the glass using 3M tape to prevent the films from detachment from the coverslip during subsequent reactions. The films were placed in the wells of a 24 well-plate. A solution of NBS (1 mL of a 14 mg/mL solution in deionized H_2O) was added to each well and the plate was kept under a UV lamp on a rocker. After every 6 h, NBS solution was removed from each well and fresh NBS solution was added. The process was repeated for 4 days. The NBS solution was removed, 1 mL of deionized H_2O was added to each well and the plate was kept on a rocker for 2 h. The films were transferred to a new 24 well-plate, deionized H_2O was added to each well and the plate was kept on a rocker for 15 mins. The films were rinsed three times with H_2O and MeOH and dried under a stream of Ar. XPS 533 (O, 1*s*, 25.9%), 285 (C, 1*s*, 67.9%), 71.2 (Br, 3*d*, 3.8%) eV.

6.3.2.2. General procedure for ATRP

Bpy (16 mg, 0.10 mmol) was added to an 8 mL solution of the methacrylate monomer (400 mg/mL) in 3:1 mixture of MeOH and H_2O in a 100 mL Schlenk flask that was previously purged with Ar. The reaction mixture was degassed by 6 freeze-pump-thaw cycles and back-filled with Ar. Four surface brominated PL films were placed in four separate round-bottom flasks and CuBr (4 mg, 30 μmol) was added to each flask. The flasks were purged with Ar for >15 min. The degassed reaction mixture (2 mL) was added to each round-bottom flask and the flasks were kept on a rocker in the dark for 16 h. The reaction mixture was removed from the flasks and the films were transferred to glass vials. The films were washed twice with MeOH, followed by water (x3) washes and dried under a stream of Ar.

Films bearing poly(QAMA) brushes, XPS 533 (O, 1*s*, 18.1 %), N (400, 1*s*. 7.6 %), 285 (C, 1*s*, 67.3 %), 71.2 (Br, 3*d*, 0.8 %) eV. Films bearing poly(ZMA) brushes, XPS 533 (O, 1*s*, 26.4 %), N (400, 1*s*, 5.7 %), 285 (C, 1*s*, 63 %), 169 (S 2*p*, 4.9 %).

6.3.2.3. Antimicrobial assay

E. coli suspension was grown in Mueller-Hinton Broth (MHB) overnight at 37 °C. The resulting culture was used to inoculate a second culture in 2 mL of MHB medium until an optical density of 0.8 at 600 nm was obtained. The bacteria were collected by centrifugation at 4,000 x g for 3 min at 4 °C, washed with sterile PBS (pH 7.4) and suspended in PBS to get a specific final concentration. Polymer films (0.01-0.04 cm^2) were added to the suspension of bacteria and the vial was shaken for 0.5 to 4 h on a rocker. A 25 µL aliquot of the suspension was spread onto a layer of LB medium containing 0.8% agar (previously autoclaved, and cooled to 37 °C) in a sterile Petri dish. Bacterial colonies were counted after overnight incubation at 37 °C.

6.4. CONCLUSIONS

In conclusion, an approach to modify the surface of PL by carrying out bromination in the presence of *N*-bromosuccinimide (NBS) under UV irradiation is described. Brominated PL surfaces serve as a surface initiator for the grafting-from atom-transfer radical polymerization (ATRP) of methacrylate monomers to afford polymer brushes. Surface initiated ATRP of [2-(methacryloyloxy)ethyl]trimethylammonium chloride, a quaternary ammonium methacrylate (QAMA) affords films that display a 400 fold increase in the antimicrobial efficacy over that of PL. The selective modification of the surface of PL films, without altering the bulk material that provides the structural integrity, would provide new opportunities to tailor interactions with the host.

6.5. REFERENCES

1. Hu, W.; Huang, Z.-M., Biocompatibility of braided poly(L-lactic acid) nanofiber wires applied as tissue sutures. *Polymer International* **2010,** *59* (1), 92-99.
2. Huh, B. K.; Kim, B. H.; Kim, S.-N.; Park, C. G.; Lee, S. H.; Kim, K. R.; Heo, C. Y.; Choy, Y. B., Surgical suture braided with a diclofenac-loaded strand of poly(lactic-co-glycolic acid) for local, sustained pain mitigation. *Materials Science and Engineering: C* **2017,** *79*, 209-215.
3. Middleton, J. C.; Tipton, A. J., Synthetic biodegradable polymers as orthopedic devices. *Biomaterials* **2000,** *21* (23), 2335-2346.
4. Eppley, B. L.; Morales, L.; Wood, R.; Pensler, J.; Goldstein, J.; Havlik, R. J.; Habal, M.; Losken, A.; Williams, J. K.; Burstein, F.; Rozzelle, A. A.; Sadove, A. M., Resorbable PLLA-PGA plate and screw fixation in pediatric craniofacial surgery: clinical experience in 1883 patients. *Plast Reconstr Surg* **2004,** *114* (4), 850-6; 857.
5. Rokkanen, P. U.; Böstman, O.; Hirvensalo, E.; Mäkelä, E. A.; Partio, E. K.; Pätiälä, H.; Vainionpää, S.; Kimmo, V.; Törmälä, P., Bioabsorbable fixation in orthopaedic surgery and traumatology. *Biomaterials* **2000,** *21* (24), 2607-2613.
6. Moya, S.; Azzaroni, O.; Farhan, T.; Osborne, V. L.; Huck, W. T. S., Locking and Unlocking of Polyelectrolyte Brushes: Toward the Fabrication of Chemically Controlled Nanoactuators. *Angew. Chem. Int. Ed.* **2005,** *44* (29), 4578-4581.
7. Cheng, G.; Xue, H.; Zhang, Z.; Chen, S.; Jiang, S., A Switchable Biocompatible Polymer Surface with Self-Sterilizing and Nonfouling Capabilities. *Angew. Chem.* **2008,** *120* (46), 8963-8966.
8. El Habnouni, S.; Darcos, V.; Garric, X.; Lavigne, J.-P.; Nottelet, B.; Coudane, J., Mild Methodology for the Versatile Chemical Modification of Polylactide Surfaces: Original Combination of Anionic and Click Chemistry for Biomedical Applications. *Adv. Funct. Mater.* **2011,** *21* (17), 3321-3330.
9. Wang, L.; Chen, J.; Shi, L.; Shi, Z.; Ren, L.; Wang, Y., The promotion of antimicrobial activity on silicon substrates using a "click" immobilized short peptide. *Chem. Commun.* **2014,** *50* (8), 975-977.
10. Pranantyo, D.; Xu, L. Q.; Neoh, K.-G.; Kang, E.-T.; Ng, Y. X.; Teo, S. L.-M., Tea Stains-Inspired Initiator Primer for Surface Grafting of Antifouling and Antimicrobial Polymer Brush Coatings. *Biomacromolecules* **2015,** *16* (3), 723-732.
11. Gutierrez-Villarreal, M. H.; Ulloa-Hinojosa, M. G.; Gaona-Lozano, J. G., Surface functionalization of poly(lactic acid) film by UV-photografting of N-vinylpyrrolidone. *J. Appl. Polym. Sci.* **2008,** *110* (1), 163-169.
12. El Habnouni, S.; Lavigne, J.-P.; Darcos, V.; Porsio, B.; Garric, X.; Coudane, J.; Nottelet, B., Toward potent antibiofilm degradable medical devices: A generic method for the antibacterial surface modification of polylactide. *Acta Biomater.* **2013,** *9* (8), 7709-7718.

CHAPTER 7

Suggestion for future work

7.1. NON-FOULING SURFACES FOR BIOMEDICAL APPLICATIONS

The biocompatibility and biodegradability of PL supports its use in the fabrication of a variety of biomedical devices such as sutures, stents, wound healing dressings, and bone regeneration scaffolds. However, the biofouling behavior of these devices still poses a challenge in its utilization for these applications. Poly(oligoethylene glycol) methacrylate, poly(OEGMA), attenuates the bio-fouling behavior of polymeric materials and metallic surfaces. In chapter 5 I described a pathway to brominate PL in solution and in Chapter 6 I demonstrated a pathway to achieve bromination of thin-films of PL. Films formed by drop-casting of Br-PL (Chapter 5) or by direct bromination of PL films (Chapter 6) can be used to carry out surface-initiated atom-transfer radical polymerization (SI ATRP) of OEGMA to afford the grafting of poly(OEGMA) brushes on the surface of PL, Figure 1.

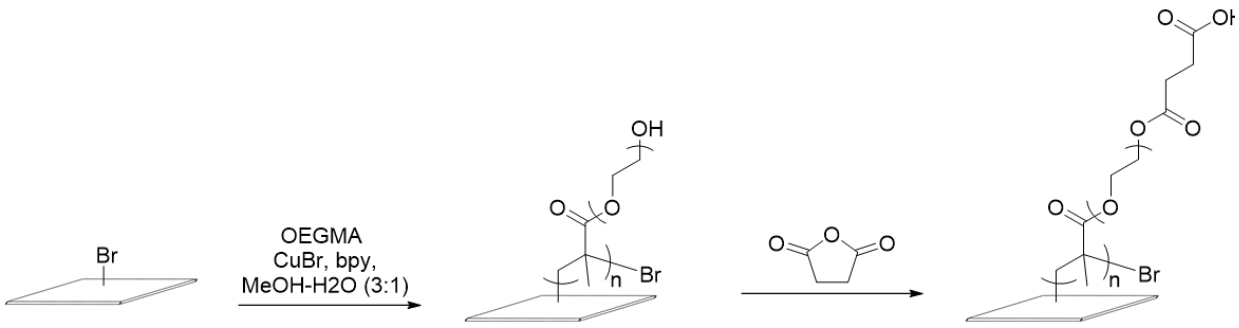

Figure 7.1. Surface-initiated atom-transfer radical polymerization of OEGMA followed by the treatment of poly(OEGMA) grafted films with succinic anhydride.

The success of the grafting of poly(OEGMA) brushes on PL can be monitored by XPS. The films grafted with poly(OEGMA) brushes would display a difference in the ratios of carbon, oxygen and bromine compared to that of brominated PL films. A cell adhesion assay of the

poly(OEGMA) grafted PL films could be carried conditions by the treatment of Human Mesenchymal Stem Cells (hMSC) with the OEGMA treated and un-treated PL films in serum. One might expect that the poly(OEGMA) grafted PL films display a significant reduction in the adherence of cells compared to untreated Br-PL films, Figure 1. Such poly(OEGMA) grafted devices could improve the utility of PL for a variety of biomedical applications.

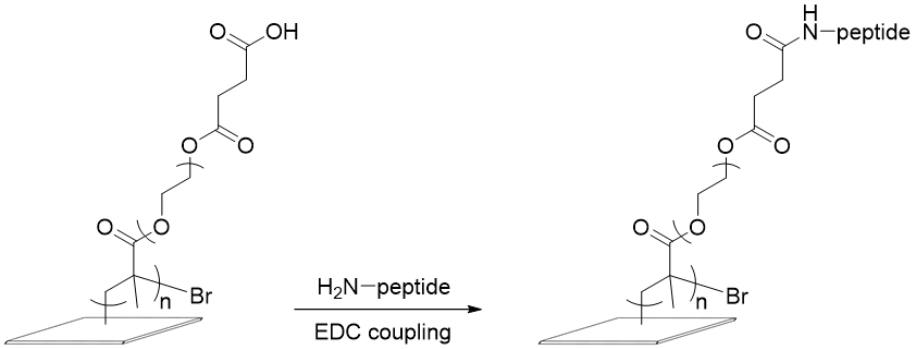

Figure 7.2. Scheme for the coupling of a peptide on a PL film

Treatment of poly(OEGMA) grafted films with succinic anhydride will result in the formation of PL films bearing polymeric brushes with carboxylic acid functional groups. The presence of an acid functional group could be exploited to couple a variety of peptides or proteins using EDC coupling chemistry. For example, the coupling of RGD-containing peptides on PL could allow for selective recruitment of osteoblast cells on the PL surface to provide a substrate with a potential to support bone growth.

7.2. CONCLUSIONS

In summary, in this thesis I have described the syntheses of five copolymers of PLA bearing different reactive functional groups. Copolymers of PLA bearing reactive functional groups offer the potential to access materials with a wide array of biomedical applications. I have fabricated

thin films and nanoparticles of selected materials to provide preliminary demonstration of these copolymers to bioconjugation, drug delivery and antimicrobial activity.

APPENDIX A

Supporting Figures

Table of Content

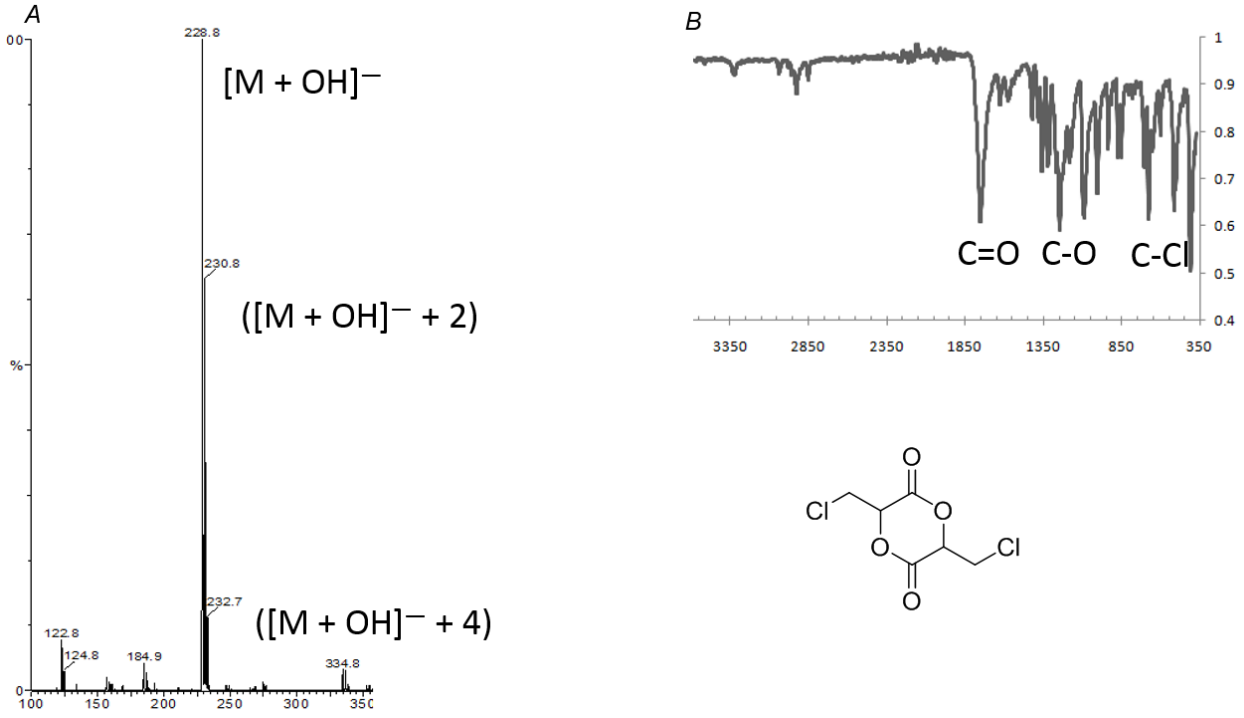

Figure A-1. 3-chlorolactide monomer: A, mass spectrum; B, IR spectrum.

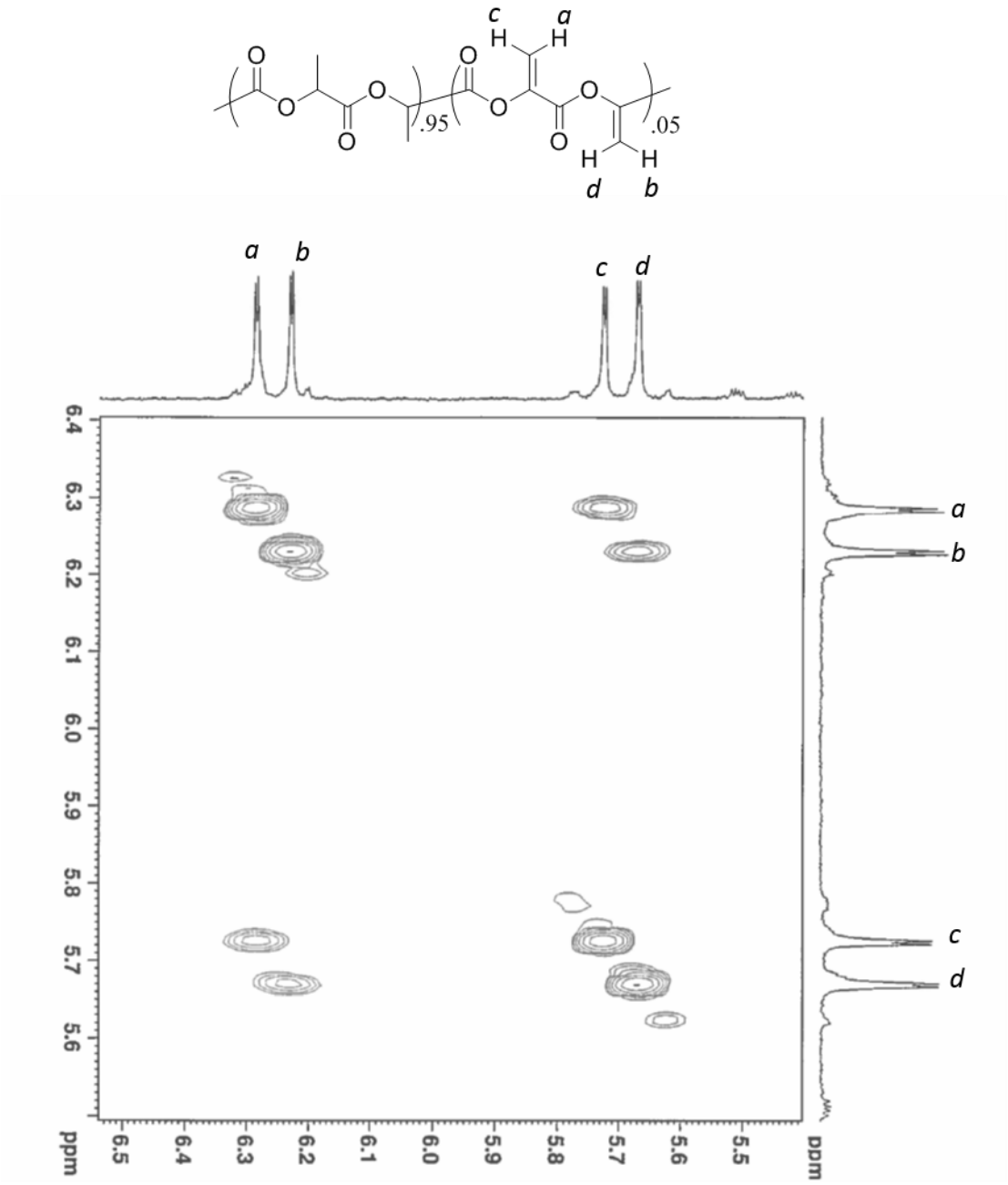

Figure A-2. ene-PL COSY NMR spectrum (500 MHz, $CDCl_3$)

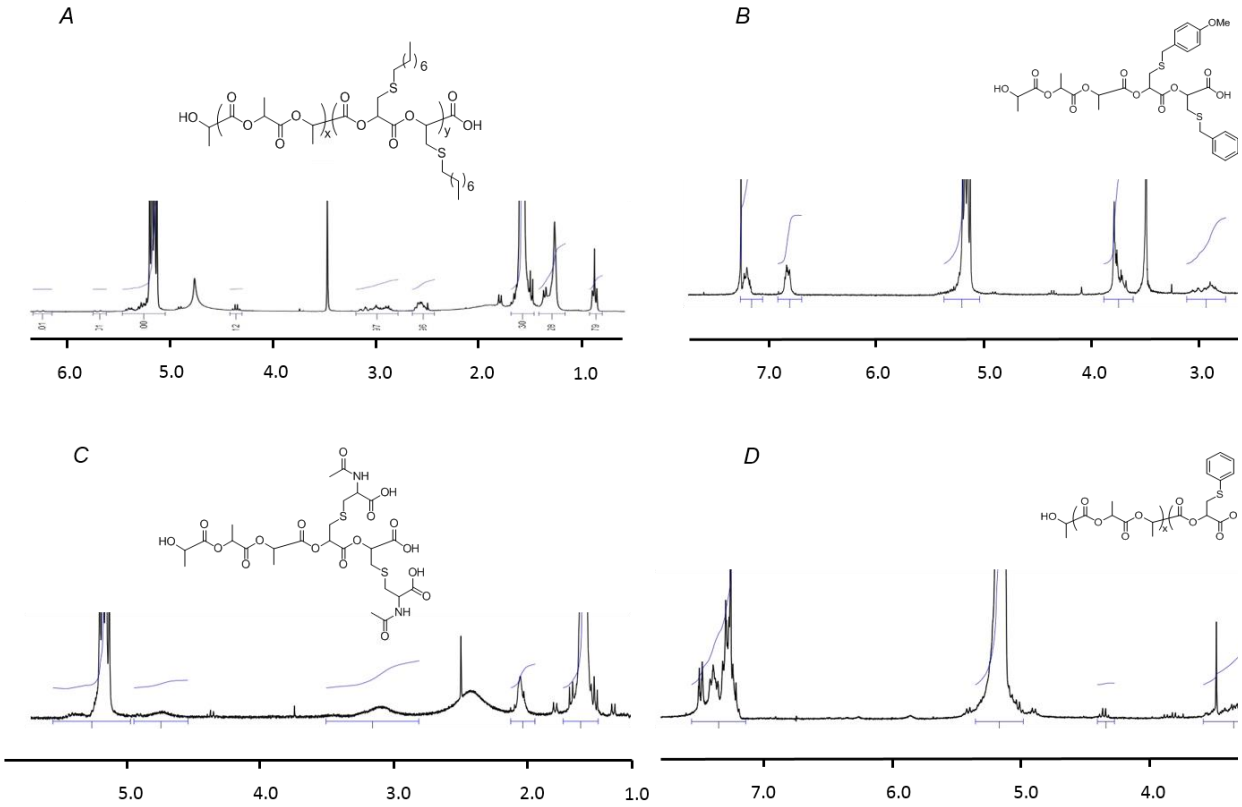

Figure A-3. Nucleophilic conjugate addition of thiol onto ene-PL. A, octylthio-PL; B, 4-(methoxy)-benzylthia-PL, C, *N*-acetylcysteine-PL; D, thiophenyl-PL.

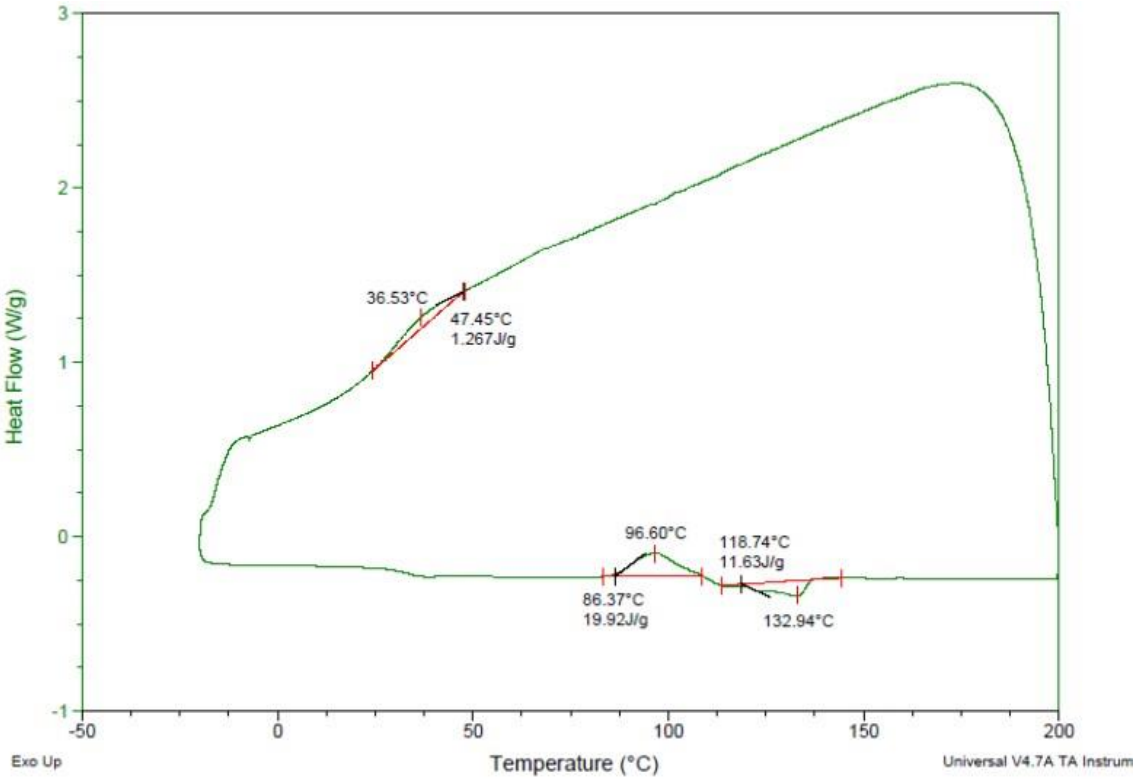

Figure A-4. DSC thermogram (5°C/min, -20 °C to 200 °C) of 3-chloro-PL.

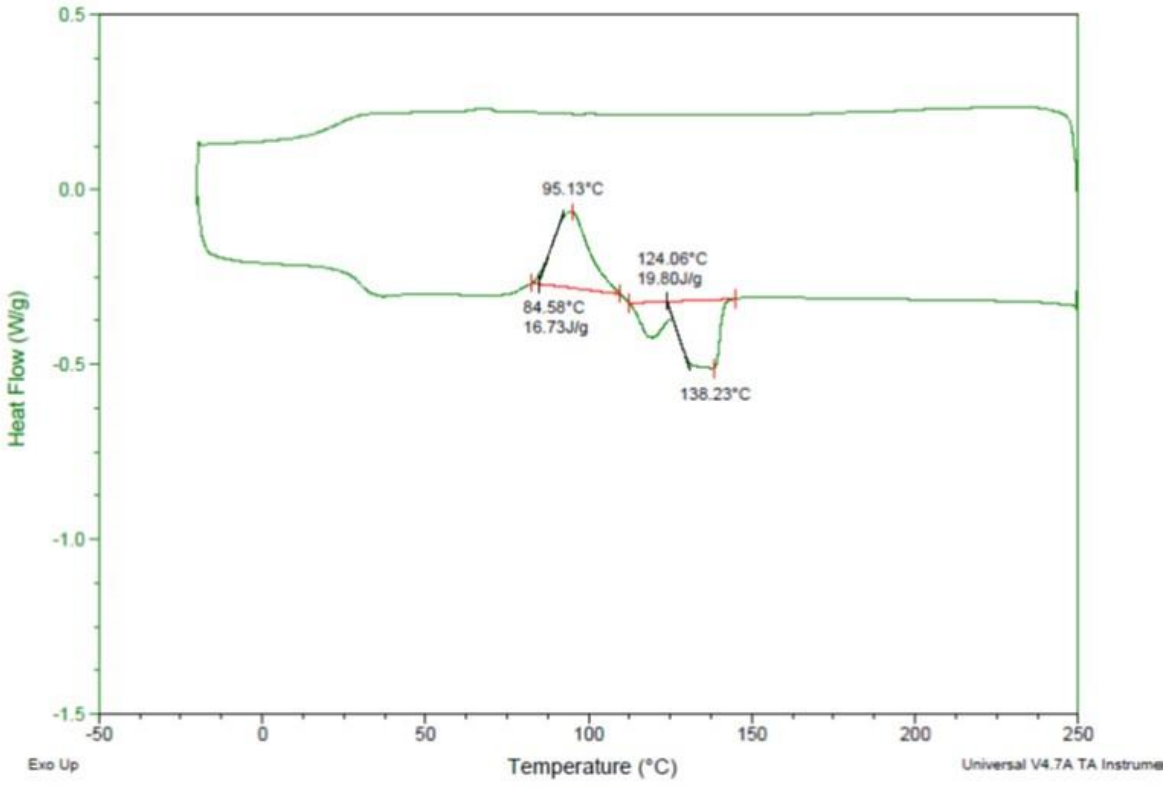

Figure A-5. DSC thermogram of ene-PL showing the second thermal cycle. 10 °C/min, -20 °C to 250 °C.

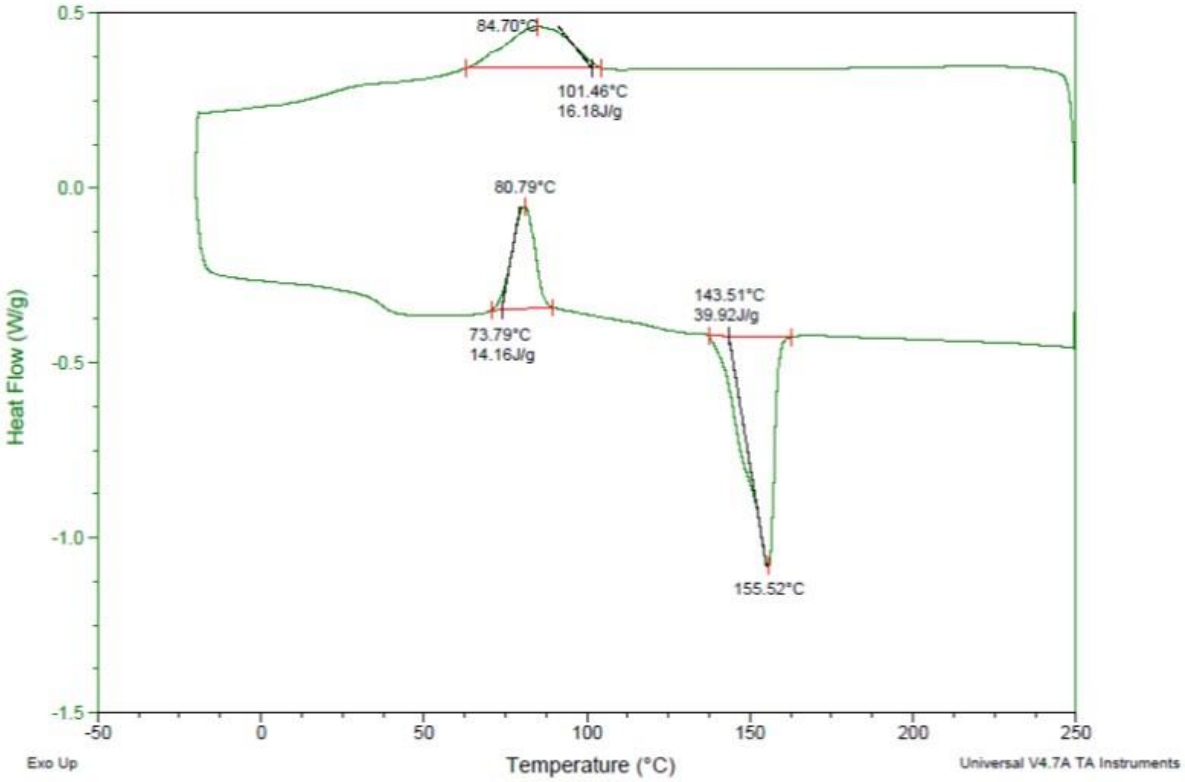

Figure A-6. DSC thermogram of MBT-PL showing the second thermal cycle. 10 °C/min, -20 °C to 250 °C.

Crystal Data and Experimental

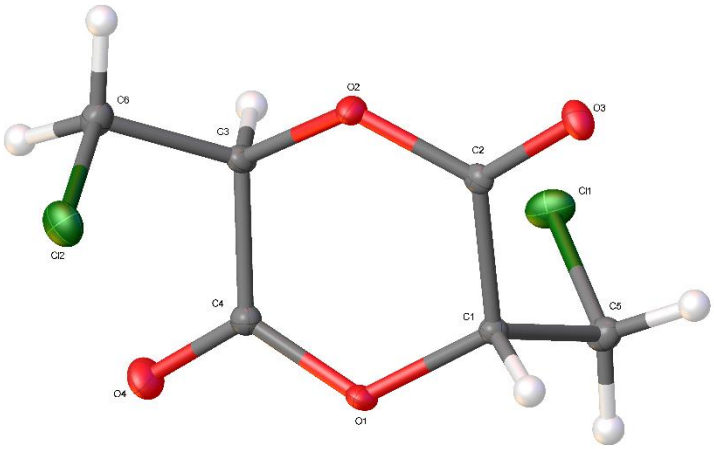

Experimental. Single colourless prism-shaped crystals of (**PK001**) were recrystallised from DCM by slow evaporation. A suitable crystal (0.93×0.34×0.32 mm) was selected and mounted on a loop with paratone oil on a Bruker APEX-II CCD diffractometer. The crystal was cooled to T = 100(2) K during the data collection. The structure was solved with **ShelXT** (Sheldrick, 2015) using direct and dual-space solution methods and by using **Olex2** (Dolomanov et al., 2009) as the graphical interface. The model was refined with version of **ShelXL-97** (Sheldrick, 2008) using Least Squares minimisation.

Crystal Data. $C_6H_6Cl_2O_4$, M_r = 213.01, monoclinic, $P2_1$ (No. 4), a = 5.2416(11) Å, b = 9.3607(19) Å, c = 8.1773(16) Å, β = 94.886(2)°, $\alpha = \gamma = 90°$, V = 399.76(14) Å^3, T = 100(2) K, Z = 2, Z' = 1, μ(MoK$_\alpha$) = 0.780, 6970 reflections measured, 2428 unique (R_{int} = 0.0252) which were used in all calculations. The final wR_2 was 0.0521 (all data) and R_1 was 0.0207 (I > 2(I)).

Compound	**PK001**
Formula	$C_6H_6Cl_2O_4$
$D_{calc.}$/ g cm^{-3}	1.770
μ/mm^{-1}	0.780
Formula Weight	213.01
Colour	colourless
Shape	prism
Max Size/mm	0.93
Mid Size/mm	0.34
Min Size/mm	0.32
T/K	100(2)
Crystal System	monoclinic
Flack Parameter	0.06(2)
Hooft Parameter	0.08(2)
Space Group	$P2_1$
a/Å	5.2416(11)
b/Å	9.3607(19)
c/Å	8.1773(16)
α/°	90
β/°	94.886(2)
γ/°	90
V/Å^3	399.76(14)
Z	2
Z'	1
Θ_{min}/°	2.500
Θ_{max}/°	30.513
Measured Refl.	6970
Independent Refl.	2428
Reflections Used	2391
R_{int}	0.0252
Parameters	130
Restraints	31
Largest Peak	0.303
Deepest Hole	-0.209
GooF	1.064
wR_2 (all data)	0.0521
wR_2	0.0518
R_1 (all data)	0.0211
R_1	0.0207

Structure Quality Indicators

Reflections:	d min 0.70	I/σ 31.6	Rint 2.52%	complete 99%
Refinement:	Shift 0.000	Max Peak 0.3	Min Peak -0.2	GooF 1.064

A colourless prism-shaped crystal with dimensions 0.93×0.34×0.32 mm was mounted on a loop with paratone oil. Data were collected using a Bruker APEX-II CCD diffractometer equipped with an Oxford Cryosystems low-temperature apparatus operating at T = 100(2) K.

Data were measured using ϕ and ω scans scans of 2° per frame for 20 s using MoK_α radiation (sealed tube, 45 kV, 35 mA). The total number of runs and images was based on the strategy calculation from the program **APEX2** (Bruker, 2014). The maximum resolution achieved was Θ = 30.5°.

Unit cell indexing was performed by using the **APEX2** (Bruker, 2014) software and refined using **SAINT** (Bruker, V8.34A, 2013) on 6759 reflections, 97% of the observed reflections. Data reduction, scaling and absorption corrections were performed using **SAINT** (Bruker, V8.34A, 2013) and SADABS-2014/5 (Bruker, 2014). wR_2(int) was 0.1458 before and 0.0488 after correction. The Ratio of minimum to maximum transmission is 0.7612. The $\lambda/2$ correction factor is 0.0015. The final completeness is 100.00% out to 30.513° in Θ. The absorption coefficient (μ) of this material is 0.780 mm^{-1} and the minimum and maximum transmissions are 0.5679 and 0.7461.

The structure was solved with **ShelXT** (Sheldrick, 2015) in the space group $P2_1$ (# 4) using direct and dual-space solution methods and by using **Olex2** (Dolomanov et al., 2009) as the graphical interface. The structure was refined by Least Squares using version of **ShelXL-97** (Sheldrick, 2008). All non-hydrogen atoms were refined anisotropically. Hydrogen atom positions were refined freely

The Flack parameter was refined to 0.06(2). Determination of absolute structure using Bayesian statistics on Bijvoet differences using the Olex2 results in 0.08(2). Note: The Flack parameter is used to determine chirality of the crystal studied, the value should be near 0, a value of 1 means that the stereochemistry is wrong and the model should be inverted.

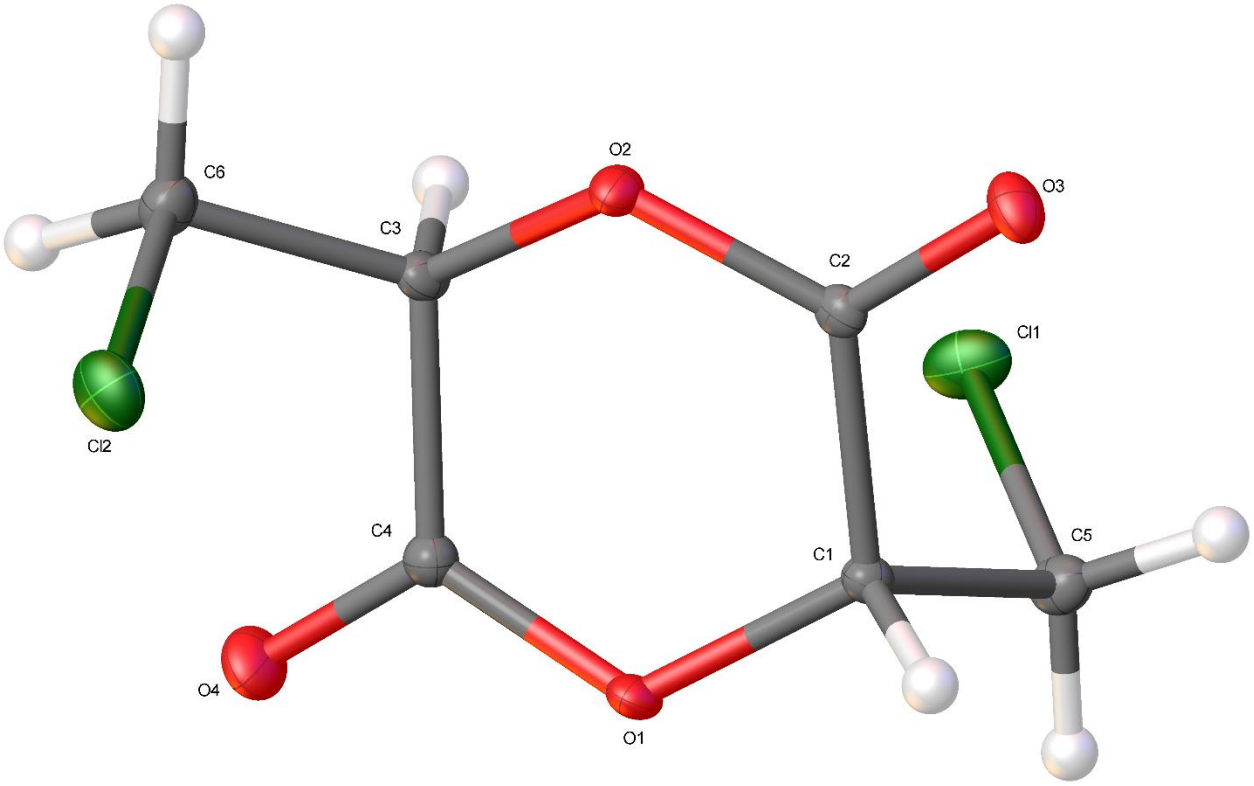

Figure A-7. Plot of the molecular structure.

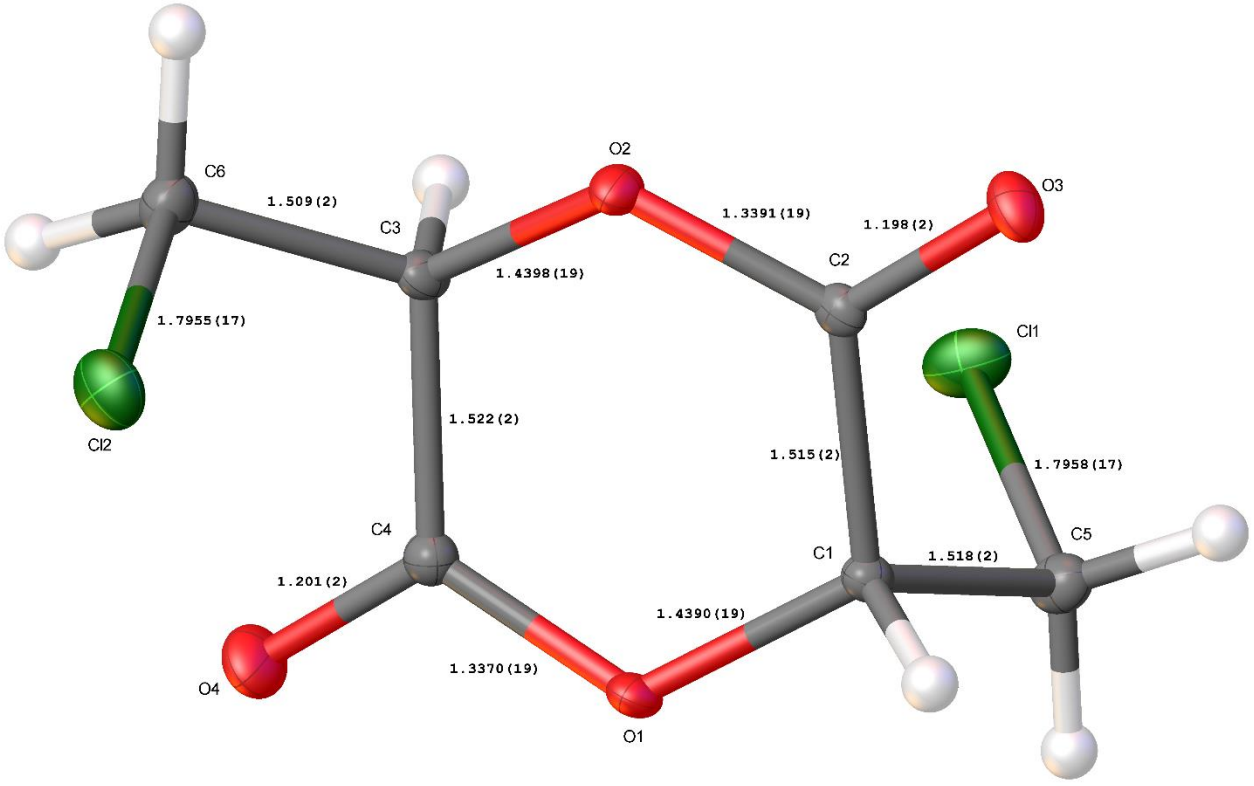

Figure A-8. Plot of the molecular structure with bond distances.

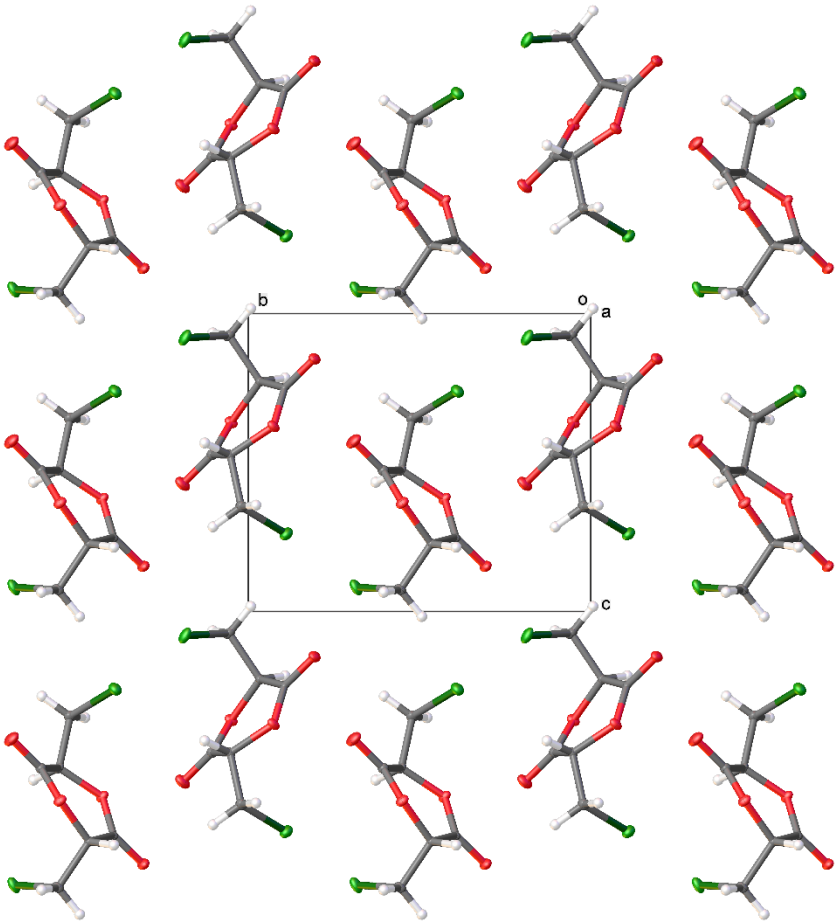

Figure A-9. Packing diagram viewed along the a-axis.

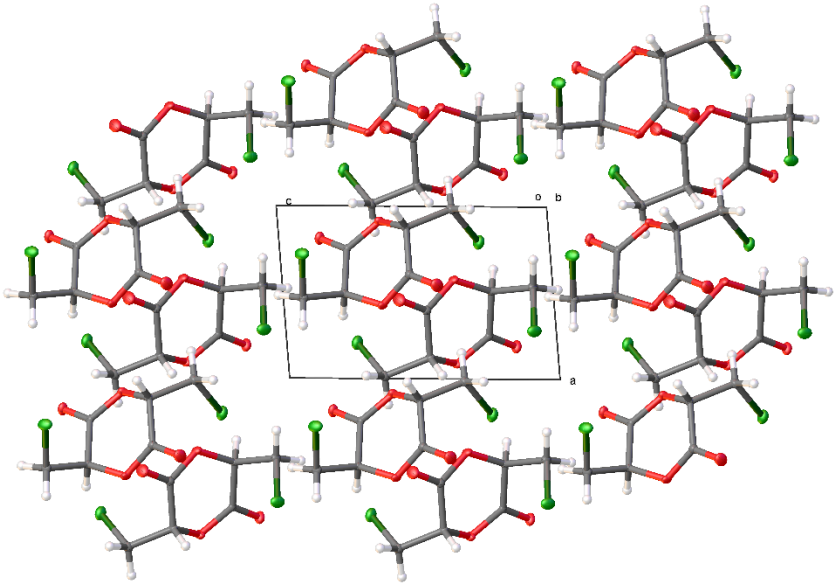

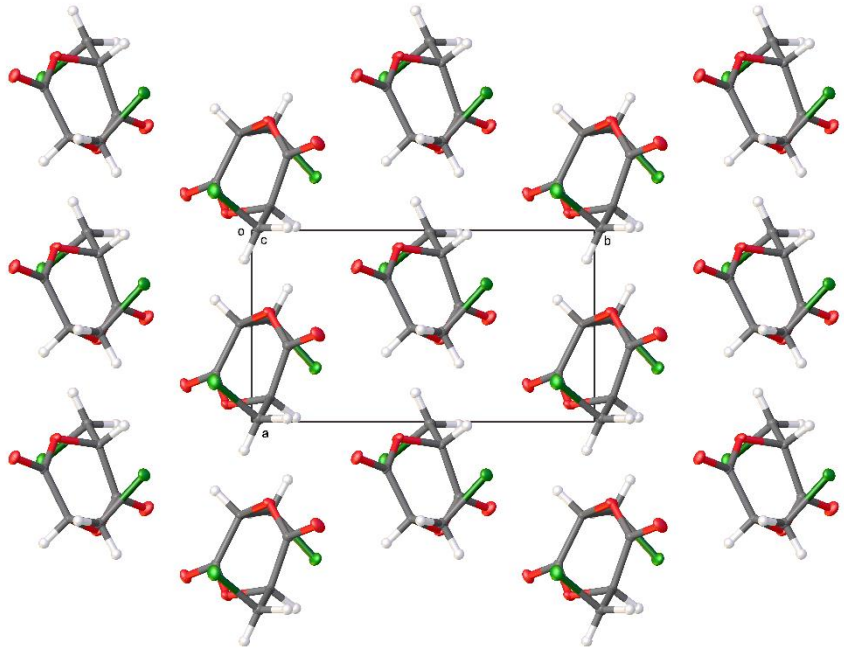

Figure A-10. Packing diagram viewed along the c-axis.

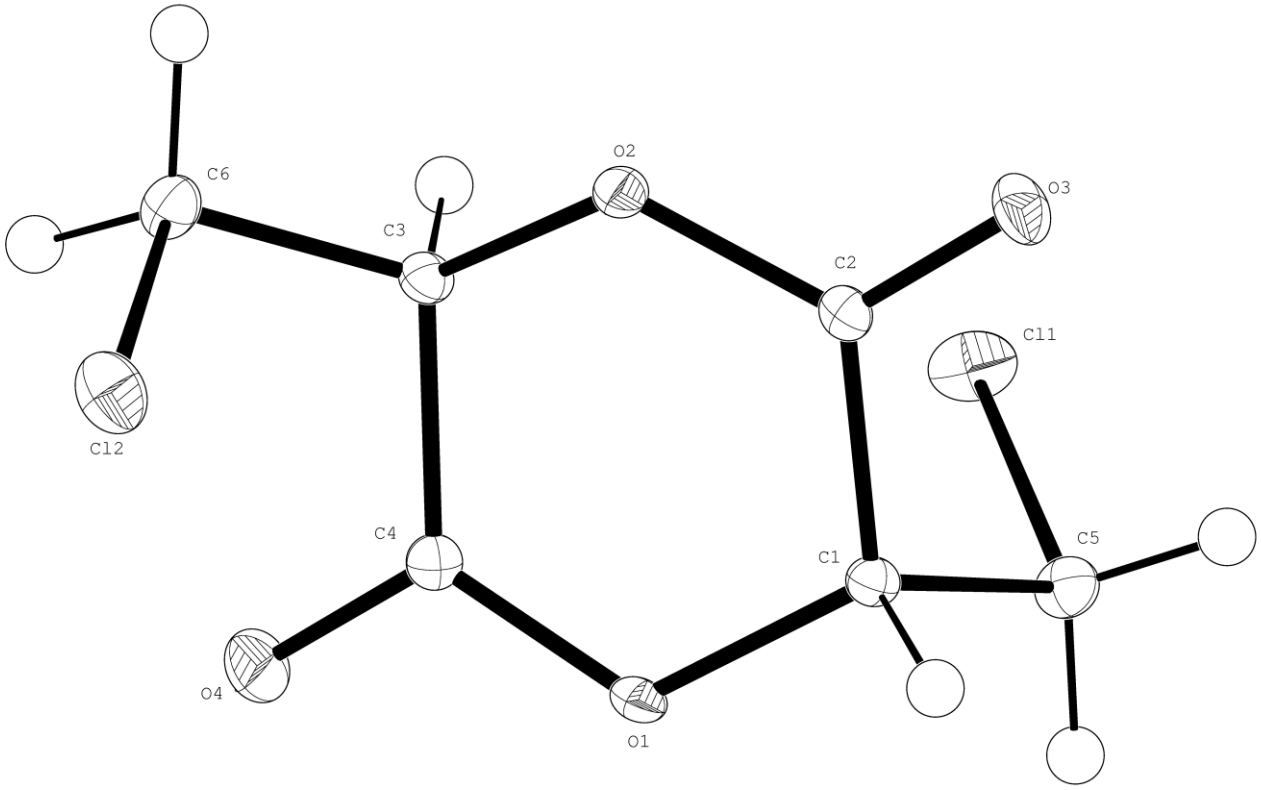

Figure A-11. Ortep plot.

Data Plots: Diffraction Data

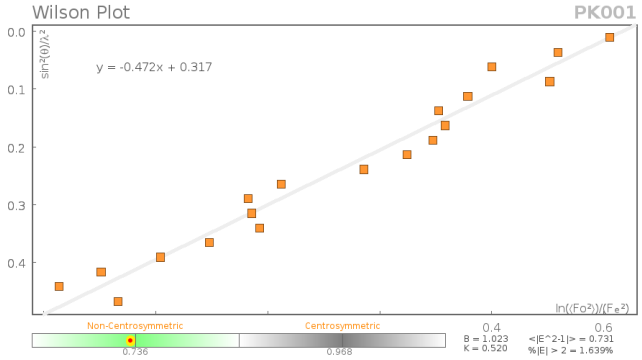

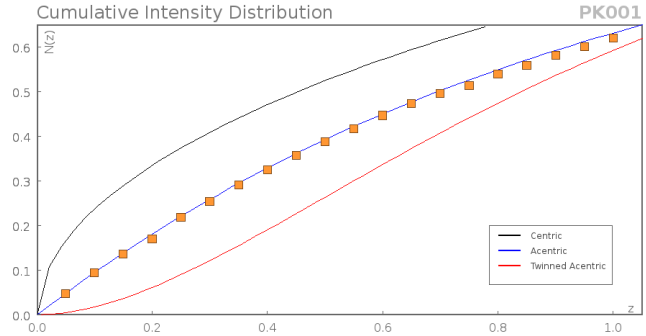

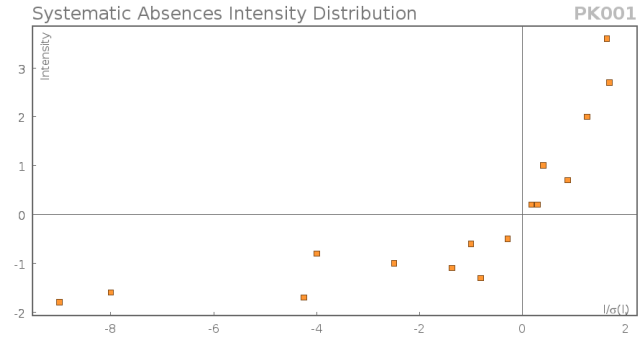

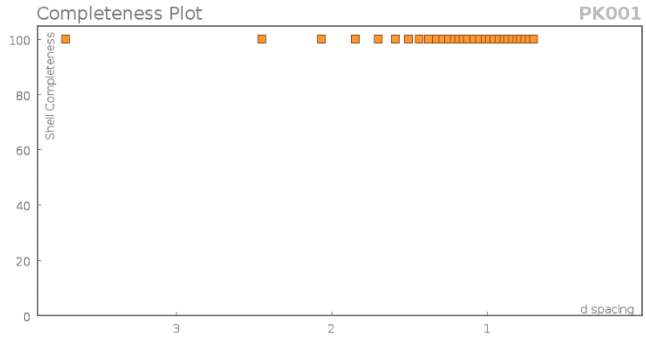

Data Plots: Refinement and Data

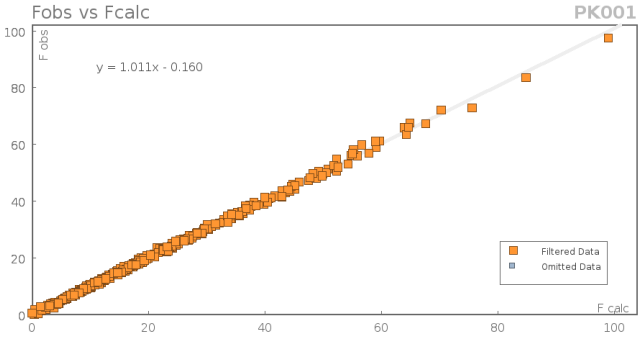

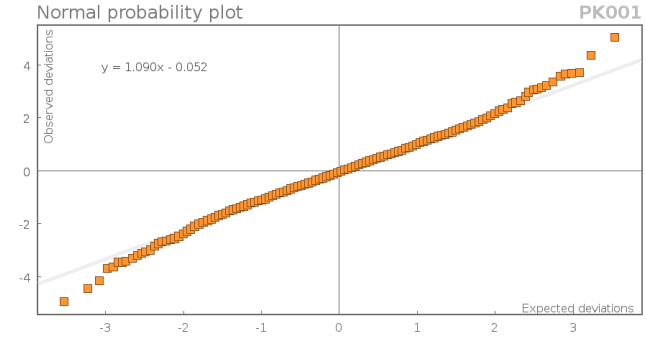

Reflection Statistics

Total reflections (after filtering)	6986	Unique reflections	2428
Completeness	0.991	Mean I/σ	31.62
hklsub>max</sub> collected	(7, 13, 11)	hklsub>min</sub> collected	(-7, -13, -11)
hkl_{max} used	(7, 13, 11)	hkl_{min} used	(-7, -13, 0)
Lim d_{max} collected	100.0	Lim d_{min} collected	0.36
d_{max} used	9.36	d_{min} used	0.7
Friedel pairs	2093	Friedel pairs merged	0
Inconsistent equivalents	0	R_{int}	0.0252
R_{sigma}	0.0253	Intensity transformed	0
Omitted reflections	0	Omitted by user (OMIT hkl)	0
Multiplicity	(2469, 1732, 279, 54)	Maximum mulitplicity	6
Removed systematic absences	16	Filtered off (Shel/OMIT)	0

Images of the Crystal on the Diffractometer

Table 1: Fractional Atomic Coordinates (×10^4) and Equivalent Isotropic Displacement Parameters (Å^2×10^3) for **PK001**. U_{eq} is defined as 1/3 of the trace of the orthogonalised U_{ij}.

Atom	x	y	z	U_{eq}
Cl2	2072.9(8)	3896.5(5)	2605.9(5)	15.66(9)
Cl1	2798.2(7)	6853.8(4)	9188.2(5)	15.53(10)
O1	5748(2)	5504.9(13)	6350.9(15)	10.2(2)
O2	877(2)	4268.9(13)	6215.1(15)	10.4(2)
O4	4567(2)	6923.1(15)	4284.5(16)	16.9(3)
O3	1890(2)	3068.9(13)	8484.9(15)	12.7(2)
C4	3964(3)	6057.7(17)	5266(2)	9.4(3)
C1	5093(3)	4657.8(17)	7723.0(19)	7.9(3)
C2	2498(3)	3937.7(19)	7514.6(17)	7.9(2)
C6	139(3)	5208.4(18)	3520(2)	11.5(3)
C3	1215(3)	5531.7(17)	5252(2)	8.6(3)
C5	5339(3)	5562.2(18)	9269(2)	11.1(3)

Table 2: Anisotropic Displacement Parameters (×10^4) **PK001**. The anisotropic displacement factor exponent takes the form: $-2\pi^2[h^2a^{*2} \times U_{11} + \ldots + 2hka^* \times b^* \times U_{12}]$

Atom	U_{11}	U_{22}	U_{33}	U_{23}	U_{13}	U_{12}
Cl2	20.43(18)	14.05(17)	12.97(17)	-3.08(14)	4.16(13)	-0.34(15)
Cl1	13.57(16)	12.59(17)	20.49(19)	-7.17(15)	1.82(14)	1.66(14)
O1	7.0(5)	13.0(5)	10.8(5)	3.5(4)	2.0(4)	-1.7(4)
O2	8.3(5)	11.8(5)	11.0(5)	3.8(4)	-0.3(4)	-2.7(4)
O4	17.6(5)	17.1(6)	15.7(6)	7.1(5)	0.6(5)	-5.3(5)
O3	16.7(6)	11.5(5)	10.0(5)	1.8(4)	2.1(4)	-4.2(4)
C4	9.2(6)	9.9(7)	9.1(6)	0.0(5)	0.8(5)	-0.3(5)
C1	7.4(6)	7.8(6)	8.7(7)	0.4(5)	1.2(5)	-0.2(5)
C2	9.2(6)	7.3(6)	7.3(6)	-1.8(5)	1.6(5)	-0.4(5)
C6	11.2(6)	12.0(7)	11.1(7)	0.4(6)	-0.7(5)	1.4(5)
C3	8.0(6)	8.2(6)	9.8(7)	1.8(5)	1.3(5)	-0.5(5)
C5	10.6(6)	11.7(7)	10.9(7)	-3.0(6)	0.2(5)	-0.1(5)

Table 3: Bond Lengths in Å for **PK001**.

Atom	Atom	Length/Å
Cl2	C6	1.7955(17)
Cl1	C5	1.7958(17)
O1	C4	1.3370(19)
O1	C1	1.4390(19)
O2	C2	1.3391(19)
O2	C3	1.4398(19)
O4	C4	1.201(2)
O3	C2	1.198(2)
C4	C3	1.522(2)
C1	C2	1.515(2)
C1	C5	1.518(2)
C6	C3	1.509(2)

Table 4: Bond Angles in ° for **PK001**.

Atom	Atom	Atom	Angle/˚
C4	O1	C1	122.08(12)
C2	O2	C3	121.67(13)
O1	C4	C3	119.20(13)
O4	C4	O1	119.71(15)
O4	C4	C3	121.04(15)
O1	C1	C2	115.39(13)
O1	C1	C5	109.47(13)
C2	C1	C5	110.70(13)
O2	C2	C1	119.29(14)
O3	C2	O2	119.75(14)
O3	C2	C1	120.96(14)
C3	C6	Cl2	110.41(11)
O2	C3	C4	114.96(13)
O2	C3	C6	107.16(13)
C6	C3	C4	110.48(13)
C1	C5	Cl1	109.55(11)

Table 5: Hydrogen Fractional Atomic Coordinates ($\times 10^4$) and Equivalent Isotropic Displacement Parameters ($Å^2 \times 10^3$) for **PK001**. U_{eq} is defined as 1/3 of the trace of the orthogonalised U_{ij}.

Atom	x	y	z	U_{eq}
H5A	5200(50)	4930(20)	10170(20)	13(4)
H5B	6940(30)	6040(20)	9350(30)	13(4)
H1	6360(30)	3930(20)	7840(30)	10(4)
H3	220(40)	6278(19)	5660(30)	10(4)
H6A	-1500(30)	4780(30)	3570(30)	18(4)
H6B	160(50)	6034(19)	2840(30)	18(4)

Citations

APEX2 suite for crystallographic software v2014.11, Bruker axs, Madison, WI (2014).

O.V. Dolomanov and L.J. Bourhis and R.J. Gildea and J.A.K. Howard and H. Puschmann, Olex2: A complete structure solution, refinement and analysis program, *J. Appl. Cryst.*, (2009), **42**, 339-341.

SAINT-8.34A-2013 •Software for the Integration of CCD Detector System Bruker Analytical X-ray Systems, Bruker axs, Madison, WI (2013).

Sheldrick, G.M., A short history of ShelX, *Acta Cryst.*, (2008), **A64**, 339-341.

Sheldrick, G.M., ShelXT, *Acta Cryst.*, (2014), **A71**, 3-8.

```
#===============================================================================#
# PLATON/CHECK-(270106) versus check.def version of 310314   for entry: pk001
# Data From: PK001.cif •Data Type: CIF          Bond Precision   C-C = 0.0020 A

#
# Cell  5.2416(11)  9.3607(19)  8.1773(16)           90    94.886(2)          90
# WaveLength 0.71073    Volume  Reported   399.76(14)  Calculated   399.76(14)
# SpaceGroup from Symmetry P 21          Hall: P 2yb
#                 Reported P 1 21 1            P 2yb
# MoietyFormula C6 H6 Cl2 O4
#      Reported C6 H6 Cl2 O4
#    SumFormula C6 H6 Cl2 O4
#      Reported C6 H6 Cl2 O4
# Mr         =    213.01[Calc],    213.01[Rep]
# Dx,gcm-3   =     1.770[Calc],     1.770[Rep]
# Z          =         2[Calc],         2[Rep]
# Mu (mm-1)  =     0.780[Calc],     0.780[Rep]
# F000       =     216.0[Calc],     216.0[Rep]  or F000' =    216.71[Calc]
# Reported   T limits: Tmin=0.568              Tmax=0.746 'MULTI-SCAN'
# Calculated T limits: Tmin=0.733 Tmin'=0.488  Tmax=0.778
# Reported   Hmax=  7, Kmax= 13, Lmax= 11, Nref= 2428       , Th(max)= 30.51
# Calculated Hmax=  7, Kmax= 13, Lmax= 11, Nref= 1295( 2451), Ratio= 1.87( 0.99)
# rho(min) = -0.21, rho(max) =  0.30 e/Ang^3
# R= 0.0207( 2391), wR2= 0.0521( 2428), S = 1.064, Npar= 130, Flack=  0.06(2)
#===============================================================================

         >>> The Following ALERTS were generated <<<
         ----------------------------------------•                  Format:    alert-
number_ALERT_alert-type_alert-level text


_ALERT_3_B Low Bond Precision on  C-C Bonds ..............       2.00 Ang.
_ALERT_4_B C-Atom in CIF Coordinate List out of Sequence ..         C1 Note
#===============================================================================
_ALERT_1_C No _chemical_absolute_configuration info given .     Please
_ALERT_4_C Crystal Size Likely too Large for Beam Size ....       0.93 mm
_ALERT_2_C Short Inter X...Y Contact  O4     ..  C2      ..       2.91 Ang.
#===============================================================================
_ALERT_4_G Rescale T(min) & T(max) by .....................       1.04
_ALERT_4_G O-Atom in CIF Coordinate List out of Sequence ..         O3 Note
#===============================================================================

             ALERT_Level and ALERT_Type Summary
             ==================================
 2 ALERT_Level_A = In General: Serious Problem
 3 ALERT_Level_B = Potentially Serious Problem
 2 ALERT_Level_C = Check & Explain

 1 ALERT_Type_1 CIF Construction/Syntax Error, Inconsistent or Missing Data.
 1 ALERT_Type_2 Indicator that the Structure Model may be Wrong or Deficient.
 1 ALERT_Type_3 Indicator that the Structure Quality may be Low.
 4 ALERT_Type_4 Improvement, Methodology, Query or Suggestion.
#===============================================================================
```

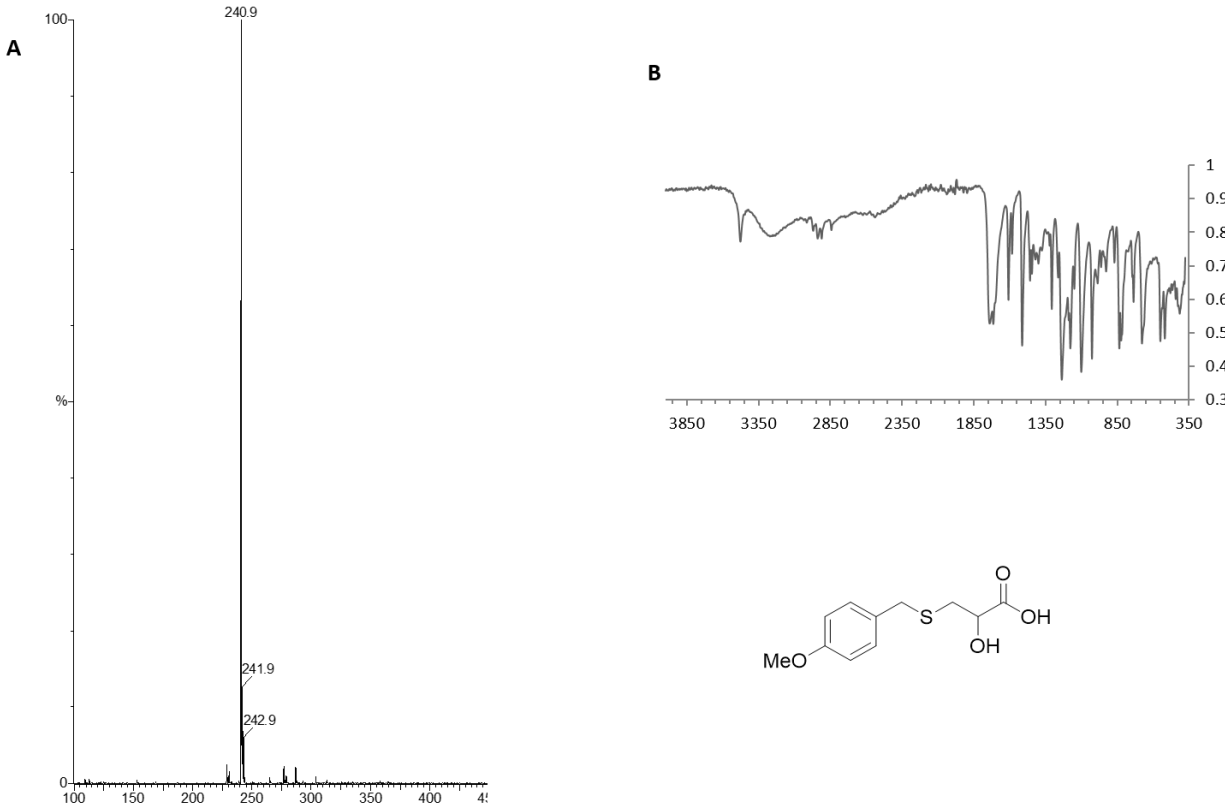

Figure A-12. 4-methoxybenzylthio-substituted lactic acid **2**. A, MS; B, IR spectrum.

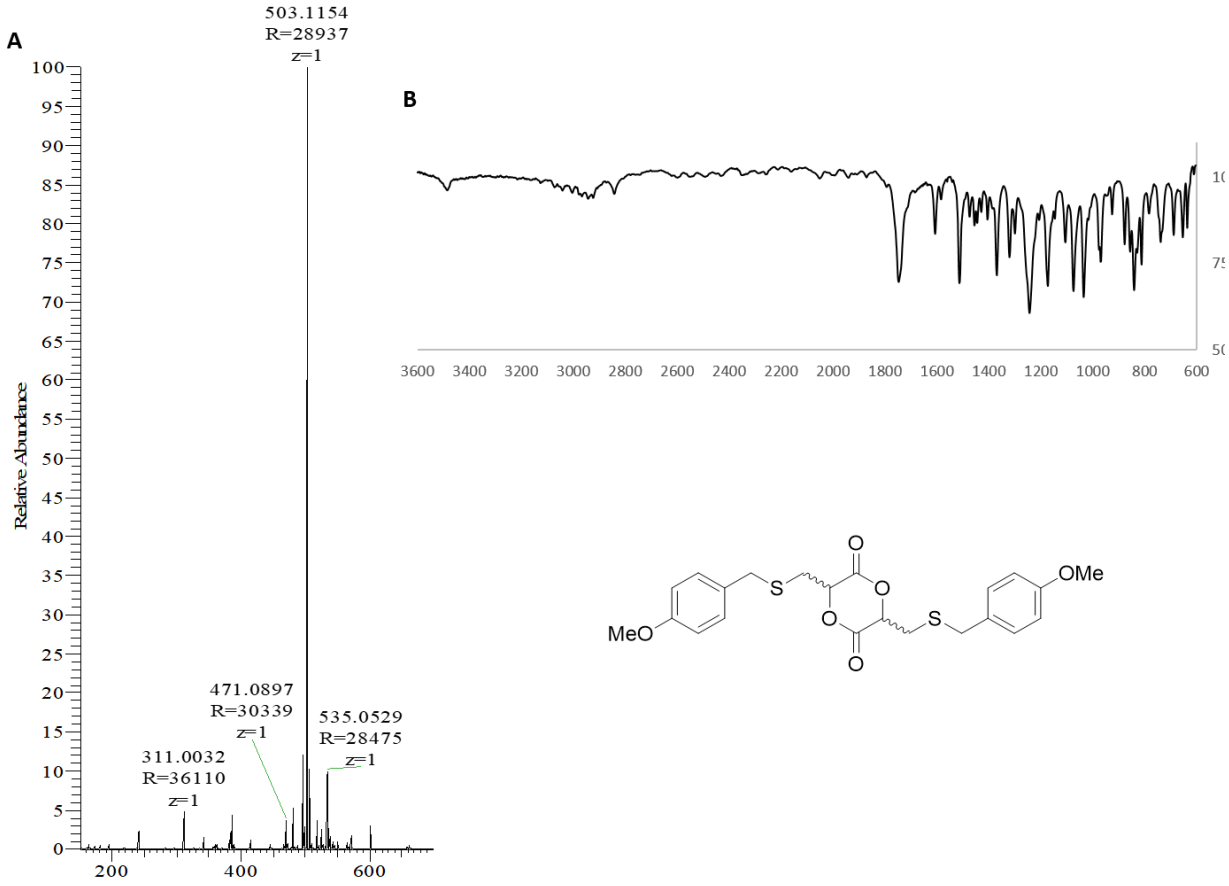

Figure A-13. 4-methoxybenzylthio-substituted lactide monomer **1.** A, HRMS; B, IR spectrum.

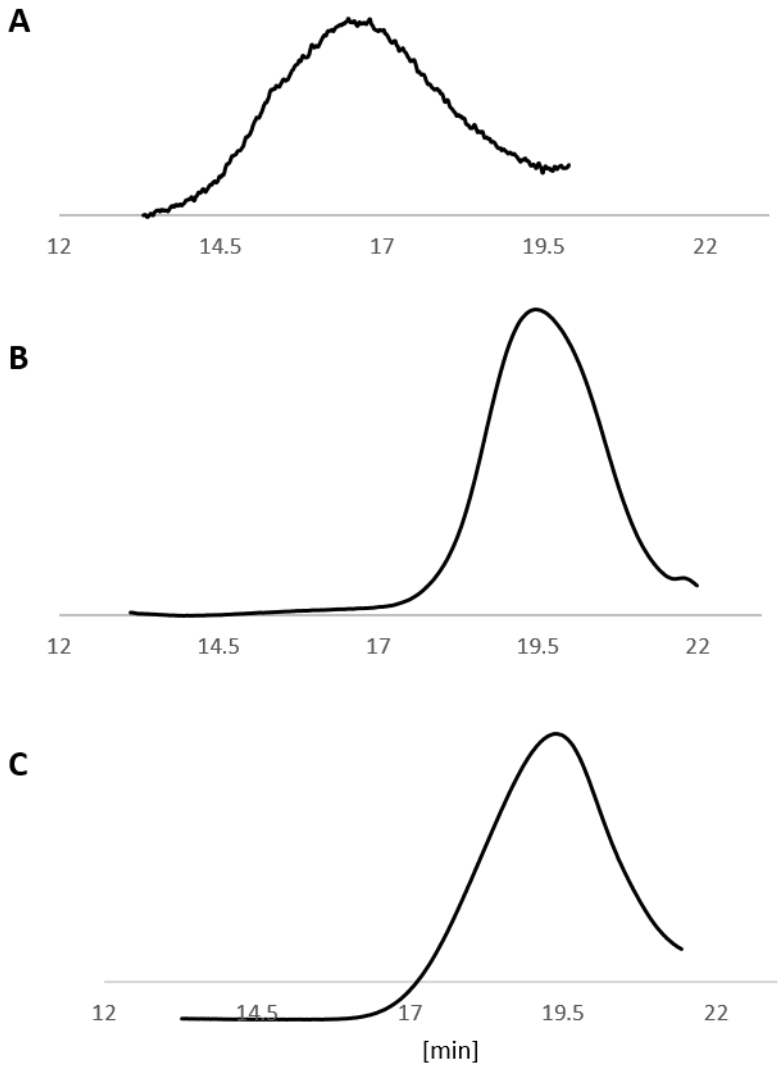

Figure A-14. GPC. A, 5 % MBT-PL obtained by copolymerization of trans MBT-lactide with L-lactide. B, 4 % thiol-PL. C, 4 % thiol-PL-phenylacrylate adduct.

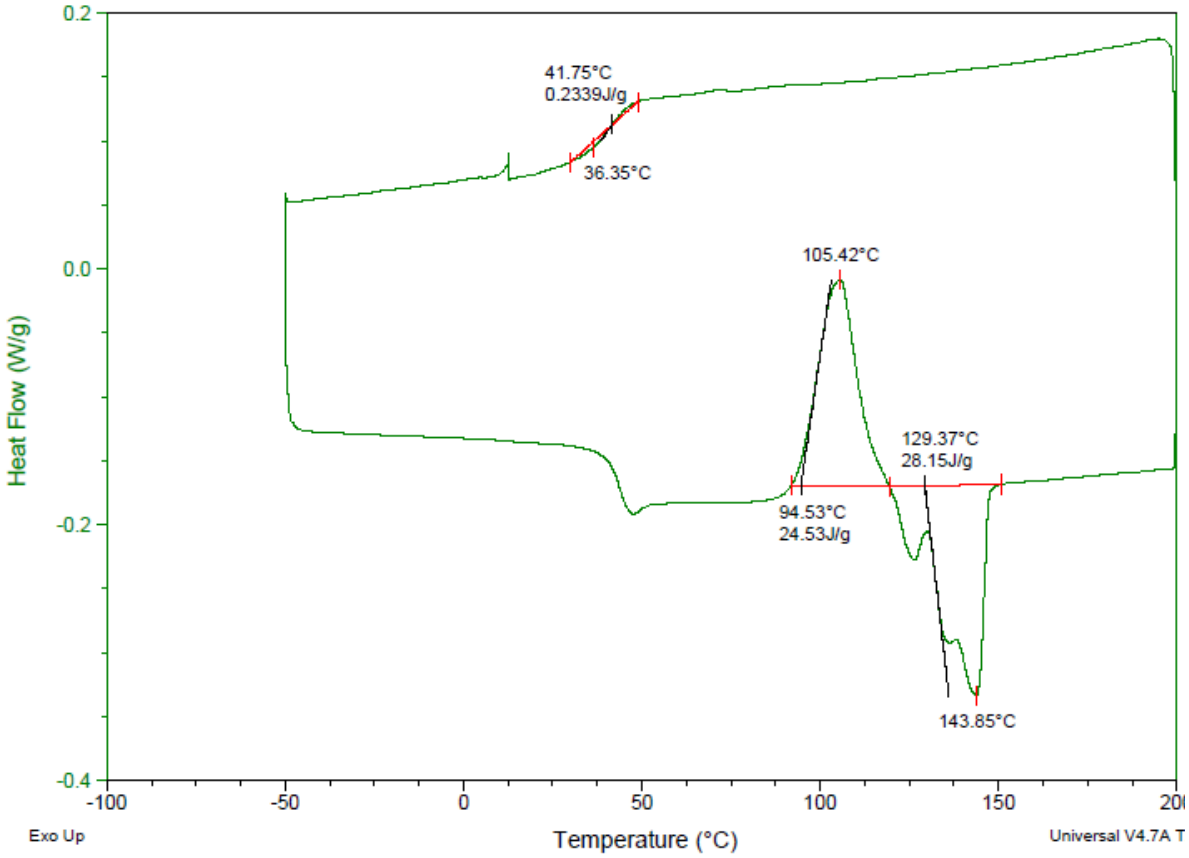

Figure A-15. DSC thermogram of 5 % MBT-PL obtained by copolymerization of the cis stereoisoform of monomer **1** with L-lactide. 5 °C/min, -50 °C to 200 °C.

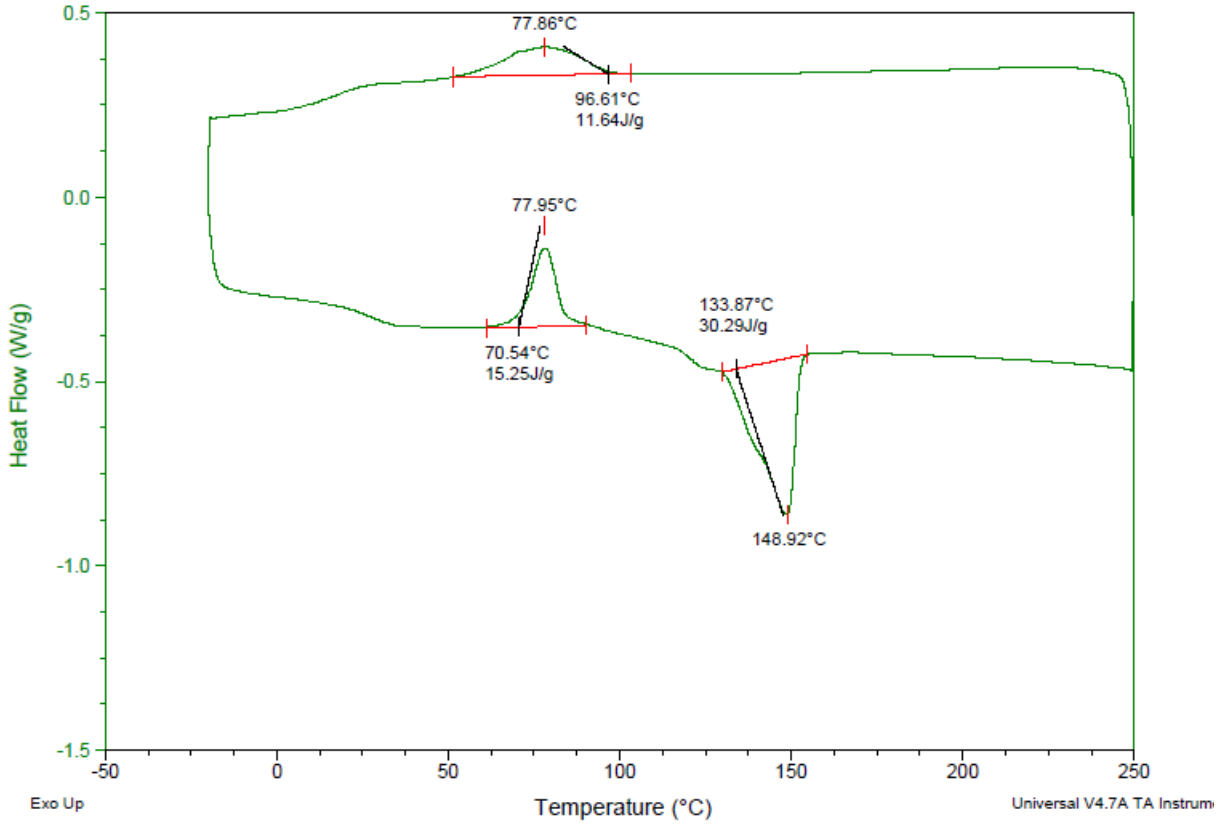

Figure A-16. DSC thermogram of 5 % MBT-PL obtained by copolymerization of the trans stereoisoform of monomer **1** with L-lactide. 5 °C/min, -10 °C to 250 °C

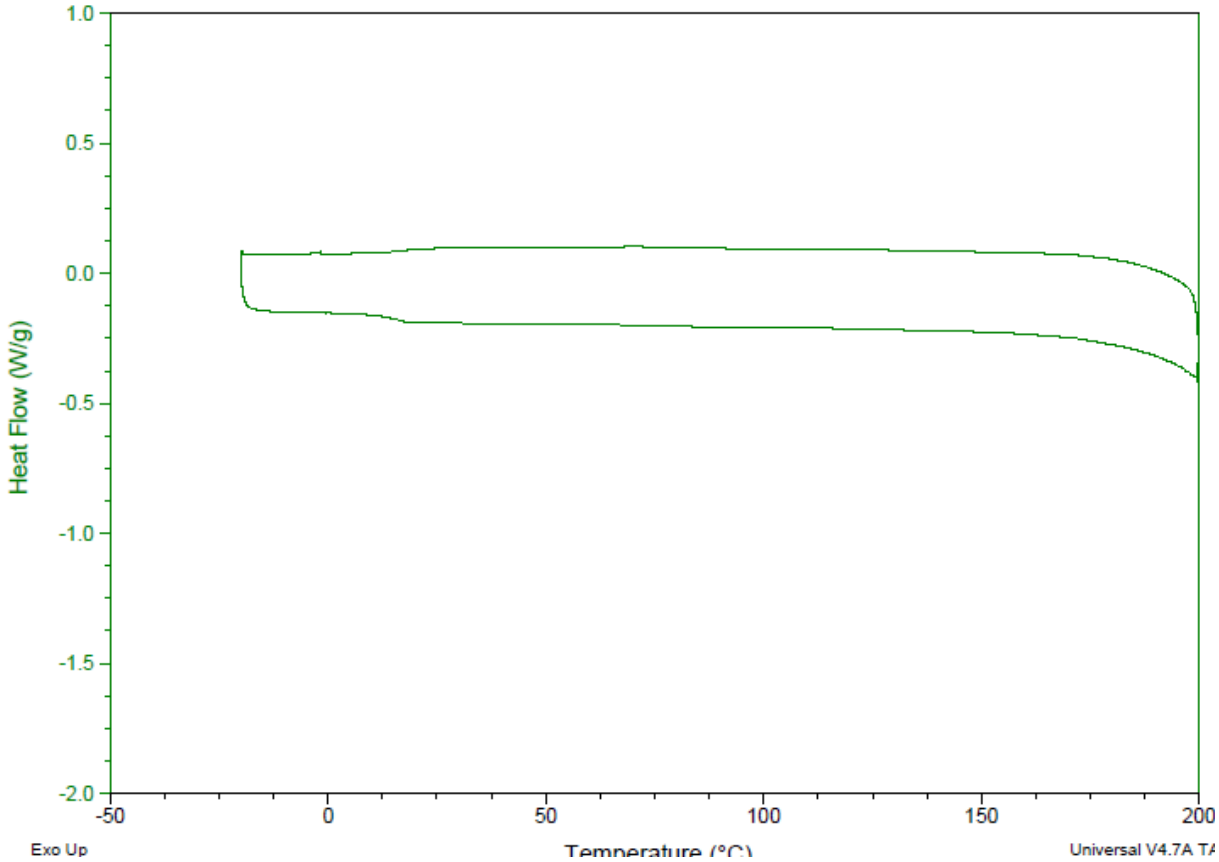

Figure A-17. DSC thermogram of 4 % thiol-PL showing the second thermal cycle. 5 °C/min, -20 °C to 200 °C.

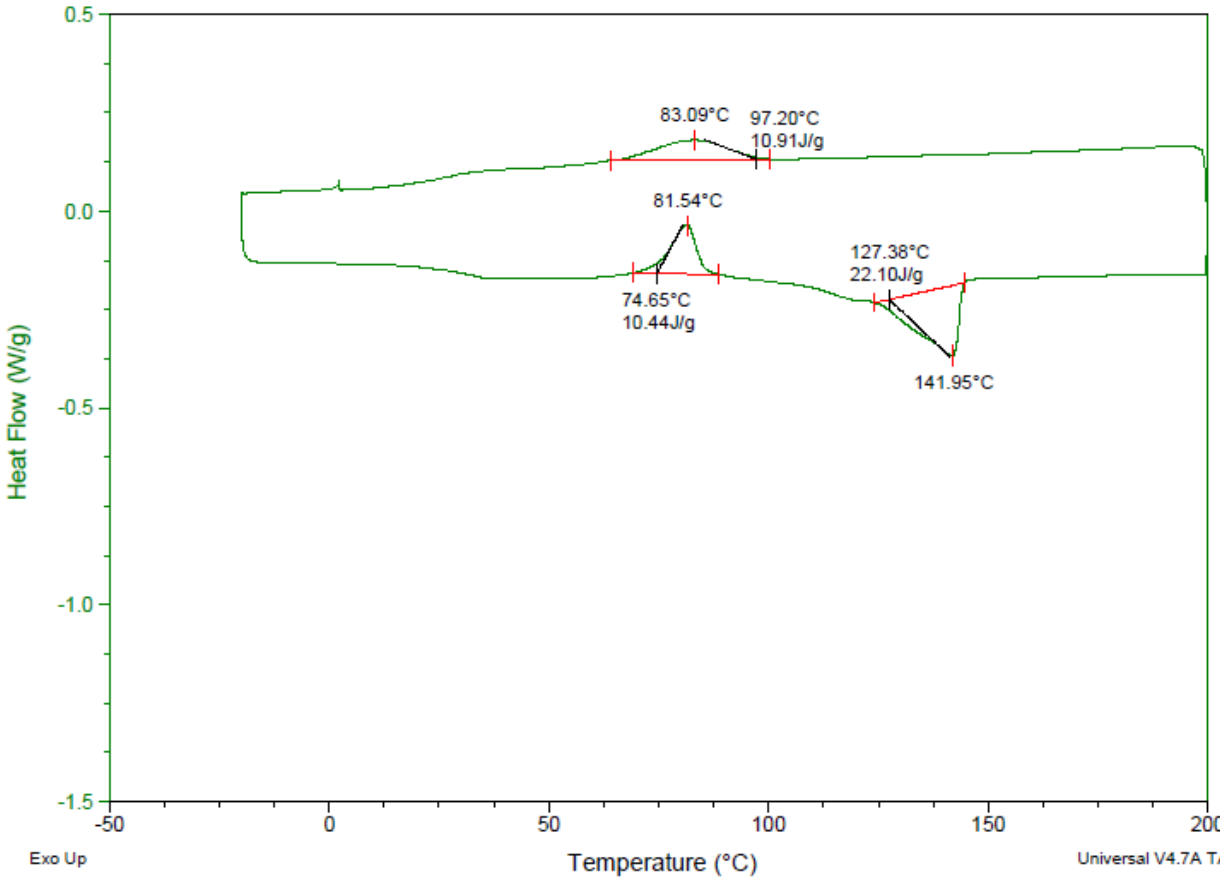

Figure A-18. DSC thermogram of phenyl acrylate adduct of 4 % thiol-PL copolymer showing the second thermal cycle. 5 °C/min, -10 °C to 200 °C.

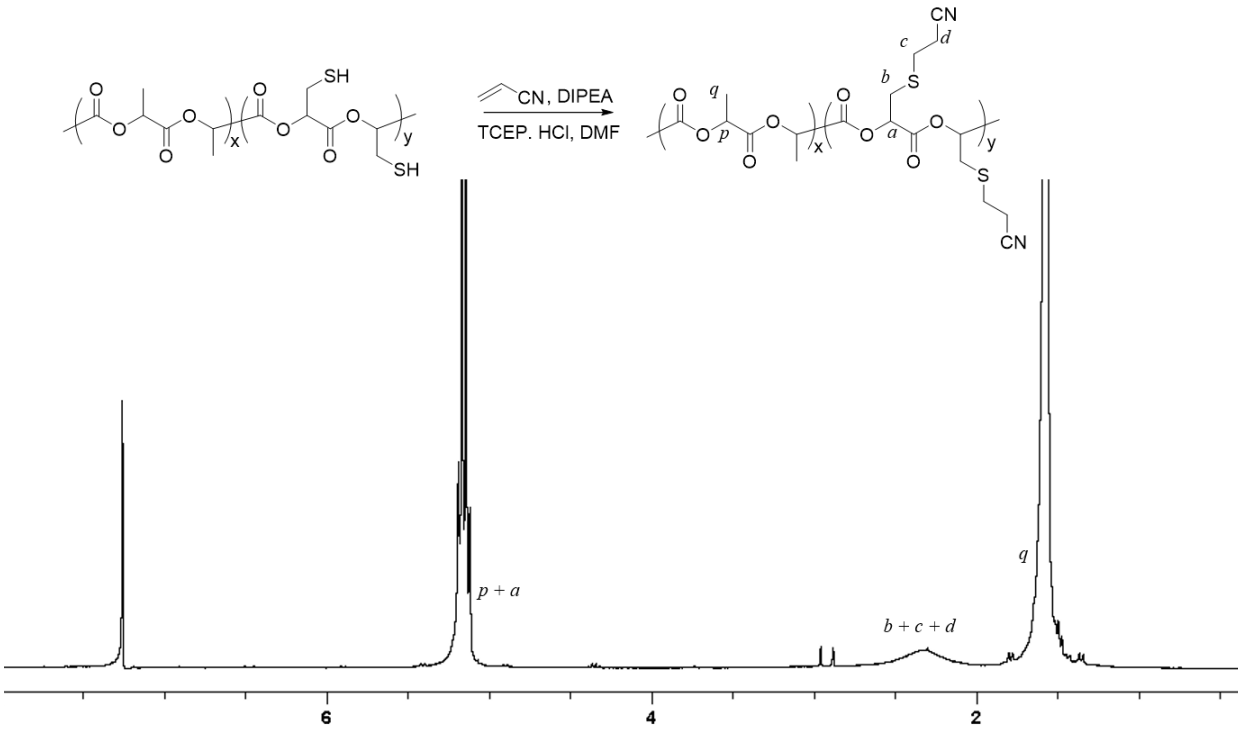

Figure A-19.[1]H NMR spectrum (300 MHz, $CDCl_3$) of acrylonitrile adduct of 4 % thiol-PL.

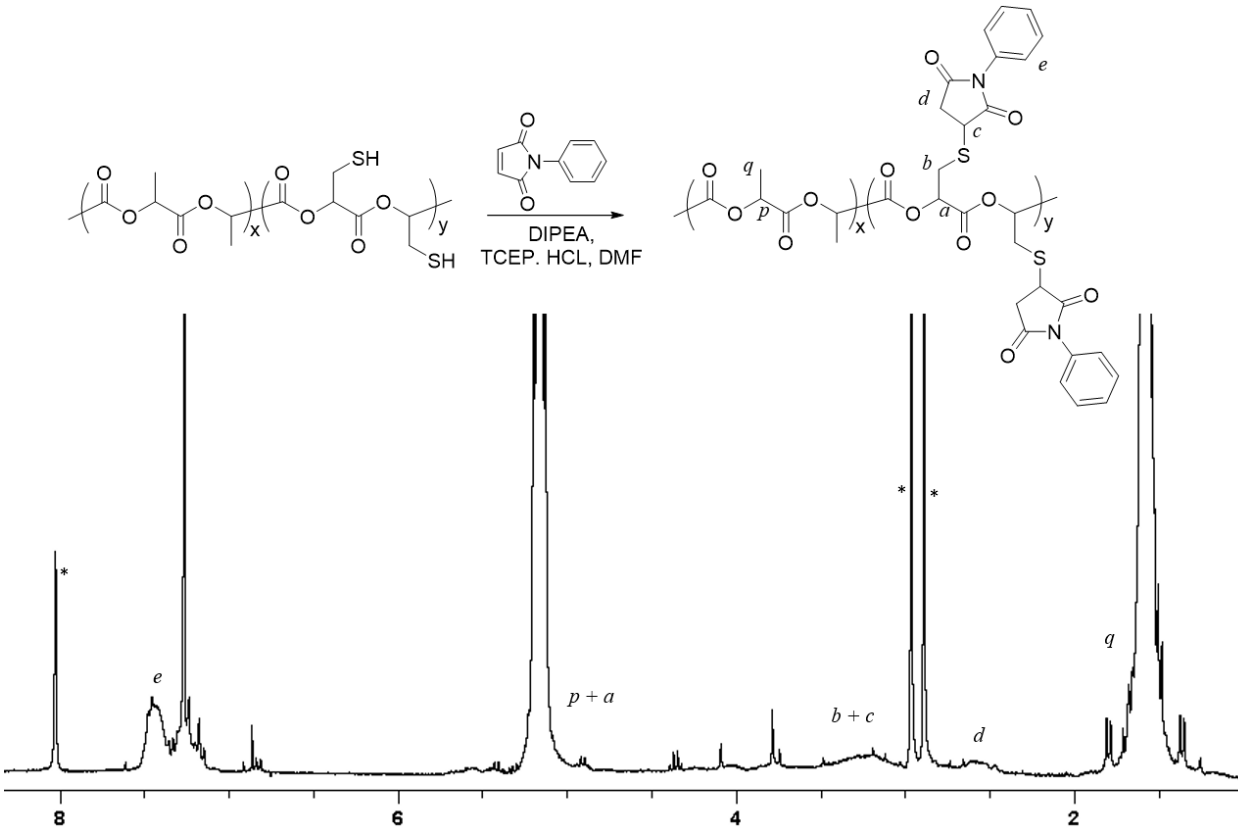

Figure A-20.[1]H NMR spectrum (300 MHz, $CDCl_3$) of *N*-phenylmaleimide adduct of 4 % thiol-PL. * residual DMF.

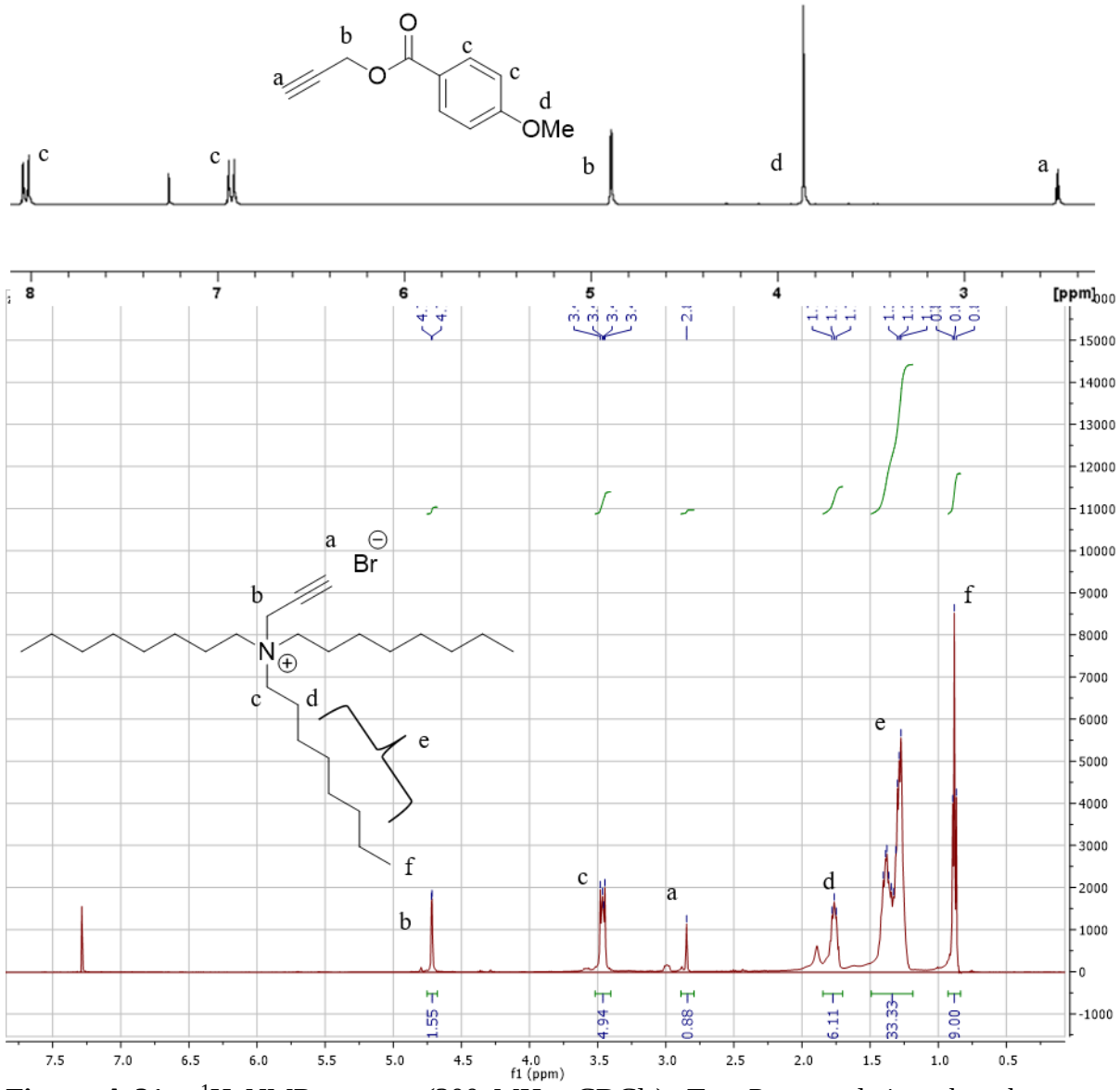

Figure A-21. ^{1}H NMR spectra (300 MHz, $CDCl_3$). Top Progargyl 4-methoxybenznoate. *N*,*N*,*N*-Trioctyl-*N*-propargylammonium bromide.

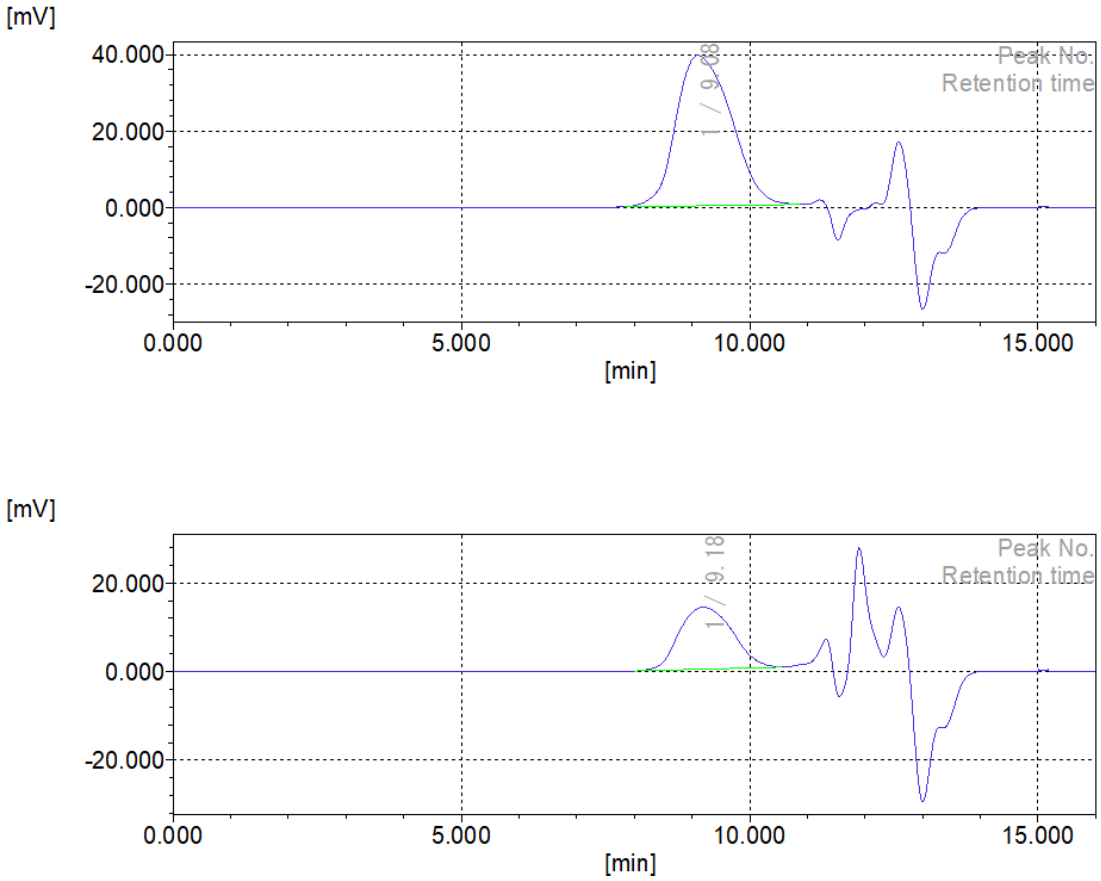

Figure A-22. Gel permeation chromatography (GPC) in THF, calibrated with polystyrene standards. Top, azido-PL; Bottom, 4-methoxybenzoate-substituted PL.

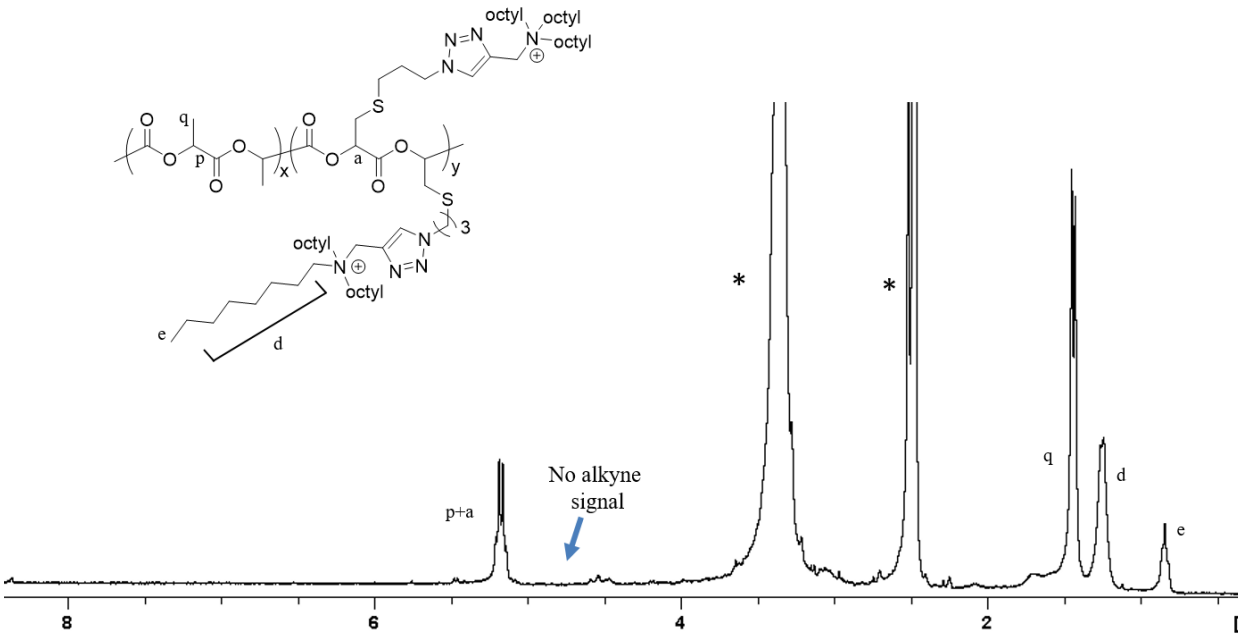

Figure A-23. ^{1}H NMR spectra (300 MHz, $CDCl_3$). Trioctylammonium-substituted PL. *residual solvents-H_2O, DMSO.

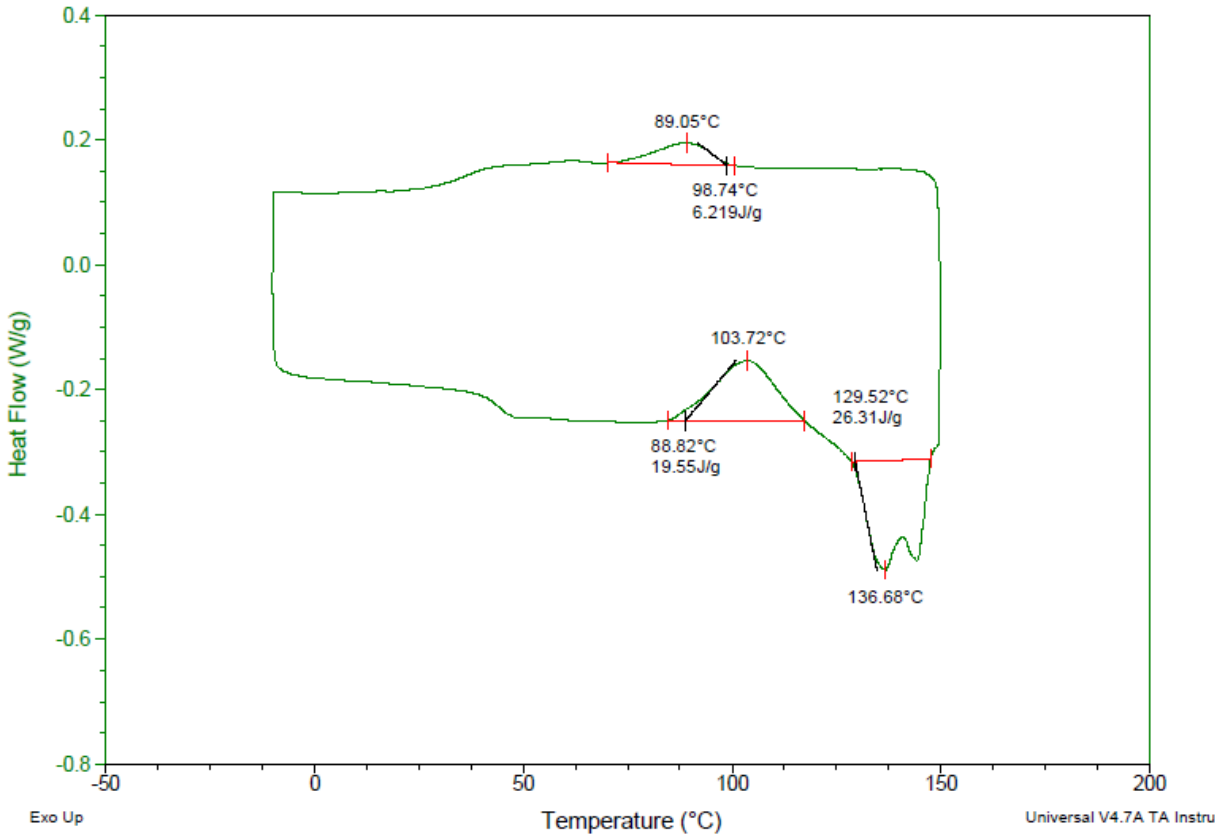

Figure A-24. Differential Scanning Calorimetry (DSC) (5 °C/min, from -10 °C to 200 °C) of Br-PL.

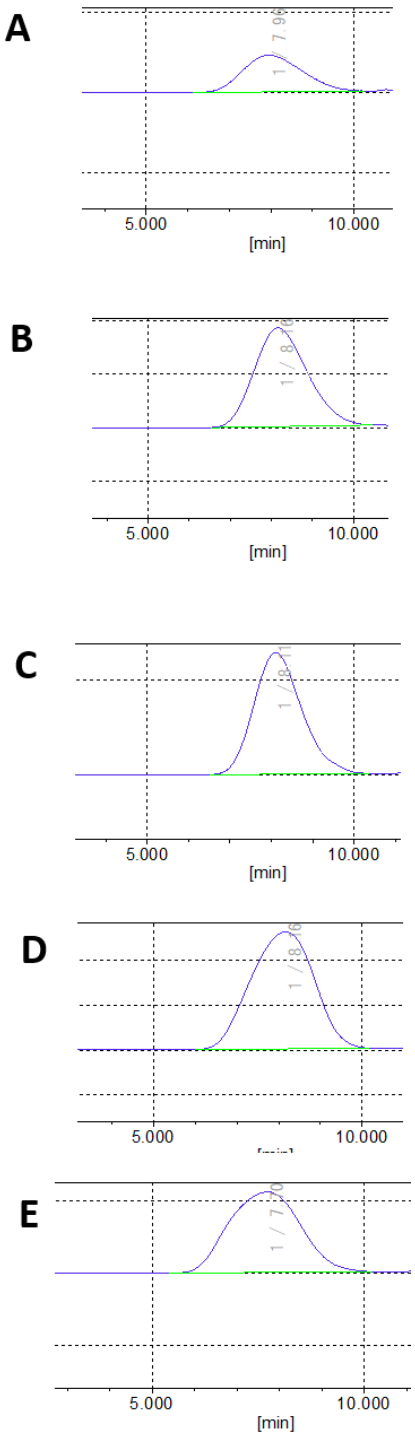

Figure A-25. Gel permeation chromatography (GPC) in THF, calibrated with polystyrene standards. A, PL. B, 5 % Br-PLA. C, C, 5% PL-$PMMA_{14}$. D, 5 % PL-$PMMA_{41}$. E, 5% PL-$PMMA_{53}$

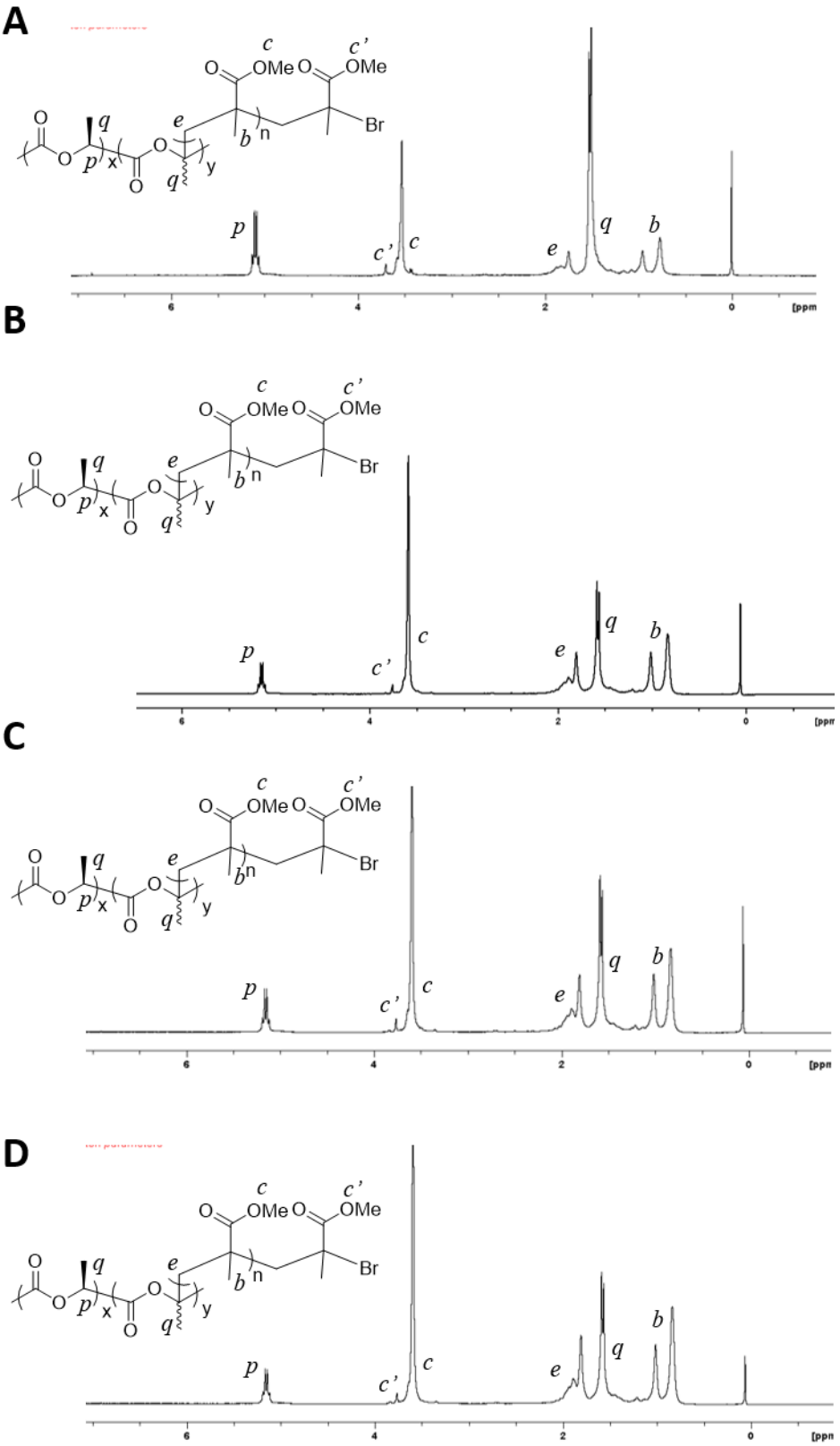

Figure A-26. ^{1}H NMR spectra (300 MHz, $CDCl_3$). A, PL-PMMA$_{14}$. B, PL-PMMA$_{22}$. C, PL-PMMA$_{41}$. D, PL-PMMA$_{53}$.

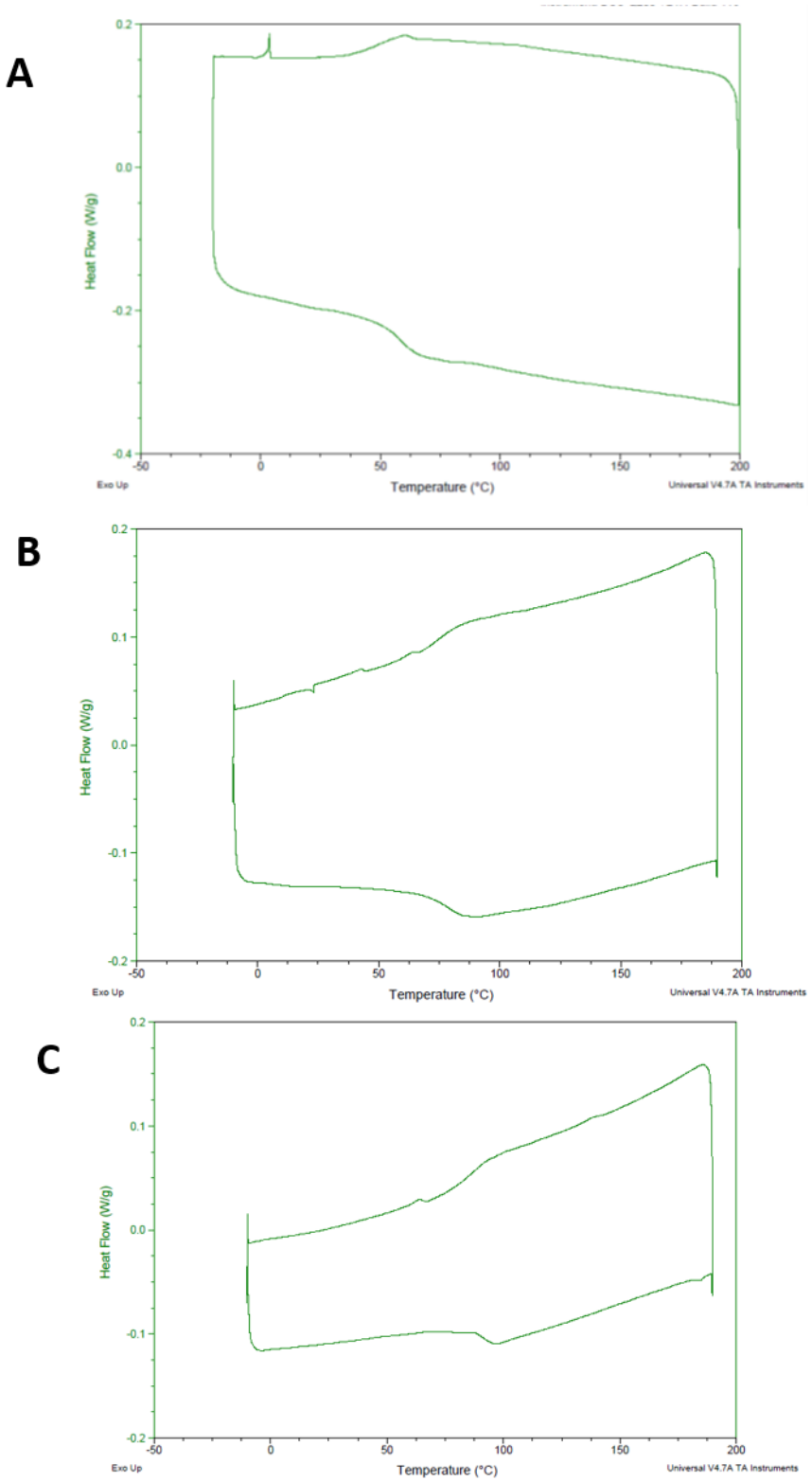

Figure A-27. Differential Scanning Calorimetry (DSC) (5 °C/min, from -10 °C to 190 °C. A, PLA-PMMA$_{14}$. B, PLA-PMMA$_{41.}$ C, PLA-PMMA$_{53}$

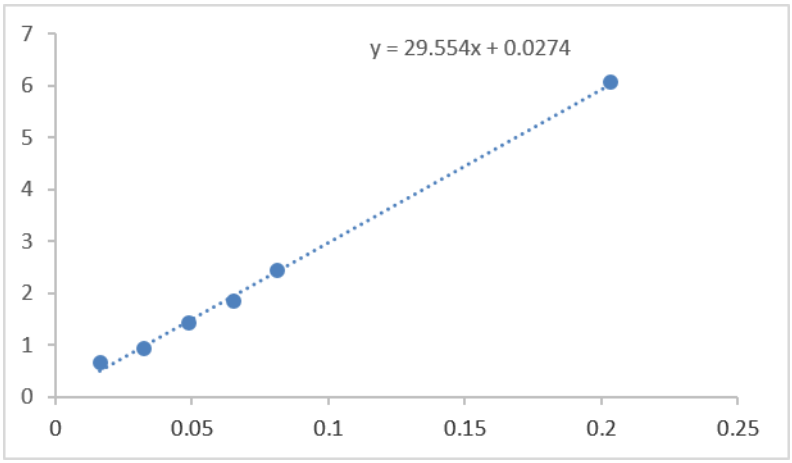

Figure A-28. Standard curve of curcumin in (4:1) H_2O-acetone mixture